PROBE, ENTRY FROM ORBIT    NASA CR-66131

# SYSTEM DESIGN

# MARS PROBE

FINAL REPORT

CONTRACT NO. NAS 1-5224

AVCO

# BOOK INDEX

# COMPARATIVE STUDIES OF CONCEPTUAL DESIGN AND QUALIFICATION PROCEDURES FOR A MARS PROBE/LANDER

## FINAL REPORT

## VOLUME III PROBE, ENTRY FROM ORBIT

## Book 1 -- SYSTEM DESIGN

Prepared by

SPACE SYSTEMS DIVISION
AVCO CORPORATION
Lowell, Massachusetts

AVSSD-0006-66-RR
Contract NAS 1-5224

11 May 1966

Prepared for

NATIONAL AERONAUTICS AND SPACE ADMINISTRATION
LANGLEY RESEARCH CENTER
LANGLEY STATION
Hampton, Virginia 23365

The results of Mars Probe/Lander studies, conducted over a 10-month period for Langley Research Center, NASA, are presented in detail in this report. Under the original contract work statement, studies were directed toward a direct entry mission concept, consistent with the use of the Saturn IB-Centaur Launch Vehicle, wherein the landing capsule is separated from the spacecraft on the interplanetary approach trajectory, some 10 to 12 days before planet encounter. The primary objectives of this mission were atmospheric sampling by the probe/lander during entry and terrain and atmosphere physical composition measurement for a period of about 1 day after landing.

Studies for this mission were predicated on the assumption that the atmosphere of Mars could be described as being within the range specified by, NASA Mars Model Atmospheres 1, 2, 3 and a Terminal Descent Atmosphere of the document NASA TM-D2525. These models describe the surface pressure as being between 10 and 40 mb. For this surface pressure range a payload of moderate size can be landed on the planet's surface if the entry angle is restricted to be less than about 45 degrees.

Midway during the course of the study, it was discovered by Mariner IV that the pressure at the surface of the planet is in the 4 to 10 mb range, a range much lower than previously thought to be the case. The results of the study were re-examined at this point. It was found that retention of the direct entry mission mode would require much shallower entry angles to achieve the same payloads previously attained at the higher entry angles of the higher surface pressure model atmospheres. The achievement of shallow entry angles (on the order of 20 degrees), in turn, required sophisticated capsule terminal guidance, and a sizeable capsule propulsion system to apply a velocity correction close to the planet, after the final terminal navigation measurements.

Faced with these facts, NASA/LRC decided that the direct entry from the approach trajectory mission mode should be compared with the entry from orbit mode under the assumption that the Saturn 5 Launch Vehicle would be available. Entry of the flight capsule from orbit allows the shallow angle entry (together with low entry velocity) necessary to permit higher values of $M/C_DA$, and hence entry weight in the attenuated atmosphere.

It was also decided by LRC to eliminate the landing portion of the mission in favor of a descent payload having greater data-gathering capacity, including television and penetrometers. In both the direct entry and the entry from orbit cases, ballistic atmospheric retardation was the only retardation means considered as apecifically required by the contract work statement.

Four months had elapsed at the time the study ground rules were changed. After this point the study continued for an additional five months, during which

period a new design for the substantially changed conditions was evolved. For this design, qualification test programs for selected subsystems were studied. Sterilization studies were included in the program from the start and, based on the development of a fundamental approach to the sterilization problem, these efforts were expanded in the second half of the study.

The organization of this report reflects the circumstance that two essentially different mission modes were studied -- the first being the entry from the approach trajectory mission mode and the other being the entry from orbit mission mode -- from which two designs were evolved. The report organization is as follows:

Volume I, Summary, summarizes the entire study for both mission modes.

Volume II reports on the results of the first part of the study. This volume is titled Probe/Lander, Entry from the Approach Trajectory. It is divided into two books, Book 1 and Book 2. Book 1 is titled System Design and presents a discursive summary of the entry from the approach trajectory system as it had evolved up to the point where the mission mode was changed. Book 2, titled Mission and System Specifications, presents, in formal fashion, specifications for the system. It should be understood, however, that the study for this mission mode was not carried through to completion and many of the design selections are subject to further tradeoff analysis.

Volume III is composed of three books which summarize the results of the entry from orbit studies. Books 1 and 2 are organized in the same fashion as the books of Volume II, except that Book 2 of Volume III presents component specifications as well. Book 3 is titled Development Test Programs and presents, for selected subsystems, a discussion of technology status, test requirements and plans. This Book is intended to satisfy the study and reporting requirements concerning qualification studies, but the selected title is believed to describe more accurately the study emphasis desired by LRC.

Volume IV presents Sterilization results. This information is presented separately because of its potential utilization as a more fundamental reference document.

Volume V presents, in six separate books, Subsystem and Technical Analyses. In order (from Book 1 to Book 6) they are:

Trajectory Analysis
Aeromechanics and Thermal Control
Telecommunications, Radar Systems and Power
Instrumentation
Attitude Control and Propulsion
Mechanical Subsystems

Most of the books of Volume V are divided into separate discussions of the two mission modes. Table of Contents for each book clearly shows its organization.

# CONTENTS

# CONTENTS (Cont'd)

## CONTENTS (Cont'd)

CONTENTS (Cont'd)

# CONTENTS (Cont'd)

# CONTENTS (Concl'd)

## ILLUSTRATIONS

ILLUSTRATIONS (Cont'd)

## TABLES

## TABLES (Concl'd)

# GLOSSARY OF TERMS

Entry Shell: The entry shell is defined as the primary load-carrying structure, including the ablative heat shield.

Entry Weight: The weight of the entry vehicle at atmospheric entry.

Entry Shell Weight Fraction: The percentage of entry weight required for the entry shell.

Launch Vehicle System: The launch vehicle system includes the three stages of the Saturn V, with its guidance subsystems and the ascent fairing which shrouds the planetary vehicle, to make up the launch vehicle (LV) as the flight hardware; plus the supporting ground equipment, software, and associated manpower.

Spacecraft System: The spacecraft system includes the flight spacecraft (FS), as its flight hardware, plus flight hardware spare parts, development models, associated operational support equipment (hardware and software), and the management and engineering teams.

Capsule System: The capsule system includes the flight capsule (FC), as the flight hardware, plus flight hardware spare parts (or spare flight capsules, depending on the time of spares replacement), development and sterilization assay models, control documentation and associated software, operational support equipment, and the management and engineering teams.

Planetary Vehicle: The planetary vehicle (PV) is defined as the composite flight spacecraft and flight capsule integrally attached and operated up to separation in the vicinity of the selected planet.

Space Vehicle: The space vehicle (SV) is the combined launch vehicle and planetary vehicle or vehicles which physically leave the launch pad in conduct of the mission.

Mission Operations System (MOS): The MOS includes that portion of the project which plans, directs, controls, and executes (with support provided by the Deep Space Network) the space flight operation after injection of the planetary vehicle on its trajectory, the mission-dependent equipment required at the Deep Space Network, and the operational teams.

Deep Space Network (DSN): The DSN is comprised of the Deep Space Instrumentation Facility (DSIF), the Space Flight Operations Facility (SFOF), the ground communications system (GCS) connecting the two facilities, and the personnel who regularly operate these facilities.

Launch Operations System (LOS): The LOS includes those elements of the project responsible for planning the executing the preflight and launch-to-injection phases of the mission.

Operational Support Equipment (OSE): The OSE includes the equipment and facilities required for the assembly, servicing, checkout, sterilization, and testing of the subsystems of the flight capsule.

Launch Opportunity: A re-occuring duration of time, every 25.6 months, when favorable Earth-Mars spatial positions allow for practial interplanetary transfer trajectories.

Launch Period: The number of days within the launch opportunity when practical Earth-Mars transfer trajectories are selected depending on mission objectives and launch vehicle constraints.

Launch Window: The duration of time each Earth day when space vehicle launch is practical to achieve desired planetary vehicle transfer orbit orientation and characteristics, depending on mission objectives and launch vehicle constraints.

Flight Capsule Terminology: Figure A presents a further breakdown of the flight capsule, identifying the terminology at the operational stages of separation and/or deployment. In summary, the flight capsule is attached to the flight spacecraft by the forward and aft sections of the flight capsule to flight spacecraft adapter. Operation of the sterilization canister lid separation mechanism, followed by the operation of the separation system on the flight capsule to flight spacecraft adapter, results in the separated vehicle. Attitude control and propulsion maneuvers are performed to place the separated vehicle on a preselected planetary impact trajectory. After these maneuvers, the propulsion and attitude control system electronics assembly is separated and the resultant entry vehicle cruises to and enters the planet atmosphere. After entry, the entry shell (including the attitude control system reaction subsystem and spin/despin rockets is separated and the suspended capsule descends through the atmosphere with the parachute. At a preselected time during descent, a separation mechanism operation extends the landed capsule from the parachute by use of a tether. At impact the landed capsule is separated from the tether for landed operations.

Note that the instrument packages are shown on the suspended capsule actually mounted to the entry shell and landed capsule support structure external to the landed capsule. In addition to the selected portions of the science instrumentation mounted externally and internally, appropriate portions of the programming and sequencing, thermal control, telecommunications, electrical power and control, and the signal and power interconnection subsystems hardware are also individually attached and operationally integrated both internally and externally, to accomplish the data acquisition and transmission functions of the capsule system mission.

Additional terminology used in this book are as follows:

CC&S: Central computer and sequencer

TVC: Thrust vector control

ACS: Attitude control system

VHF: Very high frequency

VSWR: Voltage standing wave ratio

# ACKNOWLEDGMENT

The conduct of the study and technical preparation of this report involved the participation and close coordination of many people, all of whose contributions were important to the end results.

It is impractical to single out each individual, but the major contributors to the study, reflected in the material presented in this book, are as follows:

### Responsible Manager

T. R. Ellis

### Major Contributors

| Name | Sections |
|---|---|
| R. Barnes | 4 |
| F. Boutwell | 3, 5, 12 |
| R. Davis | 4, 5 |
| P. DiCarlo | 4, 5 |
| P. Dow | 4, 10 |
| T. R. Ellis | 1, 2, 3, 4, 5, 9, 13 |
| R. Hanselman | 4, 7, 8 |
| J. Hayes | 3, 4, 11, 13 |
| H. Hurwicz | 4, 5 |
| M. Koslover | 4 |
| R. Massa | 6 |
| M. Russell | 3, 5 |
| H. Steinle | 4 |
| O. Zappa | 5 |

### Approved By

| Signature | Title |
|---|---|
| *T. R. Ellis* | |
| T. R. Ellis | Manager, Space Systems |

# 1.0 INTRODUCTION

The primary objective of this study is the design of a nonsurvivable probe to perform engineering experiments for the determination of Mars atmospheric and terrain properties. The mission is primarily engineering in nature in order to ascertain Mars properties for the definition and confirmation of assumptions that are necessary for the design of future large soft-landers for advanced missions.

The mission mode is entry from Mars orbit. The discovery by Mariner IV that the Mars atmosphere is more tenuous than previously thought tended to vitiate the earlier study results which used an entry from approach trajectory mission mode. The study was redirected to consider deployment of the flight capsule from the flight spacecraft while in Mars orbit to allow the use of shallower entry angles as is required by the new model atmospheres which vary from 5- to 10-millibars surface pressures.

The requirements of the earlier study for survivable landing has been eliminated and NASA has directed that television, surface hardness penetrometers, and wind measurement instrumentation be included in the science payload.

Flight spacecraft tradeoffs were considered insofar as possible with particular emphasis on the constraints which the flight capsule mission will place on the flight spacecraft and overall mission and trajectory selection.

The study includes all necessary parametric and systems analyses leading to a conceptual design, with particular emphasis on critical tradeoff regions and the necessary assumptions and decisions which have led to the conceptual design.

# 2.0 MISSION OBJECTIVES AND CONSTRAINTS

The entry from orbit portion of this study was conducted under a specified set of mission objectives and constraints. The more significant of these ground-rules are summarized below.

## 2.1 MISSION OBJECTIVES

The mission objectives are divided according to five missions phases: (1) pre-separation, (2) separation, (3) separation to entry, (4) entry to near chute deployment, and (5) parachute deployment to impact. Diagnostic data will be included for all mission phases. The engineering mission objective include experiments to obtain the following data:

### 2.1.1 Preseparation

None

### 2.1.2 Separation

None

### 2.1.3 Flight Capsule Separation to Entry

Trapped radiation within Mars magnetosphere.

### 2.1.4 Entry to Parachute Deployment

Prime emphasis will be placed on obtaining atmospheric data; redundant instrumentation should be utilized where possible. Data as a function of altitude is to be obtained for the following:

- Atmospheric density

- Atmospheric pressure

- Atmospheric temperature

- Atmospheric composition

- Trapped radiation within the atmosphere

- Ionosphere electron density.

## 2.1.5 Parachute Deployment to Impact

Prime emphasis will be placed on obtaining atmospheric data; redundant instrumentation should be utilized. Data as a function of altitude will be obtained for the first seven of the following: the last three pertain to surface characteristics only:

- Parachute deployment conditions

- Atmospheric pressure

- Atmospheric density

- Atmospheric temperature

- Atmospheric composition

- Trapped radiation in the lower atmosphere

- Wind speed

- Surface hardness and density

- Surface roughness

- Terrain characteristics.

## 2.2 STUDY GROUNDRULES

The following is a list of basic systems groundrules and constraints that were utilized throughout the study.

### 2.2.1 Technology Cutoff Date

September 1966 is considered the technology cutoff date for the 1971 mission.

### 2.2.2 Launch Vehicle

The reference launch vehicle for this program is the Saturn V. The dynamic envelope is to be 3 inches inside the static envelope, shown in Figure 1. The flight capsule weight will not exceed 3000 pounds. The flight capsule envelope (nominal interface and hardpoints) is shown in Figure 1.
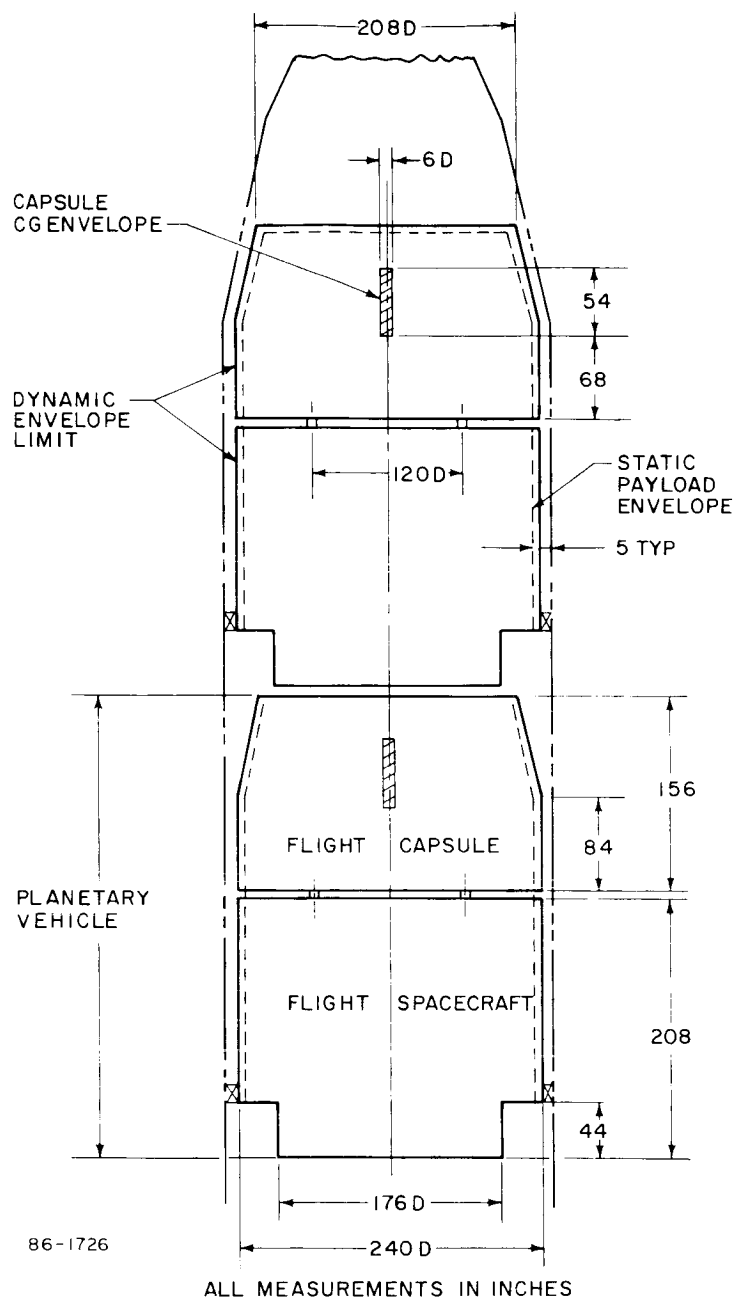
Figure 1 PLANETARY VEHICLE ENVELOPE

86-1726

ALL MEASUREMENTS IN INCHES

-4-

### 2.2.3 Atmospheric Models

The model atmospheres to be used are shown in Table I. An altitude of 800,000 feet will be used for reference entry angle and entry velocity. A surface wind profile will be assumed as shown in Table I and gusts of 200 fps for 10 seconds during parachute descent will be used.

### 2.2.4 Aerodynamic Shapes

The entry shape shall be the 60-degree blunted cone ($C_D$ = 1.63) shown in Figure 2.

### 2.2.5 Descent Subsystem

The main parachute is to be fully deployed subsonically at a minimum altitude of 15,000 feet.

### 2.2.6 Sterilization

The flight capsule system will be capable of sustaining qualification testing of three cycles of heat in a dry atmosphere at 145°C for 36 hours per cycle with sufficient time between cycles to return the flight capsule temperature to ambient and terminal sterilization of one 24-hour cycle of heating at 135°C in dry nitrogen. The probability of Mars contamination will be less than $10^{-4}$ for the flight capsule. The total internal microbial content of the flight capsule immediately prior to terminal heat sterilization will be less than $10^8$ viable organisms. The flight spacecraft is not to be sterile.

### 2.2.7 Deep Space Network

The Deep Space Network (DSN), including Deep Space Instrumentation Facility (DSIF) and the Space Flight Operations Facility (SFOF) will be utilized as defined in the footnote.*

### 2.2.8 Flight Spacecraft Characteristics

The flight spacecraft will serve as a transport vehicle for the flight capsule and provide required services until flight capsule separation. The flight spacecraft will serve as a communication relay station from flight capsule separation throughout the lifetime of the flight capsule. Consideration should be given to direct communication. A reasonable degree of flexibility will be considered during the flight spacecraft-flight capsule interface design. Separation will occur between 3 and 10 days after orbit injection. Consideration will be given to flight spacecraft-flight capsule separation, both with and without a flight spacecraft attitude maneuver prior to separation. The flight capsule will be mounted along the flight spacecraft center line (no cocked mounting).

---

* System Capabilities and Development Schedule of the Deep Space Instrumentation Facility, 1964-68, Technical Memorandum 33-83, Revision 1 (24 April 1964).

## TABLE I

## MARS MODEL ATMOSPHERES

| Property | Symbol | Dimension | VM-3 | VM-4 | VM-7 | VM-8 |
|---|---|---|---|---|---|---|
| Surface pressure | $P_o$ | millibars | 10.0 | 10.0 | 5.0 | 5.0 |
| | | lb/ft$^2$ | 20.9 | 20.9 | 10.4 | 10.4 |
| Surface density | $\rho_o$ | (gm/cm$^3$)10$^5$ | 1.365 | 2.57 | 0.68 | 1.32 |
| | | (slug/ft$^3$)10$^5$ | 2.65 | 4.98 | 1.32 | 2.56 |
| Surface temperature | $T_o$ | °K | 275 | 200 | 275 | 200 |
| | | °R | 495 | 360 | 495 | 360 |
| Stratospheric temperature | $T_s$ | °K | 200 | 100 | 200 | 100 |
| | | °R | 360 | 180 | 360 | 180 |
| Acceleration of gravity at surface | g | cm/sec$^2$ | 375 | 375 | 375 | 375 |
| | | ft/sec$^2$ | 12.3 | 12.3 | 12.3 | 12.3 |
| Composition | | | | | | |
| CO$_2$ (by mass) | | | 28.2 | 70.0 | 28.2 | 100.0 |
| CO$_2$ (by volume) | | | 20.0 | 68.0 | 20.0 | 100.0 |
| N$_2$ (by mass) | | | 71.8 | 0.0 | 71.8 | 0.0 |
| N$_2$ (by volume) | | | 80.0 | 0.0 | 80.0 | 0.0 |
| A (by mass) | | | 0.0 | 30.0 | 0.0 | 0.0 |
| A (by volume) | | | 0.0 | 32.0 | 0.0 | 0.0 |
| Molecular weight | M | mol$^{-1}$ | 31.2 | 42.7 | 31.2 | 44.0 |
| Specific heat of mixture | $C_p$ | cal/gm °C | 0.230 | 0.153 | 0.230 | 0.166 |
| Specific heat ratio | | | 1.38 | 1.43 | 1.38 | 1.37 |
| Adiabatic lapse rate | $\Gamma_o$ | °K/km | -3.88 | -5.85 | -3.88 | -5.39 |
| | | °R/1000 feet | -2.13 | -3.21 | -2.13 | -2.96 |
| Tropopause altitude | $h_T$ | kilometers | 19.3 | 17.1 | 19.3 | 18.6 |
| | | kilofeet | 63.3 | 56.1 | 63.3 | 61.0 |
| Inverse scale height (stratosphere) | $\beta$ | km$^{-1}$ | 0.0705 | 0.193 | 0.0705 | 0.199 |
| | | ft$^{-1}$x 10$^5$ | 2.15 | 5.89 | 2.15 | 6.07 |
| Continuous surface wind speed | $\bar{v}$ | ft/sec | 155.5 | 155.5 | 220.0 | 220.0 |
| Peak surface wind speed | $v_{max}$ | ft/sec | 390.0 | 390.0 | 556.0 | 556.0 |
| Design vertical wind gradient | $\dfrac{d\bar{v}}{dh}$ | (ft/sec)/1000 feet | 2 | 2 | 2 | 2 |

120°

$R_b$

$R_N$
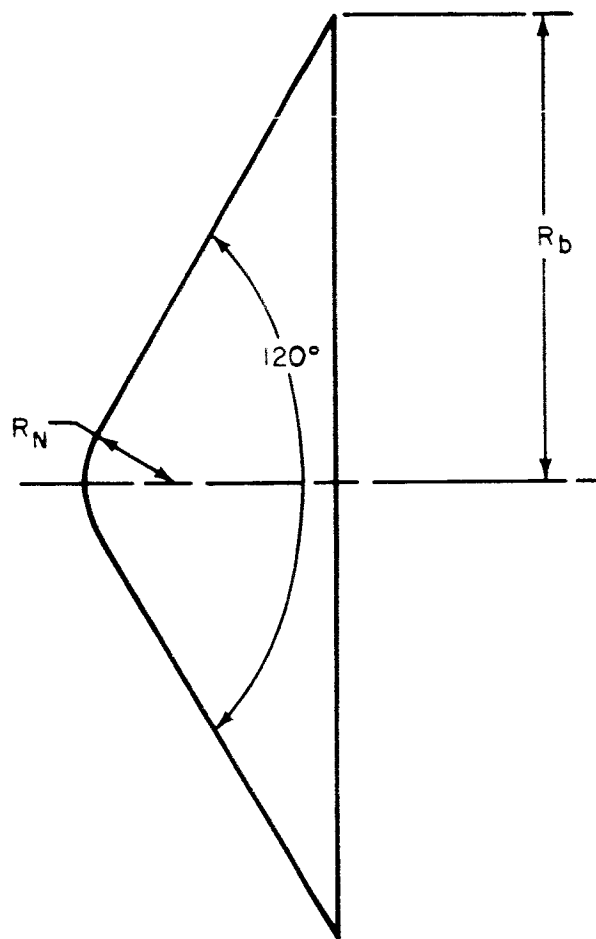
862175

Figure 2 BLUNTED CONE

The flight spacecraft orbits to be considered include periapsis altitudes from 700 to 1500 km and apoapsis altitude between 4000 and 20,000 km.

2.2.9 Structures

A shell concept capable of carrying variable size payload will be used in the design. Weight estimates will be confirmed by a detailed layout of the design. Flight capsule exterior profile will be defined as the structural shape.

# 3.0 SYSTEM DESIGN SUMMARY

This section presents a brief discussion of the flight capsule system designed to enter the Martian atmosphere from orbit and obtain data on selected atmospheric and surface properties prior to impact.

## 3.1 MISSION REQUIREMENTS AND PERFORMANCE

The discovery by Mariner 4 that the Martian atmosphere is more tenuous than previously thought tended to vitiate the earlier results of the Mars Probe/Lander Study, which used as a reference mode the deployment of the proble/lander (flight capsule, FC) on the approach trajectory. The study was then redirected to consider entry of the flight capsule from Mars orbit, to allow shallow entry angles, that are required to provide a reasonable value of $M/C_D A$ for the low surface pressure atmospheres. In addition to the changes in model atmospheres and entry conditions, the original mission requirement of a survivable lander has been eliminated. The primary objective of 1971 mission remains that of obtaining atmospheric data and, therefore, the instrumentation utilized previously is incorporated in this design with the addition of other instruments such as television, penetrometers for surface hardness measurements, and wind measurement instrumentation. The television system uses a three-camera, boresighted system, producing from 11 to 22 pictures (dependent upon the atmosphere encountered) with resolution of from 36 to 0.25 feet. The wind measurements are provided by a three-leg doppler radar. The surface roughness is determined by two radar altimeters, one each for high and low altitude measurement.

The Saturn V launch vehicle will be used for the 1971 opportunity. The Saturn V has the capability of placing two complete planetary vehicles on the desired interplanetary trajectory. The flight spacecraft will serve as a transport vehicle for the flight capsule through Mars orbit insertion up to separation. From this point through ballistic entry and parachute descent in the Martian atmosphere, the flight capsule is capable of a completely independent operation, with the exception of relay communication to the flight spacecraft. The flight capsule is capable of de-orbiting from elliptical orbits ranging for a 700 to 1500-km periapsis altitude and 4000 to 20,000-km apoapsis altitudes, utilizing a fixed $\Delta V$ de-orbit engine of 1400 fps.

For entry shell design purposes, the model atmospheres postulated in Table I were used. The aerodynamic shape used as the entry shell primary structural configuration is a 60-degree blunted cone having a hypersonic $C_D$ of 1.63. The entry shell has a diameter of 15 feet with a weight at entry of 2040 pounds, yielding an $M/C_D A$ at entry of 0.22 slug/ft$^2$. The basic structure is made of aluminum honeycomb with an ablative heat shield of Purple Blend-Mod 5. An active, cold gas attitude control system and a solid propellant hot gas system

are used for attitude control maneuvering and thrust vector control. The communication capability required to relay data from the flight capsule to the flight spacecract is supplied by a redundant 30-watt FSK 18,000 BPS system. A parachute descent system is used to provide the required time to relay the entry and descent data obtained by the flight capsule to the flight spacecraft prior to impact.

The probability of Mars contamination is to be less than $10^{-4}$ for the flight capsule. To obtain this level of sterility, the flight capsule is capable of sustaining a terminal sterilization cycle of 24 hours at 135°C in dry nitrogen. In addition, the microbial content prior to terminal sterilization will be reduced to less than $10^8$ viable organisms by the use of appropriate surface biocides such as ethylene oxide.

## 3.2 REQUIREMENTS IMPOSED ON FLIGHT SPACECRAFT

### 3.2.1 Telecommunications

#### 3.2.1.1 Flight Spacecraft Orbital Position

The severe data rate limitations associated with a direct-to-Earth radio link requires that the flight spacecraft be used as a relay terminal to transfer to Earth data collected by the flight capsule. To obtain reasonably relay link performance, it is desirable to minimize both the communications range between the flight capsule and flight spacecraft and also the look-angle variation of the flight spacecraft antenna during the entry and descent phases of the flight capsule mission. This requires that flight spacecraft be overhead at flight capsule impact, which should be at or near the subperiapsis point. For a more complete treatment see paragraph 4.3.1.2.

#### 3.2.1.2 Flight Spacecraft Relay Antenna

Satisfactory relay link performance can be obtained using the same body-fixed turnstile antenna on the flight spacecraft for all orbits considered. Two turnstile antennas would be required to satisfy the polarization diversity reception requirements discussed in the next paragraph; however, these antannas can be mounted above the same ground plane as shown in Figure 3. The relay antenna axis of major radiation should be directed along a clock angle of 282 degrees and a cone angle of 110 degrees.

#### 3.2.1.3 Flight Spacecraft Relay Receiver

Two polarization-diversity-combining receivers are desirable on the flight spacecraft for satisfactory relay link performance. A block diagram of the overall relay link receiving subsystem is shown in

ARM SUPPORTS -
DIELECTRIC

$\frac{\lambda}{4} \approx 11$ inches

MOUNTING PADS

CONDUCTING ARMS

$\frac{\lambda}{2} \approx 22$ inches

WEIGHT $\approx$ 2.5 pounds

$\frac{3}{4}\lambda \approx 33$ inches

RADIAL WIRE
COUNTERPOISE

ANTENNA FEED
SUPPORTING POST

SUPPORTING
RING
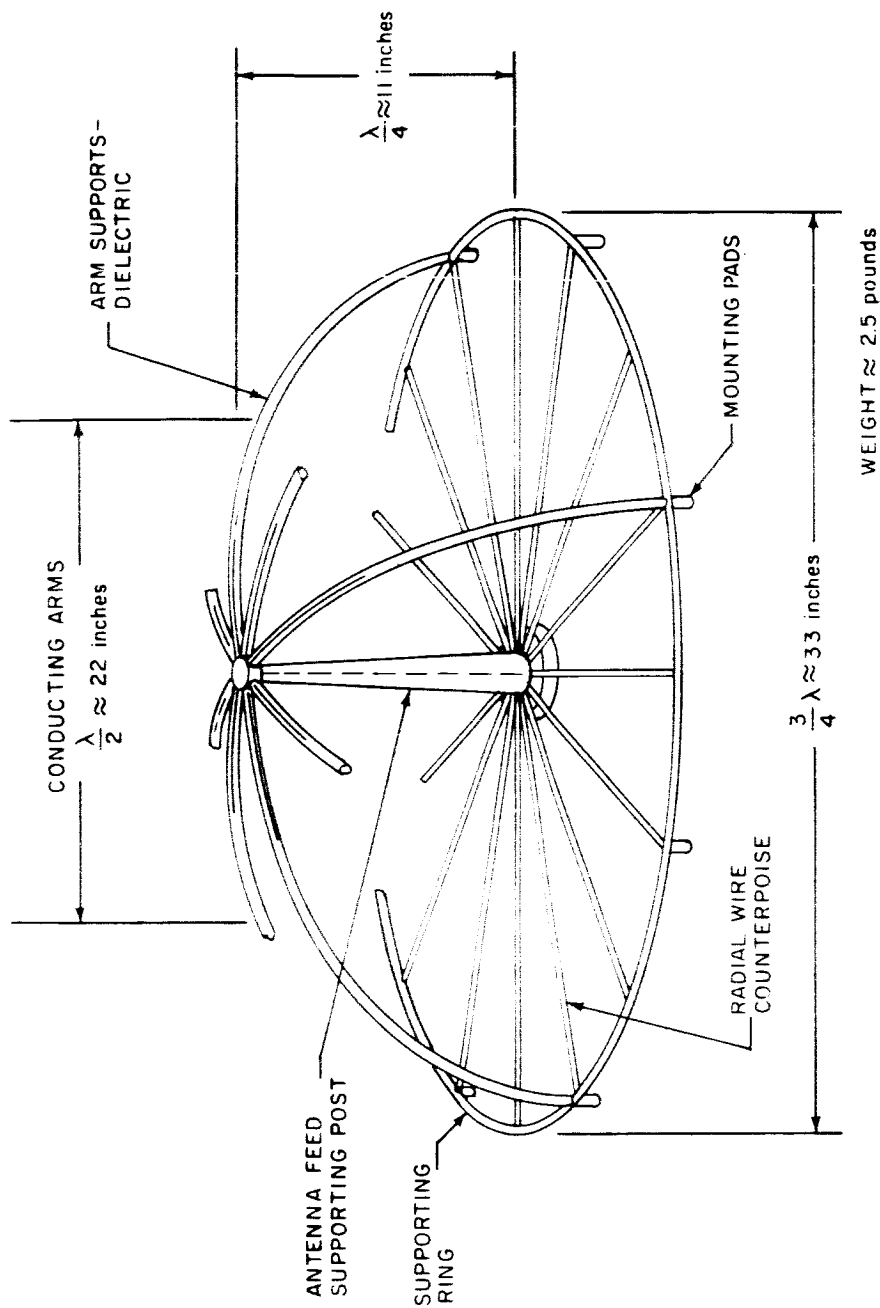
NOTE: TWO ANTENNA SYSTEMS (4 ARMS EACH)
ONE LEFT CIRCULAR AND THE OTHER RIGHT CIRCULAR

Figure 3 FLIGHT SPACECRAFT TURNSTILE ANTENNA DESIGN CONCEPT

862176

-11-

Figure 4. Both polarization senses (left and right circular) require separate detection and amplification prior to being combined in the polarization diversity combiner. This is necessary for each of the redundant relay radio links and results in a total of four receivers, two polarization diversity combiners, and two bit synchronizers are shown.

### 3.2.1.4 Flight Spacecraft Relay Data Handling

An attempt has been made to avoid a flight capsule data mode change after separation, and simultaneously to reduce the large amount of highly redundant data being transmitted at a rate of 18,000 fps real time during cruise to a degree consistent with a data rate than can be allocated by the flight spacecraft to flight capsule data.

Relay data handling consists primarily of two data storage subsystems. The first data storage subsystem uses redundant buffer memories which store 10 seconds (180,000 bits) of relay data every 5 minuts during the time from flight capsule separation until entry. During the 5 minutes between 10-second samples of cruise data, the flight spacecraft would be required to read the stored data out of each of the buffer memories at a rate of 600 bps. This data rate does not appear critical. If the 600 bps rate described here is inappropriate, the 5-minute sampling rate can be altered accordingly.

The second data storage subsystem consists of a two-track tape recorder to be used during the critical entry/descent portion of the flight capsule mission. This recorder must be turned on shortly before the flight capsule enters the Martian atmosphere. Since the time from separation to entry is a function of the orbit geometry, a quantitative command may be required from Earth to the flight spacecraft to update the recorder turn-on time. The recorder must be capable of storing about 1000 seconds of relay data since the maximum entry (800,000 feet) -to-impact time is approximately 800 seconds. This results in storage capacity requirements of approximately $1.8 \times 10^7$ bits per track (one track for each redundant relay link).

### 3.2.2 Flight Capsule Command and Sequencing

The programming and control of the flight capsule subsystems are accomplished primarily by the use of internal flight capsule equipment. The flight capsule CC&S provides stored, time-based discrete and quantitative commands as well as commands resulting from onboard computation to the various flight capsule subsystems during the normal course of the flight capsule mission. However, many of these stored command sequences must be initiated by external command. In addition, the quantitative commands stored in the flight capsule CC&S may require updating as the mission
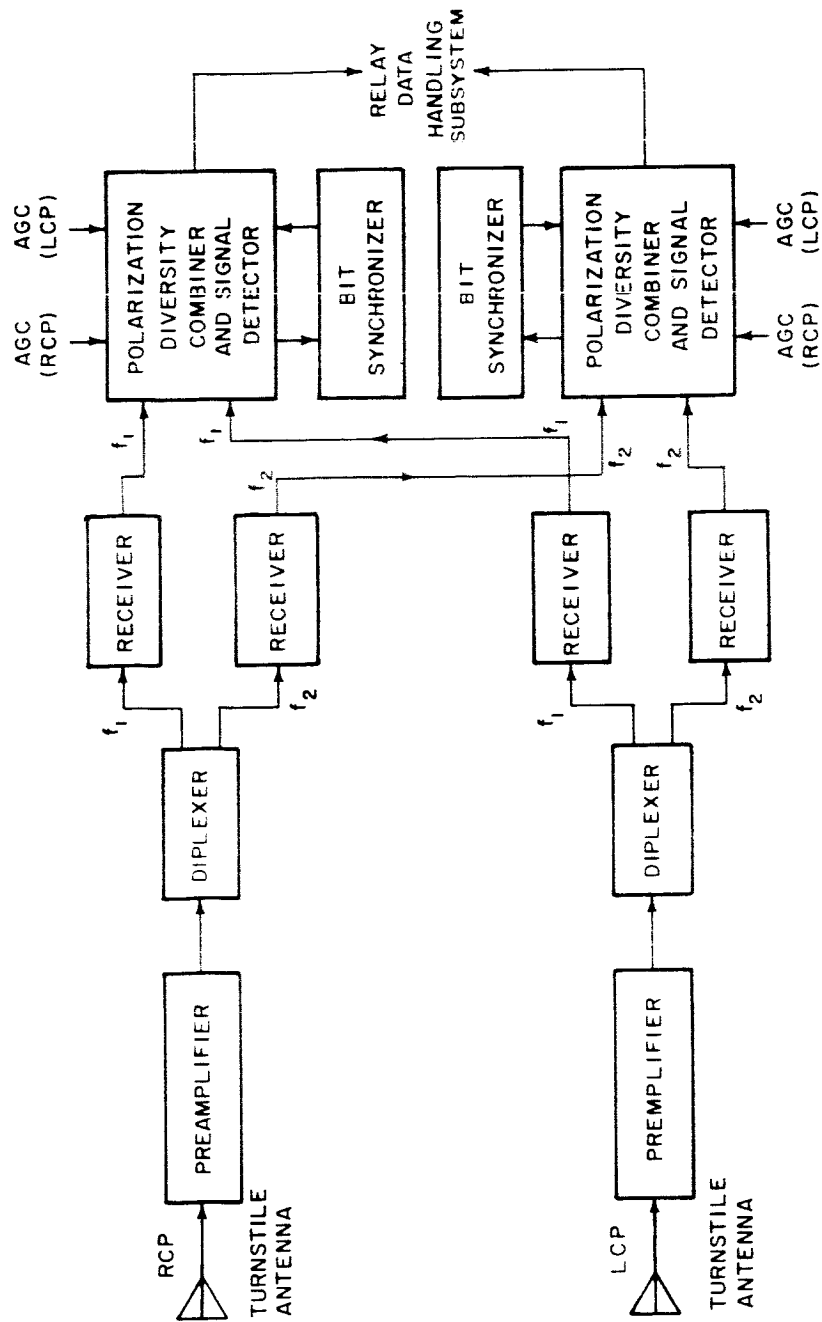
Figure 4 FLIGHT SPACECRAFT RELAY LINK RADIO SUBSYSTEM

862177

-13-

progresses to accommodate off-nominal conditions encountered during the mission. Provision for these requirements has been made in the design of the flight capsule. The flight spacecraft must provide the command link through which updated commands are transmitted to the flight capsule. The flight spacecraft must also provide stored discrete commands within its CC&S for proper checkout and separation control of the flight capsule until separation occurs.

A list of the discrete and quantitative commands which must be provided by the flight spacecraft or relayed through the flight spacecraft command link from the DSN for flight capsule control is shown in Table II.

### 3.2.3 Power

The flight capsule requires power from the flight spacecraft on a continuous basis from launch until flight capsule separation for thermal control, battery charging, and system checkout. The power requirements vary throughout the mission from about 50 watts near Earth to 200 watts in Mars orbit for thermal control (see paragraph 4.9). The maximum power requirement for battery charges is 24 watts occurring during the 3-1/2 hour recharge cycle after each flight capsule inflight checkout. During preseparation checkout, the system is operated on flight capsule power for 1/2 hour and remains operating on flight spacecraft power for 3-1/2 hours during the flight capsule battery recharge cycle. The maximum total power requirement during this phase is 505 watts.

## 3.3 DESIGN DESCRIPTION

The detailed characteristics of each subsystem within the flight capsule are presented in Section 4.0 of this report. This section is devoted to the design integration of these subsystems. The design description of the flight capsule is presented in the form of major inboard profile layouts. Each inboard profile represents a configuration at a defined phase in the operational sequence such as launch, entry, and parachute descent. In addition, significant subsystem characteristics are presented to supplement these profiles.

### 3.3.1 Launch Configuration

The launch configuration of the flight capsule as mounted to the flight space-craft is illustrated in Figure 5. This figure shows the flight spacecraft adapter interface and the general interfaces between the flight capsule sterilization canister and entry vehicle.

The Saturn V launch vehicle ascent shroud constraints are not of particular concern, since the dynamic envelope allowable for the flight capsule is 20 feet. This envelope is illustrated in Figure 6.

-14-

Figure 5  MARS PROBE FLIGHT CAPSULE LAUNCH CONFIGURATION

-16-

Figure 5 presents primarily the design of the sterilization canister and the flight capsule-flight spacecraft adapter.

### 3.3.1  Sterilization Canister

The sterilization canister provides a biological barrier around the flight capsule. The canister must prevent recontamination of the flight capsule by viable microorganisms after the terminal heat sterilization cycle. To satisfy this requirement, each residual leak in the canister must be smaller than the size of a microorganism ($\sim 0.3$ micron). The canister design presented in Figures 5 and 7 is of monocoque construction employing thin (0.030 inch) aluminum sheets welded together to form the complete shell. The canister is composed of two basic sections: a lid which is separated prior to Mars orbit injection, and a base which is attached to, and remains with, the flight spacecraft. The lid section conforms to the entry shell shape, except at the outer edge where it follows a toroidal contour to join with the base section.

A bearing pad is used between the lid and the entry shell, at the suspended capsule mounting ring, to provide a load path for the canister during launch. This plastic foam pad (in the form of a ring) consists of two pieces-- a very rigid outer ring to maintain shape and a soft inner ring to adapt to the entry shell contour and prevent damage to the heat shield.

The basic section is constructed in two pieces: 1) an outer shell, which is welded to the lid, and 2) an inner shell, located inside the flight spacecraft-flight capsule adapter. These two sections are welded to a ring at the adapter intersection. To facilitate flight capsule assembly, the outer shell section is divided a short distance from the adapter intersection. This section is welded together after final assembly of the adapter to the entry vehicle (ref. paragraph 3.6).

The canister lid separation mechanism is in a short channel located between the sterilization canister base and lid sections at the outer rim as illustrated in Figure 7 detail B. It consists of a plastic elastomer tube encasing a mild detonating fuse (MDF). The tube is clamped between the two angle rings forming a trapezoidal section around the tube. When the explosive in the tube is detonated, the tube expands, causing the thin canister wall to shear. Further expansion of the tube provides the required separation impulse to the canister lid. All gaseous products of the explosion are captivated within the tube, preventing possible damage to the flight spacecraft and possible recontamination of the flight capsule. This separation concept poses several critical development problems. At the points where the detonator is connected to the elastomer tube, in possibly two places, sealing the junction could be a problem. Long-time space vacuum storage and operation at sub-zero temperatures are also critical for this design.

Figure 7 MARS PROBE FLIGHT CAPSULE ENTRY CONFIGURATION

These potential development problems and the desire for design and fabrication simplicity led to an alternate separation design presented on Figure 7, detail B. This design utilizes a flexible, linear shaped charge (FLSC) to cut the canister wall; the resulting explosive pressure buildup provides the separation impulse. A plastic foam fragmentation absorber is employed to circumvent the safety hazards of FLSC. The plastic foam absorbs all fragments and the shape of the foam container funnels most of the gaseous debris away from the flight spacecraft. This type of separation device (FLSC) is widely used in aerospace applications. Final development screening of each technique under the proper environmental conditions will be required to establish the recommended approach.

An access door is provided on the base section of the sterilization canister to allow assembly of and access to the $\Delta V$ propulsion rocket during the latter stages of final assembly and checkout. The access door is bolted in place at the center of the canister base (Figure 5). A channel ring is welded to the main inner shell to provide a mating surface for the access door and to eliminate the need for bolting through the canister as illustrated in Figure 7, detail D.

This door is the only access panel through the sterilization canister; however, others may be added as fabrication and maintenance procedures are developed to allow assembly or removal of other subsystems. One such subsystem is the thrust vector control hot-gas reaction system located on the base ring of the entry shell. The number of access panels should be minimized to reduce potential leakage.

A pressurization control system is also incorporated on the sterilization canister to maintain a slight positive pressure differential (approximately 1 psi) across the canister from final assembly to Earth orbit injection. This pressure differential provides an indication of the maintenance of the sterile barrier by measurement of the leakage rate.

While in Earth-parking orbit, prior to transfer orbit injection, the canister is completely vented. Fill valves, relief valves, and depressurization valves, along with associated microfilters, are required in the canister for pressurization control. The main source of gas resupply during the period prior to launch is an external tank which is terminally sterilized with the flight capsule. This tank is removed prior to mating with the flight spacecraft.

One of the potential sources of flight capsule recontamination is the possibility of micrometeoroid penetration of the sterilization canister. A study was made to determine the weight required for micrometeoroid protection based on the bumper concept and a pessimistic estimate of the meteoroid flux taken from measured data. Results of this analysis

in terms of bumper weight versus probability of puncture is presented in Figure 6 along with a sketch of the micrometeoroid bumper concept. For a probability of penetration of 1.0, the canister would weigh 10,000 pounds. The canister for the present design, not utilizing a micrometeoroid bumper, weighs approximately 400 pounds. Before the sterilization canister can logically be designed for micrometeoroid protection, with such a weight penalty, the hazard of recontamination of the flight capsule by micrometeoroid puncture must be thoroughly examined.

### 3.3.3.2 Flight Capsule - Flight Spacecraft Adapter

The primary flight capsule to flight spacecraft load path is through an adapter that interfaces with the flight spacecraft at a 120-inch diameter ring. The adapter also supports the electrical cabling network and umbilical connection to the flight spacecraft and provides the mounting surface for the entry vehicle separation mechanism.

The adapter consists of two sections: an aft section, between the flight spacecraft and the sterilization canister base, and a forward section, inside the canister. Each section is constructed of an aluminum shell stiffened by 16 longitudinal hat section members and end rings. The forward section has an added ring midway along the shell to provide the required general stability. Both sections of the adapter are riveted to the sterilization canister base. Design details are presented in Figures 5 and 7, detail C.

The end ring on the forward section provides the entry vehicle mounting surface. The adapter is retained to the entry vehicle by a continuous V clamp. Four explosive bolts equally spaced around the clamp provide the separation release mechanism. Any one of the four bolts can provide the separation release. Eight coil compression springs equally spaced around the separation ring and two additional compression springs located at the electrical umbilical connectors give the required impulse for separation of the entry vehicle at 1.5 fps. The entire separation mechanism, including the springs, is retained by the adapter.

Electrical disconnect from the flight spacecraft occurs at, and is provided by, mechanical separation of the entry vehicle. Two identical 55-pin umbilical connectors are used for electrical connection between the entry vehicle and the flight spacecraft. The connectors are located diametrically opposite to each other to minimize tipoff rates induced by separation. The two electrical cabling networks from the entry vehicle run along the adapter, through the sterilization canister, to the flight spacecraft. At the sterilization canister junction, hand-disconnect umbilical plugs terminate the cables, both inside and outside

-21-
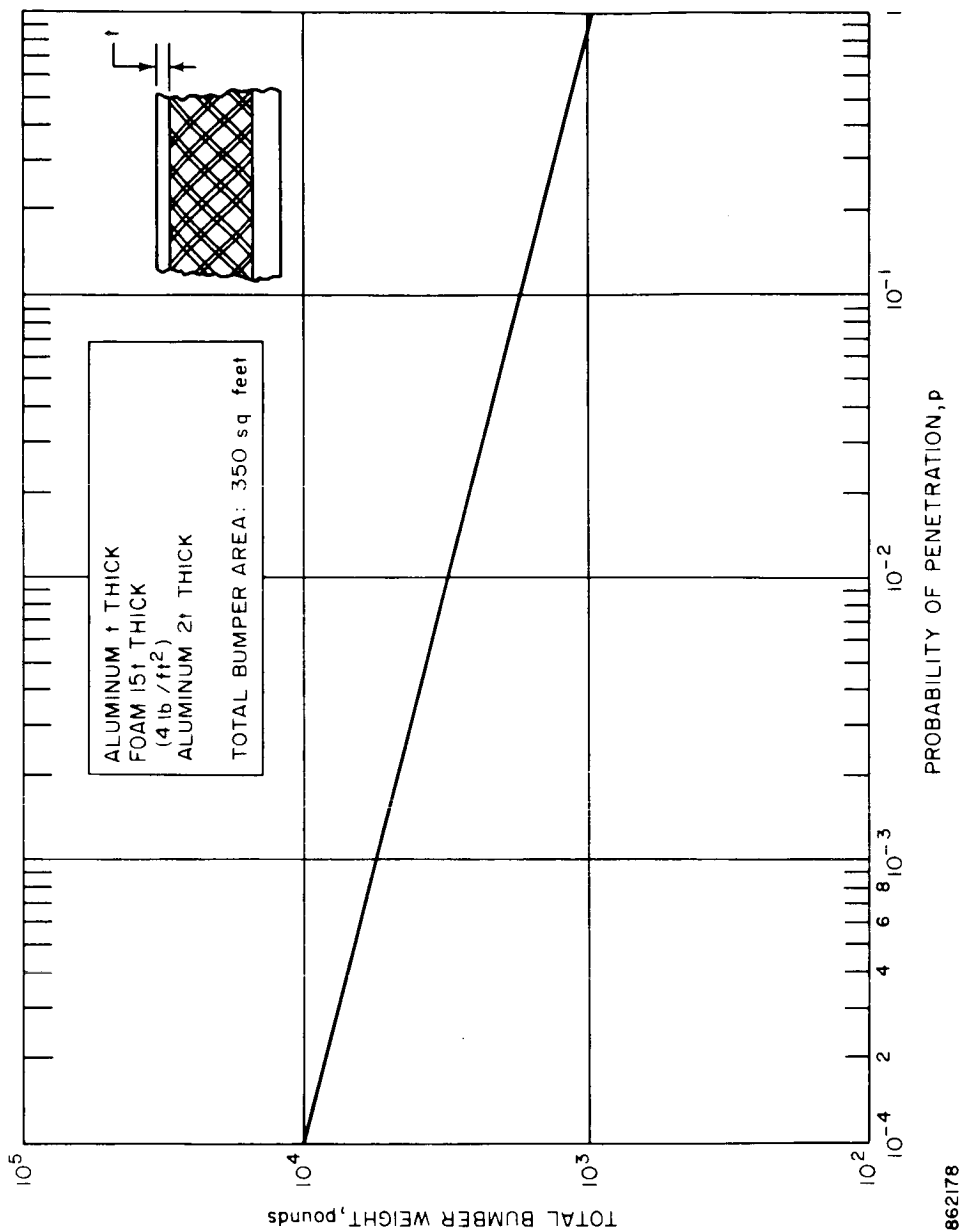
Figure 8  WEIGHT REQUIREMENT FOR MICROMETEOROID PROTECTION

862178

-22-

the canister, and are connected to a welded-in-place receptacle to reduce sealing problems. Similarly, at the flight spacecraft interface, hand-disconnect umbilical plugs are used. The general arrangement of the umbilical connectors and cabling is shown in Figure 7, detail C. This figure also shows the electrical safing and arming devices for sterilization canister lid separation and pressurization control.

### 3.3.2 Entry Configuration

The entry vehicle configuration is presented in Figure 9. A 60-degree blunted cone, 180 inches in diameter with a small nose cap ($R_N/R_B = 0.25$), provides the aerodynamic contour. Except for a small afterbody, also a 60-degree truncated cone which encloses most of the avionics, the entry vehicle aft side is essentially hollow.

Two major systems make up the entry vehicle: the entry shall--that portion forming the aerodynamic contour and separated at parachute deployment; and the suspended capsule--that portion enclosing the entry equipment and constituting the terminal descent package on the parachute. The division between these two systems is defined by the separation plane of the entry shell; i.e., all subsystems incorporated on the entry shell and separated with it are part of the entry shell, and all subsystems on the terminal descent package, including the parachute, are part of the suspended capsule. The separation mechanism between these two systems is exactly the same as that employed for entry vehicle separation from the flight spacecraft. The complete separation mechanism is retained on the entry shell; hence, separation is initiated on the entry shell side.

The design intergration of pertinent subsystems within the entry shell and the suspended capsule is described in detail in the following paragraphs.

### 3.3.2.1 Entry Shell

The design of the entry shell is presented in Figures 10 through 12. The entry shell is composed basically of a primary structure, to maintain the aerodynamic contour and to redistribute the aerodynamic loads to the internal structural network, and a heat shield, to protect the primary structure from aerodynamic heating. Several other subsystems are located on the entry shell to perform functional operations during the pre-entry and post-entry flight. Such subsystems as the ACS and TVC reaction control nozzles and tanks, the fixed flaps, to provide rearward entry instability, and the nose cap separation mechanism are located on the entry shell. Not shown on the design layouts are numerous diagnostic instruments (e.g., temperature and pressure sensors) at various locations on the shell for monitoring performance during the flight operations.

Figure 9 MARS PROBE FLIGHT CAPSULE ENTRY CONFIGURATION

Figure 10 MARS PROBE FLIGHT CAPSULE ENTRY SHELL ASSEMBLY

Figure 11 MARS PROBE FLIGHT CAPSULE ENTRY SHELL STRUCTURE
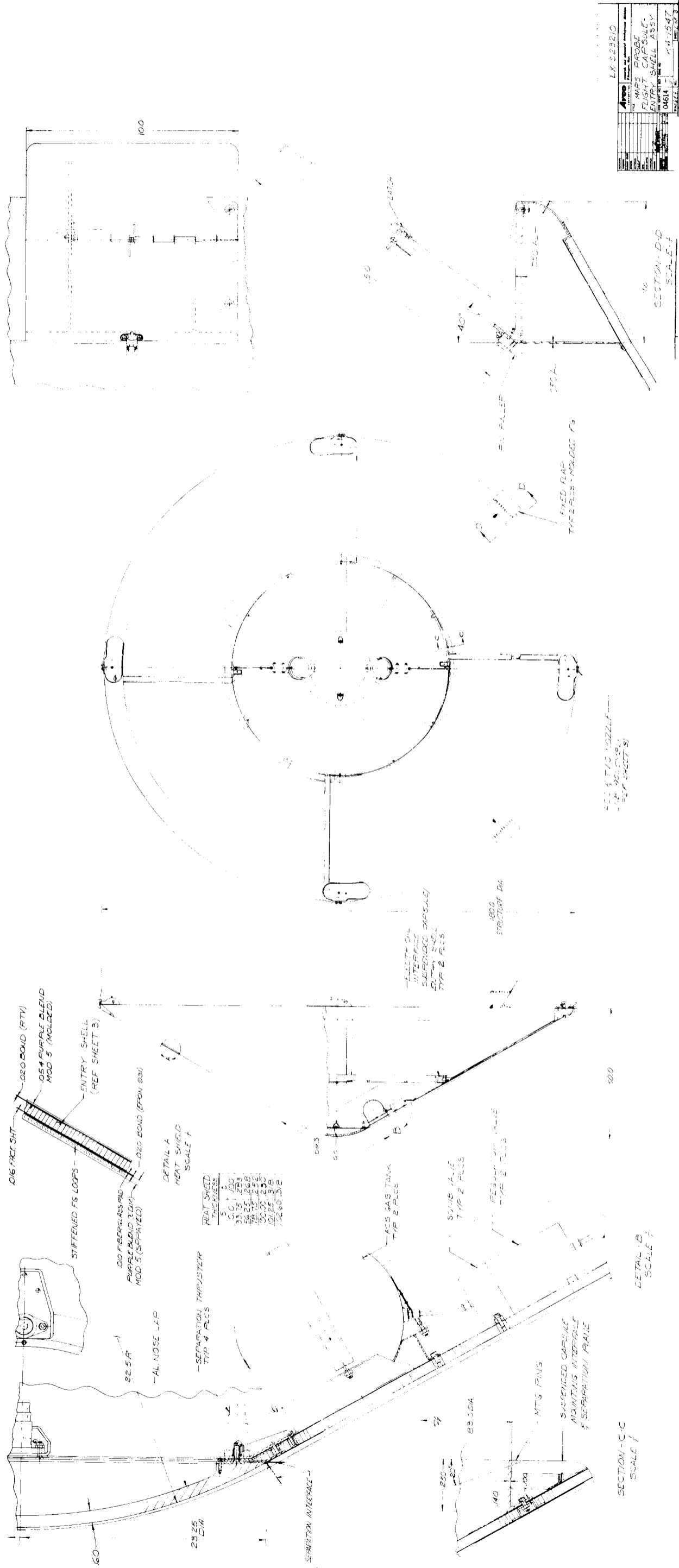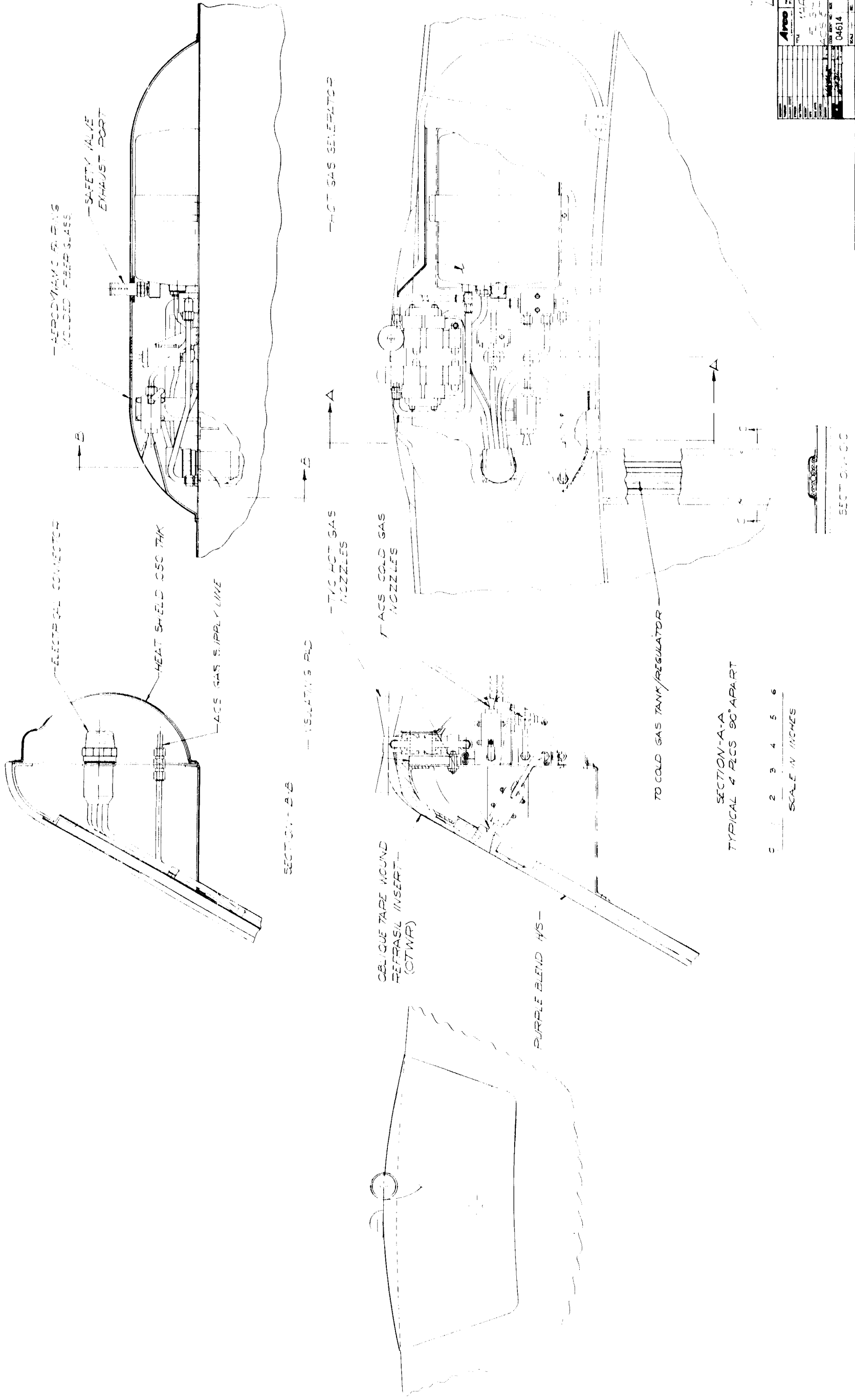
Figure 12 MARS PROBE FLIGHT CAPSULE ENTRY SHELL TVC ON ACS ASSEMBLY

-27-

2

24-1

The entry shell primary structure is of completely bonded sandwich construction, consisting of aluminum face sheets and honeycomb core. The shell is fabricated in 12 radial core sections made from standard aluminum sheet stock (approximately 48 inches) and spliced together with aluminum splice plates to form the conical configuration. A continuous closeout ring is bonded to each end of the conical shell. At the outer edge, the closeout ring provides the mounting surface to which the base ring is riveted after assembly and bonding of the conical shell. At the inner edge, the close-out ring forms the mounting surface for the nose cap and separation mechanism. An intermediate ring is bonded within the core to provide shell continuity and a bolting connection for the suspended capsule mounting ring (Figure 10, section CC). Doublers are bonded to the outside surface of both face sheets in areas of high stress concentration such as the mounting ring and the base ring. The complete shell is laid up and bonded in one process to simplify fabrication. Details of the bonded construction are illustrated in Figure 11.

The base ring is composed of two flat sections and a slightly curved section, which form the aerodynamic contour at the outer edge of the shell. These sections are riveted together to form a continuous ring, which is riveted to the bonded shell closeout ring. Mounted on the base ring at four places are the reaction control nozzles of both the TVC and ACS subsystems. These subsystems are grouped in four individual subassemblies as illustrated in Figure 12. Each subassembly consists of two TVC hot gas pitch (or yaw) nozzles, a gas generator, and three ACS cold gas nozzles (two pitch or two yaw and roll). Both hot gas nozzles (pointing forward and aft) extend outside of the maximum shell diameter to thermally isolate them from the primary structure, since they operate at 2000°F. To eliminate long lengths of hot gas tubing, each hot gas nozzle pack has its own gas generator located within the subassembly. This arrangement provides added redundancy; if one gas generator fails, the diametrically opposite pair of nozzles is unaffected. The system still has torque-producing capability to complete the mission, although the torque is not provided as a couple in this case. In case the hot gas valves fail in the closed position after generator ignition, a blowoff relief valve is provided.

The forward ACS nozzle of each set is directed through the entry shell and normal to it. Since this system operates with cold gas, thermal insulation is unnecessary. However, the hole in the heat shield, coupled with the presence of the hot gas nozzle at the maximum diameter, causes considerable aerodynamic aggravation which essentially triples the aerodynamic heating in this area. To protect the structure, a molded piece of a more efficient ablator (OTWR -- oblique tape-wound Refrasil) is used locally in the nozzle areas. The other ACS cold gas

-28-

nozzles (pitch and roll) are mounted normal to respective vehicle axes on the base ring as shown in Figure 12. The cold gas tanks, regulators, and valves are located near the center of the entry shell under the suspended capsule. Two tanks are used to feed diametrically opposite sets of nozzle packs. A redundant system is again provided; if one tank-nozzle set fails, the other set has enough stored gas to overcome the failure and complete the mission. Roll control during $\Delta V$ thrusting is provided by the cold gas subsystem. This same subsystem is also utilized for roll rate control throughout entry to reduce the spin-rate buildup to ease parachute deployment.

Each of the four reaction control subassemblies is built as a unit and mounted to a segment of the base ring. The subassembly is bolted in place on the base ring during final assembly of the entry shell. This assembly sequence was developed to facilitate final assembly and checkout of the system. The entire reaction control subassembly is covered by an aerodynamic fairing for thermal protection and to reduce the aerodynamic assymetries which could induce spin during entry.

Also located on the base ring are two fixed flaps to provide aerodynamic righting moment for the entry vehicle in case of rearward entry. Each flap is hinged at the center and folded back on itself to allow clearance between the entry vehicle and the sterilization canister while the entry vehicle is still attached to the flight spacecraft (Figure 5). After entry vehicle separation, a pin-puller releases the spring loaded flap allowing it to rotate to its nominal fixed position, where it is automatically locked in place at a 40-degree angle with the longitudinal axis of the entry vehicle. This places the flap in the maximum aerodynamic flow during rearward entry and removes it from the flow during forward entry. Each flap is 1 square foot in area and is constructed of a molded fiberglass laminate.

The nose cap of the entry shell is a 0.6 inch solid aluminum spherical cap, held in place to the conical shell by four thruster bolts (Figure 10). These bolts provide the required impulse to separate the nose cap at about 50 ft/sec in case the entry shell fails to separate at parachute deployment. This allows some of the television pictures to be taken.

To maintain the primary structure within temperature limits during entry, a modified Purple-Blend ablative heat shield is employed over the entire structure, both the primary side (forward) and the secondary side (aft). The heat-shield thickness varies from 0.10 to 0.32 inch on the primary side and is 0.005 inch thick over the entire secondary side, as shown in Figure 10, detail A. Fabrication of the primary heat shield consists of bonding a fiberglass pad with stiffened loops to

the structure, and then spraying Purple-Blend over the entire primary surface. The primary heat shield is vacuum-bag cured at approximately 300°F and machined to the proper contour. A different technique is used on the secondary side because of the irregular contour. Pre-cured molded tiles of the same material are bonded directly to the structure using a flexible bond. This bond is again vacuum-bag cured at approximately 300°F to stabilize the material and bond prior to the terminal heat sterilization cycle. The reaction control aerodynamic fairing covers utilize the same heat sheild and bonding technique.

3.3.3.2 Suspended Capsule

Design details of the suspended capsule are presented in Figures 13, 14, and 15. Configurational arrangement of the suspended capsule is dictated primarily by the required placement of some subsystems and minimization of the structural load paths. Such subsystems as the ΔV propulsion and the engineering instrumentation, particularly the television subsystem, radar antennas, and penetrometers are instrumental in determining the configuration. The ΔV propulsion must be mounted within the afterbody contour to minimize interference with the VHF relay antenna patterns. This necessitates a large cylindrical section in the middle of the suspended capsule to provide the required structural load path and mounting surface (Figure 13) at the aft end of the afterbody. The television subsystem must be on the suspended capsule center line to reduce picture distortion and to provide access through the nose cap. The center of the suspended capsule is thus completely occupied requiring that all other subsystems be located around the television and ΔV propulsion. Since the penetrometers are deployed after the entry shell is jettisoned, they were located in radial bays equally spaced around the center of the suspended capsule (Figure 13). This arrangement of the penetrometers along with the location of the radar antennas, defined the maximum diameter (85 inches) and basic structural arrangement of the suspended capsule.

The afterbody contour (60-degree truncated cone) was defined by the required volume necessary for the remaining instrumentation and functional subsystems, and by aerodynamic considerations to reduce the shadowing effects of the afterbody on the aft portion of the entry shell at high angles of attack.

The resulting basic structural arrangement of the suspended capsule consists of an afterbody shell composed of eight covers and supported by eight longerons, a continuous central cylindrical shell also containing eight longerons, an aft ring which connects these shells together and provides the mounting surface for the ΔV propulsion, a large outer ring (Figure 13, detail K), at the end of the afterbody shell, to provide a mounting surface for the entry shell and the flight capsule - flight spacecraft adapter, and finally eight radial beams, which form the

-30-
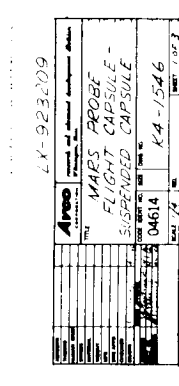
Figure 13  MARS PROBE FLIGHT CAPSULE SUSPENDED CAPSULE

Figure 14  MARS PROBE FLIGHT CAPSULE SUSPENDED CAPSULE

Figure 15  MARS PROBE FLIGHT CAPSULE SUSPENDED CAPSULE

instrumentation bays and join the outer ring to the central cylindrical section. The instrumentation mounting plates form structural webs in each of the eight bays created by the radial beams. These webs provide continuity and torsional stiffness to the structure. An additional conical shell is located in the center of the suspended capsule for mounting the television and inertial reference subsystems. The complete structure is riveted together except for the instrumentation mounting plates which are bolted in place to ease assembly and maintenance.

Three antenna subsystems are employed on the suspended capsule; 1) the VHF relay antennas, 2) the radar-altimeter antennas, and 3) the doppler-radar antennas. The two VHF (272 mc) antennas are located diametrically opposite each other on the afterbody, flush with the inner ring and tilted 15 degrees toward each other.* This location of the relay antennas also requires that the W propulsion nozzle be constructed of dielectric materials. A shorter W propulsion nozzle would create excessive heating on the afterbody and entry shell during thrusting and hence, was not utilized.

Each antenna is covered with a dielectric heat shield (Teflon) for protection against W propulsion plume heating and entry aerodynamic wake heating (Figure 14, section A-A).

Two independent radar altimeters are used on the entry vehicle for high and low altitude measurements. The high altitude altimeter utilizes the entry shell as an antenna by exciting the base ring at 18 mc. After the entry shell is jettisoned, another altimeter (at 324 mc) is employed on the suspended capsule for low-altitude measurements. The low-altitude altimeter antenna is located in one of the instrumentation bays (Figure 14, section C-C). The same antenna is used at a slightly higher frequency (400 mc) as a receiving antenna for the penetrometers.

Three antennas are employed to produce the three narrow beam legs for the doppler radar measurement. Two of these antennas are located within one enclosure and are fed at two slightly different frequencies (approximately 13 gc). The other antenna is located diametrically opposite the other enclosure (Figure 14, section A-A). Each antenna is tilted 20 degrees from suspended capsule longitudinal axis in orthogonal planes to produce the three legs of the doppler.

The remaining instrumentation, except for the numerous diagnostic instruments, is located in a module aft of the low-altitude radar altimeter antenna (Figure 14, section C-C). This module contains

-34-

*The tilting requirement was the result of antenna pattern measurement which indicated improved antenna gain. Vol. V, Book 3, paragraph 5.5.)

those instruments that require atmospheric sampling through gas ports such as the gas chromatograph, mass spectrometer, and acoustic densitometer. The programming and sequencing subsystems are also located in this module.

The television subsystem is entirely contained within one module. The three boresighted cameras are located in the forward portion of the module and are mounted on a two-degree-of-freedom gimbal platform slaved to the inertial reference platform to compensate for suspended capsule angular motions during terminal descent on the parachute. Electrical stops limit the cameras angular movements to ±45 degrees. A flexible boot is attached to the camera case and to the outside shell of the module to protect the gimbal system from debris during entry shell and nose-cap release.

Electronics and data processing for the television cameras are located in the aft portion of the module. The electrical cable from the camera to the electronics is wrapped around the gimbal system in both planes in such a manner as to reduce interference with the gimbal performance and to minimize bending of the cable.

The telecommunication, power, and data-handling subsystems are contained in modules located between the doppler radar antennas and the VHF relay antennas (Figure 14, section A-A). Each module contains identical equipment, feeding the adjacent VHF relay antenna to provide complete redundancy in the telecommunications link.

Because of the possible interference between the transmitting equipment and the data-storage equipment, the module is divided into individual sealed compartments. The power-supply equipment is also contained in an individual compartment which is thermally isolated from the rest of the module for thermal control. Heaters are provided in this compartment to maintain the batteries at -40°F during the flight capsule cruise phase. This modular construction is shown in detail on Figure 15.

After entry shell release and at about 3500-foot altitude, the penetrometers are deployed. Each penetrometer is held to the suspended capsule by three straps joined at the center of the penetrometer and attached to the instrumentation bay by explosive pin pullers on two straps and an adjustable bolt on the other. A coil compression spring is housed in the mounting cavity. At deployment, the pin pullers are activated (either of the two will release the penetrometer) and the penetrometer is pushed away from the suspended capsule at a nominal 5 ft/sec.

The parachute pack (including the pilot chute) is mounted diametrically opposite the instrumentation module as illustrated in Figure 14, section C-C . The pack is in a sealed contained maintained at approximately $10^{-4}$ psi throughout the flight. At parachute deployment, the pilot chute is mortared out of the container. The pilot chute is attached to the main chute container cover, pulling it off and extracting the main-chute closure bag. The main chute is pulled out of the container, along with its shroud lines and harness. A four-strap harness is connected to four points at the maximum diameter of the suspended capsule (Figure 14, section J-J). The apex of the harness is attached to a swivel joint which is connected by a single riser line to the main chute canopy suspension system. All parachute loads are transmitted to the primary structural load path of the suspended capsule at four hard points.

## 3.4 ASSEMBLY SEQUENCE

The complete flight capsule assembly and checkout sequence may not occur at one facility or even in one geographical location; however, the basic approach will remain the same. The major steps in such an assembly sequence are discussed as they were developed during the preliminary flight capsule design. The overall assembly sequence is shown in Figure 16 with a brief description of each step in the sequence. The assembly sequence begins with the suspended capsule skeletal structure and proceeds through installation of the subsystems into primary subassemblies which are mated in sequence to achieve a completely assembled flight capsule. The primary subassemblies are; 1) suspended capsule, 2) entry shell, 3) flight capsule - flight spacecraft adapter, and 4) sterilization canister base. After mating of these subassemblies, the sterilization canister lid and the $\Delta V$ propulsion are installed.

Special handling fixtures are required in the assembly sequence, due to the rather large size and light-weight structural members of the flight capsule. Simplified versions of these fixtures are illustrated throughout the discussion to illustrate the procedures used during the assembly.

### 3.4.1 Suspended Capsule Subassembly

The forward ring of the suspended capsule provides the mounting surface and attachement for both the entry shell and the flight spacecraft adapter. These interfaces are exactly the same size and configuration, and utilize the same type of V-clamp separation mechanism.

To handle the suspended capsule, a mating ring which conforms to this interface must be supplied. A typical handling ring fixture, is illustrated in Figure 17. Since the same interface exists at the entry shell and flight spacecraft adapter, these subassemblies, as well as the entire entry vehicle, can also be handled by this fixture. The interfacing ring on the fixture also utilizes V-clamps to attach the suspended capsule.

-36-

SUSPENDED CAPSULE STRUCTURE

AFTERBODY

ENTRY SHELL

ENTRY VEHICLE

FC - FS ADAPTER

SEPARATION RING

STERILIZATION CANISTER BASE

STERILIZATION CANISTER LID

FLIGHT CAPSULE

ΔV PROPULSION

ACCESS DOOR

SUBASSEMBLY A

1. INSTALL ELECTRICAL CABLES &
   MAKE CONNECTIONS AS FOLLOW-
   ING SUBSYSTEMS ARE INSTALLED
   a. SENSOR MODE
   b. MARTIAN REFERENCE PLATFORM
   c. ENTRY SYSTEM COMPUTER
   d. ELECTRICAL CONVERTER
   e. SUPPLY & DATA HANDLING
   f. RADAR ANTENNAS WITH VHF ANTENNA
   g. PENETROMETER ASSEMBLY
   h. PARACHUTE PACK
   i. AFTERBODY COVERS & NACELLES/EDGE
   ANTENNA & OVER ENTRY SHELL ELECTRICAL
   UMBILICALS

SUBASSEMBLY B

1. INSTALL ELECTRICAL CABLES
   a. COLD GAS TUBING & ASSEMBLY
   COVERS, MAKE CONNECTIONS TO
   DIAGNOSTIC SUBSYSTEM
   FOLLOWING SUBSYSTEMS AS
   INSTALLED
   b. PCS SUBASSEMBLY & ACCESS
   HOT GAS GENERATORS
   c. NOSE CAP SUBASSEMBLY
   d. DIAGNOSTIC INSTRUMENTATION
   e. FLAPS (FOLDED)
2. ATTACH ENTRY SHELL TO SUS-
   PENDED CAPSULE USING V
   CLAMP RINGS
3. CONNECT & ALIGN ELECTRICAL
   UMBILICALS

SUBASSEMBLY C

1. INSTALL ELECTRICAL UMBI-
   CAL & MAKE CONNECTIONS
   FOLLOWING SUBSYSTEMS AS
   INSTALLED
   a. FC-FS PRESSURIZA-
   TION VALVES & PRESSURE
   TRANSDUCERS
   b. SEA DEVICES
   c. DIAGNOSTIC INSTRUMENTA-
   TION
2. ATTACH ADAPTER TO SUS-
   PENDED CAPSULE WITH V
   CLAMP RING & REMOVE SEP-
   ARATION SPRING ASSY PINS
3. CONNECT & ALIGN ELECTRICAL
   UMBILICAL

SUBASSEMBLY D

1. INSTALL ELECTRICAL CABLES
2. SEAM WELD SEPARATION RING
   TO CANISTER BASE, INSTALL
   SEALS ON CANISTER BASE SM
3. INSTALL SEA DEVICE & MAKE
   ELECTRICAL
   CONNECTIONS
4. INSTALL PCS HOT GAS GENER-
   ATORS & PYRO/ANC RINGS
5. SEAM WELD CANISTER BASE TO
   FC-FS ADAPTER

SUBASSEMBLY E

1. BOND BEARING PADS TO
   CANISTER LID
2. SEAM WELD CANISTER TO
   BASE

SUBASSEMBLY F

1. INSTALL & ALIGN ΔV PROPULSION
   TO SUSPENDED CAPSULE
2. MAKE ELECTRICAL CONNECTIONS
   TO ΔV OPERATORS
3. INSTALL ACCESS DOOR
   WITH SEAL

Figure 16 MARS PROBE FLIGHT CAPSULE ASSEMBLY SEQUENCE

3-47-1

HOIST HARNESS

SUSPENDED CAPSULE

PIVOT RING

PIVOT POINT

V CLAMP

86 2179

Figure 17 SUSPENDED CAPSULE AND ENTRY VEHICLE HANDLING FIXTURE

Using an overhead hoist the suspended capsule is carried to the major assembly fixture for assembly of the other subsystems. This fixture is illustrated in Figure 18. Two pivot points on the suspended capsule handling fixture are attached to the major assembly fixture which allows movement of the suspended capsule to the most desirable orientation for assembly.

With the major assembly fixture in the horizontal position, the subsystems are installed to the suspended capsule in the order listed on Figure 16 subassembly A. The afterbody covers, located over the entry shell-to-suspended capsule umbilical connection are not assembled at this time to allow access during entry shell mating. Since these umbilicals are not explosively released, proper adjustment after mating must be accomplished to ensure that binding at separation does not occur.

### 3.4.2 Entry Shell Subassembly

Due to the fragile character of the entry shell heat shield, the storage containers for the entry shell after fabrication must be lined with a soft foam material fitted to the heat-shield contour to prevent damage during handling. Similarly, extreme care must be exercised in handling the entry shell during installation of the subsystems. The handling fixture used to assemble the suspended capsule (Figure 17) is also used for entry shell assembly. The entry shell is removed from the storage container and attached to the major assembly fixture (Figure 18), in the same way the suspended capsule was attached. The entry shell is held in a horizontal position and the electrical cabling installed along with the insulating covers. In the same position, the entry shell subsystems are installed along with the insulating covers. Also in the same position, the entry-shell subsystems are installed, according to the subassembly B, Figure 16.

After the entry shell subsystems are installed, the entry shell is placed back into the storage container and the handling fixture removed. The suspended capsule is then picked up and placed in the entry shell. The V-clamp separation mechanism is installed. The entry vehicle is picked up and attached to major assembly fixture at the entry vehicle - adapter separation joint to assemble and align the entry shell electrical umbilical to ensure proper fit. At this time a dummy $\Delta V$ propulsion is installed to provide proper entry vehicle balance and propulsion alignment.

### 3.4.3 Flight Capsule - Flight Spacecraft Adapter

The adapter structure is previously assembled including portion of the sterilization canister base, (the inner shell, excluding the access door, and a short portion of the outer shell). The handling fixture utilized on the suspended capsule and entry vehicle is again used to pick up the adapter and attach it to the major assembly fixture. In the assembly fixture, the

FLIGHT CAPSULE

ACCESS PLATFORM
(ADJUSTABLE)

ASSEMBLY FIXTURE BASE
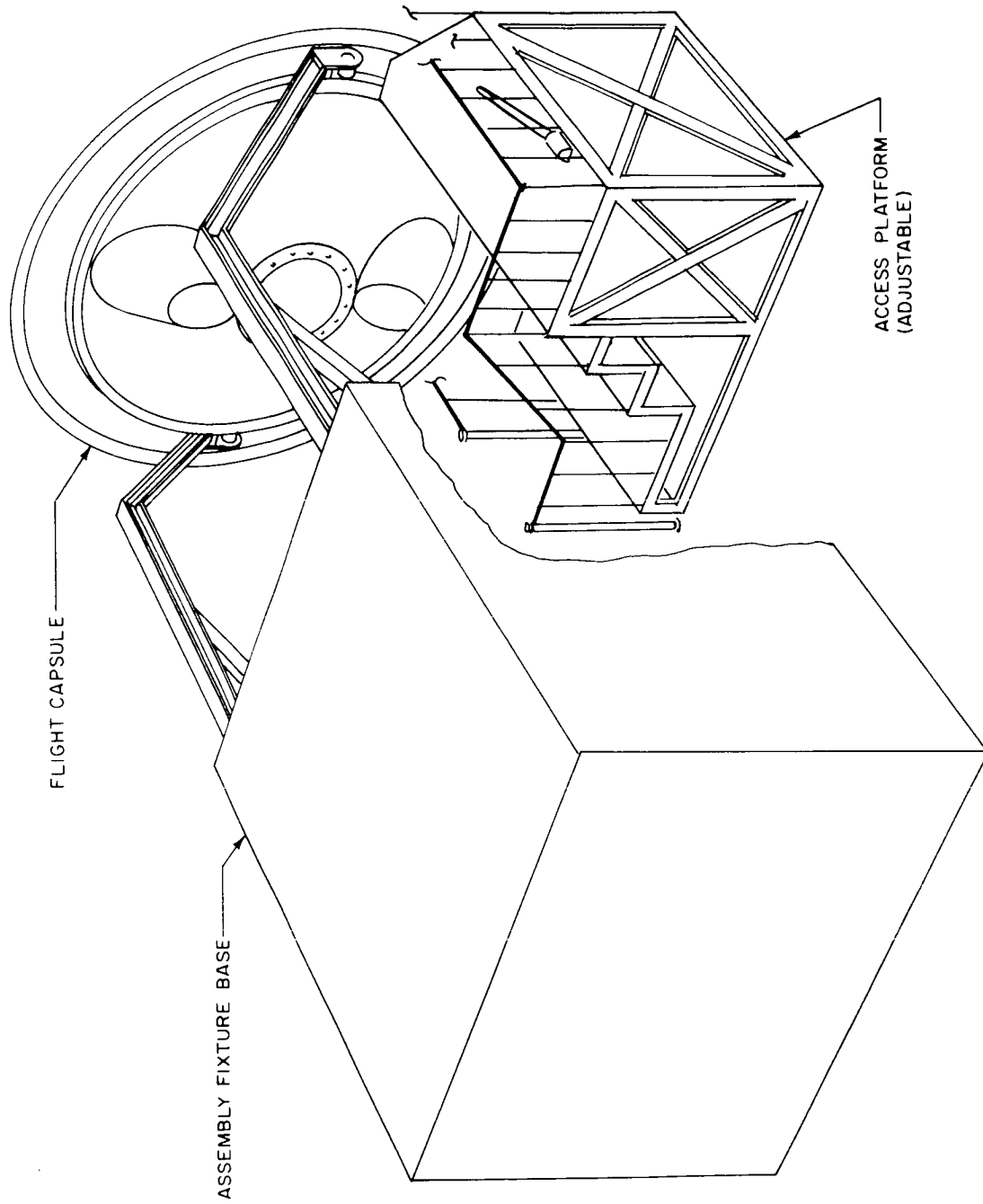
Figure 18  MAJOR ASSEMBLY FIXTURE AND STAND

-40-

two electrical cables and umbilicals, through the sterilization canister, are installed along with the electrical safing and arming devices. The remaining subsystems are installed as specified in subassembly C, Figure 16.

After final assembly of the adapter, another handling fixture is attached at the flight spacecraft interface ring, and the major assembly fixture is removed. This fixture is illustrated in subassembly A, Figure 19.

The adapter is lowered into place on the entry vehicle in its storage container. The V-clamps for the separation mechanism are attached and the handling fixture removed.

### 3.4.4 Sterilization Canister Base Assembly

Due to the extreme structural flexibility of the sterilization canister-base outer shell, handling of it should be minimized. Subsystems assembly is accomplished while the shell is in a uniformly supported cradle. In this position, the subsystems are installed as indicated in subassembly D, Figure 16.

After assembly of the subsystems, the sterilization canister outer shell is lifted by a ring fixture at the outer diameter rim and placed on the partially assembled flight capsule. The flight capsule has been placed in a rotating table stand with the entry shell nose down in a support cradle (Figure 19). Prior to final assembly of the canister outer shell, electrical connection to the adapter main cabling network is made. The outer shell is then lowered in place and a seam welder is attached to the protruding rims of each section. The table is rotated as the rims are seam welded together forming the canister seal.

Final assembly of the sterilization canister is made by inverting the flight capsule on the rotating table stand and placing the canister lid into position, then seam welding around the mating rims of the lid and base. The completed assembly is removed from the stand and attached to the major assembly fixture for assembly of the $\Delta V$ propulsion and access door. While the flight capsule is in the horizontal position, the dummy $\Delta V$ propulsion is removed. Utilizing the alignment provided by the dummy case, the actual $\Delta V$ propulsion is placed in the entry vehicle. Electrical connection is made and the access door is attached.

The use of a single major assembly fixture significantly simplifying the AGE requirement is made possible by the use of a common design for the entry shell - suspended capsule and entry vehicle - adapter separation joints. These mating surfaces provide a common attachment point for the major assembly fixture.

A. FLIGHT CAPSULE - FLIGHT SPACECRAFT
   ADAPTER FIXTURE

FC-FS ADAPTER

B. ENTRY VEHICLE
   SUPPORT STAND

ADJUSTING RING
(STERILIZATION BASE
OUTER RIM

FLIGHT CAPSULE

ROTATING
TABLE

FIXED
BASE
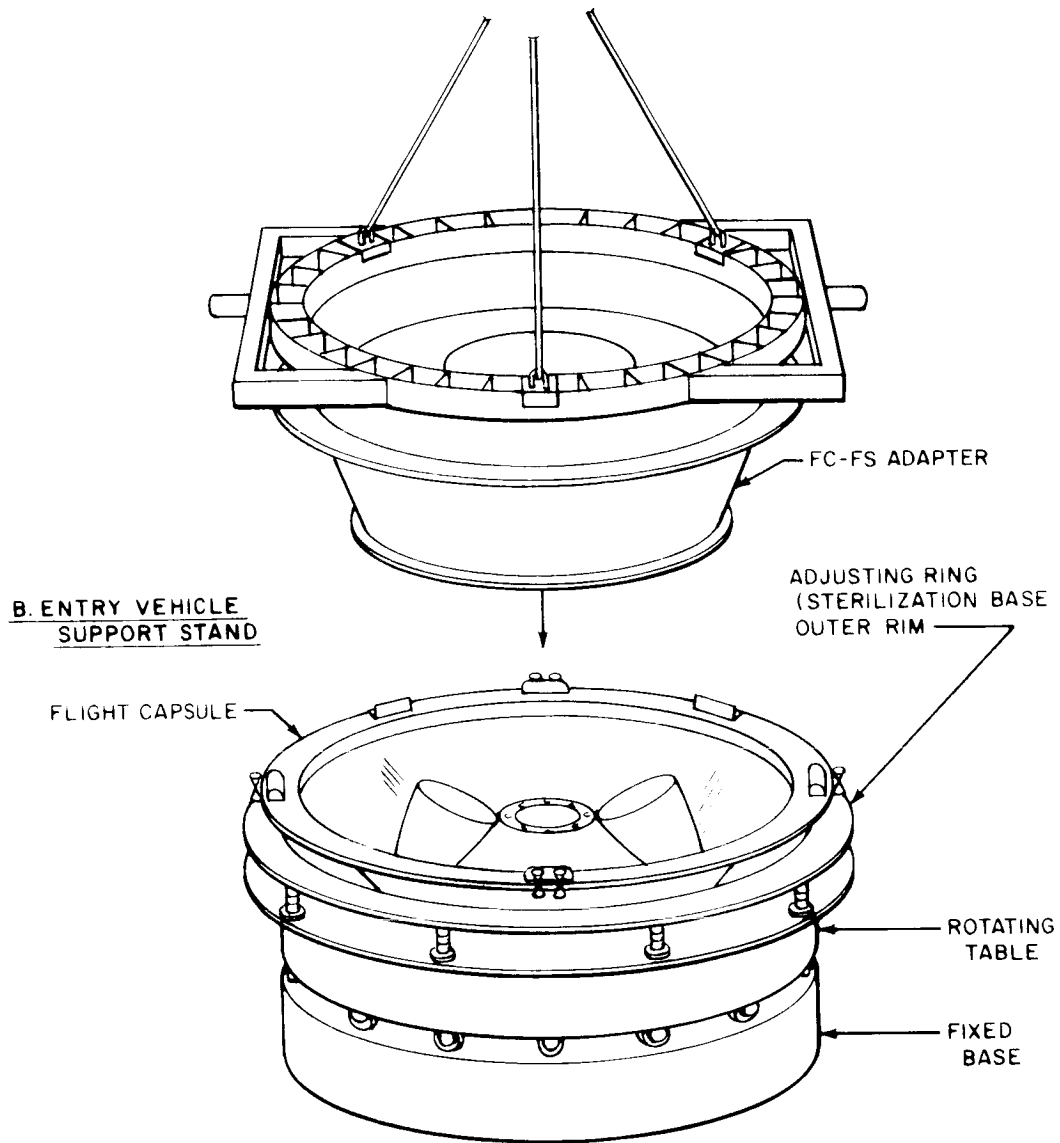
862181

Figure 19  FLIGHT CAPSULE ASSEMBLY FIXTURES

-42-

## 3.5 OPERATIONAL FLIGHT SEQUENCE

Indicated in Figure 20 are the Flight Spacecraft pre-orbit-injection maneuvers, orbit injection, orbital maneuvers and the Flight Capsule de-orbit sequence to entry. Prior to planet encounter, the sterilization canister lid is jettisoned, the canister base remaining attached to the flight spacecraft-flight capsule adapter. The flight spacecraft is subsequently maneuvered into retro-thrust attitude for orbit injection. * After the several days in orbit required for orbit-parameter determination and possibly for flight capsule landing site survey, the entry vehicle is separated from the flight spacecraft. The ACS orients the entry vehicle to the de-orbit thrust altitude. Separation could occur anywhere in orbit but should be fairly close to the entry vehicle de-orbit point in order to reduce entry vehicle power consumption and thermal control complexities. If entry vehicle de-orbit thrusting were performed too close to the flight space-craft, rocket plume interference or contamination of the flight spacecraft could result. Therefore, at least one kilometer separation between entry vehicle and flight spacecraft is provided before de-orbit thrusting.

Thrust vector control is provided by a solid propellant hot-gas reaction control system. After $\Delta V$ application, the entry vehicle is maintained under active attitude control with the cold-gas system until entry. Additional entry vehicle attitude maneuvers can be made, depending on the flight spacecraft orbit, to provide proper communications look angles and to provide a near-zero entry angle of attack. Roll control, provided by the ACS, is utilized throughout entry to maintain minimum spin rates at parachute deployment.

Figure 21 depicts the terminal descent phase of the flight capsule mission starting with parachute deployment sequence. Parachute deployment is initiated by the radar altimeter at 27,500 feet interlocked by a peak g switch and timer that indicates M = 1.2. If the entry vehicle velocity at 27,500 feet is greater than M = 1.2, deployment is delayed until that Mach number is reached. The initiation signal mortars out a 9-foot diameter ring-slot pilot chute which is attached to the main parachute closure bag, pulling the main parachute of the parachute canister on the afterbody. The 81-foot ring-sail main parachute is fully deployed by the time it reaches the end of the riser line. The entry shell separation system is initiated at peak parachute opening load by a load cell in the riser line, releasing the entry shell which falls away. The load cell deployment signal is backed-up by onboard accelerometer signals. If the entry shell fails to separate, the nose cap is then jettisoned to allow some television pictures to be taken. At an altitude of approximately 3500 feet, penetrometer deployment starts and continues at 2-second intervals until all 4 are deployed.

---

* During this maneuver and flight spacecraft orbit-injection, there could be a source of contamination to the flight capsule by the attitude control system gas and the retro-engine propellants of the flight spacecraft.
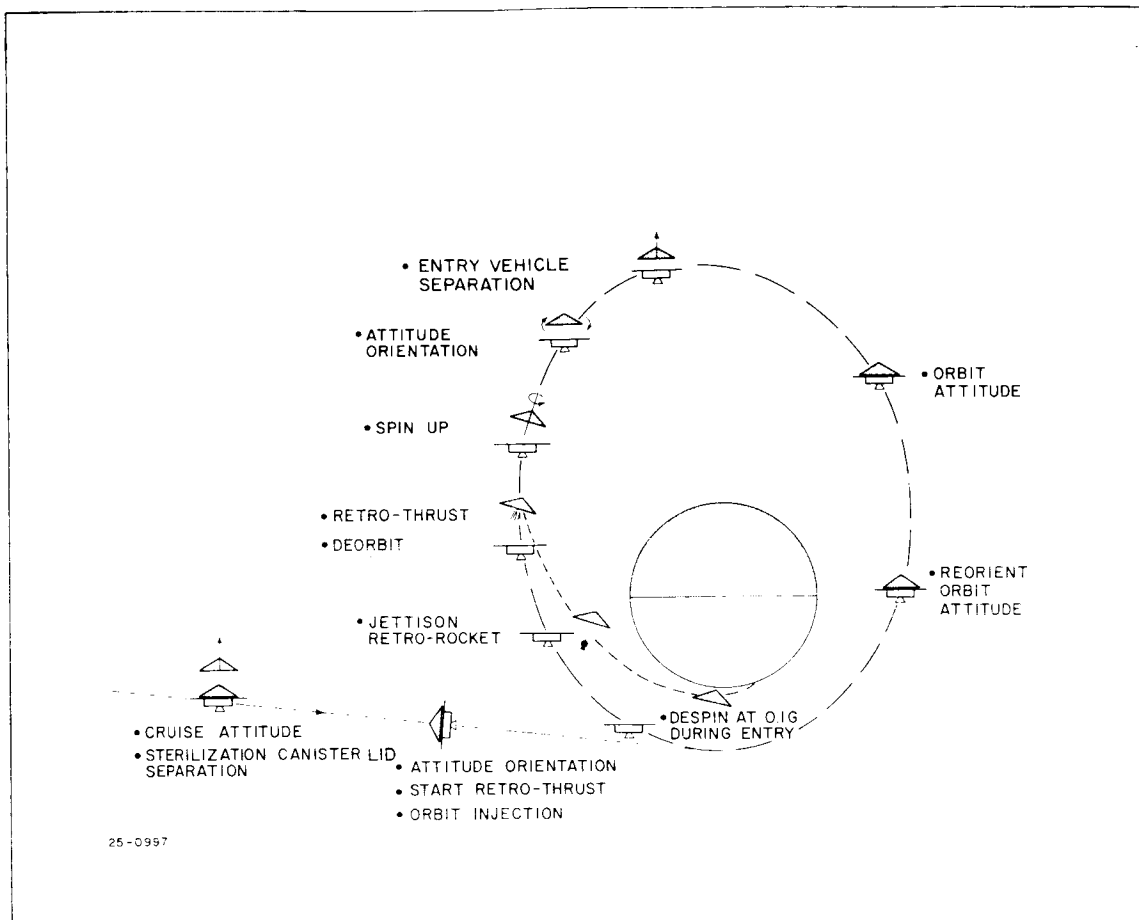
Figure 20 DE-ORBIT SEQUENCE

-44-
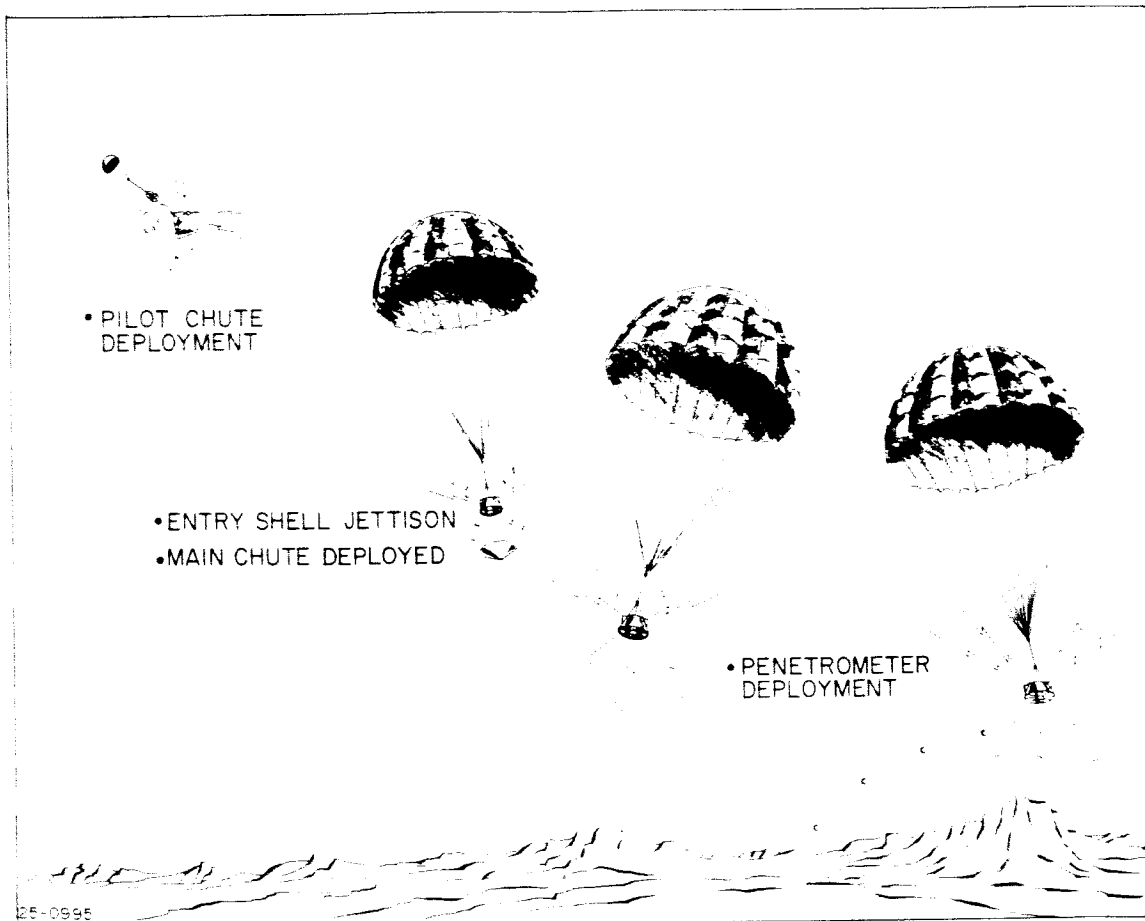
Figure 21 TERMINAL DESCENT SEQUENCE

## 3.6 WEIGHT AND BALANCE

The weight summary presented herein represents the calculated weights of the flight capsule design described in paragraph 3.3. These weights are based on the design inboard profile layouts illustrated in Figures 5 through 15. A weight summary for the total flight capsule is shown in Table III. Presented in Table IV is a detail weight breakdown to the component level for each subsystem shown in the summary table.

### 3.6.1 Weight Summary

The definition of the flight capsule as used in Table III represents the total launch weight as mounted to the flight spacecraft. The weight summary indicates the weights of jettisoned or consumed elements to arrive at the next system weight category. For example, the pressurization gas is vented in Earth parking orbit and the sterilization canister is jettisoned prior to the planet orbital injection to arrive at the preseparation weight. This weight summary presentation follows directly the operational flight sequence discussed in paragraph 3.5.

The total entry vehicle weight of 2040 pounds is based on an $M/C_DA$ of 0.22 and a diameter of 15 feet. The entry weight consists of two major categories: (1) the entry shell and associated subsystems (that portion jettisoned at parachute deployment) and (2) suspended capsule (that portion suspended on the parachute, including the parachute weight).

A contingency factor is included in most of the subsystem weight categories over and above the usual factors of safety to account for unknown brackets, and material tolerances, that cannot be determined at the preliminary design level. The contingency factor is 20 percent on all subsystems, except the instrumentation, power supply, programming and sequencing, and telecommunications where a 25 percent factor was used.

The instrumentation weight indicated in Table III includes both mission engineering experiments and diagnostic instruments. Radar subsystems are listed separately, although they supply experimental data as well as performing programming functions.

Included in the telecommunication weight are all of the relay communication link subsystems as well as the data handling and storage subsystems. All subsystem weights indicated in Table III include the weight of necessary associated hardware, such as mounting containers, wiring, fasterners (Table IV). Other bracketry, interconnecting cables, and miscellaneous hardware are included separately, 15 percent of the major weight category, excluding the weight available for growth.

## TABLE III

## WEIGHT SUMMARY

| | Weight (pounds) | cg* (inch) | Ixx (slug-ft$^2$) | Iyy (slug-ft$^2$) |
|---|---|---|---|---|
| Flight Capsule | 2922.1 | 33.2 | 1367 | 780 |
|     Sterile canister lid | 125.0 | | | |
|     Pressurization gas | 15.0 | | | |
| Preseparation | 2782.1 | 33.2 | 1262 | 720 |
|     Sterile canister base | 163.0 | | | |
|     Pressurization nozzle, valves | 6.0 | | | |
|     FC - FS adapter | 125.0 | | | |
|     Hwd., bkts., cables | 29.5 | | | |
| Separated Vehicle | 2458.6 | 30.0 | 1042 | 581 |
|     Propulsion propellant | 400.0 | | | |
|     ACS gas expelled | 1.0 | | | |
|     TVC gas expelled | 17.6 | | | |
| Entry Vehicle | 2040.0 | 29.5 | 1036 | 575 |
|     Entry shell heat shield | 370.7 | | | |
|     Entry shell structure | 343.0 | | | |
|     Thermal control | 30.0 | | | |
|     ACS-reaction control | 42.4 | | | |
|     TVC-reaction control | 48.5 | | | |
|     Hwd., bkts., cables | 83.5 | | | |
|     Available for growth | 96.9 | | | |
| Suspended Capsule | 1025.0 | 26.8 | 131 | 97 |
|     Instrumentation | 205.6 | | | |
|     Radar subsystem | 56.9 | | | |
|     Telecommunications | 117.4 | | | |
|     Programming and sequencing | 23.6 | | | |
|     Power supply | 178.0 | | | |
|     Parachute | 84.0 | | | |
|     Inertial reference system | 21.6 | | | |
|     Propulsion case | 49.0 | | | |
|     Structure | 96.0 | | | |
|     Afterbody heat shield | 36.0 | | | |
|     Hwd., bkts., cables | 131.0 | | | |
|     Available for growth | 25.9 | | | |

*Measured from the nose cap of the Entry Vehicle structural contour.

## TABLE IV

## DETAIL WEIGHT BREAKDOWN

| | Weight (pounds) | Location | | |
|---|---|---|---|---|
| | | X | Y | Z |
| | | | (inches) | |
| Flight Capsule | (2922. 1) | (33. 3) | (0. 1) | (0. 01) |
| | | | | |
| Sterile canister lid | 125. 0 | 35. 0 | 0. 0 | 0. 0 |
| Pressurization gas | 15. 0 | 40. 0 | 0. 0 | 0. 0 |
| | | | | |
| Pre-F/C separation | (2782. 1) | (32. 2) | (0. 2) | (0. 01) |
| | | | | |
| Sterile canister base | 163. 0 | 64. 0 | 0. 0 | 0. 0 |
| Pressurization nozzles, valves | 6. 0 | 72. 0 | | |
| F/C - F/S adapter | 125. 0 | 48. 0 | | |
| Hwd., bkts., cables | 29. 5 | 56. 8 | 0. 0 | 0. 0 |
| | | | | |
| Separated Vehicle | (2458. 6) | (30. 0) | (0. 2) | (0. 02) |
| | | | | |
| Propulsion propellant | 400. 0 | 33. 5 | 0. 0 | 0. 0 |
| ACS-gas expelled | 1. 0 | 10. 0 | | |
| TVC-gas expelled | 17. 6 | 10. 0 | 0. 0 | 0. 0 |
| | | | | |
| Entry Vehicle | (2040. 0) | (29. 5) | (0. 2) | (-0. 02) |
| | | | | |
| Entry shell heat shield | ( 370. 7) | | | |
| Primary - heat shield | 201. 5 | 35. 7 | 0. 0 | 0. 0 |
| - Fiberglass pad | 21. 0 | 35. 7 | ↑ | ↑ |
| - Bond | 31. 0 | 35. 7 | | |
| Secondary - heat shield | 37. 4 | 32. 8 | | |
| - Bond | 18. 0 | 32. 8 | | |
| Contingency at 20 percent | 61. 8 | 35. 2 | | |
| | | | | |
| Entry shell structure | ( 343. 0) | | | |
| Face sheets | 94. 5 | 35. 7 | | |
| Core | 39. 5 | 35. 7 | | |
| Splice plates | 7. 5 | 35. 7 | | |
| Doublers | 14. 5 | 35. 7 | | |
| Bond | 35. 0 | 35. 7 | | |
| Mounting ring | 12. 0 | 12. 0 | | |
| Base ring | 51. 6 | 48. 8 | | |
| Nose cap ring | 2. 4 | 4. 0 | | |
| Aluminum nose cap | 25. 6 | 2. 0 | | |
| Inserts and attachments | 3. 0 | 35. 7 | ↓ | ↓ |
| Contingency at 20 percent | 57. 4 | 34. 2 | 0. 0 | 0. 0 |

TABLE IV (Cont'd)

## DETAIL WEIGHT BREAKDOWN

| | Weight (pounds) | Location | | |
|---|---|---|---|---|
| | | X | Y | Z |
| | | | (inches) | |
| **Entry Vehicle (Cont'd)** | | | | |
| | | | | |
| Thermal control | ( 30.0) | 35.7 | 0.0 | 0.0 |
| ACS-reaction control | ( 42.4) | | ↑ | ↑ |
|    Cold gas- | 5.0 | | | |
|    Tanks (2) | 11.8 | 10.4 | | |
|    Valve - shut-off (2) | 0.7 | 10.4 | | |
|    Nozzles (12) | 2.2 | 48.0 | | |
|    Plumbing (2) | 6.0 | 10.4 | | |
|    Pressure transducer (4) | 2.0 | 10.4 | | |
|    Regulator (2) | 6.0 | 10.4 | | |
|    Filter (4) | 1.0 | 10.4 | | |
|    Manifold (2) | 0.5 | 10.4 | | |
|    Contingency at 20 percent | 7.1 | 12.5 | | |
| | | | | |
| TVC-reaction control | ( 48.5) | | | |
|    Gas generator (4) | 31.1 | 8.0 | | |
|    Valves and nozzles (8) | 4.2 | 48.0 | | |
|    Tubing and fittings | 5.0 | 8.0 | | |
|    Contingency at 20 percent | 8.2 | 11.5 | | |
| | | | | |
| Hwd., bkts., cables | ( 83.5) | 32.1 | ↓ | ↓ |
| Available for growth | ( 96.9) | 32.1 | 0.0 | 0.0 |
| | | | | |
| **Suspended Capsule** | (1025.0) | (26.8) | (0.4) | (-0.04) |
| | | | | |
| Instrumentation | ( 205.6) | | | |
| | | | | |
|    Penetrometer (4) | 36.0 | 24.8 | 0.0 | 0.0 |
|    Mass spectrometer | 10.0 | 20.0 | -25.5 | ↑ |
|    Acoustic sensitometer | 3.0 | ↕ | ↑ | |
|    Gas chromatograph | 5.0 | | | |
|    Pressure sensor (2) | 1.0 | 20.0 | -25.5 | |
|    Radiation detector | 2.2 | 26.0 | -35.0 | ↓ |
|    Accelerometers (3) | 1.8 | 20.0 | 0.0 | 0.0 |
|    Beta scatter | 0.8 | 21.0 | -34.0 | 7.0 |
|    Temperature sensor (2) | 0.6 | 21.0 | 0.0 | 0.0 |
|    Television subsystem | 60.0 | 14.4 | 0.0 | 0.0 |
|    Water detector | 0.5 | 21.0 | -34.0 | 7.0 |

TABLE IV (Cont'd)

## DETAIL WEIGHT BREAKDOWN

| | Weight (pounds) | Location X | Y (inches) | Z |
|---|---|---|---|---|
| **Suspended Capsule (Cont'd)** | | | | |
| **Instrumentation (Cont'd)** | | | | |
| | | | | |
| Diagnostic instruments | | | | |
| Temperature sensors (75) | 7.5 | 20.0 | 0.0 | 0.0 |
| Pressure sensors (8) | 2.4 | ↑ | ↑ | ↑ |
| Vibration sensors (11) | 5.5 | | | |
| Ablation sensors (9) | 9.0 | | | |
| Separation switches (16) | 4.8 | ↓ | ↓ | ↓ |
| Contingency at 25 percent | 37.5 | | 0.0 | 0.0 |
| Module structure + contingency at 20 percent | 18.0 | 20.0 | -25.5 | 0.0 |
| | | ↑ | ↑ | ↑ |
| Radar subsystem | (56.9) | ↓ | ↓ | ↓ |
| Doppler radar and antenna | 7.0 | 20.0 | 0.0 | 26.0 |
| Doppler radar and antenna | 14.0 | ↑ | 0.0 | -25.0 |
| Radar altimeter electronics | 11.0 | | -23.0 | 0.0 |
| Altimeter and penetration antenna | 7.0 | | -25.5 | ↑ |
| Diplexor | 1.5 | | -23.0 | |
| Penetrometer receiver | 5.0 | ↓ | -25.5 | ↓ |
| Contingency at 25 percent | 11.4 | 20.0 | 0.0 | 0.0 |
| | | | | |
| Telecommunications | (117.4) | | | |
| VHF antenna (2) | 14.0 | 28.0 | 0.0 | 0.0 |
| VHF antenna radome (2) | 8.4 | ↑ | ↑ | ↑ |
| Directional coupler (2) | 1.0 | | | |
| Ferrite circulator (2) | 5.0 | | | |
| Transmitter (2) | 6.0 | | | |
| RF load (2) | 1.0 | | | |
| Engineering data handling (2) | 10.0 | | | |
| Diagram data handling | 8.0 | | | |
| TV data storage (2) | 22.0 | | | |
| Blackout data storage (2) | 4.0 | | | |
| Contingency at 25 percent | 20.0 | ↓ | ↓ | ↓ |
| Module structure + 20 percent contingency | 18.0 | 28.0 | 0.0 | 0.0 |
| Programming and sequencing | (23.6) | 28.0 | 0.0 | 0.0 |
| Central computer and sequencer | 8.0 | ↑ | ↑ | ↑ |
| Pressure switches (3) | 0.3 | | | |
| Separation switches (3) | 0.3 | | | |
| Load switch | 1.0 | | | |
| S & A device (3) | 4.5 | | | |
| Squib isolator (18) | 4.5 | ↓ | ↓ | ↓ |
| Contingency at 25 percent | 5.0 | 28.0 | 0.0 | 0.0 |

TABLE IV (Concl'd)

DETAIL WEIGHT BREAKDOWN

| | Weight (pounds) | Location | | |
|---|---|---|---|---|
| | | X | Y (inches) | Z |
| Suspended Capsule (Concl'd) | | | | |
| Power Supply | (178.0) | 28.0 | 0.0 | 0.0 |
| Battery (2) | 105.5 | | | |
| Power converter (2) | 14.0 | | | |
| Power control switch | 8.5 | | | |
| Contingency at 25 percent | 32.0 | | | |
| Module structure + 20 percent container | 18.0 | 28.0 | 0.0 | 0.0 |
| Parachute | ( 84.0) | | | |
| Parachute | 57.8 | 26.0 | 26.5 | 0.0 |
| Pilot chute and canister | 2.5 | | | |
| Main chute container and bag | 5.0 | | | |
| Harness and swivel | 4.7 | | | |
| Contingency at 20 percent | 14.0 | 26.0 | 26.5 | 0.0 |
| Intertial Reference System | ( 21.6) | | | |
| ACS electronics package | 5.0 | 20.0 | 10.0 | 0.0 |
| Platform | 10.0 | | -10.5 | |
| Sentry gyro | 3.0 | | 10.5 | |
| Contingency at 20 percent | 3.6 | 20.0 | 10.5 | 0.0 |
| Propulsion Case + 20 percent contingency | ( 49.0) | 50.4 | 0.0 | 0.0 |
| Structure | ( 96.0) | | | |
| Rings | 25.0 | 31.0 | | |
| Beams and longerons | 30.0 | 32.0 | | |
| Shells and covers | 25.0 | 32.0 | | |
| Contingency at 20 percent | 16.0 | 32.0 | | |
| Afterbody heat shield | ( 36.0) | 32.0 | | |
| Hwd., bkts., cables | (131.0) | 27.2 | | |
| Available for growth | ( 25.9) | 27.2 | 0.0 | 0.0 |

The inertial reference system must be located in the suspended capsule since it provides the orientation reference for the television camera gimbal system during parachute descent. Similarly, the ΔV propulsion case weight is included in the suspended capsule weight since the case is retained after de-orbit thrusting.

The weight available for growth presented in both the entry vehicle and suspended capsule weight categories represents the weight remaining after all known subsystem, including contingency factors, are accounted for. This weight was purposely included when the entry vehicle diameter was selected to provide for design conservatism as well as an increase in mission objectives or further failure mode protection.

Center of gravity location and moments of inertia for each major weight category are also included in Table II. The entry vehicle mass properties and center of gravity location are of particular significance since they define the TVC, ACS and entry dynamic characteristics.

### 3.6.2 Detail Weight Breakdown

The detail weight breakdown presented in Table IV is also arranged in the same format. In Table IV, each major subsystem within the entry vehicle is subdivided into its various components. The locations of each component according to the coordinate system established on Figures 5 and 9 are shown. Each component location is presented on the respective inboard profile layouts illustrated in Figures 5, 6, and 9 through 15.

The subsystem weights, as presented in Table III, include generous contingency factors. The overall weight breakdown represents a realistic approach to the preliminary design.

# 4.0 SUBSYSTEMS CHARACTERISTICS

## 4.1 COMMAND AND PROGRAMMING

### 4.1.1 Objectives and Requirements

The central computer and sequence (CC&S) subsystem performs all timing, sequencing and related computational functions for the Flight Capsule. Computations are performed to solve equations involving time, acceleration and altitude. The timing function provides a time base to use in all computations and sequences. The sequencers perform the initiation of all events in appropriate order. by providing properly timed outputs to other subsystems.

There are seven sequences of events to be controlled. These are the checkout sequence, electrical stimulation sequence, separation sequence, master sequence, entry sequence, parachute and penetrometer deployment sequence, and TV picture sequence.

These sequences are initiated in one of two ways: either by a time-based signal (for example, a signal from the master timer) or by the occurence of a non-timed event (for example, the indication by a radar altimeter that a certain altitude has been reached). Most sequences are initiated by a timed event, and all succeeding events within the sequence are timed. In addition, some events are initiated by discrete commands from the DSN via the flight spacecraft.

### 4.1.2 Mechanization

Figure 22 shows a functional block diagram of the CC&S. This figure shows the sources of initiation signals and the sequences initiated for each phase of the mission.

Each of the sequences is defined and described below.

#### 4.1.2.1 Checkout Sequence

The checkout sequence controls the events which determine the operating status and condition of all other flight capsule subsystems. The checkout sequence is initiated by a discrete command from the flight spacecraft; thereafter the 13 events comprising this sequence are timed to occur at fixed intervals. The sequence checks out the thermal control, attitude control, power control, gas chromatograph, stable platform, and television systems, and the attitude control and accelerometer calibrators. This sequence requires 90 minutes with one minute resolution and is used as required.
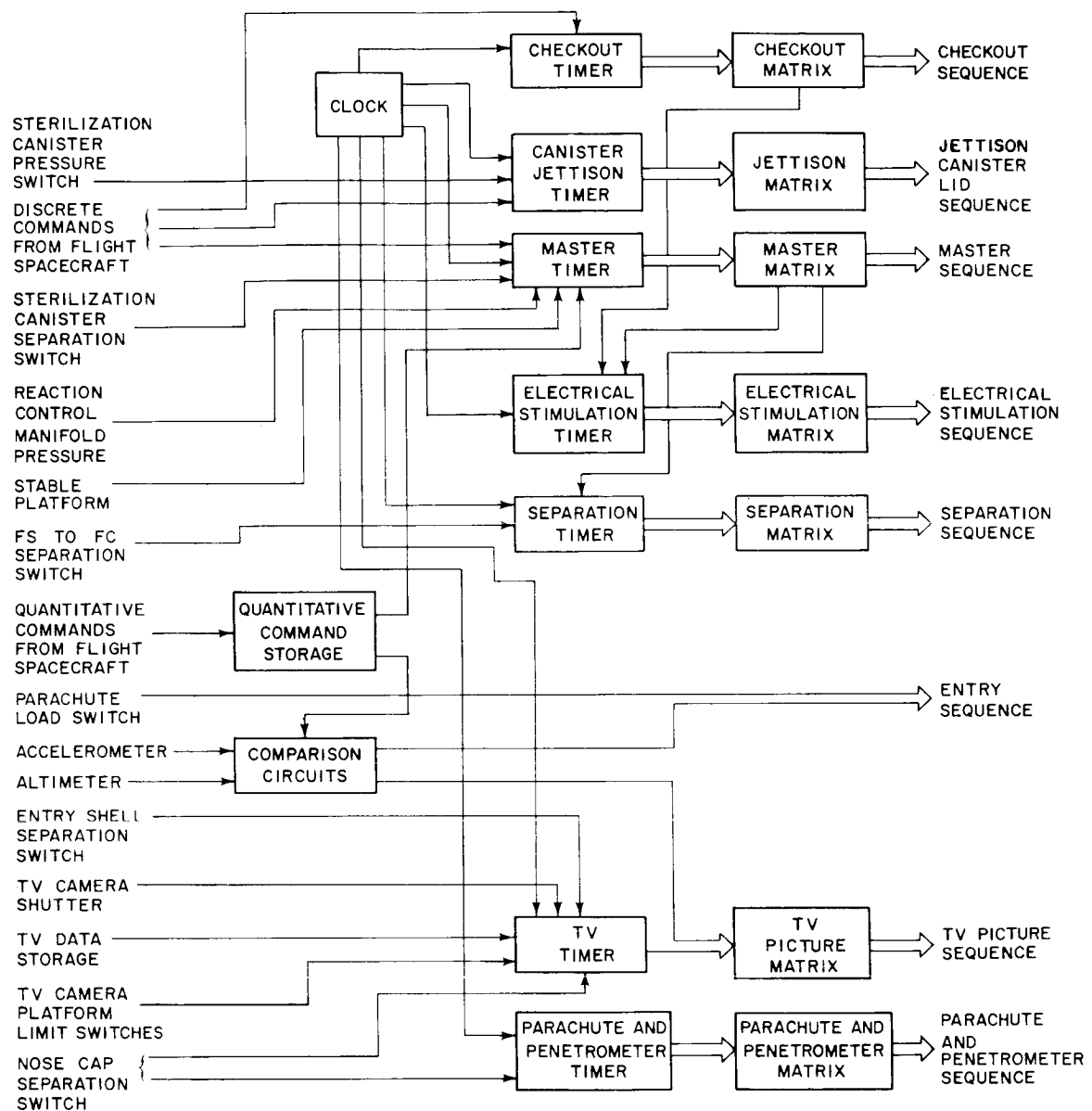
862182

Figure 22 CENTRAL COMPUTER AND SEQUENCER FUNCTIONAL BLOCK DIAGRAM

-54-

### 4.1.2.2 Electrical Stimulation Sequence

The electrical stimulation sequence is a subsequence of the checkout sequence. It is initiated by the master sequence or checkout sequence and provides a timed series of calibration signals to each of the accelerometers and gyros. The TV camera objective lenses are illuminated, and a set of pictures is taken. The gas chromatograph, acoustical densitometer, and mass spectrometer are calibrated by the release of a sample of known gas to each instrument. The high and low altitude radar altimeters are calibrated by a self-contained calibration network. This sequence of 17 events requires 2 minutes with one second resolution.

### 4.1.2.3 Separation Sequence

The separation sequence consists of three timed events initiated by the master sequence. Separation is inhibited unless a discrete enable command has been received. This sequence lasts 66 seconds with one second resolution.

### 4.1.2.4 Master Sequence

The master sequence controls all events from final checkout and calibration through entry. It is initiated by a discrete command from the DSN via the flight spacecraft and consists of 22 timed events. The master sequence initiates checkout, battery recharge, initiation of separation sequence, transfer of the stored attitude-control quantitative commands to the ACS. $\Delta V$ rocket ignition and arming of the entry pyrotechnics. $\Delta V$ rocket ignition has a two-event timed sequence as a backup, which is initiated by a separation switch. The master sequence has one minute resolution.

### 4.1.2.5 Entry Sequence

The entry sequence consists of 12 events, each of which is controlled by non-timed computer outputs. Accelerometer and radar altimeter outputs are compared with levels preset by quantitative commands to initiate pilot chute deployment, to deploy the entry shell, and to start the penetrometer eject sequence as a function of Mach number and altitude.

### 4.1.2.6 Parachute and Penetrometer Deployment Sequence

This sequence consists of five timed events initiated by the entry sequence. It deploys the main parachute and ejects four penetrometers.

### 4.1.2.7 TV Picture Sequence

This sequence is initiated by one of several timers, which start upon closure of a separation switch of receipt of a signal from the entry sequence. The TV picture sequence controls the TV camera shutters and the transfer of data into and out of the TV memories.

Signal inputs include discrete command words which provide a momentary switch closure signal to flight capsule subsystems. The discrete commands from the DSN via the flight spacecraft are as follows:

- Start Master Sequence
- Inhibit Override -- Drift of Stable Platform
- Enable Separation
- Jettison Sterile Canister Lid
- Inhibit Override -- Sterile Canister Pressure
- Start Checkout Sequence
- Release Calibration Gas Sample
- Arm Separation System
- Start Separation System
- Start Electrical Stimulation Sequence
- Open Cold Gas Supply Valve
- Separate Flight Capsule from Flight Spacecraft
- Inhibit Override -- Sterile Canister Lid Separation Switch
- Inhibit Override -- Reaction Control Pressure

Further, quantitative commands are received by the flight capsule via the flight spacecraft to be stored in the CC&S quantitative command storage, representing magnitude information. These are:

- Thrust Vector Roll Command
- Thrust Vector Pitch Command
- Times of Cruise Maneuvers (in Master Sequence)
- Maneuver Roll Angle

-56-

- Maneuver Pitch Angle

- Predicted Time of Entry

- Altitude and Constant for Parachute Deployment

- Altitude and Constant for backup Parachute Deployment

- Altitude and Constant for Penetrometer Deployment

Finally, the CC&S has signal inputs from other flight capsule subsystems, to enable various events to initiate other events. These signals are:

### Inputs: Signals

- Reaction Control Manifold Pressure

- Flight Capsule-Flight Spacecraft Separation Confirmation

- Sterilization Canister Lid Separation Confirmation

- Acceleration

- Parachute Riser Line Load

- Pressure - Sterile Canister

- Nose Cap Separation Confirmation

- Altitude - above 27, 500 feet

- Altitude - below 27, 500 feet

- Camera Platform , Limit Switch

- Altitude Confirmation

## 4. 2 ENGINEERING INSTRUMENTATION

### 4. 2. 1 Ojectives and Requirements

The primary mission objectives specified by the Langley Research Center were to obtain detailed information on the Martian atmosphere and terrain needed for the design of future landers. In addition, data which would be useful for the design of future experiments to provide scientific information on the nature of Mars with particular regard to its biological, geological and meteorological phenomena, both past and present, were to be obtained where possible.

The properties which were to be given primary importance included: atmospheric density, altitude, surface features, surface roughness, surface hardness, surface winds, atmospheric compostion, atmospheric pressure, atmospheric temperature, trapped radiation, and ionospheric composition. Since the suspended payload was not to survive the landing impact, it was desired to obtain maximum utilization of indirect techniques for measurement of surface and near-surface properties.

The ground rules imposed on the study were rather flexible when compared to the entry from approach trajectory study. No experiments were specifically excluded from consideration. It was recommended that television be seriously considered, and that penetrometrometers which might be released impact the surface, and transmit their data to the suspended capsule for relay to the flight spacecraft prior to impact of the suspended capsule, be given serious consideration. It was also later recommended that the use of smoke bombs to determine surface wind velocities also be considered. Specific deadlines on development status were not given. However, it was required that the instruments be available as needed for the test and development program.

It was stated that a master list of candidate experiments should be compiled, that various payloads should be assembled, and that these payloads should be evaluated.

4.2.2 Design

Initially three basic payloads were selected for probe missions. These were designed to represent three levels of complexity and were thus termed the minimum, nominal, and maximum payloads. The minimum payload was similar to the descent payload which had been selected for the entry from approach trajectory, and contained primarily atmosphere characterizing experiments. The nominal payload carried, in addition to the minimum payload experiments, a penetrometer experiment. The maximum payload carried, in addition to the nominal payload, a television experiment. Preliminary analysis of the three payloads and flight capsules, which would be required to carry them, raised serious doubts about the cost effectiveness of the minimum and nominal payloads. The minimum payload did not provide significantly better data than the small atmospheric probe/experiment under study by Ames Research Center. The distinctive was primarily in the amount of data rather than the kind, but the cost in entry weight was at least a factor of five greater than that of the small probe. The addition of penetrometers to provide the nominal payload still did not greatly increase the worth of the mission over small probe mission. It was only with the addition of the television, with its very extensive capabilities, that a real increase in the worth of the mission was realized. Thus it was decided to carry only the maximum mission into the detailed design phase.

The engineering instrumentation included in the reference design is shown in Table V along with some of the details of the instruments. The instruments are mounted in modules in the suspended capsule structure. A significant difference between this mission and the entry from approach trajectory is the reliance on the accelerometer and trapped radiation experiments as the only functional experiments up to sepration of the entry shell. In the entry from approach trajectory mission, there was sufficient emission from the shock wave over the stagnation point to justify the radiometer experiment and the beryllium nose cap that it required. After peak heating, holes could be opened in this cap with comparative ease and atmospheric samples allowed to flow through the sample manifold. In the entry from orbit case, the radiometer experiment would not work because of the low entry velocity. Thus, the heavy and complex nose-cap assembly was eliminated. This increased the problems of opening a hole near the stagnation point to obtain uncontaminated atmospheric samples. Since the radar altimeter and the accelerometers will provide the critical density profile data prior to parachute deployment, since high altitude (greater than 35,000 feet) measurements would probably require special instrument design and would probably not be applicable on parachute, and since aerodynamic problems were anticipated with the sampling system at velocities above about Mach 2, it was decided for this mission to defer most of the composition measurements until after parachute deployment. As a failure mode, if the entry shell fails to deploy, a large diameter hole will be cut in the heat shield and both television and composition measurements will be made through the hole. This solution reduces complexity, increases reliability, and eliminates only data whose interpretation would probably have been questionable.

Another important feature of the design is the use of a motion-stabilized platform for the television experiment. The high wind-and opening-shock-induced angular rates anticipated for the suspended capsule combined with the desire to design the television experiment for low light-levels and high resolution made the probability of obtaining undergraded television images very low if fixed cameras were used. Even with the use of high sensitivity vidicons to reduce the smear problem, the probability of the cameras pointing at undesirably high aspect angles for long periods of time (coning motions) still favored the use of the stabilized platform. This approach required the use of an inertial reference platform to provide an orientation reference for the television platform. The inertial reference platform can also be used for the active attitude control system. If later in the flight capsule development program it was desired to go to ultra-high resolution (inches or less per picture element), then no major changes in configuration would be necessary. In summary, the platform reduces the need to rely on assumptions about wind and wind-gust models as well as on assumptions about parachute dynamics, two areas of considerable uncertainty, while providing flexibility for changes in the design of a very important experiment all at relatively low cost.

TABLE V

ENGINEERING INSTRUMENTATION

| Instrument | Number Carried | Weight (pounds) | Volume (in. 3) | Power (watts) | Bits per Measurement | Outputs (per measurement) | Sampling Rate (measurement per sec.) |
|---|---|---|---|---|---|---|---|
| Radiation detector | 1 | 2.2 | 100 | 0.8 | 56 | 4 | 0.2 |
| Accelerometer | 3 | 1.8 | 15 | 10.5 | 30 | 3 | 1 |
| Radar altimeter | 1 | 19.5 | 1710 | 60.0(a) | 14(b) | 2 | 1 |
| Mass spectrometer | 1 | 10.0 | 265 | 10.0 | 1120 | 160 | 0.2 |
| Acoustic densitometer | 1 | 3.0 | 49 | 4.0 | 21 | 3 | 0.2 |
| Gas chromatograph | 1 | 5.0 | 200 | 4.0 | 56 | 8 | 0.2 |
| Pressure gage | 2 | 1.0 | 24 | 3.0 | 14 | 2 | 1 |
| Temperature probe | 2 | 0.6 | 8 | 0.2 | 14 | 2 | 1 |
| Television | 3 | 60.0 | 1922 | 27.0 | 600,000 | 3 | 0.023 |
| Beta scatter | 1 | 0.8 | 15 | 0.3 | 14 | 1 | 1 |
| Water detector | 1 | 0.5 | 16 | 0.5 | 7 | 1 | 1 |
| Doppler radar | 1 | 21.0 | 3220 | 50.0 | 70 | 10 | 1 |
| Penetrometer | 4 | 41.0 | 5110 | 5.0 | 2000(c) | 4 | 1 measurement |
| Totals | | 166.4 | 12,654 | 175.3 | | | |

(a) For high altitude mode. Low altitude mode will require only 4 watts.
(b) Also will transmit return signal waveform continuously at 1050 bits per second.
(c) Penetrometer telecommunications parameters are for all four units.

The selected payload meets all of the objectives which were discussed in paragraph 4.2.1. In Table VI, these objectives are matched with the instruments which provide data which will assist in the meeting of a given objective. In this table an X is placed under an objective if the instrument in question provides information which may satisfy the objective either alone or in a simple composition with other instruments. Certain higher order combinations have not been included. It may be seen that all of the more important objectives are supported by data from several instruments. Indeed it may appear that excessive redundancy has been achieved for several of the objectives. However, most of this redundancy is functional rather than block. Perhaps even more important, under the apparent high redundancy objectives such as atmospheric density or composition, very few if any of the individual instruments fully satisfy the objective. Under atmospheric compositions the mass spectrometer, the gas chromatograph, the acoustic densitometer, and the water detector each perform a specific task or tasks. The mass spectrometer will scan the mass to charge spectrum from ten to ninety, ideally identifying all components in this range but not readily detecting the higher mass species. In practice the interpretation is less clear even within the nominal range, since several anticipated species have identical nominal masses. For example, small amounts of carbon monoxide in nitrogen or carbon dioxide (a biologically important analysis) can't be detected. On the other hand, the gas chromatograph can handle the carbon monoxide well and can readily detect some of the higher mass species, but has trouble with separating oxygen from argon, a trivial analysis on the mass spectrometer. Further, the chromatograph is not readily programmed to scan for a broad range of species whose identity is not previously defined.

The acoustic densitometer is present primarily to determine atmospheric density, but it also allows the measurement of mean molecular weight and the heat capacity ratio, $C_p/C_v$. These latter data will provide a check on the element-specific detectors so that if an unexpected major component is present, some estimates of its identity will be available. The water detector provides data on the water content of the atmosphere, something that none of the other instruments do well at the low concentrations predicted for Mars. In addition, the accelerometer, the temperature probes, the atmospheric pressure gages, the beta scatter instrument, and the radar altimeter are credited toward the composition objective. The first four of these serve primarily to allow the reconstruction of the density profile, but knowing density, pressure, and temperature, the mean molecular weight can be calculated to provide a check on the element-specific sensors. The radar altimeter provides altitude reference points for the composition profile. Thus, although an apparent nine-fold redundancy exists, none of the instruments are present solely for the purpose of building redundancy, and each serves a well defined independent role. Similar situations exists with other objectives having an apparent high redundancy, although there actually are a few cases of almost pure block redundancy, e.g., the acoustic densitometer and the beta scatter instrument under the density profile objective.

# TABLE VI

## RELATIONSHIPS OF INSTRUMENTS TO OBJECTIVES

| Instruments | Objectives | Atm. Dens. Prof. | Atm. Comp. | Surf. Roughness | Surf. Bear. Str. | Surf. Wind | Atm. Temp. | Radiation Env. | Biology | Geology | Meteorology |
|---|---|---|---|---|---|---|---|---|---|---|---|
| Radiation detector | | | | | | | | X | X | | |
| Accelerometer | | X | X | | | | | | | | X |
| Radar altimeter | | X | | X | | X | | | | X | |
| Mass spectrometer | | X | X | | | | | | X | X | X |
| Acoustic densitometer | | X | X | | | | X | | | | |
| Gas chromatograph | | X | X | | | | | | X | X | X |
| Pressure gage | | X | X | | | | X | | | | X |
| Temperature probe | | X | X | | | | X | | | | |
| Television | | | X | X | X | X | | | X | X | X |
| Beta scatter | | X | X | | | | X | | | | |
| Water detector | | | X | | | | | | X | X | X |
| Doppler radar | | | | X | | X | | | | | |
| Penetrometer | | | | | X | | | | X | X | |

4.2.3. Performance

Although some information on the performance of the engineering instru-
mentation has been given in the previous section, it is the purpose of this
section to describe in detail the functions of the various instruments. The
three accelerometers will be mounted as close to the center of gravity of the
entry vehicle as possible with the sensitive axis of an accelerometer parallel
to the pitch, roll and yaw axes of the vehicle. By sampling the decelerations
experienced by the vehicle between entry and Mach 1, data will be obtained
which, by the application of suitable reduction methods, will allow the re-
construction of the atmospheric density profile in this region. Backup for
this calculation will be provided by the data from the radar altimeter,
the pressure gages, and the temperature probes. A failure of almost every
other experiment and even the loss of communications during the latter
phases of the mission would not compromise the achievement of the critical
parts of the most important mission objective if the accelerometers function.

The radar altimeter will provide altitude data from the end of blackout until
impact. Use of the entry shell structure as the high altitude antenna will
allow this broad range of operation without excessive power requirements.
After sepration of the entry shell, the altimeter will shift from the low
frequency (18 mc) to the high frequency (324 mc) system which includes its
own antenna. The data obtained will provide reference points for the data
taken by the other instruments. With a single altitude reference point, the
accelerometer experiment can be used to construct a large portion of the
density profile even though low-altitude density data are not obtained.

The atmospheric pressure gages will make direct measurements of ambient
pressure during the parachute descent phase of the mission. The pressure
instrumentation to be used will be either vibrating plate transducers or
diaphragms with solid state force sensors.

The atmospheric temperature probes will be two identical total temperature
probes which will be operative from entry shell deployment to impact. At
the parachute descent velocities anticipated, the measured total tempera-
ture will closely approach the static temperature. The experiment will give
information of use in the reconstruction of the density profile of meteoro-
logical interest, and also of use in the design of thermal control systems
for future missions.

The gas chromatograph will detect the concentrations of atmospheric argon,
carbon dioxide, carbon monoxide, krypton, neon, nitrogen, oxygen, and
xenon, utilizing a miniature multiple column, multiple detector system.
These are the major gases whose presence is anticipated in the Martian
atmosphere. The presence of major amounts of other gases, as perhaps
methane or nitrogen oxides will either not be detected, or will degrade the

planned analyses. However, several other experiments will either detect such components or will measure mean molecular weight.

The acoustic densitometer will transmit measurements of the acoustic velocity, acoustic impedance, and temperature of atmospheric samples. From these data, the atmospheric density, mean molecular weight, and heat capacity ratio, $C_p/C_v$ , will be calculated.. The experiment will provide low altitude density data to complement the higher altitude accelerometer data and will allow an independent check of the analyses of the major components of the atmosphere.

The mass spectrometer will utilize the scanning of a quadrupole mass filter to measure the amounts of gases which fragment to give ions with mass to charge ratios of from ten to ninety. The time from the initiation of of scan and the amplitude of up to 80 peaks in this range will be transmitted. As noted in the previous section, the mass spectrometer and the gas chromatograph rather nicely complement each other to provide, with high reliability, a broad range of analyses.

The beta scattering experiment will utilize the back scatter of beta particles from atmospheric molecules to obtain estimates of atmospheric density. The beta particles are generated by a radioisotopic source and are detected by counters shielded from the direct emissions from the source.

The television experiment will take sets of three pictures of resolution varying in the ratio of 9:3:1 with three bore-sighted cameras during the parachute descent. Depending on the atmosphere encountered, between 11 and 22 pictures will be transmitted back to the flight spacecraft. The highest resolution possible will be 0.25 foot per picture element and the lowest 36 feet per element. All images will be in a 200 by 200 element format with 32 shades of gray. The lowest resolution camera of the three will provide an image cut by a diagonal with two different color filters on either side of the diagonal line. The other two images will be unfiltered. To compensate for pointing and image smear problems caused by wind induced high angular rates and displacements from the vertical, the television cameras are mounted on a stabilized platform which is slaved to the inertial reference system. The platform can compensate angular displacements up to 45 degrees. In addition, the camera-shutter triggering sequence is programmed so that probability of triggering when the platform is on the stops is reduced. The television system is designed around conventional rather than high sensitivity vidicons. The image specifications and the shuttering sequence have been selected after careful study of the many uses to which the television experiment may be put. The breadth of utility of the experiment has been maximized without seriously compromising its usefulness in any given area.

The radiation detector will extend the range of measurement provided by flight spacecraft's radiation experiments in to the Martian surface. Electrons and protons ranging in energy from 40 kev to 8 mev will be counted by four different detectors. Although it is not currently expected that high radiation levels will be found around the planet, confirmation of this point is essential for the development of future unmanned and manned missions.

The water detector will be of the type in which changes in the capacitance across an aluminum oxide film are caused by the absorption of water and measured. Because the low levels of water anticipated will cause serious problems of absorption on exposed surfaces in other composition measuring instruments, it is planned to use a sensor which is specific for water and whose active element can be exposed directly to the atmosphere without requiring sampling manifolds. Even with this precaution, there may be some response-time problems at low temperatures and water levels.

The Doppler radar or velocity-attitude sensor will function from parachute deployment to impact as a three-leg high-frequency radar which will provide range, range rate, and Doppler signal strength on each of the three beams, as well as a cone-angle measurement. These data will be interpreted to provide estimates of horizontal velocity (wind velocity) as well as parachute dynamics and large scale surface features. The mission will also provide an opportunity to flight qualify a critical component of future soft landing systems.

The penetrometers will provide the only data on actual physical contact with the Martian surface. The experiment will consist of four penetrometers to be dropped sequentially at 2-second intervals starting at 3500 feet. Each penetrometer will contain an omnidirectional impact accelerometer and a telemetry transmitter to relay the impact acceleration data back to the suspended capsule. This analog signal will be processed on the capsule to read only the times between the crossing of 15 preselected g-level gates, and these times and gate numbers will be transmitted digitally to the flight spacecraft just prior to the impact of the capsule. From the nature of the decelerations experienced at impact, the bearing strength and vertical structure of the Martian surface will be deduced. Impacts on unyielding surfaces will be accommodated by balsa wood impact limiters.

## 4.2.4 Mechanization

In spite of the very tight development timetable allowed for this mission, the actual mechanization of the engineering instrumentation has not proceeded very far. All of the instruments can be assembled from state-of-the-art hardware, but none of them have actually been constructed to meet the various environmental conditions to be anticipated on this mission. Breadboard versions of several of the units have been constructed, and in

some cases flight prototypes have been constructed with slightly different measurement goals. Thus, the basic feasibility of the instruments is assured, but further discussion of the mechanization is not meaningful.

## 4.3 TELECOMMUNICATIONS

### 4.3.1 Requirements and Constraints

The basic requirements which must be satisfied by the telecommunication subsystem can be briefly stated as follows.

The subsystem must be able to:

a. Provide the data handling and storage services required by the flight capsule engineering and diagnostic instrumentation.

b. Transmit to Earth, via relay link through the flight spacecraft the engineering and diagnostic data collected during the cruise, entry and descent phases of the flight capsule mission.

The data transmission objectives for each mission phase are summarized in Table VII.

## TABLE VII

## DATA TRANSMISSION OBJECTIVES

| Mission Phase | Data Objective |
|---|---|
| Preseparation | Determine integrity of FC subsystems |
| Separation | Verify execution of ACS maneuvers and $\Delta V$ events |
| Cruise | Periodic status checks<br>Calibrate instruments in zero g |
| Entry* | Define upper atmosphere |
| Descent | Define lower atmosphere<br>Define surface characteristics |

\*Approximately 87 seconds of radio
blackout occurs during this phase.

-66-

The considerable difficulty associated with attitude control of the suspended capsule during the parachute descent phase of the mission make the use of directional antennas impractical, thus imposing severe limitations on the effective radiated power which can be obtained. Reflections from the planet surface further limit radio link performance by providing a multi-path signal fading environment. Plasma attenuation created by aerodynamic heating during entry, limits the time in which the communications medium is suitable for data transmission and make storage of critical entry data necessary.

Finally, the high deceleration during entry make the normally efficient coherent modulation systems less attractive due to the high carrier power required to avoid loss of phase lock. All of these factors contribute to create a situation which can severely degrade the data transmission per-formance of the flight capsule.

### 4.3.1.1 Flight Spacecraft Constraints

Because of the severe data-rate limitations associated with a direct-to-Earth radio link, the flight spacecraft must be used as a relay ter-minal to transfer to Earth, data collected by the flight capsule. In order to obtain reasonable relay link performance, the communications range between the flight capsule and flight spacecraft must be mini-mized during the entry and descent phases of the mission. This requires that the flight spacecraft be overhead at flight capsule impact which should be at or near the subperiapsis point. To maintain flight capsule to flight spacecraft look angles at high elevation angles with respect to the Martian surface, in order to minimize the effects of multi-path signal fading, it is also necessary that the flight spacecraft be near the flight-capsule zenith during entry and descent.

It is also desirable to minimize flight spacecraft complexity intro-duced by the relay-link requirements, by using only body fixed (non-tracking) antennas on the flight spacecraft. To accomplish this, with-out severely degrading relay link performance, it is necessary to orient the RF relay link antenna such that the total look-angle varia-tion required will be minimized during the entry and descent phases of the flight-capsule mission for the complete range of flight spacecraft orbits. The flight spacecraft antenna look-angle is defined as the angle between the center of the flight spacecraft antenna main lobe radiation and the line of sight to the flight capsule.

These requirements are summarized in Figure 23 which shows the geometric relationships between the flight spacecraft and the flight capsule during entry from a typical orbit.

The problem is to insure that the flight spacecraft is overhead during parachute descent no matter which atmosphere the flight capsule encounters. The flight spacecraft position during parachute descent for each atmosphere is shown on the flight spacecraft trajectory. The central angle represents the total range angle traversed by the flight capsule from entry to chute deployment.

In attempting to angle-center the flight spacecraft overhead during the parachute descent of the suspended capsule, the anticipated dispersion in the positions of the flight spacecraft and descending capsule must be considered. The flight capsule is affected primarily by dispersions in entry velocity, and entry angle, and by the atmosphere encountered. The flight spacecraft position is affected primarily by the dispersion in the time from de-orbit to entry of the flight capsule and, secondarily, by dispersion in flight spacecraft orbital parameters. The time from parachute deployment in the VM-8 atmosphere to impact in the VM-3 atmosphere is shown to be 355 seconds. For a more complete treatment see Volume V, Book 1, Section 6.0.

4.3.1.2  Design Guidelines

The following design guidlines were established to reflect a conservative approach in synthesizing a telecommunication subsystem design:

1.  Utilize a single orientation, low-gain, body-fixed antenna on the flight spacecraft for the complete range of orbits.

2.  Allow selection of a low risk flight capsule parachute. (A descent time-data rate trade-off).

3.  Utilize low voltage solid state equipment where possible, to eliminate high voltage arcing design problems.

4.  Avoid the requirement for a flight spacecraft maneuver to desired flight capsule separation attitude.

5.  Avoid the requirement for flight capsule attitude control from the viewpoint of restricting the flight capsule look-angle to increase the flight capsule antenna gain.

6.  Employ subsystem redundancy such that a single failure of any telecommunication subsystem or component would result in no loss of data.
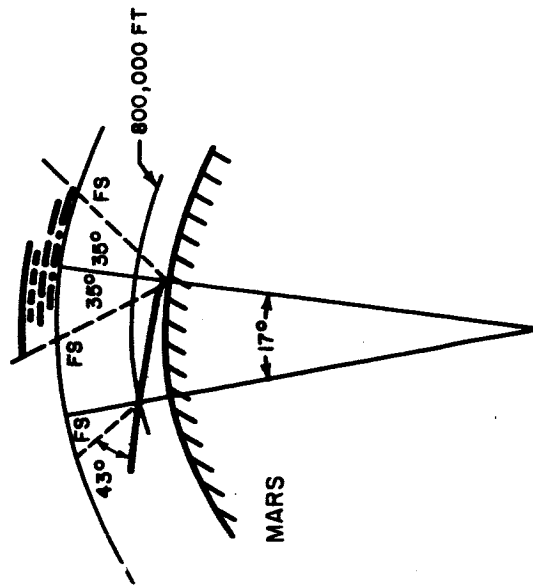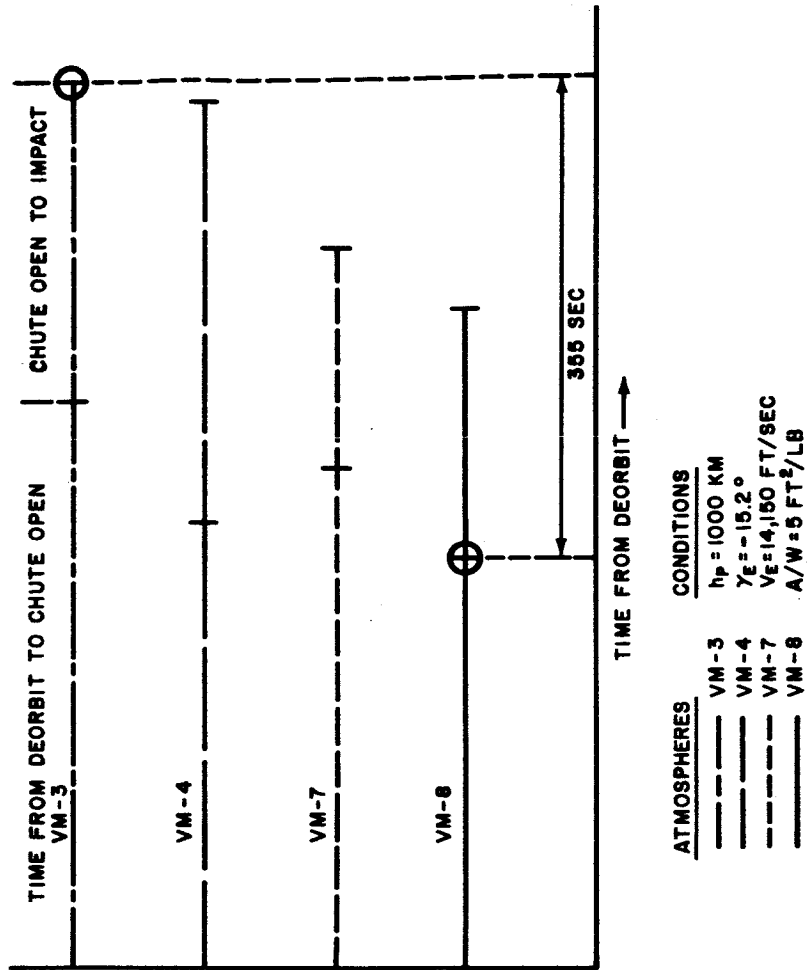
Figure 23 COMMUNICATION GEOMETRY DURING ENTRY

-69-

7.60146P

## 4.3.2 Design

The following paragraphs describe a design concept which promises to satisfy the stated requirements within the imposed constraints.

### 4.3.2.1 General Approach

The design concept features totally redundant telecommunications systems. This approach allows the use of time deversity to ensure data retrieval even under the most adverse fading conditions experienced during the mission. As shown in the simplified block diagram of the telecommunication subsystem in Figure 24 all engineering and diagnostic data is fed to the corresponding data handling equipment in both subsystems. Rather than modulate radio subsystem, 1 entirely from data handling subsystem 1 and radio subsystem 2 entirely from data handling subsystem 2 it is more advantageous to sequence the data alternately to the RF subsystems from each data handling subsystem. This scheme results in a recovery of all the data for any single failure and recovery of half the data for any two nonredundant failures.

The radio subsystems operate in the 267 mc to 273 mc band; one at 268 mc, and the other at 272 mc. They both employ 30 watt solid state transmitters and utilize frequency-shift-keying (FSK) modulation. Table VIII presents a brief resume of the telecommunication subsystem salient design and performance characteristics.

### 4.3.3. Performance

As shown in paragraph 11.6, the relay-link performance margin is well above threshold (maximum adverse tolerance) over the entire trajectory except during two periods. During entry, the radio link signal is attenuated by the flight capsule plasma wake (blackout); the magnitude of attenuation depends upon the flight capsule entry velocity and the atmosphere encountered. Provision is made in the design for continuous transmission during entry and, since blackout may occur, entry data is also stored and re-transmitted after a delay of 100 seconds.

During parachute descent, exposure to wind gusts could cause the suspended capsule to sway up to 90 degrees. As the sway angle increases, the probability of data loss also increases due to both a reduction in flight capsule antenna gain and an associated increase in the probability of signal fading due to multipath reflections from the planet surface.

However, the time diversity technique utilized in this design more than compensates for this loss since, to lose information, the suspended assembly must be at high swing angles during both time seperated periods of transmission and when the same data is sent over each transmitter, a highly unlikely event.
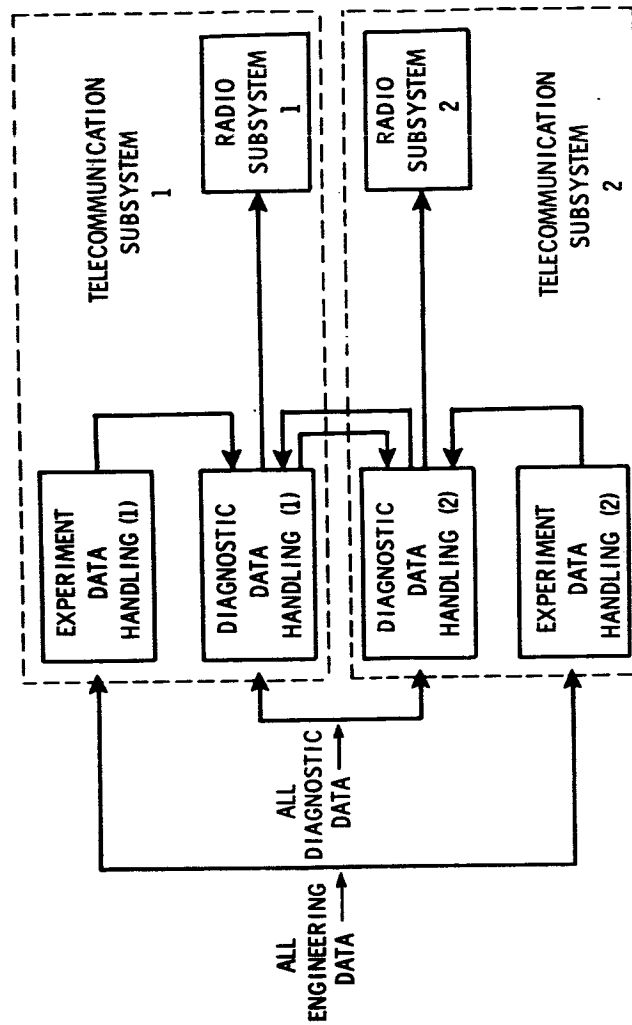
PROPOSED MECHANIZATION PROVIDES FOR:

- Total Data Retrieval For Any Single Failure
- Partial To Total Data Retrieval For Multiple Failures
- Time Diversity
- Delayed Transmission of Blackout Data

Figure 24  TELECOMMUNICATION SUBSYSTEM MECHANIZATION

760231P

## TABLE VIII

## TELECOMMUNICATION CHARACTERISTICS

| FLIGHT CAPSULE | |
|---|---|
| Frequency | 267 - 273 Mhz/band |
| Bit rate | 18, 000 bits/sec |
| Radiated power | 30 watts |
| Modulation | FSK |
| Range | 1, 700 km maximum |
| Antenna type | Log spiral |
| Weight (total) | 89. 6 pounds |
| Power consumption | 183 watts |
| Ancillary features | Redundant systems |
| Delay Memory Prevents Loss of Data in Blackout | |
| FLIGHT SPACECRAFT | |
| Antenna type | Body fixed turnstile |
| Receiver noise figure | 5 db |

## 4.3.4 Mechanization

Figure 25 shows the overall telecommunication subsystem in detailed block diagram form. As previously noted, two completely redundant subsystems are used. Each 30 watt solid-state transmitter is protected against the the effects of high VSWR occurring during blackout at entry by a 3-port circulator in the antenna feed line. The reflected power is dissipated in the RF load. The VHF antennas are log spiral types located on the after-body adjacent to the longitudinal (roll) axis of the flight capsule. These antennas are tilted approximately 15 degrees towards the longitudinal axis to obtain symmetrical antenna gain patterns in planes perpendicular to this axis. Without tilting the antennas, extensive antenna pattern measurements made by Avco on a mock-up model of the flight capsule show that deep nulls in the antenna patterns occur. See Volume 5, Book 3, Section 5.0 for a complete treatment. The data handling subsystem is split into two parts, a diagnostic data handling subsystem and an engineering experiment data handling subsystem. The reasons for doing this are:

1.  A failure in either subsystem will not compromise the operation of the other.

2.  The data-acquisition requirements are dissimilar.

3.  The engineering experiment instrumentation requirements are more susceptible to change than the diagnostic requirements, therefore, a less complex interface results with use of two subsystems.

Two storage subsystems are shown; one for television data storage, and the other for storage of certain critical data collected during entry when radio blackout may occur. The television storage capacity is 850,000 bits consistent with independent storage of 4 television pictures; one storage section for each of the three television cameras and one additional storage section for camera-A pictures. See paragraph 11.10.2 for a discussion of television storage requirements.

The redundant telecommunication subsystems are not totally independent. The reasons for not making them independent were discussed earlier in paragraph 4.3.2.1.

The selected data format scheme interlaces 34 frames of television data with 9 frames of non-television data every 2.5 seconds as shown in Figure 26.

The radar, engineering, diagnostic, and penetrometer frames shown in the first 2.5 second interval of radio subsystem (1) via data handling subsystem (1) are repeated 2.5 seconds later; but this time over radio subsystem (2) via data handling subsystem (2). The data frames transmitted over radio subsystem (1) during the first 5 second interval are entirely from data
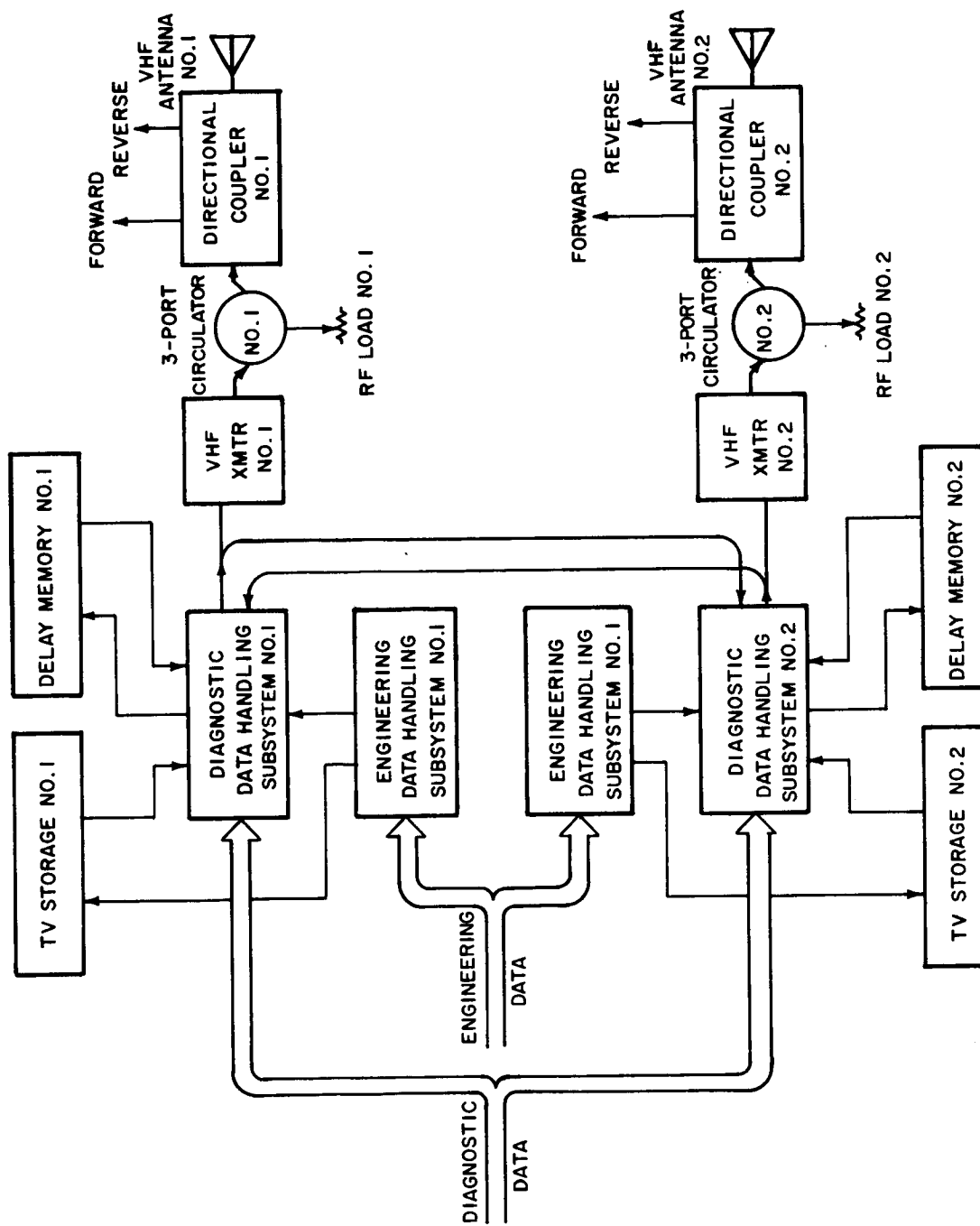
Figure 25 TELECOMMUNICATION SUBSYSTEM BLOCK DIAGRAM

862183

-74-

RADIO SUBSYSTEM NO. I

| TV(34 LINES) | R | R | R | E | E | E | D | D | P₁₂ | TV(34 LINES) | R | R | R | E* | E | E* | D* | D | P₃₄ |

| TV(34 LINES) | R | R | R | E* | E | E* | D* | D | P₁₂ |  TV

⊢———— 2.5 SECONDS ————⊣———— 2.5 SECONDS ————⊣

ETCETRA

RADIO SUBSYSTEM NO. 2

| TV(34 LINES) | R | R | R | E* | E | E* | D* | D | P₁₂ | TV(34 LINES) | R | R | R | E | E | E | D | D | P₁₂ | TV(34 LINES) | R | R | R | E | E | E | D | D | P₃₄ | TV

KEY

TV – TELEVISION
R – RADAR
E – ENGINEERING
P – PENETROMETER
D – DIAGNOSTIC

\* — DELAYED DATA

▮ DHS NO. 2

▯ DHS NO. I
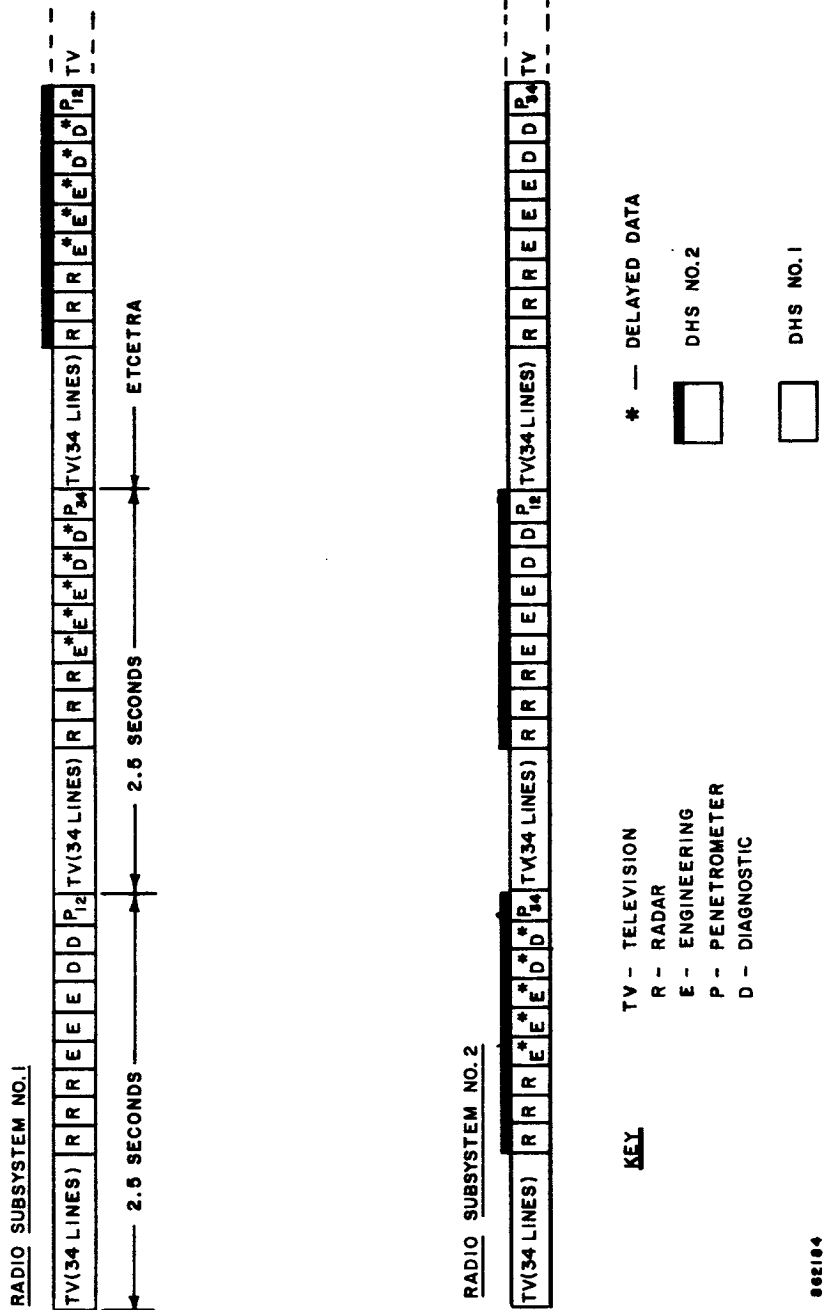
Figure 26  DATA TRANSMISSION SEQUENCE

862184

-75-

handling subsystem (1) and those transmitted over radio subsystem (2) are entirely from data handling subsystem (2). During the next 5 second interval each of the two data handling subsystems feeds data to the alternate radio subsystem. In this way, no data is lost in the event of a single failure of any subsystem.

The television transmission sequence is similarly shown in Figure 27. Each television camera has two redundant memories except the A camera which has four memories. After a set of three television pictures is taken, each picture is read into both memories for that camera. The picutre transmission sequence is C, B, A. Camera A has four memories to allow the next set of pictures to be taken before all the stored data of the first camera A picture has been transmitted. The second set of camera A memories is used to store the second camera A picture while the first camera A picture is still being transmitted. As shown in Figure 27 radio subsystem (1) transmits even numbered lines of the camera C picture from the prime camera C memory via data handling subsystem (1). This data is repeated 2.5 seconds later from the redundant camera C memory via data handling subsystem (2) providing the 2.5 seconds of time diversity. Odd numbered lines of the camera C picture are transmitted first over radio subsystem (2) from the prime camera C memory via data handling subsystem (1) and then 2.5 seconds later over radio subsystem (1) from the redundant camera C memory via data handling subsystem (2).

The second block of 34 lines of camera C data are interleaved in the second block of 34 television lines transmitted to be repeated redundantly in the third block of 34 television lines and so on. Each block of 34 television lines is thus transmitted twice with complete redundancy, and with 2.5 seconds time diversity except the first 34 lines of camera B which are transmitted first interleaved with the camera C data in the first block of 34 television lines and redundantly 14 seconds later. This was done to eliminate transmitter dead air time otherwise occuring every other frame in the first 2.5 second interval.

## 4.4 POWER AND CONTROL SUBSYSTEM

### 4.4.1 Objectives and Requirements

The power requirements are summarixed in Table IX and the equivalent power profile is shown in Figure 28. Electrical power subsystem requirements are as follows:

a) Supply all power to the flight capsule during preseparation checkout;

b) Supply all power to the flight capsule from separation to impact;

c) Be capable of being maintained fully charged by the flight spacecraft power supply;

RADIO SUBSYSTEM NO. I

| $B_1$ | $C_2$ | $B_3$ | $C_4$ | $B_5$ | ≡ ≡ ≡ ≡ ≡ ≡ | $C_{34}$ |

| $C_1$ | $C_{36}$ | $C_3$ | $C_{38}$ | $C_6$ | ≡ ≡ ≡ ≡ | $C_{66}$ |

|← 2.5 SECONDS →|

RADIO SUBSYSTEM NO. 2

| $C_1$ | $B_2$ | $C_3$ | $B_4$ | $C_5$ | ▪ ▪ ▪ ▪ ▪ | $B_{34}$ |

| $C_{35}$ | $C_2$ | $C_{37}$ | $C_4$ | $C_{39}$ | ▪ ▪ ▪ ▪ | $C_{64}$ |

KEY

A — TV CAMERA A
B — TV CAMERA B
C — TV CAMERA C

☐ DHS NO. I

■ DHS NO. 2
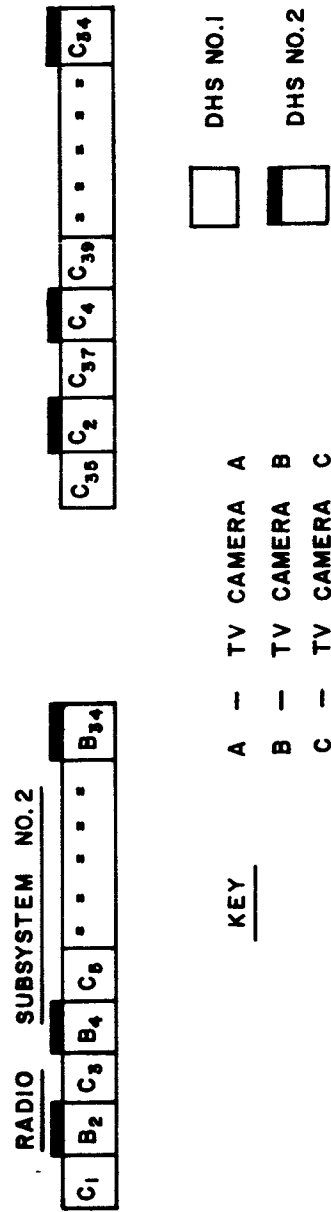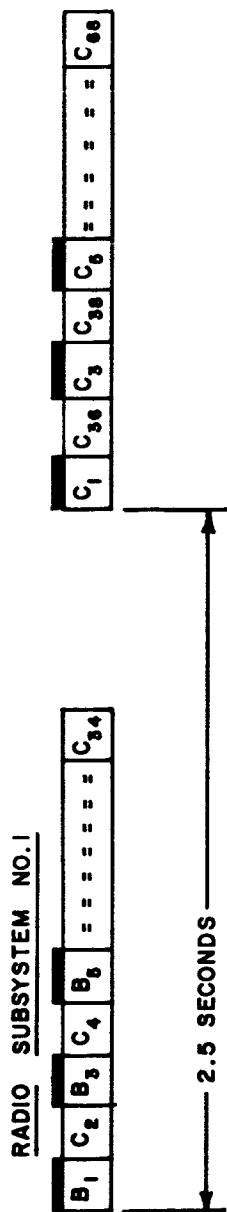
Figure 27 TELEVISION TRANSMISSION SEQUENCE

862185
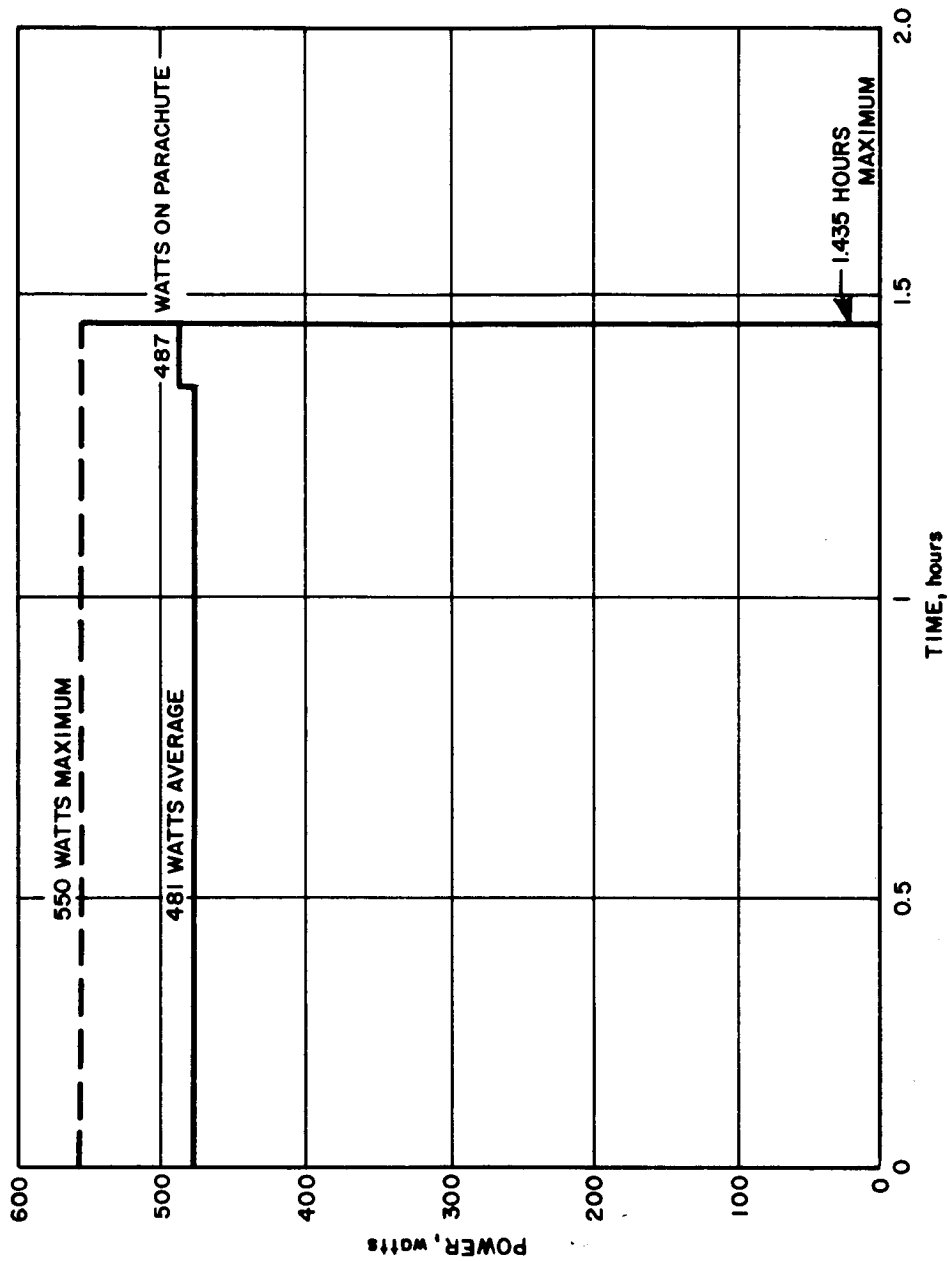
Figure 28 POWER PROFILE FOR FLIGHT CAPSULE

86-1732

## TABLE IX

### POWER REQUIREMENTS

| Part | Average Power (watts) |
|------|:---------------------:|
| Transmitters | 170* |
| Engineering data handling | 6 |
| Diagnostic data handling | 4 |
| Data storage | 1 |
| Delay data storage | 2 |
| Doppler radar | 50 |
| Mass spectrometer | 10 |
| Radiation detector | 0.8 |
| Accelerometer | 10.5 |
| Acoustic densometer | 4 |
| Gas chromatrograph | 4 |
| Pressure sensor | 21.1 |
| Beta scatter | 0.3 |
| Temperature sensors | 7.7 |
| Radar altimeter | 35 |
| Vibration | 0.5 |
| Ablation | 0.8 |
| Penetrometer receiver | 5.0 |
| Water detector | 0.5 |
| Television | 37 |
| ACS electronics | 10 |
| Inertian reference system | 45 |
| Sentry gyro | 10 |
| Power converter/regulator | 86 |
| Total | 521.2 |

*Unregulated power

d) Be capable of being fully checked out electrically before and after heat sterilization.

A basic design objective is to obtain maximum system reliability and component redundancy consistent with weight limitations.

Design constraints consist of heat sterilization at +145° C, an ambient flight capsule temperature from +40 to +200° F, and possible nuclear radiation levels to be defined.

## 4.4.2 Design

Application of the electrical requirements and design constraints to a comparison of power sources led to the selection of a nickel cadmium battery as the only possible candidate at this time. Both the silver-zinc battery and the Lithium Chlorine fuel cell system were investigated as alternates. The silver-zinc battery is awaiting evaluation for heat sterilizability and the Lithium Chlorine fuel cell system has yet to be fully developed.

Table X shows the characteristics of the candidate power sources. In addition to the usual power conditioning regulators, a power control unit has been incorporated in the power subsystem to switch all flight capsule power upon receipt of signals from the CC&S. In this manner, the CC&S is relieved from on power switching. The power control unit includes blocking diodes and fuses in addition to switches to protect the batteries and isolate any component that has experienced a short circuit failure and may cause a heavy drain on the batteries. All components are in parallel from each battery. Each battery-regulator power-control circuit is capable of carrying the entire load at any time. A schematic diagram of the power and control subsystem is shown in Figure 29. Complete power control system redundancy is achieved.

Tables XI show performance characteristics for the power conditioning and power control equipment. The total power subsystem weight (excluding charge regulators) is 139 pounds, of which 106 pounds is battery weight. The volume is approximately 1.38 ft$^3$ of which 0.92 ft$^3$ is battery volume.

## 4.4.3 System Mechanization

### 4.4.3.1 Power Source

The recommended power source consists of hermetically-sealed nickel cadmium cells connected in series to form a battery.. The cells are placed in an unsealed container for the purpose of mounting and thermal dissipation. Full battery design characteristics are shown in Table XII. Two batteries are to be used.

-80-

EXTERNAL POWER ──── FROM F S POWER SUPPLY ──── EXTERNAL POWER

```
           CHARAGE                           CHARAGE
          REGULATOR                         REGULATOR
```

────────────────── INTERFACE F S ──────────────────
                        F C

```
            POWER                              POWER
           CONTROL                            CONTROL
         MAIN SWITCH                        MAIN SWITCH
            IA                                  IB
```

```
           BATTERY                            BATTERY
             I                                   2
```

```
            POWER                              POWER
           CONTROL                            CONTROL
           SWITCH                             SWITCH
            2A                                  2B
```

```
                      DUAL POWER
INPUT SIGNALS                            INPUT SIGNALS
FROM CC AND S          CONTROL           FROM CC AND S
```

```
            VOLTAGE                            VOLTAGE
          REGULATOR                          REGULATOR
             I                                   2
```

TO CC AND S ◄                                  ► TO CC AND S

```
ALL USERS                                ALL USERS
VIA POWER CONTROL                        VIA POWER CONTROL
```

RADIO

862186

Figure 29  SCHEMATIC DIAGRAM OF POWER AND CONTROL SUBSYSTEM

-81-

TABLE X

COMPARISON OF POWER SOURCE CHARACTERISTICS

| Characteristic<br><br>Power Source | Nominal Capacity (Design) | | Voltage Under Load (volts) | Charge Efficiency (percent) | Weight (pounds) | Volume (in. 3) | Notes |
|---|---|---|---|---|---|---|---|
| | Amp-Hours | Watt-Hours | | | | | |
| Nickel-cadmium battery | 27 | 740 | 22 to 32 | 70 | 53 | 790 | -- |
| Silver-zinc battery | 27 | 800 | 25 to 37 | 75 | 27 | *330+ | Projected data only |
| Lithium chlorine fuel cell system | 50 | 1350 | 22 to 31 | See Notes | 10 | 200 | Primary, not chargeable |

*Does not include allowance for case

# TABLE XI

## POWER CONTROL CHARACTERISTICS
### ONE SECTION

| | |
|---|---|
| Power Capacity | 550 watts continuous |
| | 700 watts intermittent |

Number of solid-state switches:

| | |
|---|---|
| Low-power | 11 |
| High-power | 24 |

Maximum forward voltage drops:

| | |
|---|---|
| Low-power | 1.1 volts at 1.1 amps |
| High-power | 0.8 volt at 5.5 amp |

| | |
|---|---|
| Average turn-on time | 2 $\mu$ sec |
| Maximum thermal dissipation | 50 watts |
| Mechanical switching relays | 2 |

### ELECTRICAL CHARACTERISTICS OF LOAD VOLTAGE REGULATOR

| | |
|---|---|
| Rated load | 560 watts |
| Input | 22 to 35 vdc |
| Output | 28.0 vdc ±1 percent |
| Ripple | Less than 0.10 volts peak-to-peak |
| Transients | Less than 0.75 volts for 7 amp load change |
| Overload | 100 percent (intermittent) |

### CHARACTERISTICS OF CHARGE REGULATOR

| | |
|---|---|
| Charge rates (trickle) | 50 to 250 ma |
| Outputs | 2 |
| Temperature cut-offs | Max. +160°F |
| | Min. +30°F |
| Reference set (trickle only) | by zener |
| Full-charge rate | to 3 amps |
| Weight | 3 pounds |
| Volume | 20 in.[3] |

-83-

## TABLE XII

### NICKEL-CADMIUM BATTERY CHARACTERISTICS

| | |
|---|---|
| Nominal capacity (1 hour rate) | 27 amp-hours |
| Output voltage under load | 22 to 32 vdc |
| Rated energy at +40°F | 740 watt-hours |
| Maximum open circuit voltage at 40°F | 35 vdc |
| Minimum charge efficiency | 70 percent |
| Continuous trickle charge rate | 150 to 250 ma |
| Maximum weight | 53 pounds |
| Maximum volume | 790 in.$^3$ (0.46 ft$^3$) |

### 4.4.3.2 Power Conditioning

1. <u>Load Voltage Regulator</u> -- The load voltage regulator is a buck-boost regulator capable of accepting input voltages above or below the required output level. With this technique, more than 90 percent of the battery capacity can be used. Two voltage regulators are used.

2. <u>Charge Regulator</u> -- The charge regulators are located on the flight spacecraft and are disconnected from the flight capsule at separation. They are capable of providing two modes of charging, trickle or float charge, and fast charge. The trickle charge is applied during the interplanetary cruise. The fast charge is applied after preseparation checkout.

3. <u>Power Control Unit</u> -- A schematic of the power control unit (one section) is shown in Figure 30.

TRIGGER ON
AND SHUT OFF
SIGNAL
(11 INPUTS)

POWER IN

TYPICAL ELEMENT

SIGNAL

SCR SWITCH
AND TRIGGERING
CIRCUIT

LOW POWER SWITCHES

POWER OUT
TO 11 SEPARATE
USERS

TRIGGER ON
AND SHUT OFF
SIGNAL
(2 INPUTS)

POWER IN

TYPICAL ELEMENT

SIGNAL

POWER

SCR SWITCH
AND TRIGGERING
CIRCUIT

CRITICAL COMPONENT
SWITCHES

TO ACS
TO ALTIMETER

TRIGGER ON
AND SHUT OFF
SIGNAL
(22 INPUTS)

POWER IN

TYPICAL ELEMENT

SIGNAL

SCR SWITCH
AND TRIGGERING
CIRCUIT

HIGH POWER SWITCHES

POWER OUT
TO 22 SEPARATE
USERS

INTERNAL/EXTERNAL
TRIGGER
CHARGE/TRICKLE
TRIGGER
FROM BATTERY

FROM EXTERNAL
SOURCE

2 ELECTRO MECHANICAL
RELAYS

TO CONVERTERS
AND NON-REGULATED
USERS

86-1733

Figure 30  POWER CONTROL SUBSYSTEM

## 4.5 PROPULSION

### 4.5.1 Objectives and Requirements

The primary objective of the propulsion subsystem is to alter the separated vehicle trajectory such that the vehicle impacts the planet. To accomplish this objective, four types of mission approaches were studied:

1. Fixed $\Delta V$ for all orbits.

2. Fixed $\Delta V$ for each orbit, selected to achieve minimum entry angle dispersion.

3. Fixed $\Delta V$ for each orbit, selected to require the minimum $\Delta V$ rocket size.

4. Variable $\Delta V$, fixed entry angle.

Comparison of these techniques as discussed in Section 9.0 resulted in the selection of the approach using a fixed $\Delta V$ for all orbits.

For this deorbit technique, following the over-all objective of simplicity and conservatism, performance and design requirements were established for the propulsion subsystem. The requirement for only one firing cycle had the largest impact on the selection of the propulsion subsystem. Only subsystems with state-of-the-art established by September 1966 were considered. These two requirements allowed the consideration of solid propellant rocket motors as well as liquid propulsion systems. Both systems were compared with respect to other propulsion subsystem requirements such as: sterilizability, reliability, space storability, total impulse accuracy and the 101,600 lb-sec total impulse required. A solid propellant rocket motor was selected as the propulsion subsystem.

### 4.5.2 Design

The propulsion subsystem consists of a solid propellant rocket motor which is fired to deorbit the separated vehicle such that the vehicle impacts the planet. Rocket firing is controlled by the Flight Capsule CC&S which stores the start time and is updated as needed through the DSN-planetary vehicle-flight capsule command link. After the attitude control subsystem has re-oriented the Separated Vehicle to the correct firing attitude, the rocket is ignited at the prescribed time, by an electrical signal originated in the flight capsule CC&S. The rocket burns for 33.5 seconds to exhaust the total propellant loading.

The rocket motor is a new design but is similar to the Surveyor main retro motor in design concept. The propellant (TP-H-3105) is sterilizable.

-86-

The motor is spherical in shape, 22.3 inches in diameter and 24 inches long having a 6 A$_1$ 4V titanium case. The exhaust nozzle is completely submerged with an area ratio of 18.7 and is made of vitreous silica phenolic. An exhaust nozzle extension has been added to the basic motor to facilitate exhaust gas ducting away from the structure and other equipments. The extension is made of dielectric materials to prevent antenna attenuation. This extension is 11 inches long, mounted to the motor nozzle exit with machine screws into heli-coil inserts. The established nozzle contour is continued. The extension structure is fiberglass coated with Teflon on both the interior and exterior surfaces. The rocket motor without nozzle extension weighs 432 pounds loaded which is a propellant mass fraction of 0.925. The nozzle extension adds 9 pounds to the total weight.

The motor is mounted in the flight capsule by bolting its flange to a matching one on the flight capsule structure. The motor is buried within the flight capsule structure and is not jettisoned after firing. This buried installation was employed instead of jettisoning because failure of the motor to jettison it would place the nozzle in the antenna field of view disrupting antenna patterns.

To contribute to the reliability design goal of 0.990 dual ignitors are used and each has a minimum firing current of 4 amperes.

### 4.5.3 Performance

The rocket has a total impulse of 101,600 lb-sec, required to give the separated vehicle a $\Delta V$ capability of 1400 ft-sec. This total impulse is repeatable within ± 1 percent 3 sigma.

The propellant specific impulse is 254 seconds which results in acceptable subsystem weight. The requirement that only gaseous exhaust products shall result from the combustion process and the fact that the propellant is to be sterilizable prevents, at this time, improving the specific impulse of the propellant by using metal additives. The above specific impulse does not consider the performance increase obtainable from the nozzle extension because of the greater area ratio, 53 instead of 18.7. This would increase the effective specific impulse by approximately 7 percent an equivalent increase in specific impulse of 18 seconds.

The average thrust level is 3000 pounds and offers no problems for the separated vehicle due to acceleration loads; the thrust to weight ratio is approximately 1.2. The thrust level was designed as low as possible to reduce thrust vector control requirements. The 3000 - pound level was the lowest that could be obtained for the type and quantity of propellant being used based on achievable propellant burning rates.

## 4.6 ATTITUDE CONTROL AND THRUST VECTOR CONTROL

### 4.6.1 Objective and Requirements

The attitude control system (ACS) is required to orient the separated vehicle to the proper attitude for application of the velocity increment following separation from the flight spacecraft, to maintain it in this attitude while thrusting, and then to place the entry vehicle in the proper attitude to optimize communications and entry conditions and to maintain limit cycle attitude until entry. After entry, the internal reference system will continue to act as a reference for the television camera. More specifically, the systems must perform the following functions:

a.  Stabilize the tip off rates due to separation from the flight space-craft and realign the separated vehicle to the flight spacecraft reference attitude.

b.  Maneuver the separated-vehicle thrust axis into a preselected attitude, with respect to the flight spacecraft reference attitude, for $\Delta V$ thrust application.

c.  Provide thrust vector control (TVC), by an ancillary hot gas system, in conjunction with the cold gas roll nozzles during the operation of the $\Delta V$ propulsion system.

d.  Reorient the entry vehicle from the thrust application attitude to the proper attitude which optimizes communications and entry conditions.

e.  Maintain limit cycle conditions by means of the cold-gas reaction control system until entry.

f.  Maintain roll rate control during entry to reduce any spin up due to aerodynamic asymmetries.

g.  Provide a reference via the internal reference system for the television camera gimbal system during the parachute descent phase.

The design of the ACS provides for the following modes of failure:

1.  Redundancy permits a single failure in the cold-gas reaction control system.

2.  Redundancy permits a single failure in the hot-gas thrust vector control system.

3.  A sentry system, consisting of body-mounted rate gyros/ prevents high tumble rates if the inertial reference system fails. The

-88-

reaction control system is deactivated by the sentry system should angular rates about any axis exceed 6 deg/sec.

## 4.6.2  Design

The selected design utilizes active attitude control from separation to entry. Maneuvers and initial stabilization are accomplished by a cold-gas reaction control system, whereas control during $\Delta V$ thrusting is provided by an ancillary hot-gas system. Commands to control the operation of the nozzle valves are generated in the inertial reference system. These signals are a function of angular error and its time rate of change. The reaction control system provides three axis control in couples by means of twelve nozzles. Eight hot gas nozzles provide control over the disturbing torques in pitch and yaw arising during the thrusting mode. Roll disturbances arising during this phase are handled by the cold gas roll nozzles. Upon completion of the thrusting phase, the ACS maintains the attitude of the entry vehicle with the cold gas system. It may reorient the vehicle to optimize communication performance. An orientation will be performed prior to entry to an attitude which minimizes the entry angle of attack.

During early entry, the reaction control system will be disabled in pitch and yaw, but roll control will be maintained in a roll-rate limiting mode. The inertial reference system will remain operative and will provide acceleration data during the entry phase for the purpose of event control and also for entry wind and atmospheric density measurements. Upon parachute deployment, the IRS will provide the television camera gimbal system with commands required to maintain the optical axis of the cameras along the local vertical.

Several alternatives were available in the design of the ACS and TVC. These are discussed in greater detail in Volume V, Book 5, but are mentioned here very briefly. An active system was mandatory to obviate a flight spacecraft maneuver and to improve accuracy. With a spin stabilized system, rate damping of the entry vehicle during early entry to improve angle of attack convergence and damping of the suspended capsule for camera stabilization during the parachute descent phase may be necessary. With an active control system, rate damping is unnecessary since the entry vehicle will possess a nominally zero angle of attack. To minimize system weight, an ancillary reaction control system is used for TVC. Systems investigated included:

    a.   Bipropellant

    b.   Monopropellant

    c.   Cold Gas

    d.   Spin Stabilization

e.   Gimballing of Rocket Motor

f.   Solid Propellant

The last of which was chosen.   Approximately 100 pounds reduction in weight is realized by using the auxiliary (or hybrid) control.

## 4.6.3  Performance

The most stringent requirement on the performance of the ACS is the control of the direction of the imparted velocity perturbation.   System accuracy during thrusting is 0.5 degree (1 sigma) and 1.0 degree (1 sigma) at entry.

Operation is divided into the following phases:

1.   Separation to thrusting        0.5 hour

2.   Thrusting                      35 seconds

3.   Cruise                         1.0 hour

The total stored impulse is 3500 lb-sec of hot gas and 248 lb-sec of cold gas as compared with the required values of 1225 lb-sec and 68 lb-sec, respectively   System weight is 90 pounds.

The ACS is characterized by a limit cycle amplitude of less than 0.5 degree in pitch and yaw and 1.0 degree in roll, and a maximum rate during orientation of 1.0 degree per second.   The limit cycle amplitude and rate limit were selected to minimize fuel requirements subject to the system accuracy constraints.   In addition to the limit cycle itself, other contributors to the pointing error are drift of the inertial reference system gyros and alignment errors.   More than three times the required total impulse is stored in the cold gas system to provide for leakage and possible failure.   There are two completely redundant systems with sufficient extra impulse in each system to compensate for a valve stuck open in either system.   Similar redundancy and provisions for failure exist with the hot-gas system.

Performance of the inertial reference system for use after entry is characterized by:

a.   Pointing Performance        1.0 degree

b.   Operating Time              0.5 hour

## 4.6.4 Mechanization

A subsystem block diagram is shown in Figure 31. Three axis control is provided by a cold-gas reaction system for portions of the mission exclusive of the thrusting phase, where control in pitch and yaw is accomplished by a hot gas system.

Commands to control the action of the reaction control system are generated in the inertial reference system. This system consists of a four gimbal inertial platform, a digital computer, and a three axis rate sensor Sentry System for rate limiting. Use of four gimbals provides full angular freedom. The platform also contains the accelerometers for data purposes, thus providing inertially referenced acceleration data. Transformation of the platform gimbal angles into the proper reference frame for commanding the reaction control system is accomplished by the computer. After entry the computer performs the proper transformation from the inertial reference system gimbal angles to command the television camera gimbal angles so as to position the camera line of sight along the local vertical.

A schematic of the cold gas nozzle and plumbing portion of the reaction control system is presented in Figure 32. These twelve nozzles provide three axes control in couples about each of three axes. The reaction control system has a dual-operating feature, such that failure of one nozzle will not cause a system failure. The cold gas (N2) tanks are capable of withstanding sterilization after being fully charged. Figure 33 illustrates the solid propellant TVC system. Each of four solid propellant hot gas generators supplies two normally-open solenoid valves to provide couples about both axes. Utilization of two independent thrust modules per axis (each consisting of a gas generator and two valves) permits the complete loss of one module per axis without causing failure of the TVC function. Roll control during thrusting is accomplished by the cold-gas roll nozzles.

## 4.7 PARACHUTE

### 4.7.1 Objectives and Requirements

The primary objective of the parachute descent system is to decelerate the suspended capsule after entry to provide adequate communications time at altitudes between 20,000 feet and the surface of the planet. The parachute descent system must satisfy both a minimum and maximum required descent time. A minimum of 160 seconds is required for data acquisition and playout, and a maximum of 360 seconds is available before the flight spacecraft passes out of the flight-capsule antenna pattern. It is further required that the terminal-descent parachute be fully inflated and subsonic at 15,000 feet altitude.
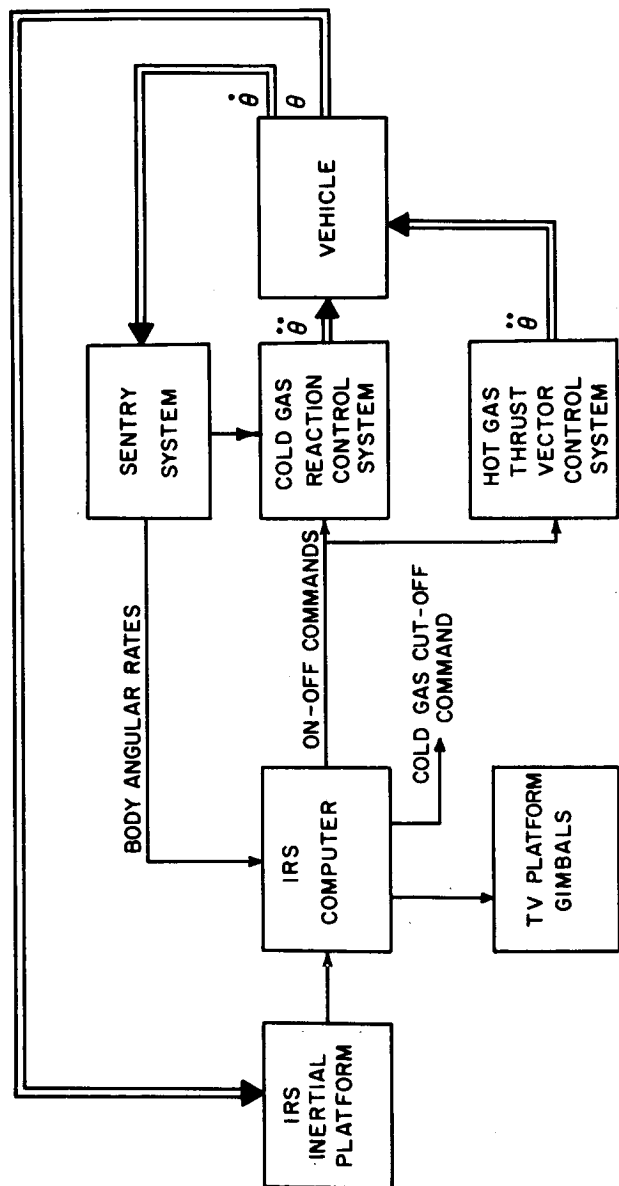
Figure 31 BLOCK DIAGRAM OF ACS-TVC

86-1192

-92-
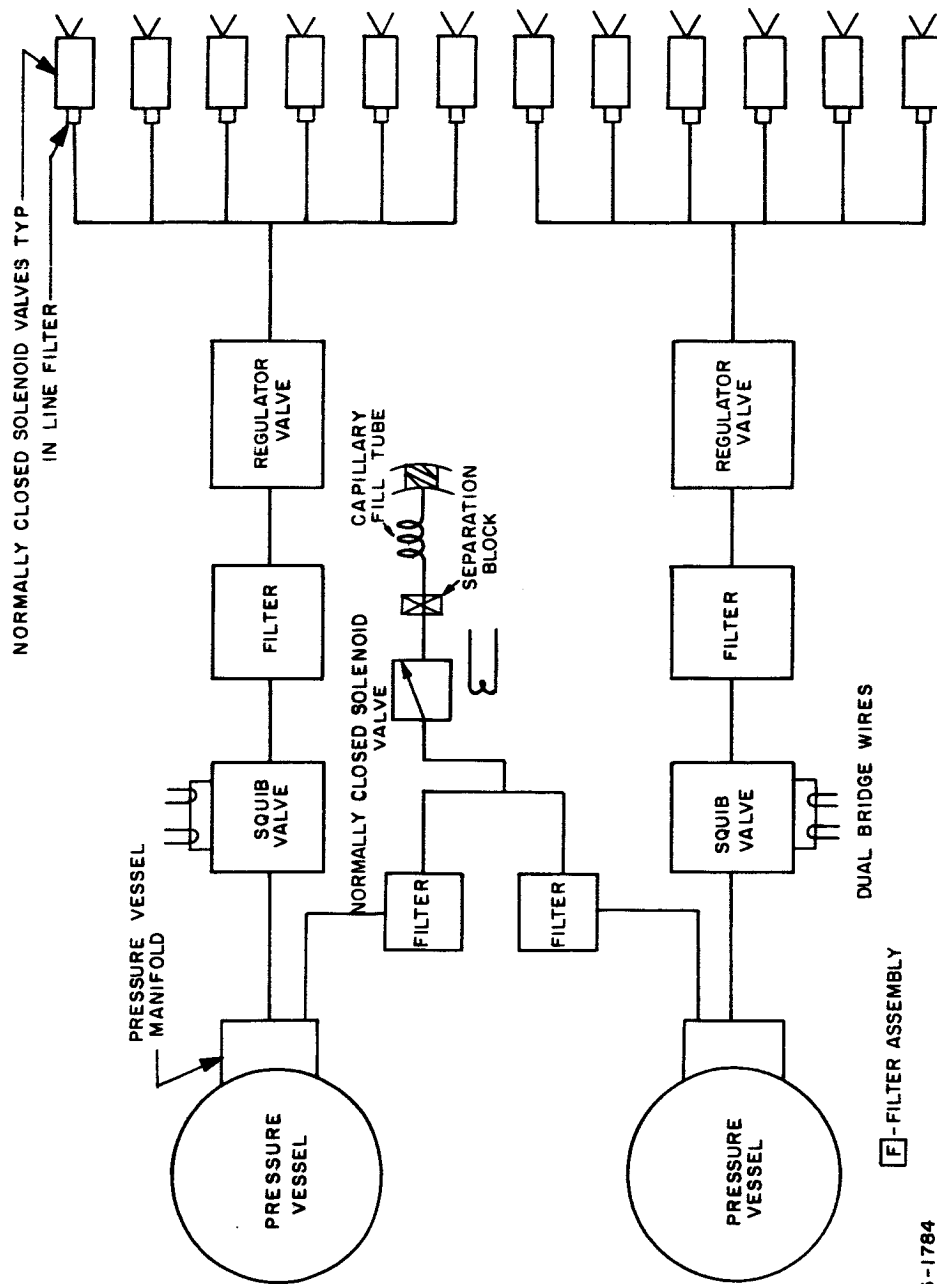
Figure 32 COLD-GAS REACTION SYSTEM

85-1784

-93-
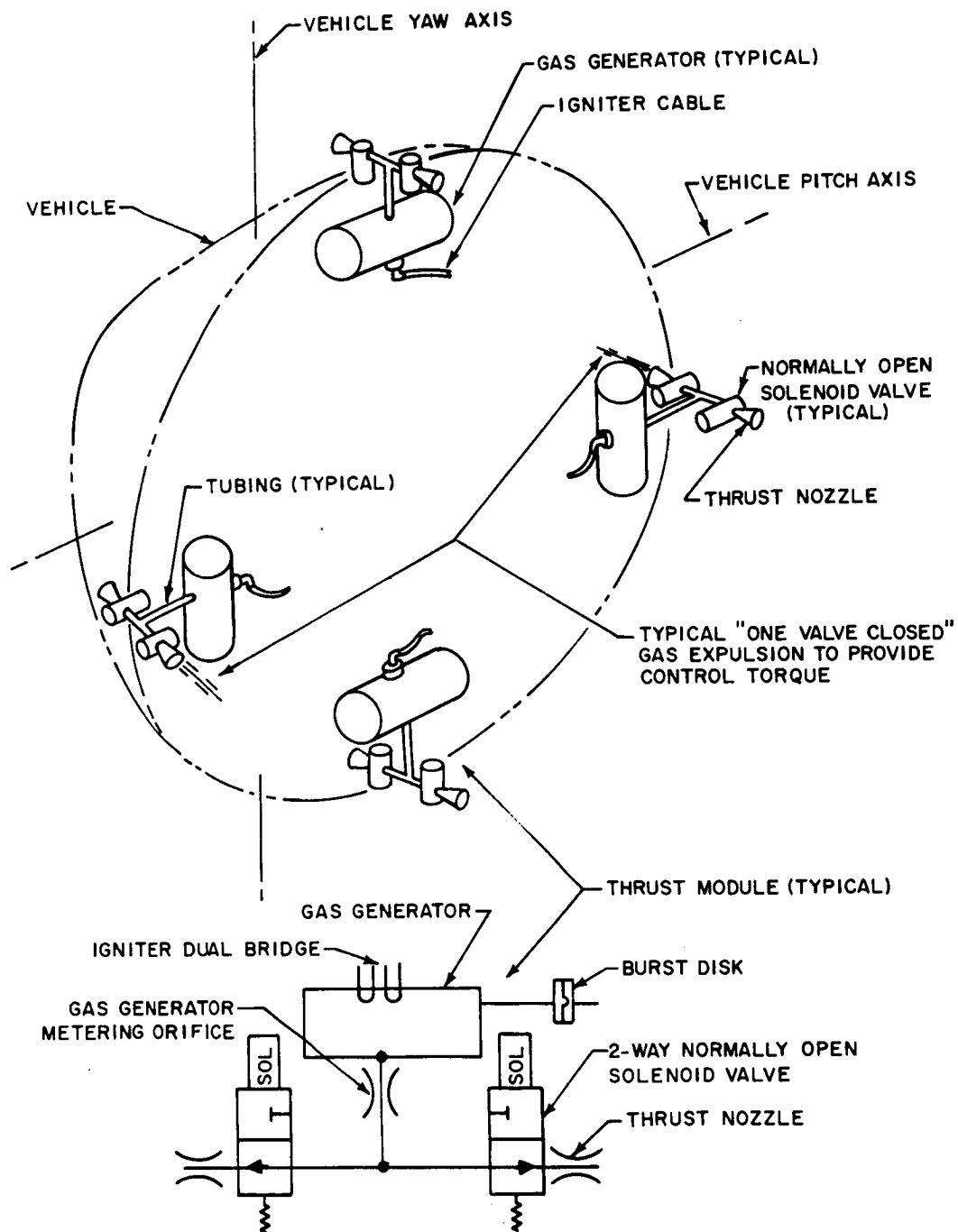
86-1194

Figure 33  SOLID PROPELLANT OPEN CENTERED TVC SYSTEM

-94-

The parachute system and attendant deployment conditions (altitude and Mach number) dictate, to a large degree, the maximim $M/C_D A$ that can be achieved for a vehicle entering a given atmosphere with particular entry conditions. The final selection of the parachute system was based on reliability, performance and development risk, in that order.

## 4.7.2 Design

The Model atmospheres used were the 5 to 10 mb pressure VM-3, 4, 7, and 8 atmospheres. Neither a two parachute drogue-main nor reefing of a single main chute is necessary to accomplish the intended mission under the design constraints. Hence, the selected reference descent system is a conventional single stage ring-sail parachute which is deployed at a maximum Mach number of 1.2 (Mach 1.2 was selected as the upper limit for reliable deployment and operation).

Trajectory results indicate that for the range of entry conditions considered, the VM-8 atmosphere results in the lowest parachute deployment altitudes. However, for terminal descent deceleration, the VM-7 atmosphere requires a greater drag area than the VM-8 if all other conditions are equal. This cross over in behavior between the two atmospheres is due to the larger scale height and lower sea level density of the VM-7 atmosphere in comparison with the VM-8. In summary, the VM-8 atmosphere dictates the maximum allowable $M/C_D A$ for given parachute deployment conditions, but an appreciably greater parachute deployment altitude is required in the VM-7 atmosphere in order to achieve equal descent time.

Utilizing the terminal descent velocity expression, a useful parameter involving parachute drag area and suspended weight can be evolved.
(i.e., $A_{MC}/W_{Susp} \propto \frac{1}{V_v^2} at$, where $V_v$ is the vertical impact velocity and $t$ is the chute descent time). Based on chute deployment at Mach 1.2 for all entry conditions considered, the minimum deployment altitude is approximately 19,9000 feet in the VM-8 atmosphere (0.22 M/CDA). Figure 34 which is a plot of chute descent time versus altitude for a range of $A_{MC}/W_{Susp}$ ratios in the VM-8 atmosphere, indicates that in order to satisfy the minimum descent time requirement of 160 seconds an $A_{MC}/W_{Susp}$ ratio of approximately 4.9 ft²/pound is required. A value of 5.0 ft²/pound was chosen in the reference design in order to adequately allow for sensing and initiation errors and also allow time for parachute deployment and inflation. The reference flight capsule design has a suspended weight of 1025 pounds. Figure 35 which presents nominal chute diameter versus suspended weight, indicates that a 81 foot nominal diameter ring-sail parachute is required for the reference $A_{MC}/W_{Susp}$ of 5.0 ft²/pound. The maximum opening dynamic pressure is approximately 5.0 psf for deployment at Mach 1.2, for the reference $M/C_D A$ of 0.22 slug /ft². Figure 36 plots parachute weight versus opening dynamic pressure for a range of nominal parachute diameters.
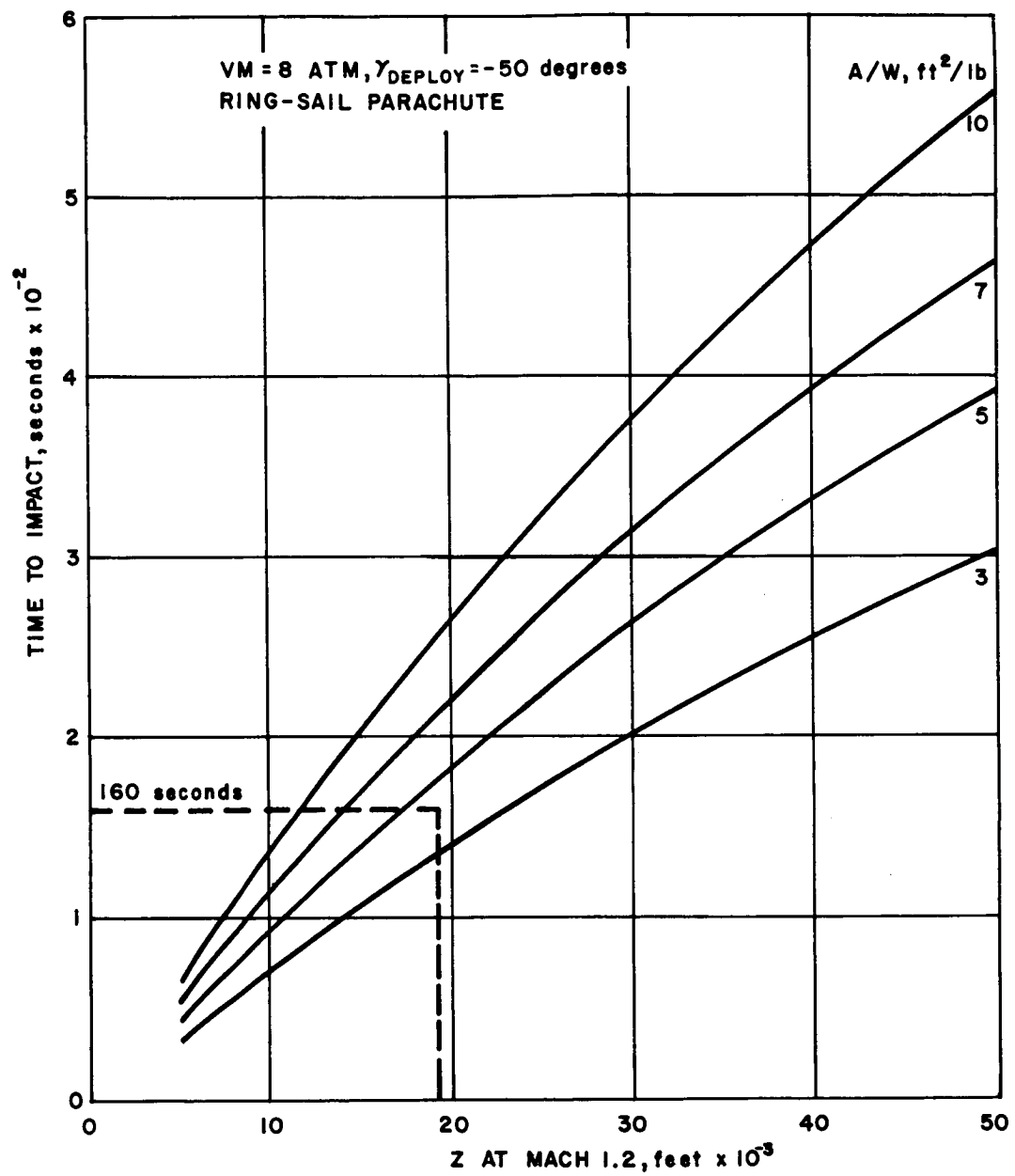
Figure 34 TIME ON PARACHUTE VERSUS ALTITUDE

862187
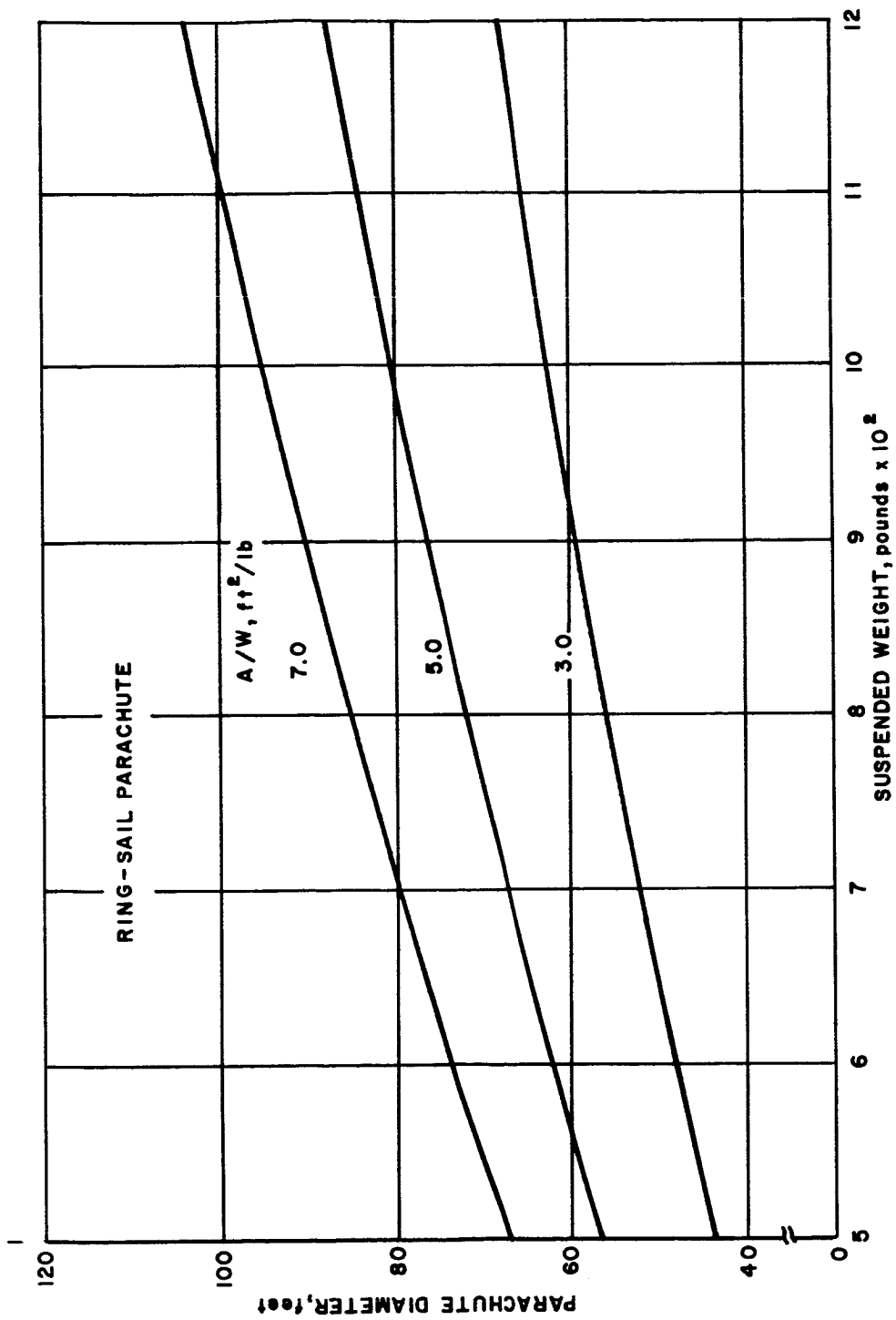
Figure 35  NOMINAL DIAMETER VERSUS SUSPENDED WEIGHT
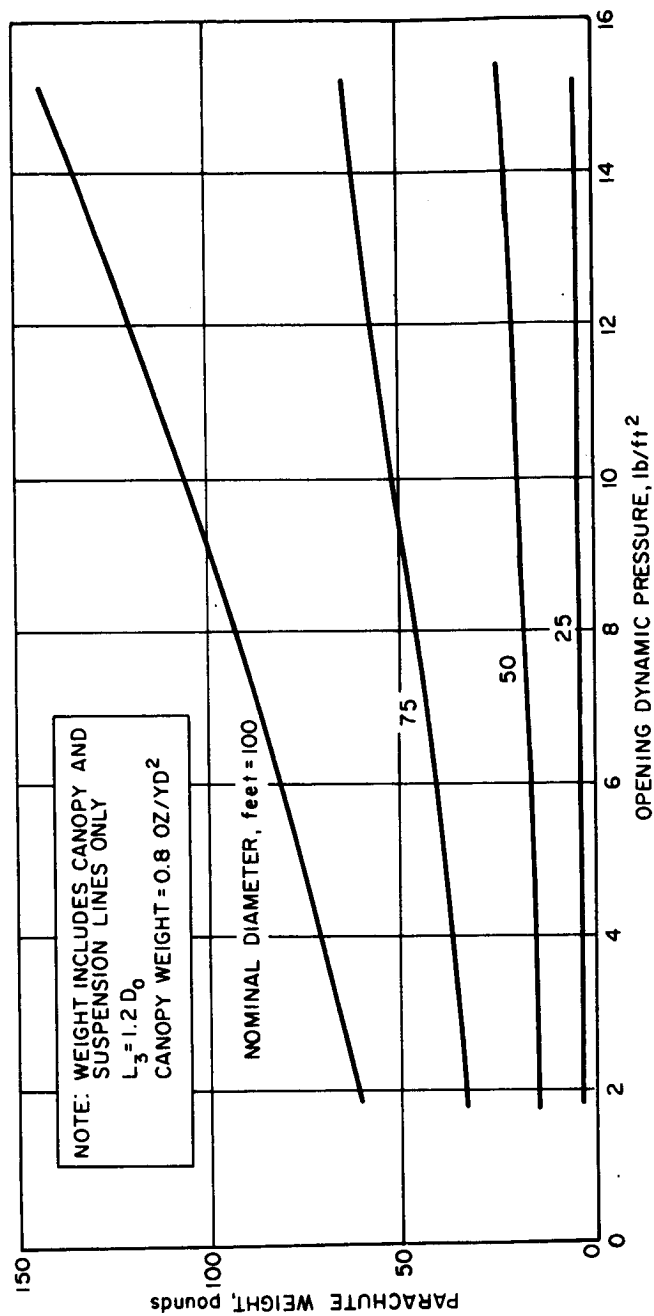
Figure 36 PARACHUTE WEIGHT VERSUS DYNAMIC PRESSURE

86-1643

The indicated parachute weight reflects only the canopy and shroud lines. The weight of the riser line swivel, pilot parachute, and canisters would additionally have to be included. For the reference 81-foot nominal diameter parachute and an opening dynamic pressure of 5 psf, Figure 36 indicates a canopy and shroud line weight of 54 pounds. An additional 14 pounds for the riser line, swivel, pilot chute and deployment canisters brings the total parachute system weight to 70 pounds (see Volume 5 Book 6, paragraph 2.5.5.5).

Table XIII presents the extreme range of deployment altitudes at Mach 1.2 for each of the atmospheres considered. The maximum parachute deployment altitude results in the VM-3 atmosphere. Figure 37, which plots descent time versus deployment altitude for the reference $AMC/W_{Susp}$ of 5.0 $ft^2$/pound, indicates descent times as high as 660 seconds in the VM-3 atmosphere (a 2500-foot altitude excursion is assumed for initiation, deployment, and full inflation). This exceeds the maximum allowable descent time by some 300 seconds. Hence, in order to ensure descent times within the minimum and maximum range for all atmospheres and trajectories, considered, a restriction on the deployment altitude must be imposed. For the VM-7 atmosphere, a deployment altitude of approximately 27,500 feet is required for minimum descent-time considerations (see Figure 37). A radar altimeter and peak acceleration-time correlation are combined such that parachute deployment occurs when the altitude is less than 27,500 feet and the Mach number is less than 1.2 (see paragraph 6.8.4 of this book). The last column of Table XIII indicates that with these deployment conditions, the maximum descent time is 320 seconds while the minimum is 168 seconds. This satisfies the design constraints. The vertical impact velocities for the $AMC/W_{Susp}$ of 5.0 $ft^2$/lb, are 90, 68, 128 and 89 fps in the VM-3, 4, 7, and 8 atmospheres, respectively.

TABLE XIII

TRAJECTORY AND DEPLOYMENT CONDITIONS
$(M/C_DA = 0.22$ slug/$ft^2$)

| ATM | $V_e$ (ft/sec) | $\gamma_e$ (degrees) | $Z_M = 1.2$ (feet) | $(D/W)_{max}$ | t Z at M= 1.2 (seconds) | t Z = 27,500' (seconds) |
|---|---|---|---|---|---|---|
| VM-3 | 12,000 | -14.7 | 72,556 | 4.41 | 630 | 258 |
| ↑ | 15,000 | -14.0 | 77,213 | 4.06 | 660 | ↑ |
| VM-4 | 12,000 | -14.7 | 38,552 | 11.87 | 437 | 320 |
| ↑ | 15,000 | -14.0 | 42,438 | 7.62 | 475 | ↑ |
| VM-7 | 12,000 | -14.7 | 40,404 | 4.42 | 255 | 170 |
| ↑ | 15,000 | -14.0 | 44,801 | 3.86 | 280 | ↑ |
| VM-8 | 12,000 | -14.7 | *20,631 | 12.24 | *168 | N/A |
| ↑ | 15,000 | -14.0 | *25,096 | 7.45 | *205 | N/A |

*Deployment occurs at Mach 1.2 in the VM-8 atmosphere (note the asterisk altitudes) and at 27,500 feet in the VM-3, 4 and 7 atmospheres.
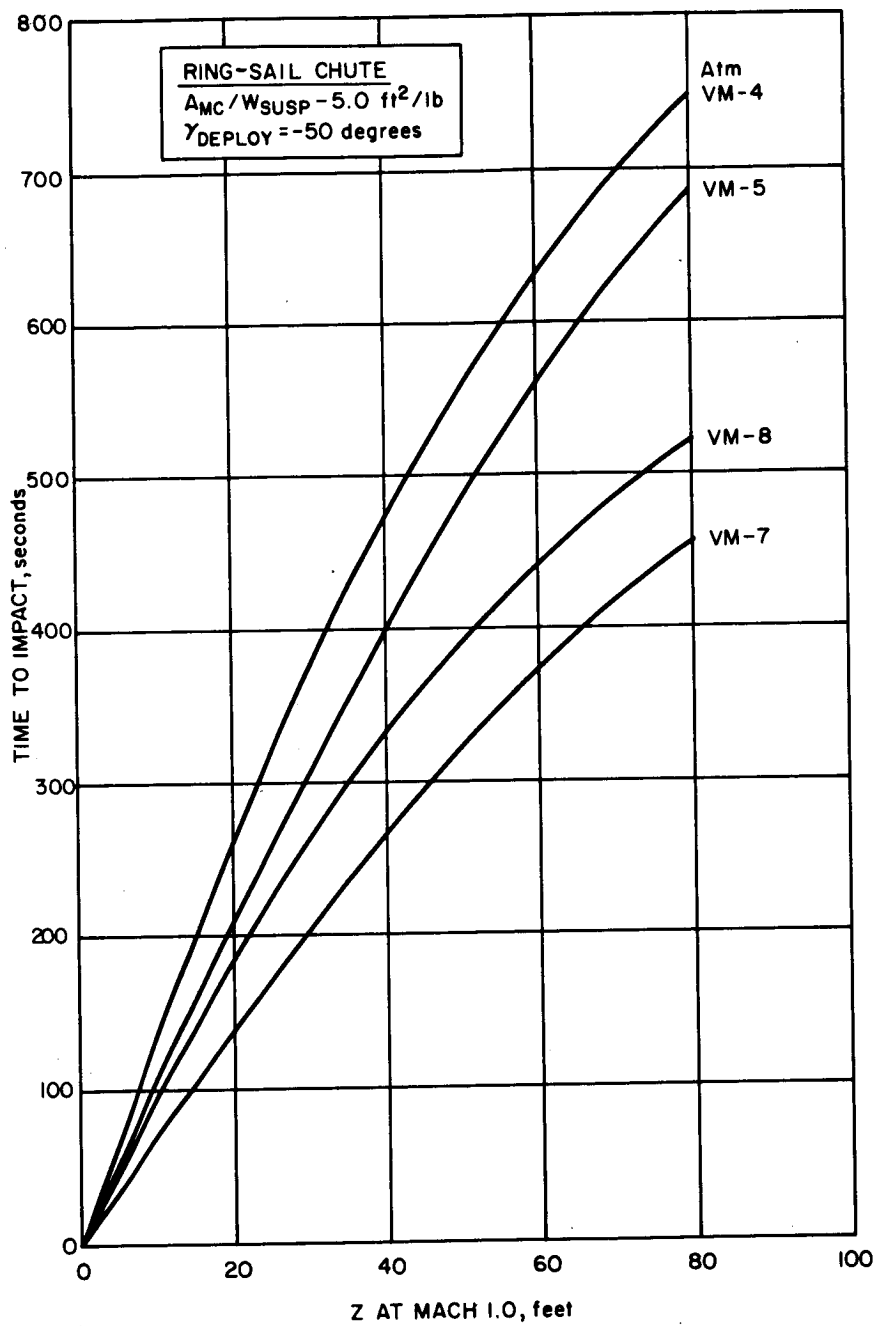
Figure 37 PARACHUTE DESCENT TIME VERSUS DEPLOYMENT ALTITUDE

862189

-100-

### 4.7.3 Mechanization

The descent system consists of a pilot chute which is mortared out of its canister. The pilot chute in turn pulls the main parachute out of its canister in a fully inflatable condition. Satisfactory operation of the descent system is dependent upon proper initiation of the system and, to an even larger degree, the separation mechanisms used to accomplish the deployment sequence. Mach number cannot be sensed directly, but it is correlated with the magnitude of the peak entry acceleration and the time from peak acceleration to the Mach number desired.

Figure 38 is a plot of peak acceleration versus time from peak acceleration to Mach 1.2. Data are shown for the range of entry velocities, atmospheres, and entry angles considered (see Volume 5, Book 6, paragraph 2.5.3). A curve fit of all the data results in the expression shown on Figure 38 which relates entry velocity, ($V_e$) peak acceleration (Gmax) and the resultant time excursion ($\Delta t$). The curve fit ensures initiation at Mach 1.2 or less for all trajectories considered and also results in a minimum deployment altitude of 19,900 feet.

Implementation of this reference initiation system requires the sensing of altitude via a radar altimeter and also the sensing of vehicle axial acceleration. The magnitude of the peak acceleration is read into an analog circuit along with the entry velocity to ascertain the required $\Delta t$. At peak acceleration, a timer is started and at the end of the required $\Delta t$, initiation takes place.

At initiation, a signal is sent to an electrical squib which in turn ignites the mortar change. The mortar fires the pilot chute out of its canister at 100 ft/sec. The pilot chute in turn pulls the main chute out of its canister. In the event the mortar fails to fire the pilot chute, a gas generator is employed as a backup, ejecting the main parachute directly out at 30 ft/sec.

## 4.8 ENTRY SHELL

### 4.8.1 Design Environments

The variation of entry shell-design conditions with entry mode is significant, although the entry conditions are mild compared to the previously studied entry from the approach trajectory. Nominal entry, with proper operation of the ACS results in near zero entry angle of attack. The possible failure modes must be considered however, to establish the actual design conditions. The designing failure mode results from an ACS failure. The ACS is designed with full redundancy in the reaction control system. A single failure can be accommodated without loss of full control. However, the inertial reference system might fail, resulting in an erroneous command signal to the reaction control system. A rate sentry is used to disable the reaction
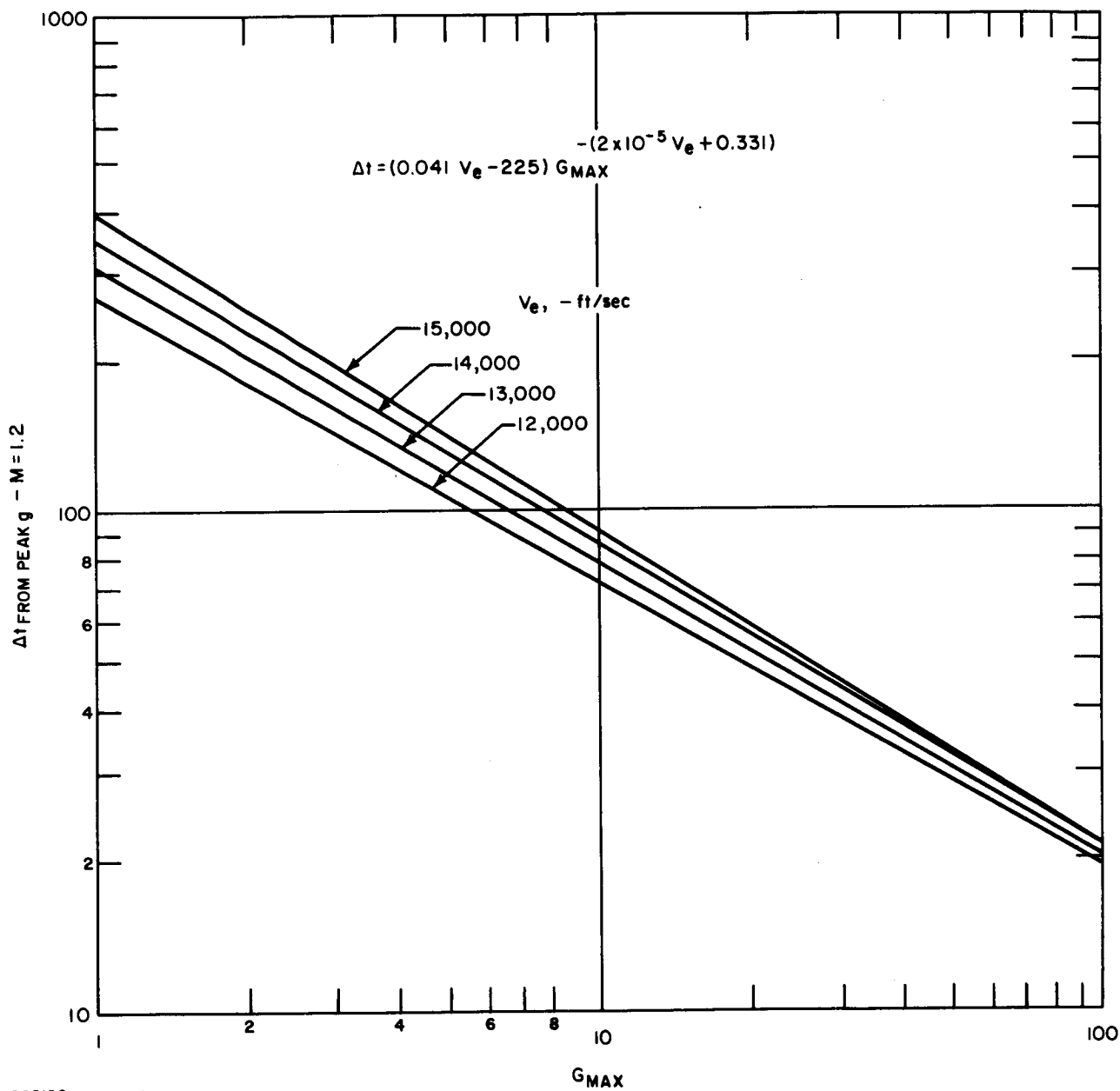
Figure 38  PARACHUTE DEPLOYMENT LOGIC

862190

-102-

control system if the rates about any axis exceed 6 deg/sec. Failure mode entry, therefore, must consider the entry vehicle at a random entry angle of attack and body rates up to 6 deg/sec (0.1 rad/sec) about any axis.

A $V_e$ - $\gamma_e$ map was established (see paragraph 5.1) which defines the range of entry velocities and entry angles for which the entry shell must be designed. The $V_e$ - $\gamma_e$ map considers the entire range of orbits and the predicted dispersions in these parameters due to execution errors at flight capsule separation and deorbit. Figure 45 shows the established $V_e$ - $\gamma_e$ map. The nominal $V_e$ - $\gamma_e$ conditions are indicated as well as the range extension conditions, included to improve the operational flexibility of the flight capsule (see Section 9.0).

Syrtis Major was considered as the desired impact area, taking into account the rotating planet effects with entry from southwest to northeast (entering with the planet rotation), at an angle of 40 degrees to the equatorial plane. The latitude at entry (800,000 foot altitude) was 5 degrees south.

### 4.8.1.1 Loads

The maximum loads were associated with rearward entry at a spin rate of 0.1 Rad/sec. The loads are summarized in Table XIV. The design loads were obtained for entry along the equator in the direction of planet rotation since initial analysis indicated that this resulted in maximum loads. When considering Syrtis Major as the desired impact area (with orbital inclinations between 40 to 60 degrees) the critical loads experienced differ. The nominal case was obtained for the nominal entry angle ($\gamma_e$ = 15 degrees) at the maximum velocity under consideration with entry inclined at 50 degrees to the equator. The loads to be experienced for the critical heating entry (VM-7 atmosphere) occur when the orbit is at a maximum inclination, the entry angle being -14 degrees. The actual maximum loads encountered for a Syrtis Major impact show the conservative nature of the selected design loads. The primary effect of considering planet rotation on the loads is reflected in the effective steepening of the trajectory, due to the lower relative entry velocity. This effect also results in a shallower entry angle for the skipout limit.

### 4.8.1.2 Heating

The heating environments are summarized in Table XV in terms of peak rates and integrated heating for the stagnation and the maximum diameter points. The design conditions were selected without rotating planet effects on the basis of preliminary analyses which indicated that maximum integrated heating was associated with no rotation. The critical heating associated with Syrtis Major as the impact area is lower as shown in the table. The evaluation of the heating for the critical loads entry case results in significantly lower heating as is to be expected

## TABLE XIV

### LOADS SUMMARY

$( a_e = 179 \text{ degrees} \quad P = 0.1 \text{ rad/sec} )$

| | Reference | Syrtis Major Impact | | |
|---|---|---|---|---|
| | Design | Nominal (particle) | Heating (Critical Design Point) | Loads (Critical Design Point) |
| $V_e$ Inerital $\gamma_e$ Coordinates | 15,200 | 15,200 | 15,200 | 15,200 |
| | -16 | -15 | -14 | -16 |
| Atmosphere | VM 8 | VM 8 | VM 7 | VM 8 |
| Aximuth (deg) | non-rotating | 50 | 60 | 40 |
| Maximum x/w | | | | |
| x/w (g) | 15.9 | 10.1 | 4.1 | 13.6 |
| n/w (g) | 0.61 | 0.01 | 0.22 | 0.54 |
| $q_\infty$ (psf) | 114.6 | 72.0 | 31 | 98.3 |
| $a_E$ (deg) | 10.3 | 0.28 | 13.5 | 10.1 |
| $\dot{a}_E$ (rad/sec) | 1.63 | 0.03 | 0.9 | 1.6 |
| $\ddot{a}_E$ (rad/sec$^2$) | 15.0 | 0.25 | 4.3 | 15 |
| Maximum n/w | | | | |
| x/w (g) | 15.7 | 8.5 | 3.2 | 11.5 |
| n/w (g) | 0.71 | 0.01 | 0.25 | 0.61 |
| $q_\infty$ (psf) | 113.2 | 60 | 27.5 | 83 |
| $a_E$ (deg) | 13.8 | 0.39 | 16.7 | 13.5 |
| $\dot{a}_E$ (rad/sec) | 1.53 | 0.03 | 1.2 | 1.84 |
| $\ddot{a}_E$ (rad/sec$^2$) | 9.8 | 0.31 | 5.6 | 15.1 |

## TABLE XV

## HEATING SUMMARY

| | Reference | | Syrtis Major Impact | |
| --- | --- | --- | --- | --- |
| | Design (nonrotating planet) | Nominal (particle) | Heating (critical design point) | Loads (critical design point for structure) |
| $V$ (ft/sec) ⎫ Inertial Coordinates | 15,200 | 15,200 | 15,200 | 15,200 |
| $\gamma$ (degrees) ⎭ | -14 | -15 | -14 | -16 |
| Atmosphere | VM 7 | VM 7 | VM 7 | VM 7 |
| Azimuth (degrees) | - | 50 | 60 | 40 |
| $Q_s$ (Btu/ft$^2$) | 2227 | 1666 | 2030 | 1300 |
| Max $\dot{q}_s$ (Btu/ft$^2$ sec) | 18.6 | 17.8 | 20.0 | 34.0 |
| $Q_s R/N = 4.5$ (Btu/ft$^2$) | 1705 | 550 | 1333 | 745 |
| Max $\dot{q}_s$ $R/N = 4.5$ (Btu/ft$^2$ sec) | 24 | 5.9 | 15.3 | 32.2 |

-105-

(VM-8 atmosphere). The heating includes low-density effects which increase the heating by approximately 15 percent due to vorticity interaction and an additional 40 percent over the conical portion of the probe due to varying entropy effects.

## 4.8.2 Structure

### 4.8.2.1 Objectives and Requirements

The objective of the entry-shell structure design is to provide a light-weight structure which will support the ablator of the thermal protection system, maintain the proper aerodynamic contour and transmit the aerodynamic drag forces to the remainder of the flight capsule.

An efficient but not necessarily minimum weight type of construction was required for the design of the entry shell. The design was subject to practical limitations such as minimum sheet thickness so that no undue manufacturing or ground handling problems would arise. Practical structural materials whose mechanical properties were well established and manufacturing technology well developed were also specified.

The design conditions for the mission phases for the reference design are given in Table XVI. The entry conditions are also given in the table.

### 4.8.2.2 Design

An aluminum-honeycomb sandwich structure was selected for the entry shell structure.

A typical cross section of the entry shell wall consists of two 2024 aluminum alloy face sheets, 0.016-inch thick, bonded to a nominal 0.40-inch deep aluminum honeycomb core. The density of the honeycomb core is 5.7 pounds per cubic foot. It has a 3/16-inch cell and a 0.002-inch aluminum alloy foil. The outer edge of the shell is stiffened by an aluminum end ring which also supports the ACS rockets. An integral ring is provided for attachment of the suspended capsule to the entry shell and for reducing the bending and shear stresses induced by the inertial forces of the suspended capsule during the entry phase.

The forward edge of the conical portion of the shell is supported by a ring which also is the attachment point for the deployable aluminum spherical nose cap. The spherical cap is joined to the conical shell

## TABLE XVI

### SUMMARY OF DESIGN CONDITIONS FOR THE 15 FOOT DIAMETER BLUNT CONE

| Mission Sequence | Design Condition |
|---|---|
| Sterilization | 294° F for 36 hours (3 cycles) |
| Ground handling | Vibration<br><br>$\pm 2.0\ g_e$ (rms)    2 to 50 cps<br>$\pm 1.5\ g_e$           50 to 300 cps<br><br>Packaged<br><br>$\pm 1.3\ g_e$        2 to 26 cps<br>$\pm 0.036$ in da    26 to 52 cps<br>$\pm 5.0\ g_e$        52 to 300 cps<br><br>Shock<br><br>Unpackaged<br>10 $g_e$ for 11 milliseconds |
| Launch | Sustained Acceleration<br><br>-4.7 $g_e$   axial<br>2.0 $g_e$   lateral |
| Booster Separation | Unknown |
| Midcourse maneuver | -1.0 $g_e$ |
| Spaceflight cruise | Spaceflight temperature distribution<br>-100 to 150° F |
| Mars orbit injection | -2.9 $g_e$ |
| Separation of flight capsule and flight spacecraft | 1200 pound force |
| De-orbit | 3200 pound force |
| Capsule entry (Maximum axial) | Stagnation pressure      229 lb/ft$^2$<br>Angle of attack        10.3 degrees<br>Axial $g_e$             15.9<br>Normal $g_e$         0.61<br>Structure temperature    300° F |
| Capsule entry (Maximum lateral) | Stagnation pressure      226 lb/ft$^2$<br>Angle of attack        13.8 degrees<br>Axial $g_e$             15.7<br>Normal $g_e$         0.71<br>Structure temperature    300° F |
| Parachute deployment | 18,000 pounds |

at four points by explosive bolts and thrusters. Details of structure are down in the design layout, Figure 9.

4.8.2.3 Performance

The design criteria for the entry shell was shell buckling. The shell stresses had little influence on the design because of the small aero-dynamic surface pressures during entry. The maximum expected stagnation pressure is approximately 229 lb/ft$^2$. For this low surface pressure, the theoretical face-sheet thickness required for shell stability was well below practical minimum thicknesses. As a consequence, the stresses in the minimum-gage face sheet, with the corresponding core depth required for stability, were a factor of two or more lower than the allowable yield stress of the 2024 aluminum alloy.

The shell structure was analyzed for both symmetrical and unsymmetrical design loading. Unsymmetrical design loading at an angle of attack of 10.3 degrees and a stagnation pressure of 229 lb/ft$^2$ was approximately 9 percent more critical than symmetrical loading with the same stagnation pressure. The effect of the unsymmetrical loading was an increase of the circumferential stresses on the windward side with a resulting decrease in the margin of safety in buckling.

Failure modes typical of honeycomb sandwich structures such as face sheet wrinkling, extra cellular buckling, and core shear were not predicted to be critical due primarily to the minimum core density specified.

The fundamental frequencies of the entry shell were computed as a function of circumferential wave number or harmonic. The frequency of the second harmonic will be as low as 20 cps. Although this frequency approaches that of the rigid body motion of the capsule during entry, little coupling is expected because the only significant unsymmetrical component of the external surface pressure loading occurs in the first harmonic, i.e. the unsymmetrical pressure varies as the $\cos \theta$ around the circumference. The minimum frequency of the structure in this harmonic is approximately 40 cps.

The compatibility of the entry shell structure and heat shield was investigated using the limited data available on mechanical properties of the heat shield material and assuming that the zero stress temperature of the composite structure was 300°F. The results showed that at a -100°F spaceflight cold-soak condition the margin of safety of the Mod 5 purple blend ablator was 2.64 for a tensile strain failure. The results also indicated that the compressive stresses developed in the substructure were equal to the critical buckling stresses due to

-108-

the entry pressure loading. Whether the substructure could buckle due to this thermal loading depends upon the integrity of the bond between the ablator and substructure. No information is presently available on the bond strength requirement for this mode of failure; hence a conservative approach should be used which assumes that the structure can buckle when subjected to the above conditions. This problem can be alleviated with a very small weight penalty by increasing the core depth.

After establishing the design of the shell for the entry design loading condition, the design was varied as a function of pressure and diameter using a symmetrical pressure distribution. For the reference design condition, the structural shell weight was 268 pounds, including any contingency weight. It does, however, include a margin of safety of 1.25.

## 4.8.3 Heat Shield

### 4.8.3.1 Objectives and Requirements

The requirements imposed on the heat shield parallel those for the structure through the mission sequence from the factory to parachute deployment. During the spaceflight phase, the heat shield is aided by the thermal control system and together they assure integrity of the structure and of the payload.

The assurance of the integrity of the structures and of the payload through attenuation of the external thermal environment during entry is the primary objective of the heat shield. Practical ablative materials were to be considered; minimum weight was not the overriding consideration.

The satisfaction of the design conditions is predicated on the availability, selection, and understanding of the behavior of appropriate heat shield materials, i.e., materials displaying a proper combination of thermal, optical and ablative characteristics. As a result, complex interactions have to be considered in establishing the heat-shield design and material specifications.

On the other hand, the weight of the heat shield is sensitive to the initial conditions (temperatures) existing at the onset of entry. These temperatures depend on the thermal control exercised prior to entry with the attendant flight spacecraft-flight capsule interface, (see paragraph 4.9) and post separation problems. In addition to the environmental, structural and material requirements present in any entry vehicle design, a set of thermal control design constraints exists on the heat shield (or vice versa).

Finally, the requirement for decontamination and sterilization imposes a constraint on the selection of heat-shield materials from the beginning of the design process, limiting the choice to only such materials as can satisfy this stringent requirement.

A summary of design conditions used for the reference design is given in Table XVII.

The additional system requirements imposed by the definition of the normal and failure modes of entry are discussed in paragraph 5.3. These failure mode requirements involve consideration of critical atmosphere (VM-7), entry angle (-14 degrees) and velocity (15,200 ft/sec), $M/C_DA$ selection, (0.22 slug/ft$^2$) planet rotation (influenced by landing site selection), and spin, tumble and angle of attack effects.

## 4.8.3.2 Design and Performance

An ablative thermal protection system consisting of Purple Blend, Mod 5 ablator, backed up by a ply of fiberglass with stiffened loops protruding into the ablator (for improved mechanical integrity of the decomposed material) was selected for the reference design. This composite was then bonded to the load-carrying structure. The detail of this design was shown previously in Section 3.0. A similar concept but without fiberglass and loops was utilized on the secondary and afterbody heat shield. In local areas of possible aggravation, higher density refrasil phenolic inserts were recommended. The heat-shield thickness requirement for the primary (forebody) is shown in Table XVIII, and for other areas requiring thermal protection (except the rocket nozzle) in Table XIX, for the design condition and criteria summarized in Table XVII. The performance of the heat shield (temperature and density distributions and history and mass loss variation) was calculated for various design conditions and subsequently used in thermo-structural analysis. The required heat-shield weight and weight fraction for the various entry modes was also calculated and the resulting weight fraction (primary) for the reference design was determined as 12 percent. The calculated weight for the primary heat shield not including contingency, but including allowance for manufacturing, mounting pad and bond was 253.5 pounds while the secondary was 55.4 pounds.

The design criteria utilized in the design were nominal. Depending on the actual initial entry temperatures, and allowable bond-line temperature the weight-requirements or heat-shield response will deviate from nominal. For example, the initial temperature at entry calculated for the assumed flight spacecraft-flight capsule interface was found to be less than 25°F (see paragraph 4.8) rather than the nominal 100°F. This would either permit lower heat-shield

## TABLE XVII

## SUMMARY OF HEAT SHIELD DESIGN CONDITIONS
## BLUNTED CONE

| | |
|---|---|
| Diameter | 15 feet |
| Entry weight | 2040 pounds |
| Entry velocity | 15, 200 ft/sec (max) |
| Entry angle | -14 degrees |
| Atmospheric model | VM-7 |
| $M/C_D A$ | 0.22 slug/ft$^2$ |
| Entry angle of attack | 90 degrees |
| Total integrated heating | 2227 Btu/square foot |
| Maximum heating rate | 18.6 Btu/ft$^2$-sec |
| Duration of heating pulse | 240 seconds |
| Heat shield material | Purple Blend (Mod 5) |
| Structure material | Aluminum Honeycomb (2024) |
| Bond-line temperature | 500 °F |
| Entry temperature | 100 °F |
| Safety factor | 1.2 |

## TABLE XVIII

### PURPLE BLEND HEAT-SHIELD REQUIREMENTS

| Station S/RN | Purple Blend (inches) | Fiberglass (inches) | RTV Bond (inches) | Total Local Weight (lb/ft$^2$) | Structure (inches) |
|---|---|---|---|---|---|
| 0.0 | 0.100 | . 0.010 | 0.020 | 0.45 | 0.600 AL |
| 1.5 | 0.283 | | | 1.08 | 0.452 HC |
| 2.5 | 0.268 | | | 1.03 | |
| 3.5 | 0.252 | | | 0.97 | |
| 4.0 | 0.239 | | | 0.93 | |
| 4.5 | 0.318 | | | 1.2 | |
| 4.56 | 0.318 | ↓ | ↓ | 1.2 | 0.050 AL |

## TABLE XIX

### AFTERBODY, SECONDARY, AND ANTENNA HEAT-SHIELD REQUIREMENTS

Afterbody Heat Shield Requirements
    0.072 inch
    Bond 0.020 inch RTV
    Structure 0.020-inch aluminum

Secondary Heat Shield Requirement
    0.054 inch
    Bond 0.020 inch RTV
    Structure 0.020-inch aluminum

Antenna Heat Shield Requirement
    Teflon 0.217 inch

OTWR Inserts
    0.66 inch

weight, or would increase the present safety margin. However, until the thermal control interface is defined, a flexible design must be maintained. The considerations involving selection and characteristics of the material, the effect of the entry velocity-entry angle-diameter- and entry mode variations are discussed in paragraph 5. 3.

## 4.9 THERMAL CONTROL SYSTEM

### 4.9.1 Objectives and Requirements

The main objective of the thermal control system is to maintain the electronic components, batteries, structural members, and heat shield within their operating temperature limits as prescribed by their operative and nonoperative conditions in the various phases of flight. The thermal-control subsystem must be compatible with the spacecraft, including the heater power available, within the general weight allocations. The thermal control system must be compatible with other systems, allowing for departures from nominal performance conditions (failure modes) during all the phases of the mission. To provide for reliable operation, it should minimize the requirement for active elements and assure that its passive elements do not degrade the performance of other materials and are not degraded by other materials.

A specific requirement was imposed on the thermal control system to minimize the disturbance to the flight capsule at flight capsule separation. Prior to separation, power available from the flight spacecraft for flight capsule heating was limited to a reasonable level; specific determination of the heater power requirements await detailed specification of the flight capsule-flight spacecraft thermal interface. It is necessary for proper design and performance evaluation, to specify the thermal interface between the flight spacecraft and the flight capsule. This is necessary to determine the relationships between the various allowable capsule temperatures, power available for heating and the optical property requirements for the control coatings. The lack of such thermal interface information made it necessary to make certain assumptions with respect to either the interface geometry or its thermodynamic state. Several alternatives were studied. Assumptions relating to interface geometry were made based on data published in the literature. This interface assumption was shown to be conservative, resulting in the lowest temperatures for critical components and the heat shield.

The temperature limitations of the system components, the critical phases of their operation, and design approach used are shown in Table XX, the design conditions and requirements for each mission phase are shown in Table XXI, while Figure 39 below shows the geometrical configuration of the flight spacecraft -flight capsule interface.

TABLE XX

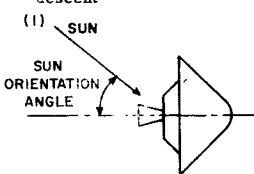## TEMPERATURE LIMITATIONS FOR STRUCTURAL MEMBERS AND COMPONENTS

| Subsystem or Component | Location | Typical Temperature Specification (°F) | | Critical Phase of Operation or Environment | Thermal Design Approach |
|---|---|---|---|---|---|
| | | Nonoperative | Operative | | |
| 1. Flight Capsule | – | | | | |
| Entry shell structure | – | -100 (a) | | Mars cruise and orbit | Heaters installed in the H/S (1) using FS power |
| Entry shell heat shield material | | -100 to +300 | -100 (b) | | |
| Sterilization canister | | -150 to +300(c) | | Cruise, midcourse maneuver | High $a/\epsilon$ |
| 2. Power and power control Battery | Telecommunication & Power Module | -65 to +160 | +40 to +160 | Mars cruise and orbit (low temperatures) Preparation to entry (high temperatures | Insulation and (2) heaters using FS power. Insulation and heat sink. |
| 3. Telecommunications | Same as battery | -65 to +275 | 0 to +175 | Same as battery | Same as battery (2) |
| 4. Data handling | Same as battery | -65 to ±275 | 0 to +175 | Same as battery | Same as battery (2) |
| 5. Engineering experiment | Instrumentation module | -40 to +140 | 0 to +100 | Same as battery | Same as battery (1)(2) |
| Accelerometers | Suspended capsule | -65 to +275 | 0 to +175 | Same as battery | Same as battery (2) |
| Penetrometers | Same as accelerometers | -65 to +275 | 0 to +175 | Same as battery | Same as battery (2) |
| Television | Suspended capsule | 0 to +140 | +20 to +100 | Parachute descent to impact | Insulation and (1)(2) heaters using FS power |
| 6. Retrorocket subsystem | Suspended capsule structure | -40 to +175 | -40 to +175 | Mars cruise and orbit | Insulation and (1) heaters using FS power (if required) |
| 7. Attitude control subsystem | | | | | |
| Reaction control | Entry shell | -100 to +275 | | Preseparation to entry | None |
| Tank-cold gas | Suspended capsule structure | -100 to +275 | | Preseparation to entry | None |
| Platform | Suspended capsule structure | -65 to +275 | 0 to +175 | Preseparation to entry | Insulation and (2) heaters and FS power during cruise (if required) and preseparation |
| Sentry gyro | Suspended capsule structure | -65 to +275 | 0 to +175 | Preseparation to entry | (2) |
| 8. Thrust vector control subsystem | Entry shell | -100 to +300 | | Preseparation | None required |
| 9. Parachute subsystem | Suspended capsule structure | -100 to +150 | | Entry parachute descent | Insulation for entry heating |
| 10. Separation systems | Various | -160 to +300 | | Mars cruise to entry | None required |

(a) As required by thermal structural compatibility with the heat shield
(b) Tentative for Purple Blend Mod 5
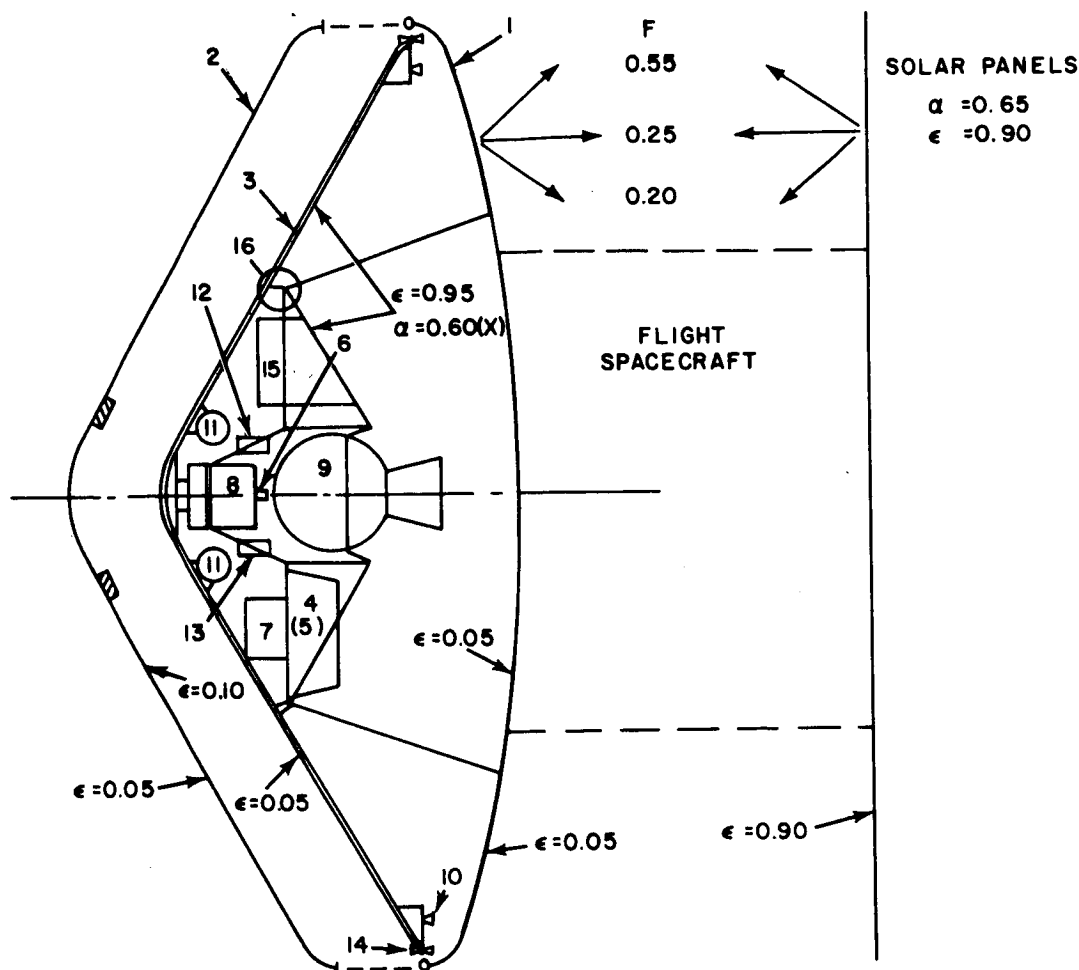(c) Limitations defined by structural design requirement

(1) Power required during FS cruise and orbit
(2) Preseparation power required for heating to minimum operating temperature

TABLE XXI

REFERENCE DESIGN CONDITIONS AND REQUIREMENTS

| Phase | Environment | Condition or Requirement |
|---|---|---|
| 1. Prelaunch Decontamination/ sterilization | ETO decontamination and temperature cycle (294°F) | Conductive, convective and radiative heat interchange. Internal power to reduce temperature gradients and shorten heat-up times. |
| 2. Cruise* <br> Near Earth | Space; FC in shade of FS | Radiative heat interchange between FS solar panel backface and canister base. Power from FS available if required to heat critical components. |
| Midcourse maneuver | Space; FC in Sun (Earth intensity) | Total maneuver time assumed 3 hours. No fixed FC orientation relative to the Sun. |
| Near Mars | Space; FC in shade of FS | Decrease radiative FS solar panel backface/canister base interchange. Power from FS available if required to heat critical components. |
| 3. Mars Orbit* <br> Orbit injection maneuver | Space; FC in Sun (Mars intensity) | Maneuver time: 1 to 4 hours. No fixed FC orientation relative to the Sun. |
| Orbit | Space; FC in shade of FS, planetary thermal effects | Time in orbit: 3 to 10 days <br> Orbital data: hp = 700, 1000, 1500 km <br> ha = 4000, 10,000, 20,000 km <br> Orbit inclination: 40 to 60 degrees <br> Selected orbits: $h_p$ $h_A$ <br> (A) 700 x 20,000 <br> (B) 1000 x 10,000 (nominal case) <br> (C) 1500 x 4000 |
| Preseparation | | Power available from FS to heat H/S and critical components. Time: 242 minutes before separation; all equipment "on". |
| 4. Postseparation | Space; Entry vehicle in Sun, orientation depends on orbital parameters | Maximum time in orbit after separation: 0.5 hours. |
| De-orbit | | Maximum time de-orbit to entry: 0.5 hours. |
| De-orbit to entry | | Non spinning (tumbling) vehicle <br><br> Sun orientation: Orbit    Sun orientation angle (1). <br> (A) 14 degrees <br> (B) 24 degrees <br> (C) 61 degrees <br><br> All equipment "on" through impact; power from FC battery. |
| 5. Entry | Entry heating | Time from entry to chute deployment: <br><br> Min: 301 seconds (VM8, $V_e$ = 14,150 ft/sec, $\gamma_e$ = 15.8 degrees) <br><br> Max: 415 seconds (VM3, $V_e$ = 15,200 ft/sec, $\gamma_e$ = -14.6 degrees) <br><br> Max heating:    (VM7, $V_e$ = 15,200 ft/sec, $\gamma_e$ = 14.6 degrees $t_e$ = 348 sec) |
| 6. Parachute descent | Mars atmospheric environment | Parachute descent time |

(1)

SUN

SUN ORIENTATION ANGLE

| | | Chute Deployment | |
|---|---|---|---|
| Atm | time | Velocity (fps) | Altitude |
| VM3 | 249 | 660 | 27,500 feet |
| VM4 | 324 | 540 | 27,500 feet |
| VM7 | 171 | 915 | 27,500 feet |
| VM8 | 163 | 816 | at M = 1.2 |

(All data for $\gamma_e$ = 50 degree; A/W = 5 ft$^2$/lb)

*FS-FC interface data not available for assumed configuration and conditions (See figure 39).

F
0.55
0.25
0.20

SOLAR PANELS
$\alpha$ =0.65
$\epsilon$ =0.90

$\epsilon$ =0.95
$\alpha$ =0.60(X)

FLIGHT
SPACECRAFT

$\epsilon$ =0.05

$\epsilon$ =0.05

$\epsilon$ =0.10

$\epsilon$ =0.05

$\epsilon$ =0.05

$\epsilon$ =0.05

$\epsilon$ =0.90

1. CANISTER BASE
2. CANISTER LID
3. ENTRY SHELL
4. TELECOMMUNICATIONS AND POWER
   MODULE (2)
5. INSTRUMENTATION MODULE
6. ACCELEROMETERS (3)
7. PENETROMETERS (4)
8. TELEVISION
9. ΔV PROPULSION

10. ACS REACTION NOZZLES (12)
11. ACS COLD GAS TANKS (2)
12. ACS ELECTRONICS
13. ACS SENTRY GYRO
14. TVC REACTION SUBSYSTEM (4)
15. PARACHUTE
16. ENTRY SHELL SEPARATION
    MECHANISM
X. PURPLE BLEND,
   UNCOATED

86 2191

Figure 39  FLIGHT CAPSULE – FLIGHT SPACECRAFT INTERFACE

## 4.9.2 Design and Performance

The trade-off studies performed for the reference design and typical mission sequence revealed that a) the critical consideration governing the selection of the thermal control system and, thus, the power drain imposed on the flight spacecraft was the flight capsule-flight spacecraft thermal interface configuration, and b) the near-Mars orbit phase was the critical phase of the operation (although space cruise was quite similar) because of separation of the sterilization canister lid prior to orbit injection.

The recommended thermal control system is shown in Figure 39 together with the interface configuration and characteristics used in the design and performance studies. The system consists of low emissivity ($\epsilon = 0.05$) coatings on the external surface of the sterilization canister lid ($\epsilon = 0.10$ internal) as well as $\epsilon = 0.05$ coating on the face of the primary heat shield and on both faces of the sterilization canister base facing the flight-capsule afterbody and the flight spacecraft. The face of the secondary heat shield and the afterbody surface are not coated with a thermal control coating, since the emissivity of the heat shield material (or of a selected sealer/paint) is acceptable from the thermal control viewpoint. This acceptability simplifies the development and manufacturing efforts. Heating elements required to maintain the heat shield temperature above the specified minimum are imbedded in the heat-shield substructure, and those required either to maintain the components within specified limits during interplanetary cruise and Mars orbit, or to warm the components up to their operative temperatures prior to separation, are located near the components. The components are insulated as required. Power requirement to the heat shield amounted to a nominal 200 watts, while additional power requirement to the components varied from 10 watts during cruise and Mars orbit to a peak additional requirement for warm up prior to separation of up to 180 watts, depending on the mode of power supply (on-off) selected for the heat shield. The total peak demand would amount to 30 to 130 watts above the nominal 200 watt requirement. The actual power usage will be regulated by thermostatic controls, preset to the desirable temperature limits.

The performance studies for the preceding system were made in several steps. First, power requirement was established for heating the components only, and the resulting heat-shield temperatures were established. Secondly, the power was supplied to the heat shield alone, and component temperatures were calculated. It was thus determined that a feasible and efficient system design definitely required power to the flight capsule as, otherwise, the heat shield temperatures fell below -150°F, while the component environment reached approximately -140°F. Furthermore, it was established that heat must be supplied to the heat shield in larger proportion than to the components. Supplying the latter would burn them out before the heat shield reached minimum allowable temperatures while

heating of the heat shield to acceptable levels (200 watts and -27°F heat-shield temperature) would also raise the temperature of most components (telecommunications) to levels above -65°F not requiring separate heating, while others (instrumentation, TV) could be warmed up with a minimum of power (approximately 20 watts). Heaters, however, will be required for most components for warm-up prior to separation. The performance of the thermal control system reflecting the above approach for the reference configuration, typical orbit, separation and post separation mission phases is shown in Table XXII and Figure 40.

The postseparation phase did not entail any performance difficulties because of its short duration. The anticipated variation of the sun orientation angles from 14 to 61 degrees resulted in initial entry temperatures from -76 to 22°F in various parts of the vehicle which should be conducive to large heat shield weight savings (or increased safety margins), while imposing very small penalties in the structure weight (potential increase in honey-comb core depth).

Finally, the power requirement was correlated with that of the coating emissivity to establish the allowable excursion in the emissivity values due to space exposure, or to allow leeway in coating specifications, without detriment to either the component or heat-shield temperatures. The performance temperatures of components and heat shield are shown in Figure 41 as a function of the power and emissivity. This figure indicates satisfactory performance for power levels from 100 to 250 watts and emissivities ranging from 0.05 to 0.10. These performance characteristics are quite favorable as they indicate relatively small sensitivity of emissivity-power relationship within quite feasible limits.

**TABLE XXII**

**TEMPERATURE SUMMARY FOR REFERENCE DESIGN AND REFERENCE FLIGHT**

| Subsystem or Component | Ground (Sterilization) (Temp. °F) | Cruise — Near Earth Temp. (°F) | Cruise — Near Earth Power (watts) | Cruise — Near Mars Temp. (°F) | Cruise — Near Mars Power (watts) | Planetary Orbit (1) — Orbit Temp. (°F) | Orbit Power (watts) | Preseparation Warmup Temp. (°F) | Preseparation Warmup Power (watts) | Component Checkout Temp. (°F) | Component Checkout Power (watts) | Postseparation (1) Temperature (°F) | Entry Temperature Rise (°F) | Parachute Descent Temperature (°F) |
|---|---|---|---|---|---|---|---|---|---|---|---|---|---|---|
| Primary Heat Shield | 294 | | 90(2) | | 140 | | 200 | | 50(2, 4) | | 200 | | | N.A. |
| Stagnation Point | | 1-43 | | 26 | | -27 | | -69 | | -57 | | -60 | 320 | N.A. |
| Maximum Diameter | | -45 | | -39 | | -27 | | -70 | | -58 | | 53 to -12 | 320 | N.A. |
| Sterilization Canister | 294 | | | | | | | | | | | | | |
| Base | | -57 | - | -70 | - | -85 | - | -86 | - | -86 | - | N.A. | N.A. | N.A. |
| Lid | | -80 | - | -80 | - | N.A. | N.A. | N.A. | N.A. | N.A. | N.A. | N.A. | N.A. | N.A. |
| Telecommunications and Power Module (2) | 294 | | | | | | | | | | | | | |
| Battery | | -55 | - | -55 | - | -52 | - | +40 | 60 | | - | | | |
| Electronics | | -55 | - | -55 | - | -52 | - | 0 | 60 | | - | | | |
| Engineering Experiment | 294 | | | | | | | | | | | | | |
| Instrumentation Module | | -35 | 7 | -35 | 7 | -35 | 7 | 0 | 30 | | | | | |
| Television | | 5 | 3 | +5 | 3 | +5 | 3 | +20 | 30 | | | | | |
| Afterbody | 294 | -55 | - | -55 | - | -52 | - | -52 | - | -49 | | -12 to +17 | 360 | |
| ΔV Rocket | 294 | -55 | - | -55 | - | -52 | - | -52 | - | -49 | | -20 | N.A. | N.A. |
| Total Power Required, watts | | | 100 | | 140 | | 210 | | 230 | | 200 | | | |

Postseparation note (Battery / Electronics group): Temperatures approach maximum allowable operating temperatures from internal power generation before impact.

(1) Typical case (nominal orbit).

(2) Additional 50 watts during cruise near Earth would raise the heat shield temperature level by approximately 25 °F.

(2) Additional 50 watts during preseparation warmup would raise the heat shield temperature level by approximately 14 °F.

(4) Additional 100 watts during preseparation warmup would raise the heat shield temperature level by approximately 28 °F.
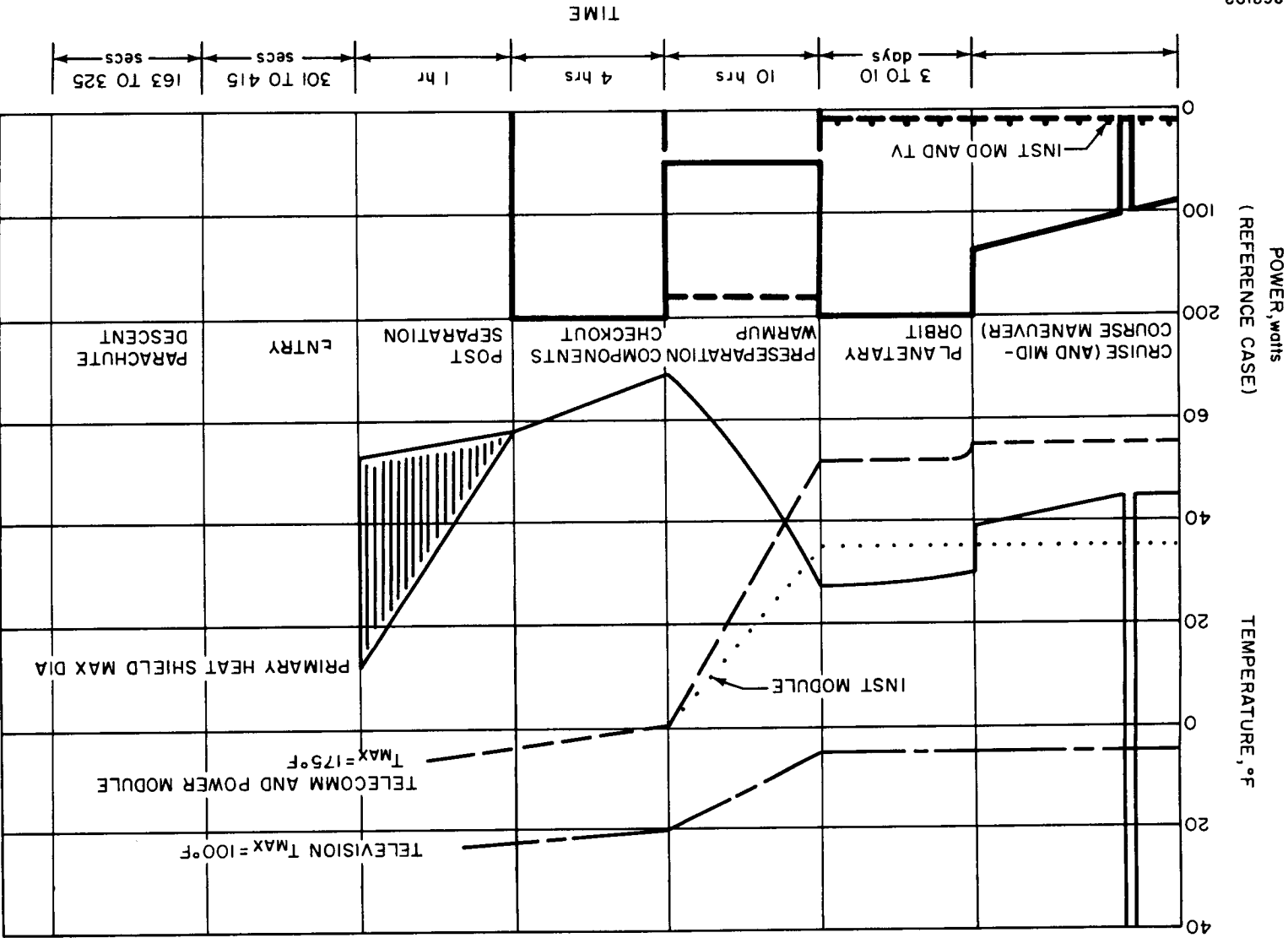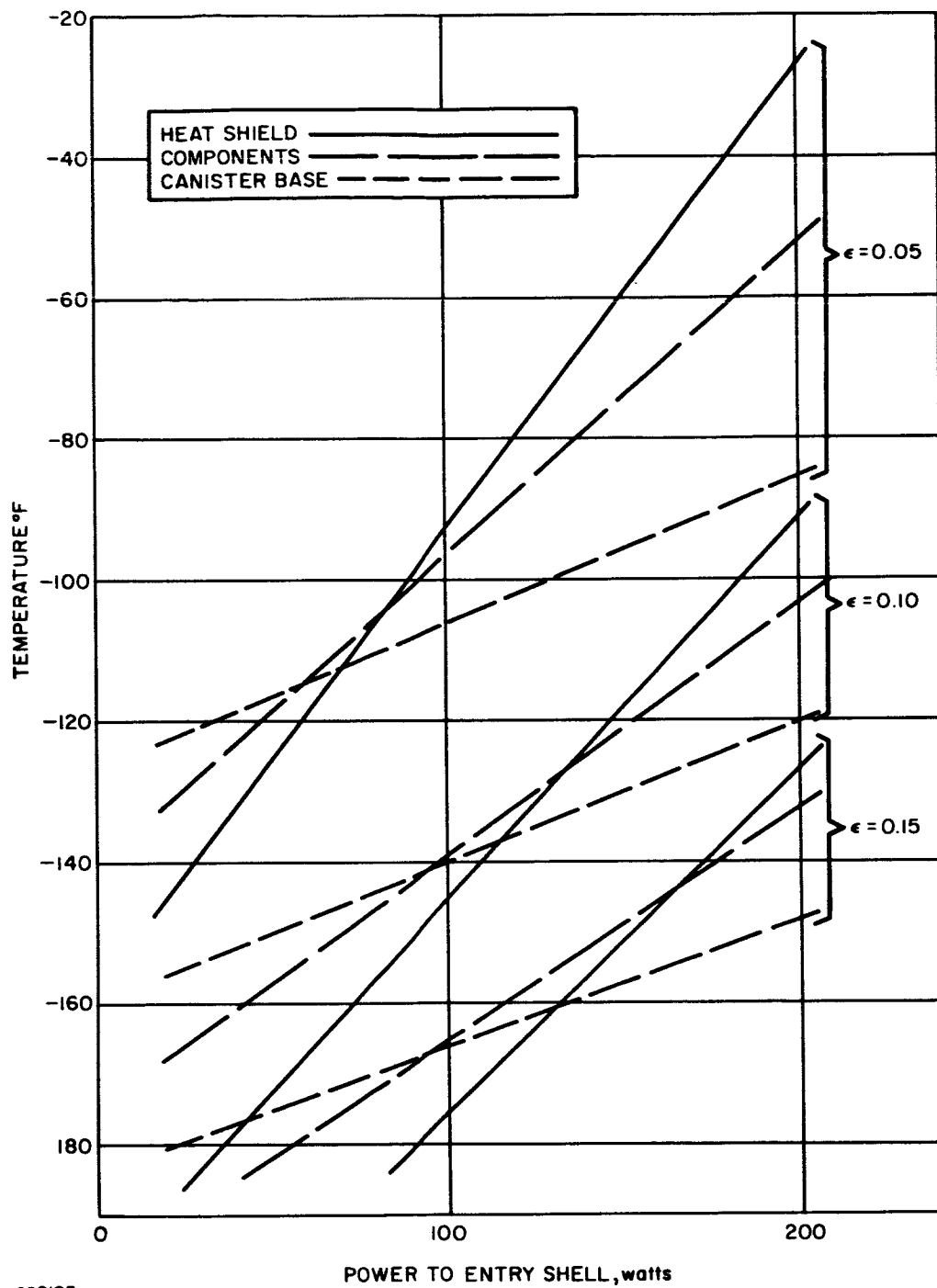
Figure 40 TEMPERATURE HISTORY AND POWER REQUIREMENTS FOR CRITICAL COMPONENTS

862192

862193

Figure 41   HEAT-SHIELD TEMPERATURE VERSUS POWER FOR ENTRY SHELL

# 5.0 ENTRY VEHICLE

## 5.1 M/$C_D$A SELECTION

The flight capsule M/$C_D$A is determined by the entry conditions, model atmospheres, and parachute deployment altitude and Mach number. Allowance must be made in the selection of M/$C_D$A for expected dispersion in each of the controlling parameters. The selected M/$C_D$A should be as high as possible to minimize the entry shell weight fraction.

### 5.1.1 Skip Out Boundary

The skip-out boundary is the minimum entry angle as a function of velocity for which the flight-path angle does not change sign during entry for the least dense model atmosphere (VM-8) considered. The skip out boundary based on particle trajectory analysis is shown on Figure 42. A dynamic trajectory skip-out boundary exists at a slightly steeper entry angle, about 1/2 degree above the particle trajectory contour. In making the M/$C_D$A selection, entry angles near the skip-out boundary should be avoided.

### 5.1.2 Parachute Deployment Conditions

The primary requirement defining parachute deployment conditions is the necessity for at least 160 seconds descent time to complete transmission of the desired data at 18,000 bits per second. This requirement can be met with various combinations of parachute size and deployment altitude in each of the model atmospheres. The VM-7 and VM-8 model atmospheres are the designing atmospheres for the parachute and M/$C_D$A respectively. Figure 43 shows parachute size as a function of deployment altitude for 170 seconds descent time (10 seconds allowed for dispersion in deployment conditions) and a suspended capsule weight of 1025 pounds in the VM-7 and VM-8 atmospheres. Reasonable parachute size, to minimize the parachute development problems, was determined to be about 80 feet diameter. This is the size of each parachute in the cluster of three used for Apollo. An 81-foot diameter parachute (area of main parachute/suspended weight, A/W of 5.0 ft$^2$/lb) was selected for the reference design. Figure 43 shows the necessary altitude for deployment of the main parachute to achieve the minimum descent time to be 19,500 feet in the VM-8 atmosphere and 27,500 feet in the VM-7 atmosphere. These deployment altitudes include a 2500 feet altitude increment for parachute inflation.

The parachute deployment Mach number should be as high as practicable to maximize the achievable M/$C_D$A. After consultation with Langley Research Center, a parachute deployment Mach number of 1.2 was selected resulting in subsonic velocities at full deployment.
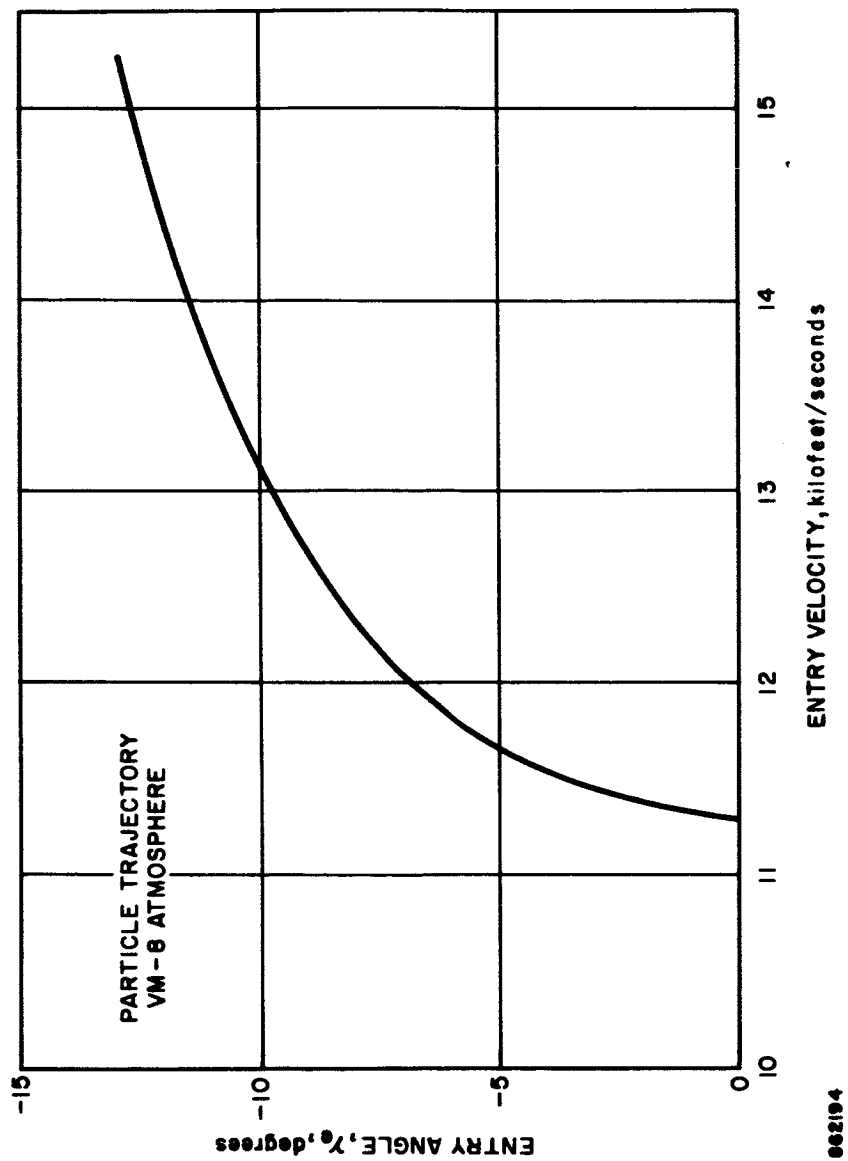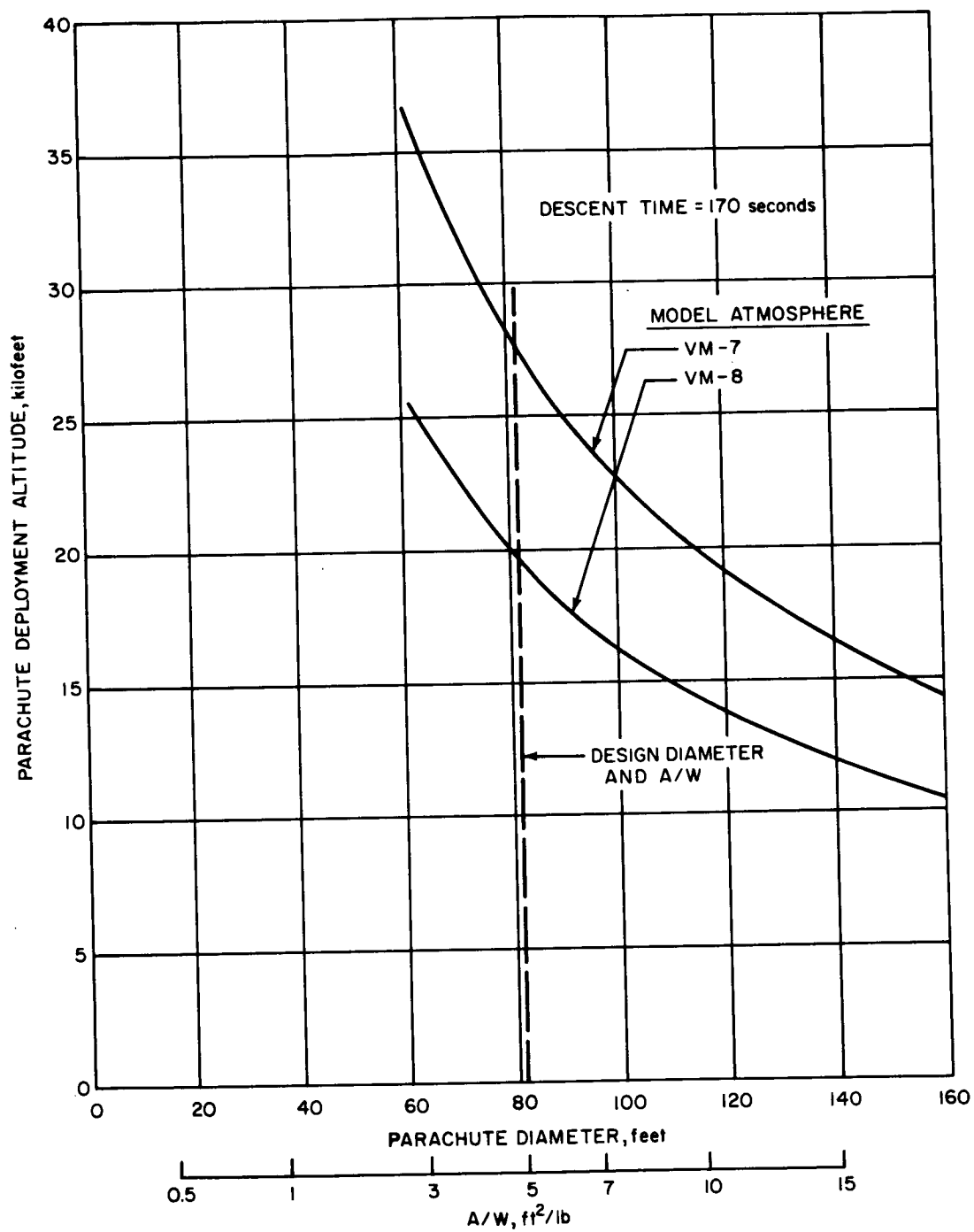
-122-

PARTICLE TRAJECTORY
VM – 8 ATMOSPHERE

ENTRY VELOCITY, kilofeet/seconds

ENTRY ANGLE, $\gamma_e$, degrees

Figure 42  SKIP-OUT BOUNDARY

662194

-123-

Figure 43  PARACHUTE SIZE VERSUS DEPLOYMENT ALTITUDE

862195

-124-

Figure 44 presents constant $M/C_D A$ contours on the entry velocity-entry angle map for the deployment conditions (20,000 feet altitude, Mach. 1.2) associated with the VM-8 atmosphere.* The skip out boundary can be seen to constrain the $M/C_D A$ achievable.

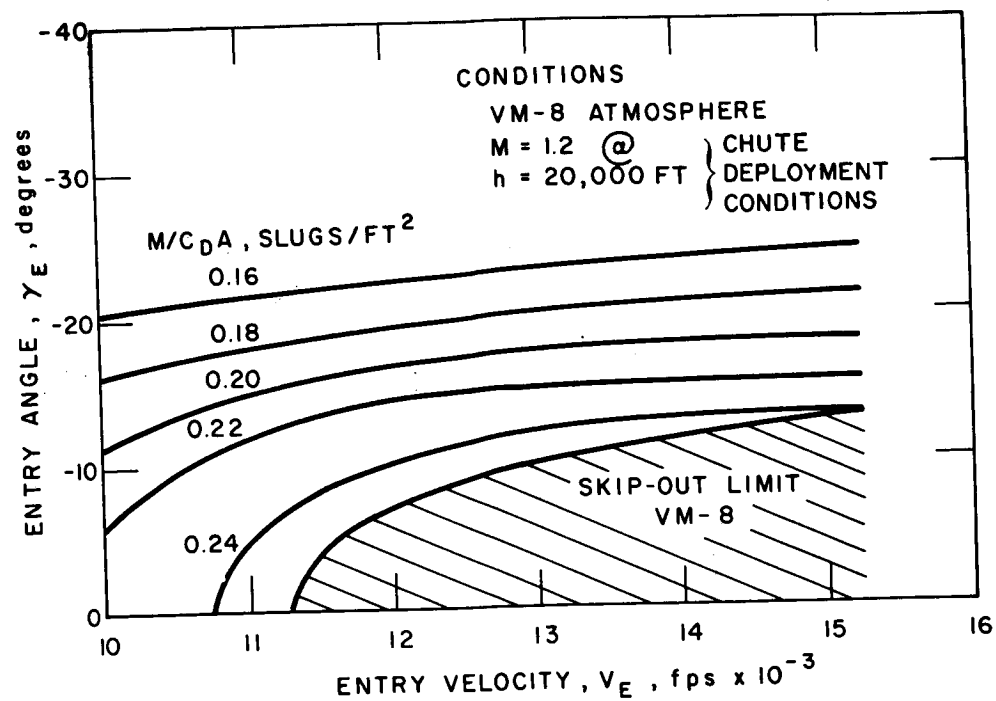### 5.1.3 Entry Angle Dispersion

Figure 45 shows the flight capsule $V_e$-$\gamma_e$ operational limits on the same entry velocity - entry angle map. The operational limits were established by examining the expected entry angle dispersion within the entry velocity limits (12,500 to 15,200 ft/sec) resulting from the range of orbits considered. The boundaries of the map labeled <u>NOMINAL</u> $V_e$ - $\gamma_e$ <u>MAP</u> represent the three sigma dispersion limits about a nominal entry angle. The $M/C_D A$ is constrained at the high velocity limit by the dynamic skip out boundary. The <u>NOMINAL</u> $V_e$-$\gamma_e$ <u>MAP</u> follows the selected $M/C_D A$ contour to lower velocities. The <u>RANGE EXTENSION</u> $V_e$ - $\gamma_e$ <u>MAP</u> is also indicated. This boundary extends the range of entry angles to lower values constrained by the dynamic skip-out boundary at all velocities. With the fixed $\Delta V$ de-orbit concept, it is possible to extend the impact point by using shallower entry angles (see Section 9.0).

### 5.1.4 Terrain Model Effects

Parachute deployment on the basis of Mach number (correlation of the time from peak entry deceleration and the value of peak deceleration with Mach number - see Volume V, Book 6, paragraph 2.5) results in proper parachute deployment in the VM-8 atmosphere, however, deployment at Mach 1.2 in the VM-3 atmosphere results in a 680-second descent time. The flight spacecraft does not remain overhead within practical communications antenna look angles for over 360 seconds for the most constraining orbit (700 x 20,000 kilometers). As a result, the parachute must not be deployed above a 27,500-foot altitude. Parachute deployment then occurs whenever the entry vehicle is below 27,500 feet altitude and below Mach 1.2. The descent time ranges from 170 to 322 seconds over the range of model atmospheres.

The parachute deployment technique results in deployment at 27,500 feet in the VM-3, VM-4 and VM-7 atmospheres; the altitude measurement being made by a radar altimeter as altitude above the local surface. In the VM-8 atmosphere, the Mach number deployment criteria governs. The deployment at 19,500 feet above mean surface altitude could result in a significantly different altitude above the local surface. The only major impact of this terrain altitude effect, for reasonable terrain altitude models

---

* The VM-7 atmosphere is denser at high altitudes than the VM-8, more than compensating for the higher parachute deployment altitude required.

CONDITIONS

VM-8 ATMOSPHERE

M = 1.2 @ } CHUTE
h = 20,000 FT } DEPLOYMENT
} CONDITIONS

$M/C_D A$, SLUGS/FT$^2$

0.16
0.18
0.20
0.22
0.24

SKIP-OUT LIMIT
VM-8

ENTRY ANGLE, $\gamma_E$, degrees

ENTRY VELOCITY, $V_E$, fps x $10^{-3}$

25-1005

Figure 44 ENTRY ANGLE VERSUS ENTRY VELOCITY ACHIEVABLE $M/C_D A$



NOMINAL $V_E$-$\gamma_E$ MAP

$\Delta\gamma_E = 6\sigma$

$M/C_D A = 0.22$

RANGE EXTENSION
$V_E$-$\gamma_E$ MAP

PARTICLE TRAJECTORY
SKIP-OUT BOUNDARY

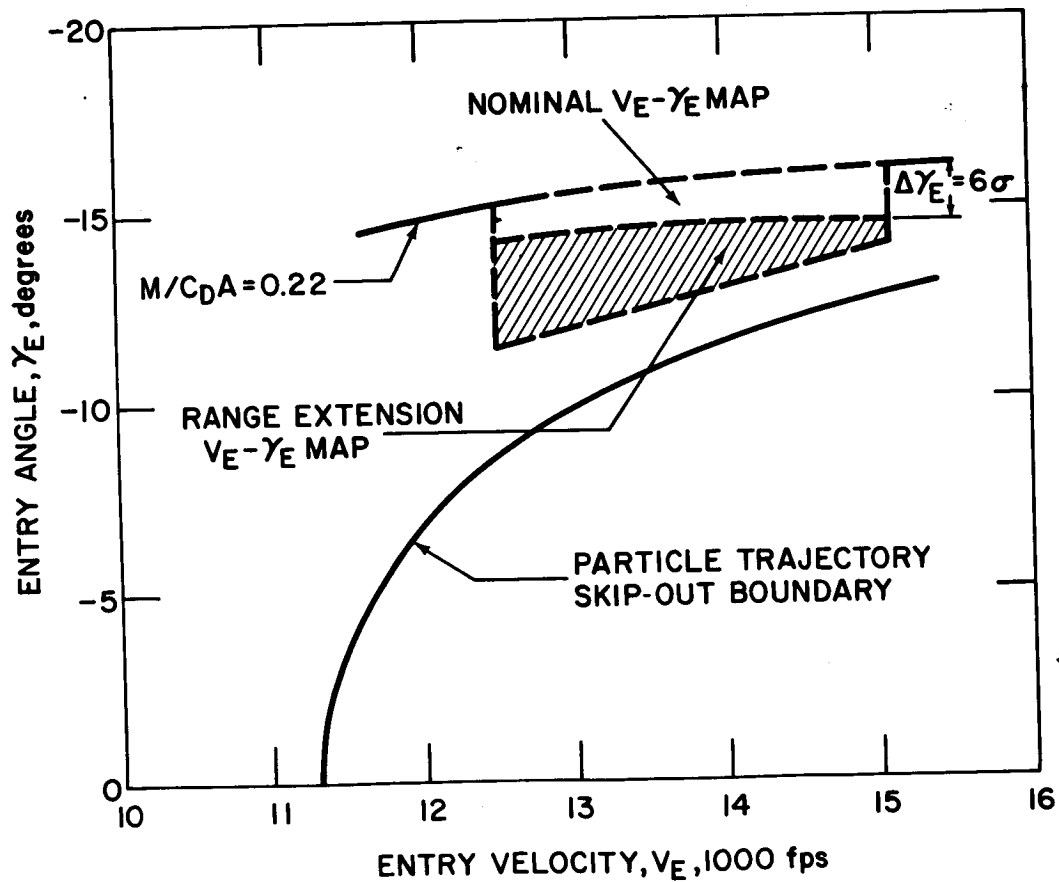ENTRY ANGLE, $\gamma_E$, degrees

ENTRY VELOCITY, $V_E$, 1000 fps

Figure 45 DISPERSION, RANGE EXTENSION, AND $M/C_D A$ SELECTION

-126-

(<5000 feet) could be on the maximum achievable resolution of the television pictures. However, the television shutter sequencing is independent of altitude; taking pictures as rapidly as possible. The maximum resolution achievable is therefore unaffected by terrain altitude.

## 5.2 STRUCTURES

### 5.2.1 System Requirements and Design Guidelines

The primary requirement of the structural design was the development of a simple lightweight, easily-manufactured structure, while at the same time adhering to design limitations such as minimum skin-gage thickness and core density so that existing test data would be applicable and no undue ground-handling problems would arise. Practical structural materials whose properties and manufacturing technology was well developed were specified. The entry environment and the other design conditions are specified in paragraph 4.8.2.

Early in the evaluation of various entry shell design approaches, the failure mode entry conditions were examined. The failure mode resulting from an inertial reference system malfunction, commanding continuous torque to be applied in one direction, allows the entry vehicle to enter at body rates up to 4.0 rad/sec. This failure mode resulted in a relatively large entry shell-weight penalty, primarily in additional heat-shield weight. A sentry system, which deactivates the reaction control system if the body rates ever exceed 0.1 rad/sec was incorporated to eliminate this failure mode from consideration (a double failure is necessary to achieve this failure mode). The designing entry-shell failure mode is random entry angle of attack with body rates limited to 0.1 rad/sec.

The effect of the two failure modes on structure weight is shown in Table XXIII to be negligible.

TABLE XXIII

## FAILURE MODE STRUCTURAL SHELL WEIGHT

|  | 40 rpm No Despin | Tumbling Rearward Entry |
|---|---|---|
| Diameter, feet | 15 | 15 |
| Shell design weight, pounds | 358 | 358 |
| Entry velocity, ft/sec | 15,200 | 15,200 |
| Entry angle, degrees | -18.0 | -16.0 |
| Atmosphere model | VM-8 | VM-8 |
| $M/C_D A$ | 0.20 | 0.20 |
| Entry angle of attack, degrees |  | 179 |
| Stagnation pressure lb/in.$^2$ | 358 | 229 |
| $A_x$ g | 23 | 15.5 |
| $A_n$ g | 2.1 | 0.6 |
| Structural material and concept | Aluminum Honeycomb sandwich | Aluminum honeycomb sandwich |

### 5.2.2  Material Selection

The material selection for the entry shell structure is influenced by the failure mode of the shell, the operating temperature at maximum loads, the state of technology for the material, and the structural weight fraction.

For a minimum gage-limited sandwich structure, where buckling is the dominant failure mode, the relative efficiency is determined primarily by the product of the density and minimum attainable gage of the structural material. Because beryllium and magnesium have the lowest values of this product, they can be seen in Figure 46 to have a lower relative weight over the stagnation pressure range of 50 to 550 psf as compared to aluminum. A 300°F structural temperature at maximum loads was assumed, since it represented the typical maximum value to be expected in a cold gas structure with thermal protection.
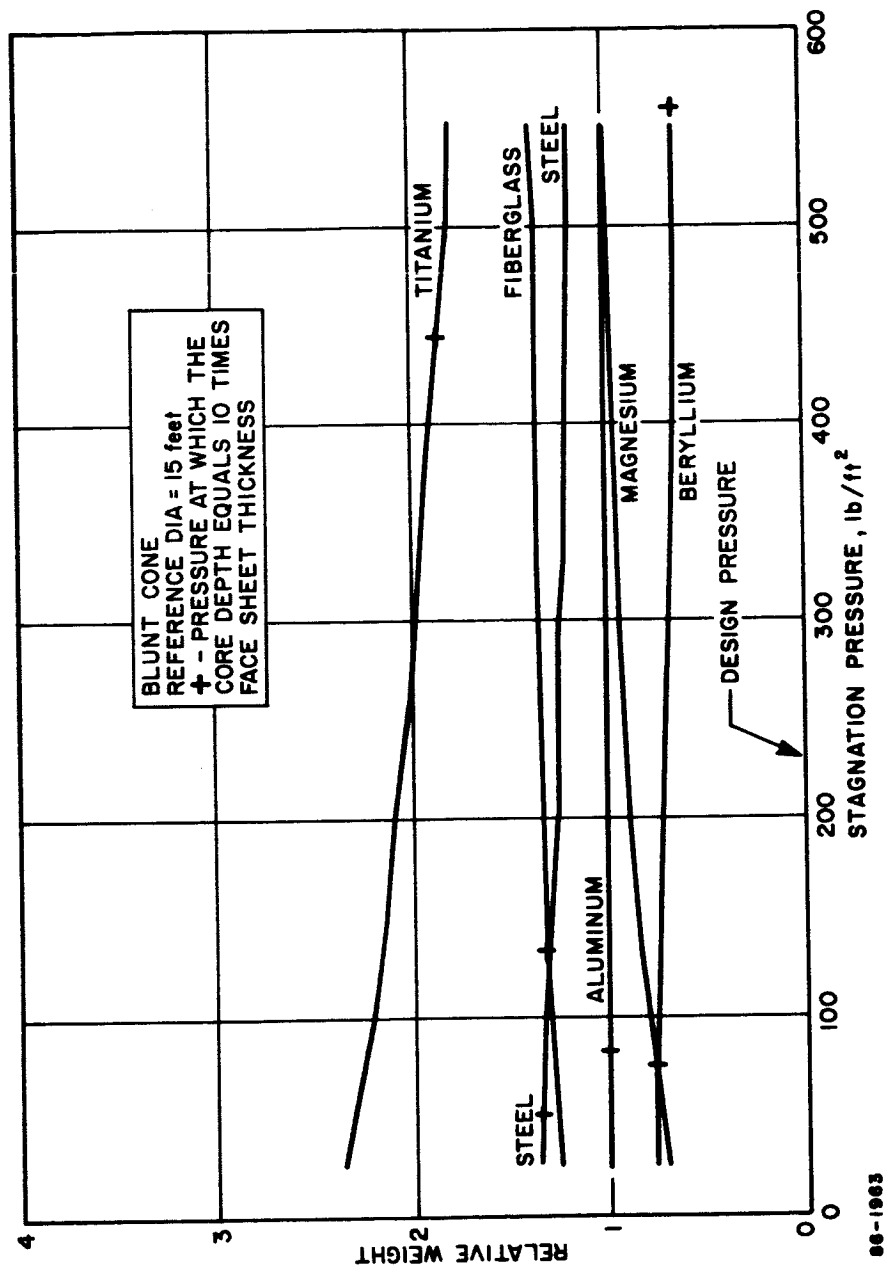
Figure 46 RELATIVE EFFICIENCY OF STRUCTURAL MATERIALS FOR HONEYCOMB SANDWICH CONSTRUCTION

86-1963

-129-

At higher stagnation pressures for minimum gage limited sandwich shells, the ratio of the core density to the product of the extensional stiffness becomes more important. Magnesium is inferior in this respect to most other structural materials; it tends to lose its relative weight advantage.

At even higher stagnation pressures, where a sandwich shell is no longer minimum-gage limited, with the shell having the optimum combination of face sheet and core depth required to satisfy a buckling criterion, the efficiency of a structural material is determined by the ratio of the Young's modulus to the face sheet density raised to the 2/5 power. This relationship holds if the stresses in the face sheet are less than the allowable yield stress. Beryllium is the most efficient of available structural materials for this application at the temperature levels under consideration.

When the stresses in the face sheet are sufficient to cause yielding, the failure mode of the shell becomes both buckling and yielding. In a comparison of materials, the most efficient material has the lowest value of the ratio of the face-sheet density to the allowable yield stress, if the Young's moduli of the materials are approximately the same. When there are relatively large differences in Young's modulus, the ratio of the yield stress to the Young's modulus raised to the 2/3 power becomes important. Materials, such as fiberglass, with a low Young's modulus, would be inefficient for this application.

At higher temperature levels, the mechanical properties of magnesium and aluminum are rapidly degraded, and therefore, materials such as stainless steel and titanium become more efficient. Beryllium, however, retains its advantages up to at least 1000°F.

From a manufacturing viewpoint, the technology of aluminum is better developed than that of beryllium or magnesium. In the face of the relative unimportance of the weight difference between the three materials, of Figure 46, aluminum was chosen as the structural material.

5.2.3 Structural Concept Selection

The selection of the structural concept is also influenced by the failure criteria, operating temperature, manufacturing methods, and importance of the structural weight fraction as in the material selection. To some extent, the degree of development of the methods of analysis also enter into the selection process.

A monocoque, ring-stiffened, or sandwich structure would be logical candidates for a shell under external pressure, which could fail due to instability. A sandwich construction would likely be more efficient than monocoque for a shell which could fail due to both the instability and high bending stresses.

-130-

The governing failure criteria of the entry shell is instability under an external surface pressure. As shown in Figure 47, the design stagnation pressure is within the range where sandwich construction is more efficient with respect to weight. This result is generally true because the stiffness of sandwich construction can be increased by increasing the depth of the relatively light-weight core. This places the highest strength and density material in the highest stressed regions. A monocoque structure will be more efficient only when its wall-thickness requirement is less than twice the face-sheet thickness of a sandwich structure. Ring stiffened semi-monocoque construction is more efficient than monocoque construction and less efficient than sandwich within the expected pressure range. An optimized ring-stiffened structural shell would have many small closely spaced rings which would be more difficult to manufacture than honeycomb sandwich.

Honeycomb core material was selected for the sandwich construction because it is less difficult to manufacture than a truss or corrugated core.

### 5.2.4 Entry Mode Effect

The various entry conditions affect the structure primarily by varying the external surface pressure distribution and magnitude. The varying pressure distribution is due to entry angle of attack. The resulting structural weights can be related approximately to the maximum stagnation pressure on a given trajectory. For angles of attack less than 30 degrees the structure weight, as a function of stagnation pressure given in Figure 48 can be used to determine the weight as a function of entry mode. The weights were determined using the maximum stagnation pressure for each combination of entry conditions.

Figure 49 gives the structure shell weight as a function of entry angle and velocity for the nominal zero entry angle of attack trajectories. The weights shown include the individual weights of the face sheets, core, bond, end ring, support ring, splices, and doublers. The flight capsule $V_e$ - $\gamma_e$ map is shown superimposed on the structural weight-carpet plot to identify the design condition. Both the normal and the range extension $V_e$ - $\gamma_e$ maps are shown. At zero entry angle of attack, the design condition occurs at an entry velocity of 15,200 ft/sec and an entry angle of -16 degrees. The tumbling entry resulting from attitude control system failure is shown to result in a weight penalty of 35 pounds.

## 5.3 THERMAL PROTECTION SYSTEM

### 5.3.1 System Requirements and Design Guidelines

The design objectives and requirements discussed under subsystem characteristics in paragraph 4.8.3, establish the design guidelines to be followed in the thermal protection system trade-off studies. Basically, they result
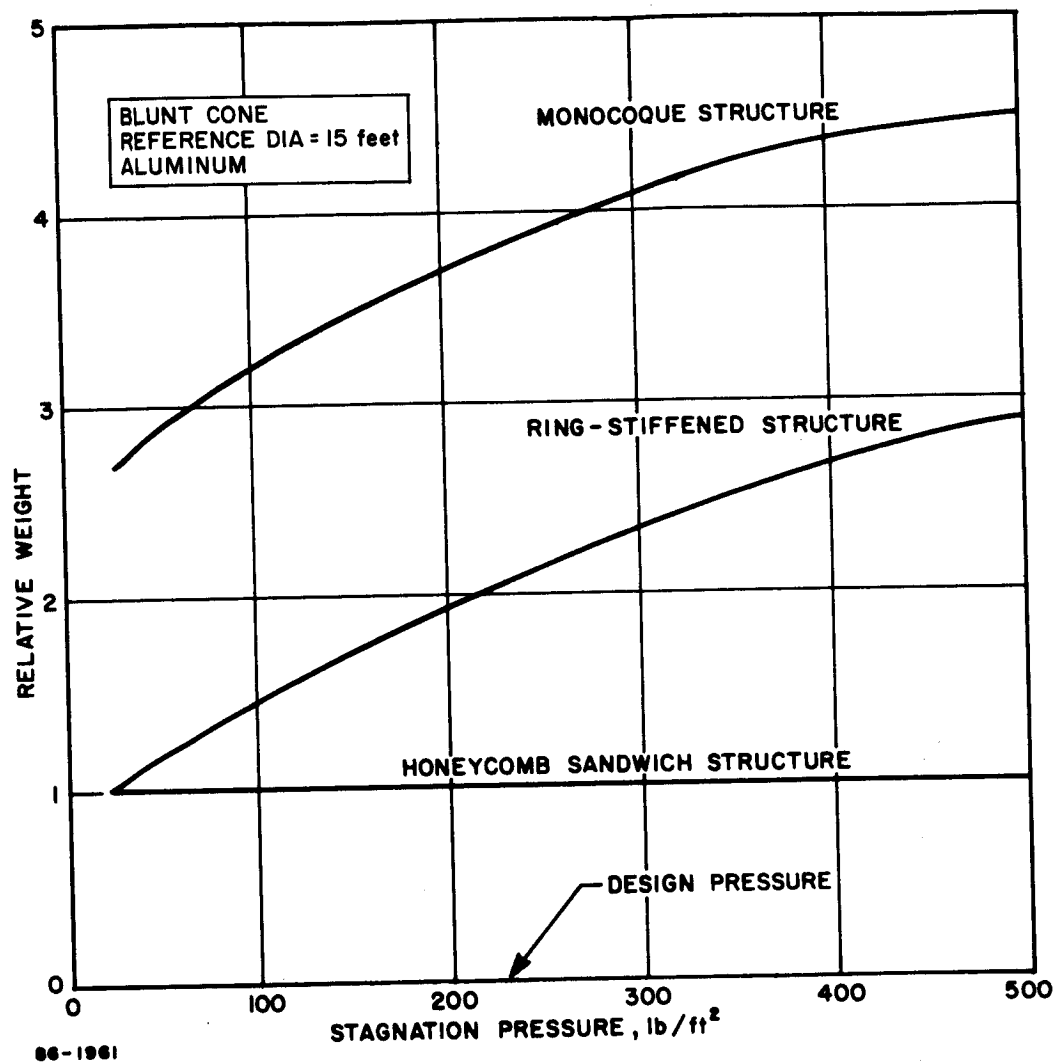
-131-

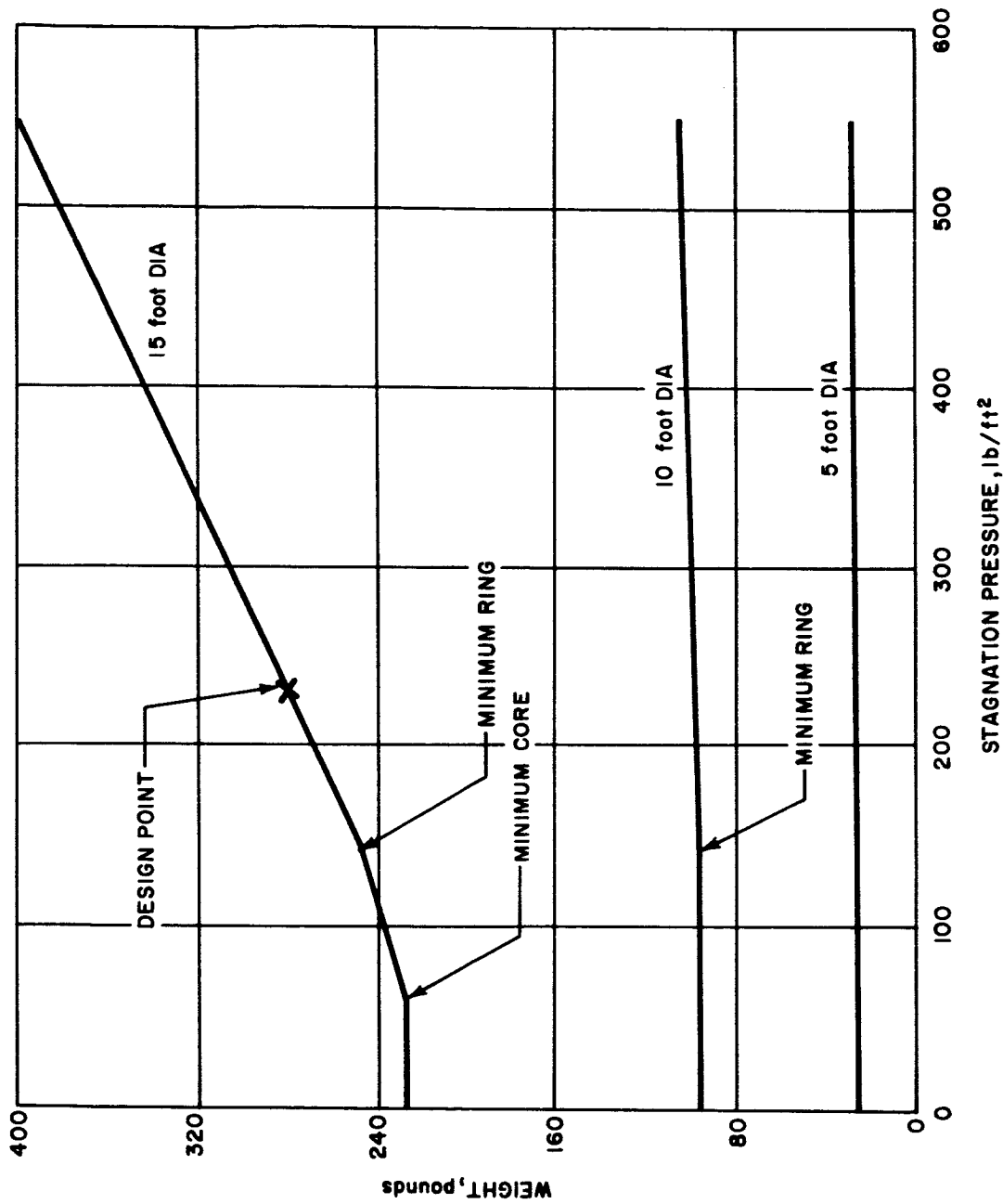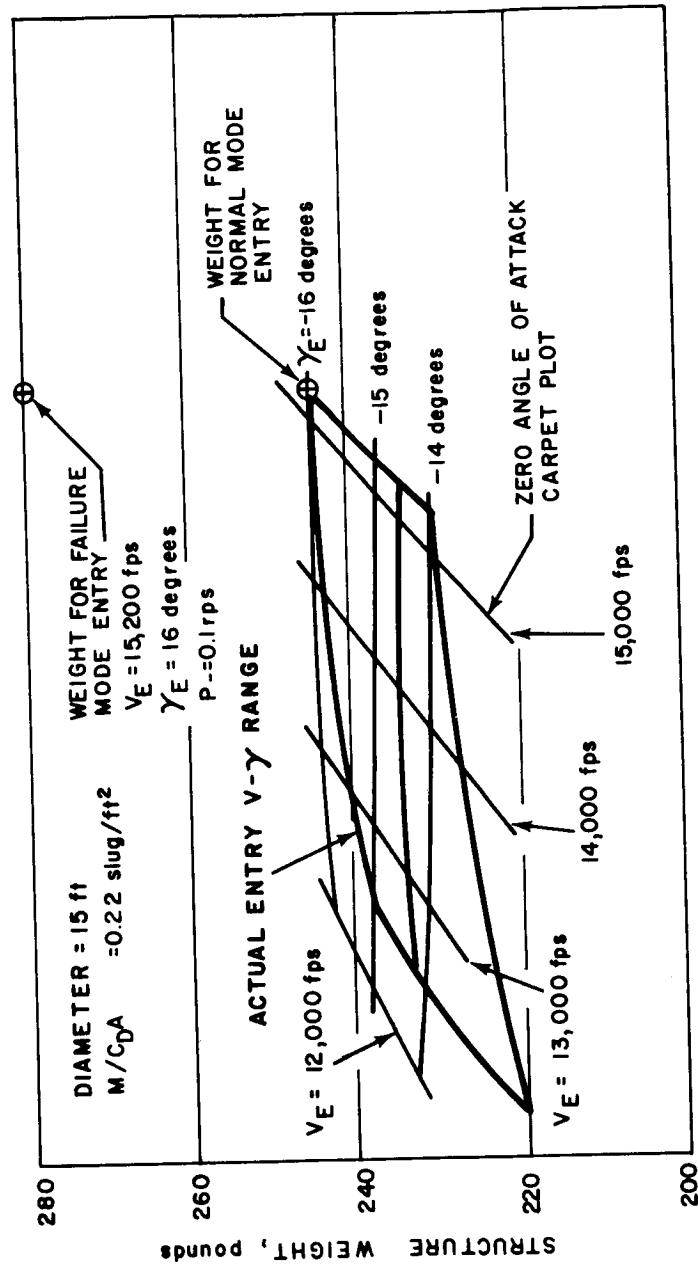Figure 47 RELATIVE EFFICIENCY OF STRUCTURAL CONCEPTS

Figure 48 BLUNT-CONE SHELL STRUCTURE WEIGHT VERSUS STAGNATION PRESSURE

062197

-133-

Figure 49  ENTRY SHELL STRUCTURE WEIGHT

862198

-134-

in a design goal of a lightweight heat shield compatible with the structure and thermal control requirements. The over-riding consideration, however, is the attainment of overall mission objectives. These mission objectives and constraints define the entry environment (paragraph 4.8.1) which will be experienced by the thermal protection system. Nevertheless, in the process of subsystems integration and reconciliation of often diverse subsystem requirements, major tradeoffs are possible which will materially affect the weight fraction of an individual subsystem such as the heat shield. These tradeoffs are reflected in changes of the basic aerodynamic environment and require a number of parametric studies. The requirements imposed by the selection of the landing site, communications and de-orbit philosophy, and evaluation of failure modes translated into the heat shield environment design conditions and weights are shown in Table XXIV for three entry modes. The design conditions and criteria shown in this table also reflect the usual entry vehicle requirements. The heat shield designs considered were limited to ablative shields, and although an efficient heat shield system was required, only available materials were to be considered even if some weight penalty was incurred. Weight savings of course were desirable, but the design was not critically weight limited, thus ample safety factors and somewhat conservative allowances for the initial and bondline temperature were used.

### 5.3.2 Material Selections

Materials used in the study were reviewed prior to this phase of the program. The examination of the experimental data acquired concurrently with this program indicated that the ranking of the materials previously examined may well be reversed, and especially that Purple Blend, Mod 5 may perform more efficiently than was assumed previously, in the absence of adequate data. Even though no formal evaluation was conducted on other materials due to limitations of the time and scope of the contract, it was jointly agreed with NASA-LRC that Purple Blend, Mod 5 was to be used in heat-shield weight calculations because (1) the material characterization experiments conducted at Avco indicated a significant reduction in the weight estimates made during the previous phase of the study. The analysis of the data indicated that Purple Blend Mod 5 may be lighter than other materials previously considered, (2) the availability of more complete material characteristics for Purple Blend Mod 5 permitted more realistic calculations of weight requirements, (3) manufacturing and development problems associated with Purple Blend Mod 5 appeared to present less difficulties than those of other materials.

Subsequent evaluation of the Cork Silicon material confirmed this selection.

The properties and ablative characteristics of the Purple Blend Mod 5 used in the design analysis are shown in Table XXV. A rigorous ablation analysis

TABLE XXIV

### SUMMARY OF HEATING AND HEAT SHIELD PERFORMANCE DATA
### (BLUNT CONE)

| Design Concept / Flight Parameters | 40 rpm Spin | Despin | Present Design |
|---|---|---|---|
| Diameter, feet | 15.0 | 15.0 | 15.0 |
| Weight, pounds | 1855 | 1855 | 2040 |
| Entry velocity, ft/sec | 12,900 | 12,900 | 15,200 |
| Entry angle, degrees | -12.8 | -12.8 | -14 |
| Atmospheric model | VM-7 | VM-7 | VM-7 |
| $m/C_dA$, slug/ft$^2$ | 0.20 | 0.20 | 0.22 |
| Entry angle of attack, degrees | 86 | 86 | 90 |
| Total integrated heating, Btu/ft$^2$ | 2052 | 1790 | 2270 |
| Peak heating rate, Btu/ft$^2$/sec | 23.6 | 18.8 | 18.6 |
| Duration of heat pulse, seconds | 320 | 310 | 240 |
| Angle of attack-peak heating, degrees | 59 | 30 | 11 |
| Material heat shield | Purple Blend Mod 5 | | |
| Material structures | Aluminum Honeycomb | | |
| Limiting bondline temperature, °F | 500.0 | 500.0 | 500.0 |
| Entry temperature, °F | 60 | 60 | 100 |
| Saftey factor | 1.2 | 1.2 | 1.2 |
| End of heating pulse | Parachute Deployment | | |
| Approximate weight fraction (forebody only) percent | 12.7 | 9.3 | 12 |
| Total weight fraction, percent | 23 | 15 | 16 |

TABLE XXV

## THERMAL PROPERTIES AND ABLATIVE CHARACTERISTICS
## OF PURPLE BLEND MOD 5
## INTERNAL PROPERTIES

|  |  | Virgin | Fully charred |
|---|---|---|---|
| $\rho$ | - lb/ft$^3$ | 41.8 | 16.7 |
| $C_p$ | - Btu/lb-°F | 0.34 | 0.34 |
| $\kappa$ | - Btu/ft-hr-°F | 0.075 | 0.049 (760°R) |
|  |  |  | 0.080 (1100°R) |
|  |  |  | 0.180 (2250°R) |
|  |  |  | 0.240 (4060°R) |

### REACTION CONSTANTS

| $\Delta H$ | Btu/lb | 1000 |
|---|---|---|
| A | * | $3.9 \times 10^5$ |
| B | * | $2.0 \times 10^4$ |
| $\eta$ | * | 1.0 |

*Units compatible with $\dot{\rho}$ (lb/ft$^3$-sec) = A $(\rho - \rho_c)^n \exp(-B/T)$

### GASEOUS EFFUSION

| $C_{p_g}$ | 0.40 | Btu/lb-°F |
|---|---|---|

### CONDUCTIVITY EXPLICIT FUNCTION RHØK

| Density, lb/ft$^3$ | RHØK |
|---|---|
| 16.7 | 1.0 |
| 29.8 | 0.66 |
| 36.2 | 0.44 |
| 40.2 | 0.21 |
| 41.8 | 0.0 |

### SURFACE ABLATION CHARACTERISTICS

| | |
|---|---|
| ETA | 0.3937 |
| $\epsilon$ | 0.62 |

| Density, lb/ft$^3$ | A3 |
|---|---|
| 16.7 | $6.73 \times 10^8$ |
| 41.8 | $1.0 \times 10^6$ |
| $3.987 \times 10^4$ | B3 |
| $1.0 \times 10^4$ | HC |

| Density, lb/ft$^3$ | TW |
|---|---|
| 16.7 | 2.02 |
| 41.8 | 5.0 |
| $1.066 \times 10^4$ | HV |

employing the combustion mechanism was employed in the design calculations; however, it was assumed that the Martian atmosphere would sustain the same type of surface reaction as Earth, and that only a small, even if complete, body of experimental data were available for the analysis.

### 5.3.3 Entry Mode and Design Concept Effects

A correlation of the heat-shield thickness, integrated aerodynamic heating and bondline temperature allowances was established and used to calculate heat-shield weights and the effect of allowable temperature rise on this weight. This effect was found to be significant, approximately a 25 percent decrease in weight per $100^\circ F$ allowable temperature rise.

The same relationships including a correlation of entry angle, entry velocity, heating, diameter, and atmospheric scale height were used to determine the heat shield requirements for various modes of entry.

The variation in the heat-shield weight requirement over the operating $V_e - \gamma_e$ map is shown in Figure 50. The heat shield consists of Purple Blend Mod 5, calculated for application on the reference design structure. The lower carpet plot of the figure assumes zero angle of attack at peak heating, the heat shield is calculated for various combinations of entry velocity and angle. The carpet plot shows a strong influence of entry angle on heat-shield weight, primarily due to the relationship between heat soak time and entry angle. The increase of weight with entry velocity is also significant. The actual Flight Capsule $V_e - \gamma_e$ map is superimposed upon the carpet plot. The entry heat-shield design point occurs at an entry velocity of 15,200 ft/sec and an entry angle of -14 degrees. To account for the failure mode of tumbling entry and increase in the $M/C_DA$ to 0.22 relative to the conditions of this plot, a heat-shield weight penalty of 114 pounds must be taken; the failure mode weight was incorporated in the reference design. The weights shown in this chart are for the primary heat shield (on the shell forward face) and includes bond and a mounting pad between the structure and the bond. The weights shown do not include the weight of the secondary heat shield (on the back side of the shell) and bond which totals 55 pounds.

General dependence of the heat-shield weight on the variation of the ballistic coefficient and the diameter was evaluated for a typical structure and is shown in Figure 51. The weight is relatively insensitive to $M/C_DA$, reflecting a small increase in total heating for increasing $M/C_DA$. The larger effect of the diameter is due to the increase in the total area exposed to heating moderated by the decrease in local heating. As in the previous figure, the conditions are for zero angle of attack with a Purple Blend Mod 5 heat shield.
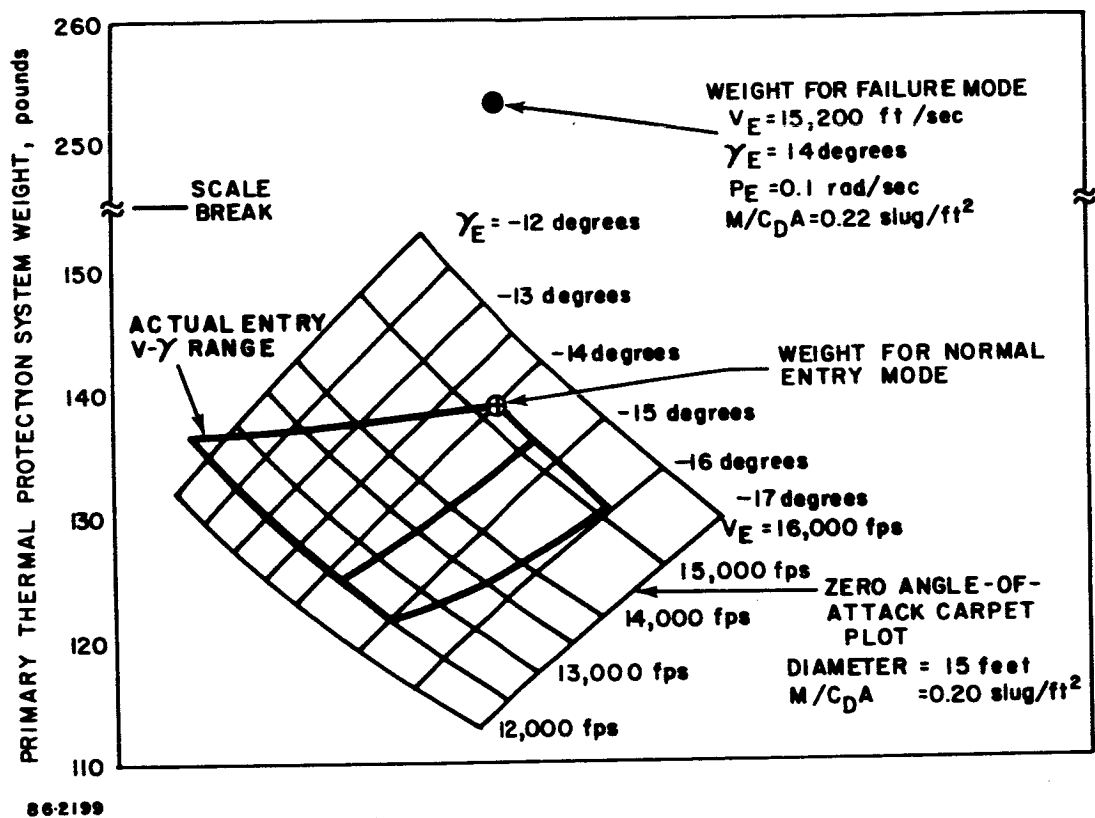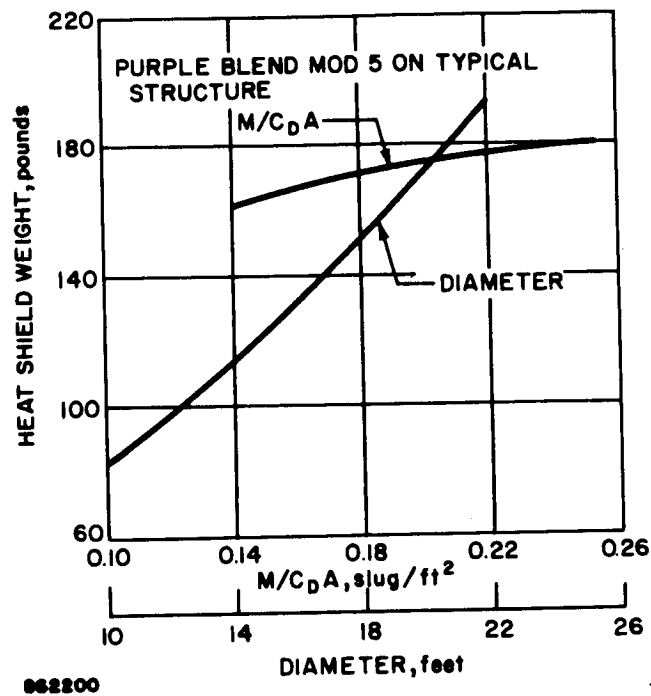
Figure 50 ENTRY SHELL HEAT-SHIELD WEIGHT

86-2199

Figure 51 THERMAL PROTECTION SYSTEM
WEIGHT VERSUS M/$C_D$A AND DIAMETER

Other modes of entry considered during the parametric studies were concerned with the spin and associated angle of attack effects and were previously shown in Table XXIV. These effects are shown for a fixed entry angle of -12.5 degrees in Figure 52 for various entry velocities. For this case, each particular entry mode may result in various combinations of $V-\gamma-a$ depending on de-orbit and communication requirements. The effect of angle of attack existing at peak heating is very large over the range of interest. Total required heat shield weights (not including contingency or manufacturing considerations) for the forebody primary, secondary, and afterbody thermal protection are compared for the three designs evaluated on a particle trajectory basis in Figure 53 indicating the advantage of the adopted design.

## 5.4 AFTERBODY SELECTION

The afterbody performs two vital functions: 1) It provides a turn-around capability in the event of rearward entry, and 2) It protects the internal flight capsule subsystems from the thermal environment associated with this mode of entry. Such thermal protection is also necessary for the normal entry mode, zero angle of attack, although the thermal environment is significantly less severe.

### 5.4.1 Candidate Afterbody Shapes

Three basic afterbody shapes were considered as shown in Figure 54. These afterbodies were synthesized based upon the specified LRC minimum afterbody (A), eliminating a major portion of the flight spacecraft-flight capsule adapter (B) and minimizing the afterbody weight (C).

### 5.4.2 Comparison of Candidate Shapes

The three candidate afterbodies were compared on the basis of:

- Aerodynamic performance
- Weight
- Antenna Performance
- Separation clearance.

#### 5.4.2.1 Aerodynamic Performance

The dearth of data on optimum afterbody configurations restricts the designer to using forebody technology with the concommitant weight penalty. Shallow afterbody angles (such as used in the Apollo Command Module) are necessary to provide only one stable trim point; the result is excessively large afterbody surface area and $\Delta V$ rocket integration complexity (large moment arm for thrust misalignment).
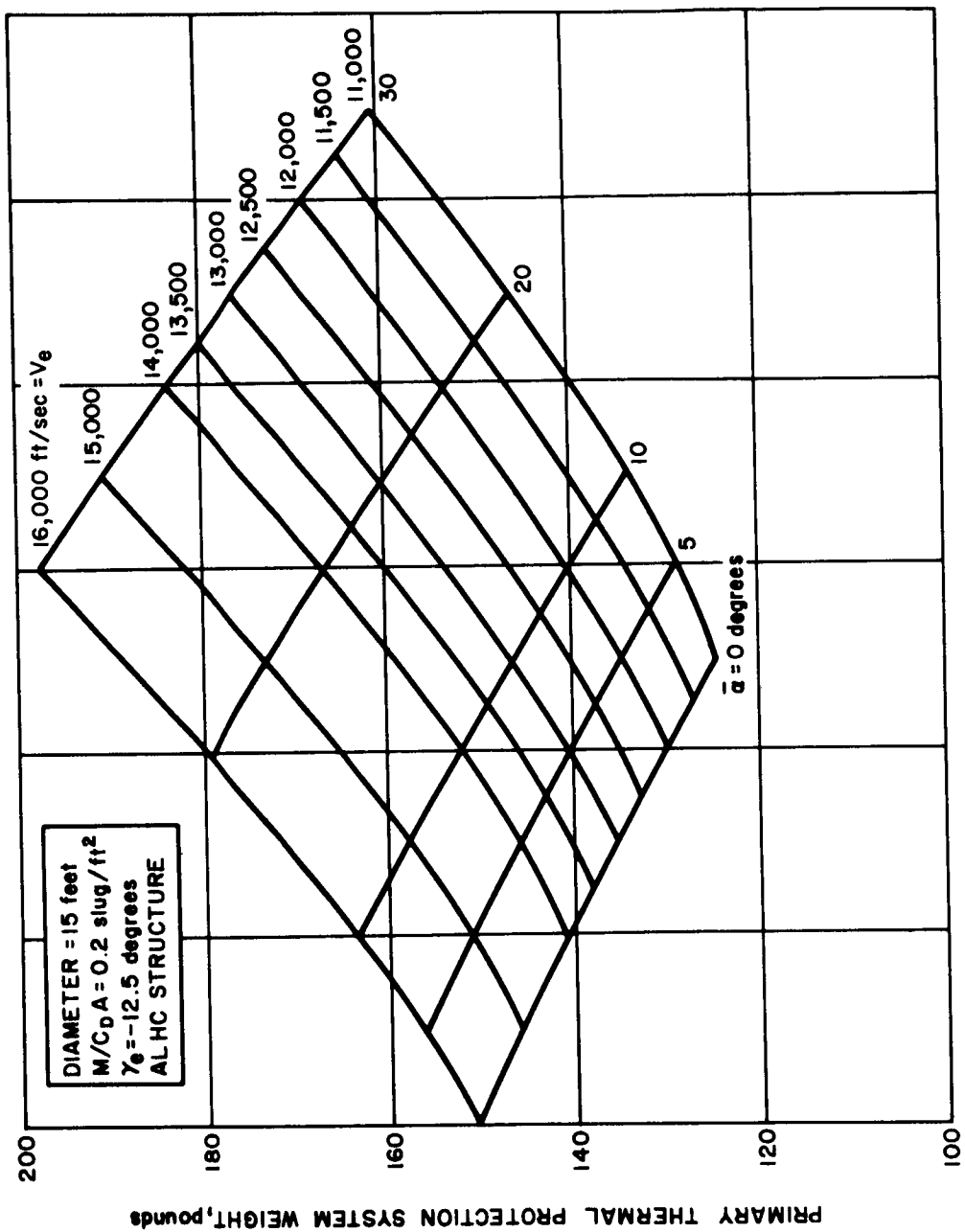
Figure 52 VELOCITY AND PEAK HEATING ANGLE OF ATTACK EFFECTS

862201

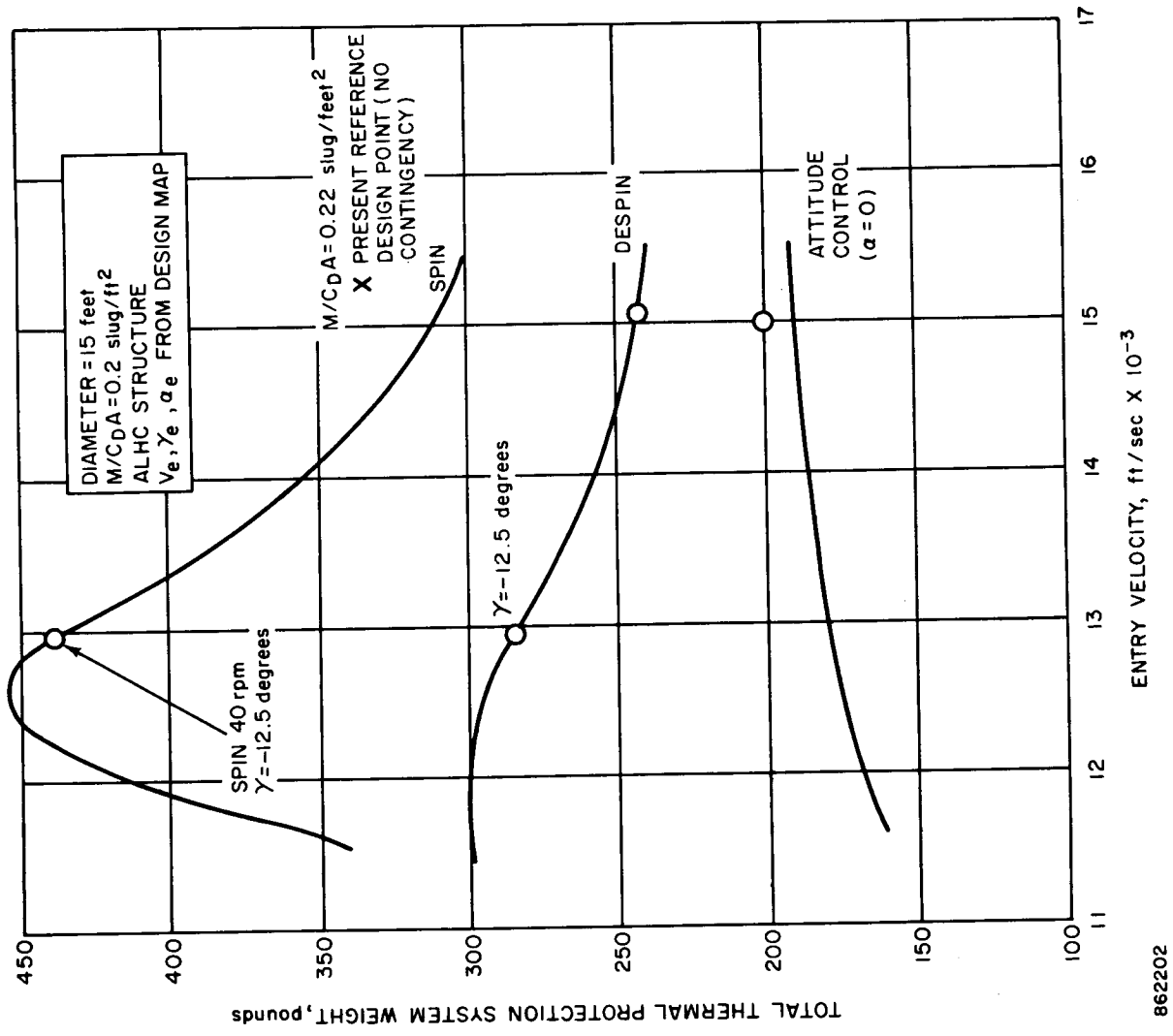-142-

Figure 53  TOTAL THERMAL PROTECTION SYSTEM WEIGHTS

862202

CONCEPT "C"

ADAPTER

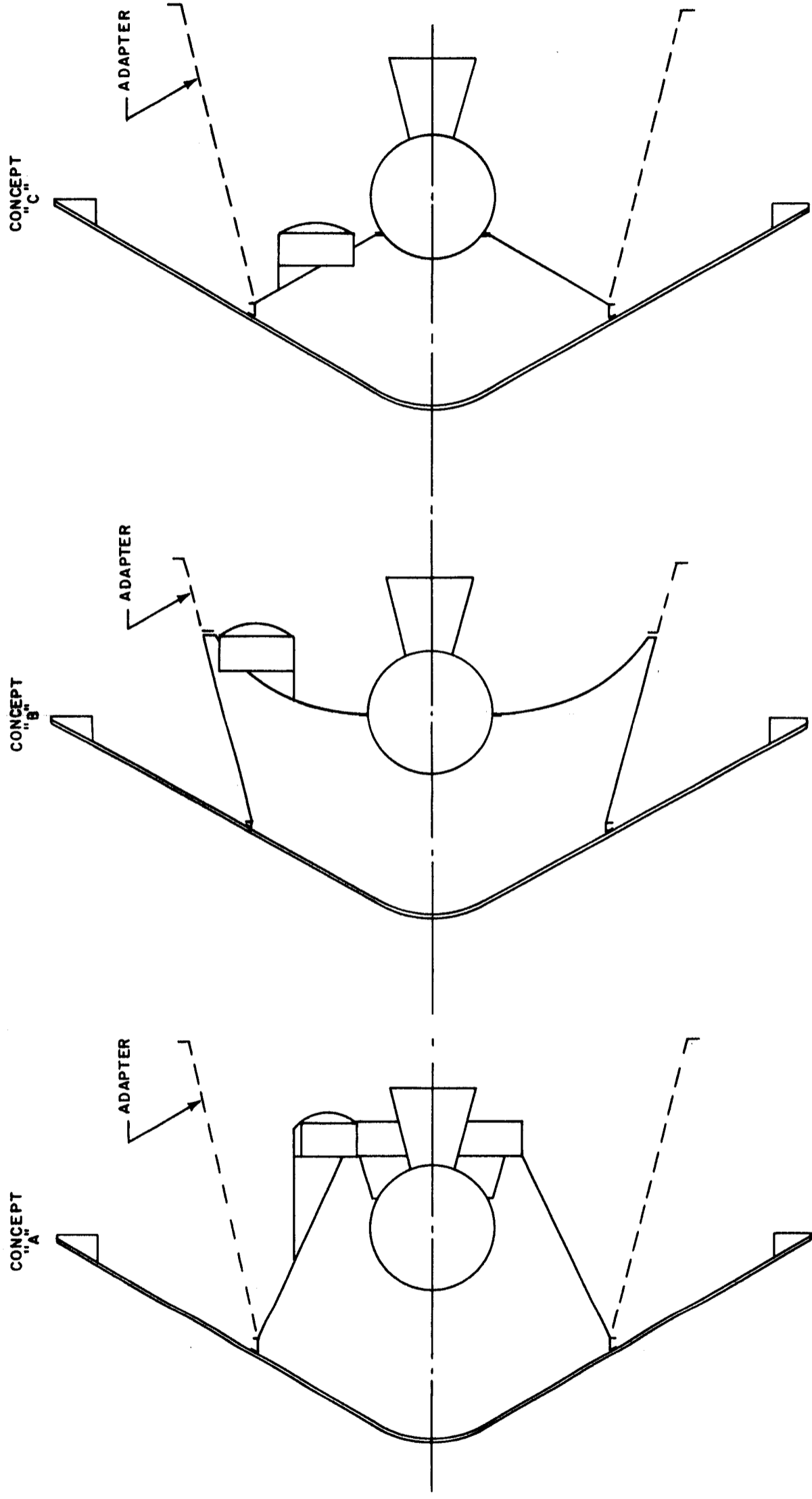CONCEPT "B"

ADAPTER

CONCEPT "A"

ADAPTER

Figure 54  AFTER BODY DESIGN CONCEPTS

86-2203

144-2

Using these afterbodies, a serious problem is introduced during the transonic phase of flight. Vehicles using forebody-shaped afterbodies exhibit dynamic instability associated with the hysteresis movement of the shock boundary layer separation phenomenon at transonic velocities (Mach 0.8 to 2.0).

To circumvent this problem, a stable separation point can be provided by providing a pronounced step from the maximum diameter to the afterbody, the step must be sufficiently large to avoid re-attachment of the boundary layer to the afterbody. The problem now is that of predicting the rearward stability. On the basis of Newtonian theory, adequate turnaround capability is available for the afterbody configurations shown in Figure 54 particularly when the dish effect on the moment is accounted for. Available data indicate a pronounced effect associated with the dish shape at angles of attack other than 180 degrees. At 180 degrees, however, the sparse data available show a region of stability for the configurations tested. These afterbodies were tested in conjunction with large forebodies. The data do provide a means for factoring out the forebody and sting contributions since data were taken about several moment centers. A neutrally stable condition is indicated for the dish shaped afterbodies. This situation is easily overcome by assymetrical flaps.

The comparison of these three afterbody configurations used Newtonian theory, accounting for the dish shape as well as shadowing. The resulting moment coefficients are shown in Figure 55. These co-efficients consider the weight associated with the respective configurations as reflected in a center of gravity location for each shape. The effect of the afterbody on forward stability is due to this center of gravity difference.

The performance of each afterbody was evaluated using these coefficients for a rearward entry with the expected spin rate of 0.1 rad/sec associated with an attitude control system failure. The resulting angle of attack envelopes are presented in Figure 56. These results indicate adequate convergence for all three afterbodies, afterbody B performing slightly poorer than the others.

Afterbody configuration C experiences the lowest heating environment for rearward entry since the afterbody is recessed within the dish.
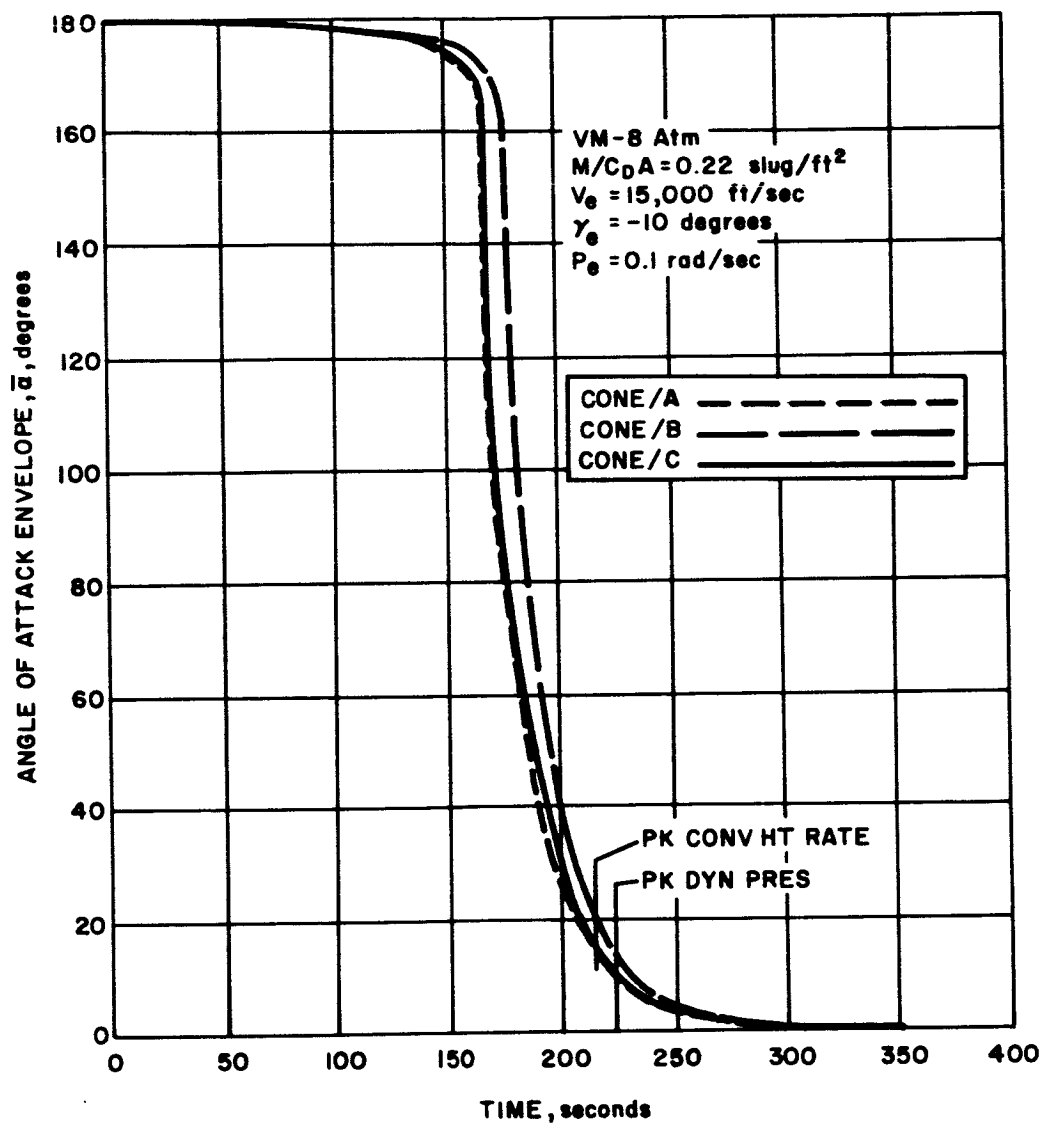
5.4.2.2 Weight

The weight and center of gravity location of each of the three afterbodies is shown in Table XXVI.
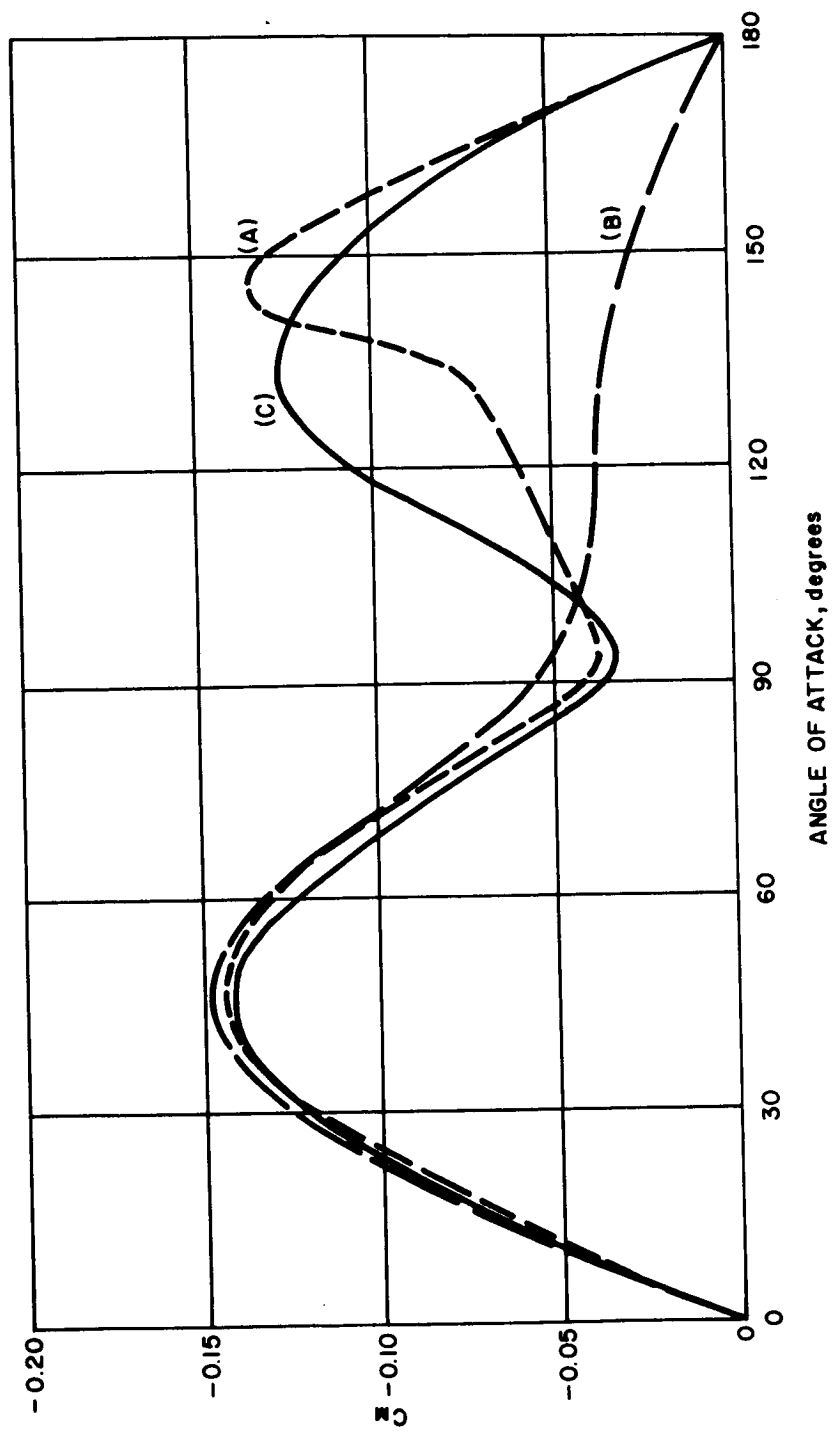
Figure 55 NEWTONIAN MOMENT COEFFICIENTS

ANGLE OF ATTACK, degrees

062204

-146-

Figure 56 ANGLE OF ATTACK CONVERGENCE--AFTERBODY COMPARISON

862205

## TABLE XXVI

### AFTERBODY WEIGHT COMPARISON

| Afterbody | | | |
|---|---|---|---|
| | A | B | C |
| Afterbody Weight (H/S and STR) (pounds) | 239 | 332 | 186 |
| $X_{cg}$ (from nose) (inches) | 35.2 | 35.9 | 34.0 |

Afterbody C shows a 53-pound weight saving as compared with afterbody A and results in a significantly more forward center of gravity providing better packaging flexibility for the payload and a better static margin for rearward entry.

5.4.2.3 Antenna Performance

In paragraph 11.2.2 it is shown that the total flight capsule antenna look angle requirements are dictated by conditions during descent when the suspended capsule may swing up to 90 degrees due to wind gusts. The total look-angle variation for all orbits considered is approximately 270 degrees during this portion of the mission. Such a large look-angle requirement makes the selection and placement of antennas on the afterbody very difficult since, at look angles of 90 degrees and beyond (total look angle variation of 180 degrees or more) the performance of the antenna is practically impossible to predict. This is due, in part, to signal reflections, from the afterbody and other structural elements, causing signal cancellation and enhancement, thus affecting the antenna performance. Since prediction was not a reliable means of determining antenna performance, extensive antenna pattern measurements were conducted by Avco on scaled mock-ups of the flight capsule concept. The results of these measurements, which included placement of the antennas above and below the topmost edge of the afterbody showed little dependence on the main afterbody shape. The $\Delta V$ rocket casing and nozzle, however, had a significant bearing on antenna performance. Removal of the rocket and nozzle if both extended beyond the top edge of the afterbody, or removal of the nozzle if it alone extended beyond the edge showed improvements such as filling in nulls that otherwise occurred in the patterns. The best performance of the antennas occurred with tilting

them slightly (15 degrees) toward the longitudinal axis of the flight capsule.

In summary, acceptable antenna performance can be obtained with any of the afterbody shapes considered, however, either the rocket or nozzle as the case may be, must be removed or made of dielectric (RF transparent) materials.

5.4.2.4 Separation Clearance

Afterbody A exhibits severe separation clearance problems at flight spacecraft-flight capsule separation. The afterbody angle is quite shallow with separation occurring at the afterbody-entry shell junction. The flight spacecraft-flight capsule adapter is a frustrum of a cone extending from the flight spacecraft through the sterilization canister to the separation joint. This adapter remains with the flight spacecraft and in separating, has little clearance around the aft end of the afterbody at the VHF antennas.

Both afterbodies B and C reduce the clearance problem. Afterbody B eliminates the problem by using a section of the adapter as the afterbody placing the separation joint at the aft edge of the afterbody. Afterbody C reduces the clearance problem greatly by using a much shorter afterbody with a steeper angle cone.

Afterbody C was selected for the preliminary design as the best compromise between these competing criteria.

## 5.5 DIAMETER SELECTION

The selection of a diameter for the entry vehicle was made on the basis of estimated weight of the entry shell as a function of diameter, estimated weight of the subsystems, and the selected $M/C_D A$.

In the upper curve of Figure 57, the entry weight available, at the required $M/C_D A$, is presented as a function of flight capsule diameter. The two lower curves present the weight required for the reference flight capsule configuration as a function of diameter. The lowest curve is the weight of the design excluding all the contingency factors presented in the previous weight-summary charts. The middle curve represents the weight required if all contingency factors (as presented in the weight summary charts) are incorporated. This curve represents conservative preliminary design weights. An additional weight is allowed, over and above this weight, for growth in the system to the hardware stage and for possible moderate increases in capability. Hence, the diameter selection of 15 feet gives approximately 6 percent weight for growth which is thought to be sufficient, since it is felt that the calculated weights presented are somewhat on the conservative side in most of the major subsystem categories.
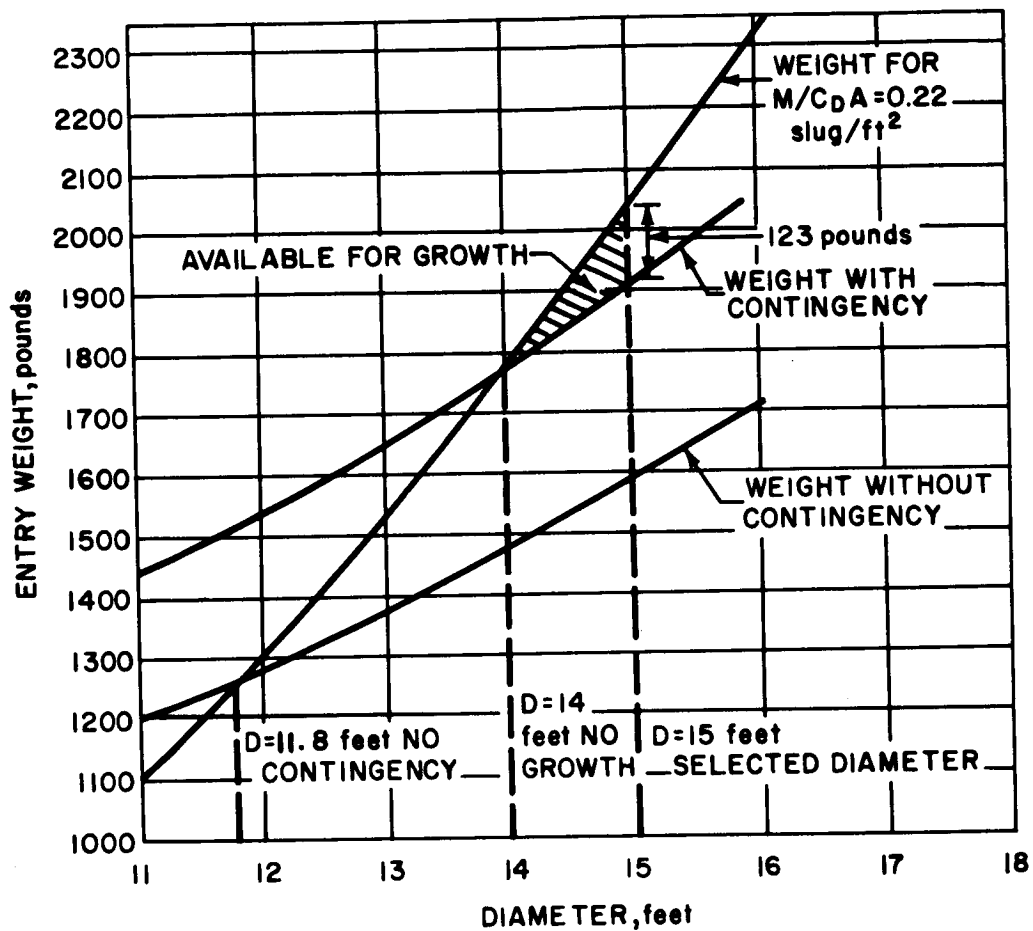
Figure 57 DIAMETER SELECTION AND WEIGHT AVAILABLE FOR GROWTH

862206

# 6.0 TELEVISION EXPERIMENT DESIGN

## 6.1 EXPERIMENT OBJECTIVES

The basic objective of the flight capsule television experiment is to provide unique imagery data required for the future exploration of Mars. These data primarily relate to characteristics of the Martian surface of engineering importance and, to a lesser extent, to properties of the Martian atmosphere.

In the integration of a television experiment into the instrument payload of the flight capsule and into the overall flight capsule - flight spacecraft mission, several major factors must be considered:

1. The flight capsule television experiment is only one part of the overall image generating program of the mission. It must be designed to effectively augment and complement image experiments performed with flight spacecraft payload.

2. It must be integrated with the other instruments in the flight capsule payload to take advantage of the potential of television images to improve interpretation of the results of other experiments.

3. The flight capsule has two significant advantages for television pictures over the flight spacecraft -- range to the surface and less potential atmospheric deterioration of images. The flight capsule television experiment must make the best possible use of these advantages in performing its mission and should concentrate on mission objectives for which these favorable conditions are necessary.

4. Like all other spaceborne television experiments, video data transmission accounts for the vast bulk of communication capability required in the flight capsule and, in fact, significantly influences other major aspects of the flight capsule system. Thus, it is especially important to closely integrate the television experiment and subsystem with the remainder of the flight capsule and support subsystems. These factors play a major role in the definition of television mission objectives and the design of the television hardware required to satisfy these objectives.

The television experiment objectives may be grouped into the four (4) categories shown in Table XXVII. The actual television images from the flight capsule will be used to generate engineering data through the analysis of topological statistics, the measurement of surface roughness, the identification of discrete surface object hazards, the generation of topographical maps to provide slope information, and the identification and description of geological features in larger maps. The desired image resolutions, nesting requirements, and solar elevation angles -- a key aspect of flight spacecraft trajectory selection -- are determined

-151-

TABLE XXVII

OBJECTIVES OF FLIGHT CAPSULE TV EXPERIMENT

1.  Resolution of surface character and surface objects to assist in landing and lander operations on the Martian surface

    • Discrete object hazards
    • Surface texture and roughness
    • Slopes

2.  Determination of significant features of local albedo and photometric properties to assist in the design of future imaging experiments

    • Photometric function
    • Skylight effects
    • Spectral characteristics
    • Albedo variations

3.  Assistance in interpreting flight spacecraft television images taken from Mars orbit

    • Generalization of surface features to large areas
    • Identification of geological features

4.  Supporting other experiments in the engineering payload

    • Wind measurement
    • Penetrometer experiments
    • Atmospheric measurements
    • Radar-optical correlations of surface roughness

by considering each of these subexperiments. In addition, the image characteristics required to effectively support wind measurements, atmospheric measurement, radar roughness measurements, and penetrometer bearing strength measurements are also reflected in generating the image requirements summarized in Table XVIII.

Effectively complementing and augmenting the flight spacecraft television experiments is a major consideration in the design of flight capsule television experiments. It has been assumed that the flight spacecraft will utilize high- and low-resolution camera systems and that the high-resolution system will map the region in which the flight capsule lands. The resolution which can be obtained from the flight spacecraft high-resolution camera is assumed to be 10 to 100 meters/television line.

In order to effectively locate the flight capsule television images in the maps obtained from the flight spacecraft cameras, at least one image at no worse than 3:1 flight spacecraft - television resolution is required. The reference design presented is based on actually achieving 10 to 30 meters/television line resolution from the flight spacecraft. Modification of the flight capsule television design presented would be required if this resolution is not available. Several other aspects of the flight capsule television experiment, such as the use of color, can benefit from compatibility with flight spacecraft-television concepts.

## 6.2 ALTITUDE RANGE -- MISSION PHASE FOR TELEVISION

The de-orbit, pre-entry, entry, and parachute-descent regions of the flight capsule trajectory have been examined to determine the most advantageous period during which to take television pictures. The flight capsule has two major advantages over the flight spacecraft, range to the surface and less potential atmospheric distortion of images. The television experiment must use both of these advantages to accomplish the high resolution mission required for future lander operations. The parachute-descent phase has been selected as the best region for flight capsule image experiments, although it has certain limitations. The primary advantages are long duration at low altitudes and an unobstructed view of the surface from near vertical orientation. The major limitation of on-parachute television pictures is the relatively small total area covered and the flight capsule dynamics on the parachute. The major advantages and disadvantages of each mission phase are outlined in Table XXIX.

## TABLE XXVIII

### TV IMAGE REQUIREMENTS

| Purpose | Surface Resolution (ft/tv line) Max. | Min. | Nesting Desirable | Location in FS Images Desirable | Wide Area Coverage Desirable | Two-Colors Desirable | Desired Solar Elevation Angle (degrees) |
|---|---|---|---|---|---|---|---|
| Roughness and object hazards | 0.1* | 1.0 | | | X | | 20-40 |
| Topological statistics | 1 | 100 | | X | X | | 10-30 |
| Experiment support | 3 | 30 | | | X | X | 20-40 |
| Photometric topography | 3 | 100 | X | X | X | | 20-30 |
| Geological mapping | 10 | 100 | X | X | X | X | 20-60 |

*Desired resolution increased from previous value of 1 ft/tv line based on Luna IX results

Other Considerations

Lowest resolution FC TV should be no worse than 3:1 better than FS TV
Highest resolution FC TV should meet object hazard resolution requirement
Steady winds prevent picture nesting by means of altitude change
Nested images must have no worse than 3:1 resolution relationship
At least 32 grey levels are required
Cameras should operate at minimum surface brightness of 30 ft-Lamberts

## TABLE XXIX

## ALTITUDE RANGE FOR FLIGHT CAPSULE TV PICTURES

| Altitude | Advantages | Disadvantages |
|---|---|---|
| De-orbit ↓ ~800,000 ft | Long communication time<br><br>Relatively wide area coverage | Probably cannot do as well as FS TV<br><br>Stable platform required for camera pointing |
| 800,000 ft ↓ ~200,000 ft | Perhaps better resolution than FS TV<br><br>Fairly good dispersal | Uncertain environment difficult orientation problem<br><br>Short times require high power communications<br><br>Cannot obtain very high resolutions required (1 - 2 ft) |
| 200,000 ft ↓ ~25,000 ft | Better resolution than FS TV | Impossible environment |
| 25,000 ft ↓ Impact | Correlate with FS TV<br><br>High resolution (1 ft - 1/4 ft) | Limited sample<br><br>Stable platform required to compensate for FC dynamics on parachute. |

## 6.3 CAMERA DEPLOYMENT AND IMAGE FORMAT

The wind-induced suspended-capsule drift velocity on the parachute (up to 200 ft/sec) coupled with suspended-capsule descent velocities from 70 to 150 ft/sec precludes the use of conventional image nesting concepts based on obtaining resolution increments due to lower altitude while retaining common area coverage. Before a sufficient resolution improvement occurs, capsule drift reduces the common image area to zero.

To simultaneously satisfy image resolution and nesting requirements during parachute descent, a three-camera system with boresighted optical axes has been selected. The cameras are designed with boresight resolutions in a 9:3:1 ratio and identical 200 x 200 element formats. They are exposed simultaneously to generate a nested set of three images. The 200 x 200 image format has been chosen as the best compromise in the light of data-transmission limitations between area coverage and the variety and number of images required to achieve

the experimental objectives. At least 11 pictures can be taken and transmitted during parachute descent even in the sparsest atmospheres, in denser atmospheres additional images may be taken in a variety of ways to increase the total number of samples. The pictures are taken at altitudes between 24,500 feet and 1400 feet to yield a resolution range of 36 to 0.25 ft/TV line. The image format resolution, and area coverage of the 3-camera system is illustrated in Figure 58.

## 6.4 EXPOSURE TIME -- TUBE SENSITIVITY -- LIGHT LEVEL

The anticipated light levels for television pictures of the Martian surface depend upon the surface albedo and photometric function. Both are uncertain at present. Figure 59 indicates the anticipated average surface brightness levels for two photometric models of the Martian surface. The actual photometric function of the surface is believed to lie between the Lunar surface function and the Lambertian surface model. From this illustration, the anticipated range of surface background brightness in the desired solar elevation angle range (20 to 30 degrees) is 100 to 580 feet-lamberts.

Of greater significance in the design of the television experiment is the selection of the light level for which the camera signal-to-noise-ratio is unity. This level must be sufficiently below the average background brightness to produce adequate contrast in the television images. The unity signal to noise ratio brightness has been selected at 30 feet-lamberts. If higher sensitivity vidicons were available for this mission, 15 feet-lamberts could be used.

After consideration of sterilization and reliability requirements, two candidate image tubes were analyzed - a standard 1-inch vidicon and a higher sensitivity, 2-inch return-beam vidicon. Both tubes have antimony sulphide-oxy-sulphide photoconductors. Figure 60 indicates the exposure times required to achieve unity signal to noise ratio at a surface background brightness of 30 feet-lamberts for each tube. The standard vidicon selected for the mission - by Langley Research Center direction - requires approximately 1.0 msec exposures for adequate image contrast.

## 6.5 FLIGHT CAPSULE DYNAMICS - IMAGE SMEAR

In order to meet the light sensitivity requirements of the television experiment, exposure times of 1.0 msec are required. Flight capsule motions during this exposure interval in turn limit allowable resolution for unsmeared images. In analyzing the effect of flight capsule dynamics, images were considered unsmeared if total image motion was less than 1/2 of a television line.

### 6.5.1 Image Smear Considerations

During parachute descent the flight capsule (and camera) may experience the following dynamics components:

-156-
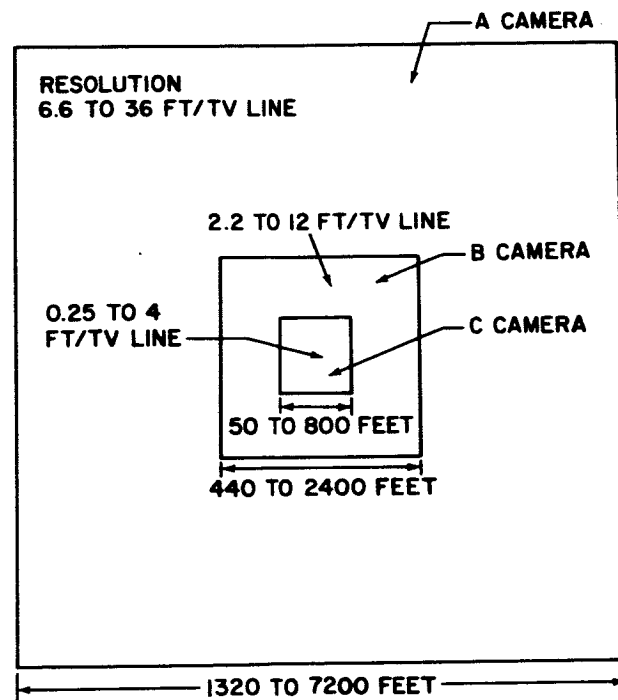
RESOLUTION AND FIELD OF VIEW DEPEND UPON ALTITUDE
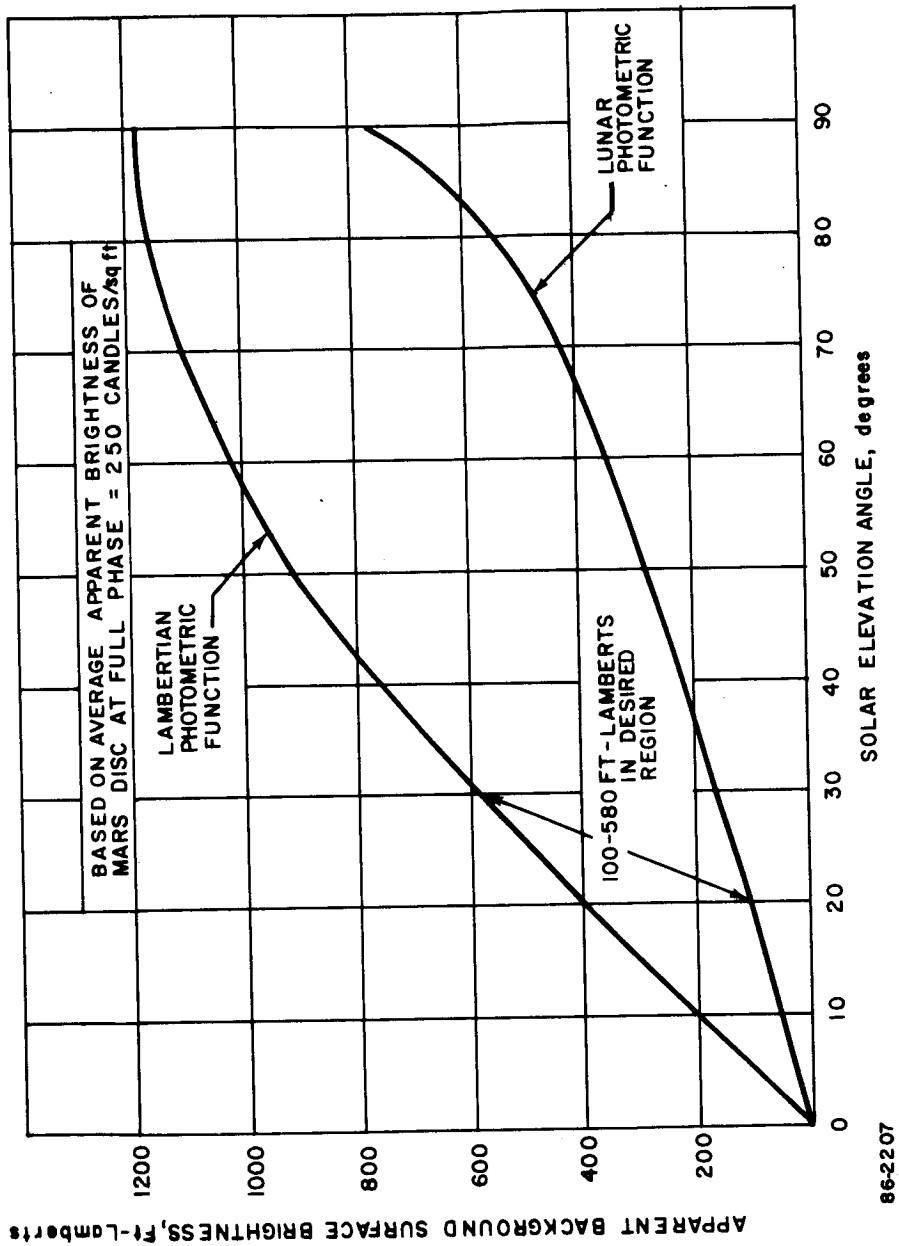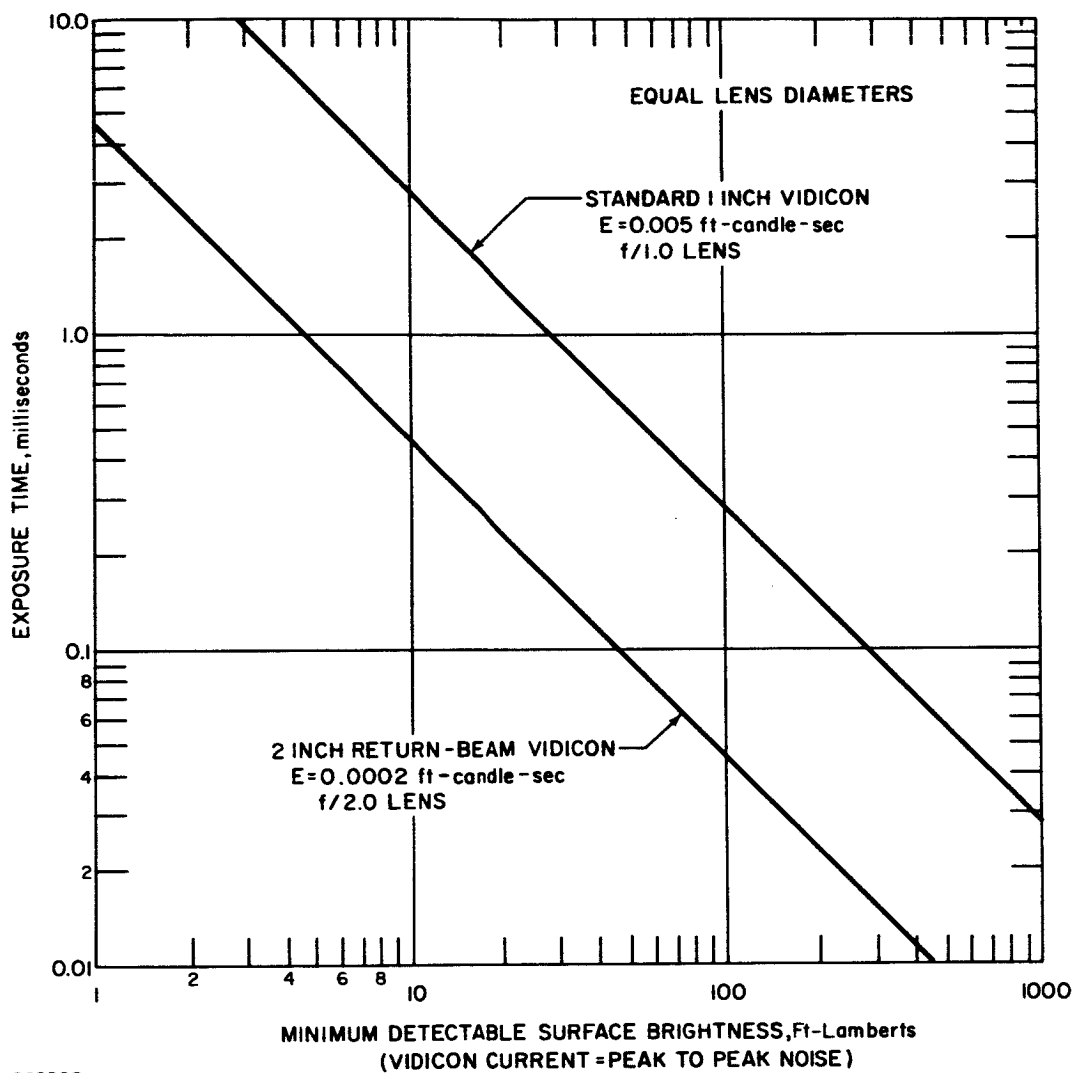


Figure 58  TELEVISION IMAGE FORMAT

Figure 59 MARTIAN PHOTOMETRIC PROPERTIES

86-2207

-158-

Figure 60  COMPARISON OF STANDARD AND RETURN-BEAM VIDICONS

862208

$V_H$ = Horizontal drift velocity (up to 200 ft/sec)

$V_v$ = Vertical descent velocity (from 70 to 150 ft/sec)

$\theta_c$ = Camera look angle with respect to local vertical (up to 90 degrees)

$\dot{\theta}_c$ = Camera swing rate (up to 100 deg/sec)

$\dot{\beta}$ = Camera spin about the flight capsule roll axis (up to 10 rpm)

These motions contribute to image smear as indicated in equation (1) below. *

$$\left( V_H + \frac{\pi}{180} \ Z \dot{\theta}_c \ \sec^2 (\theta_c + \delta) + V_v \tan (\theta_c + \delta) + \frac{\pi}{30} \ Z \dot{\beta} \ \frac{\tan \delta}{\cos^2 \theta_c} \right) T_E = S \qquad (1)$$

where

Z = Camera altitude (feet)
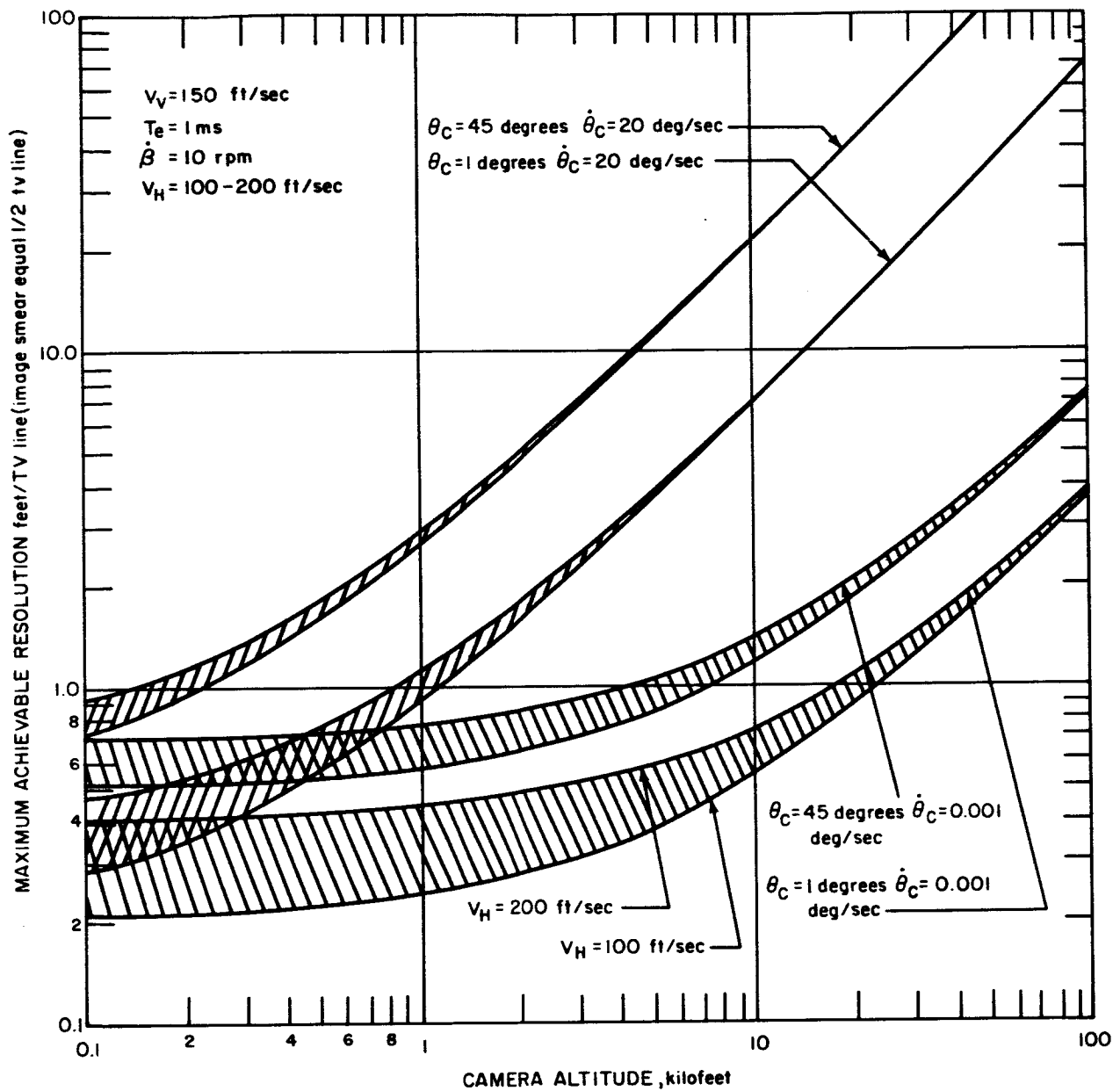
$T_E$ = Exposure duration (seconds)

S = Image smear (feet)

$\delta$ = Angle between an image element and the camera optic axis (degrees) ($\delta_{max} \approx$ camera field of view half-angle)

Using the criterion that the best resolution obtainable occurs when the smear component is less than 1/2 of a television line, S may be set equal to R/2 to establish a relationship between flight capsule dynamics and resolution. It is apparent from equation (1) that reducing the camera angle $\theta_c$ toward 0 degree, minimizes the effects of swing rate, vertical descent velocity and roll. In general, as $\theta_c$ approaches 0 degree, capsule swing rate $\dot{\theta}_c$ is the primary dynamics factor which limits resolution. The ultimate resolution limit is determined by horizontal drift velocity, especially at low altitudes where the highest resolution images can be obtained.

Figure 61 illustrates the extent to which various dynamics factors limit resolution at altitudes of interest. Note that both swing rate and camera angle in the worst case depicted are below those which might be encountered on the parachute. Thus, the 1.0 msec exposure times required for adequate light sensitivity for standard vidicon tubes, in fact limit effective resolution to worse than 5 ft/TV line on the parachute.

---

* The approximate formula indicates smear of image elements within the camera field of view and is useful for illustrating the relation of each of the dynamics factors to image smear. The formula is valid only for short exposure durations during which camera velocity is constant, and assumes that all smear components add linearly (a conservative assumption).

Figure 61  TELEVISION RESOLUTION LIMITATIONS -- FLIGHT CAPSULE DYNAMICS

Chart labels:

MAXIMUM ACHIEVABLE RESOLUTION feet/TV line (image smear equal I/2 tv line)

CAMERA ALTITUDE, kilofeet

$V_V = 150$ ft/sec
$T_e = 1$ ms
$\dot{\beta} = 10$ rpm
$V_H = 100 - 200$ ft/sec

$\theta_C = 45$ degrees  $\dot{\theta}_C = 20$ deg/sec
$\theta_C = 1$ degrees  $\dot{\theta}_C = 20$ deg/sec

$\theta_C = 45$ degrees  $\dot{\theta}_C = 0.001$ deg/sec
$\theta_C = 1$ degrees  $\dot{\theta}_C = 0.001$ deg/sec

$V_H = 200$ ft/sec
$V_H = 100$ ft/sec

862209

-161-

### 6.5.2 Allowable Flight-Capsule Rates

To achieve unsmeared images at 1.0 ft/TV line at an altitude of 2000 feet (approximately the lowest altitude from which an entire image can be transmitted), cameras must be exposed under the following dynamics conditions:

$T_E$ = 1 msec,

$V_H$ 200 ft/sec

$V_v$ 150 ft/sec

1) For $\theta_c$ = 0 degree and flight capsule spin alone - $\dot{\beta} \leq 85$ rpm

2) For $\theta_c$ = 0 degree and flight capsule swing alone - $\dot{\theta}_c \leq 6.3$ deg/sec

3) For $\theta_c$ = 30 degrees and flight capsule spin alone - $\dot{\beta} \leq 44$ rpm

4) For $\theta_c$ = 30 degrees and flight capsule swing alone - $\dot{\theta}_c \leq 4.5$ deg/sec

5) For $\theta_c$ = 45 degrees and flight capsule spin alone - $\dot{\beta} \leq 21$ rpm

6) For $\theta_c$ = 45 degrees and flight capsule swing alone - $\dot{\theta}_c \leq 3.1$ deg/sec

Beyond $\theta_c$ = 45 degrees resolution is rapidly degraded because of increased range to the surface, and thus, higher look angles are not considered desirable.

## 6.6 FLIGHT CAPSULE PARACHUTE EFFECTS

In order to satisfy the television-image resolution requirements on the parachute, rather stringent dynamics constraints (discussed in the previous section) are imposed on the cameras. These conditions may be difficult to meet during parachute descent in a still atmosphere; they are even more difficult to meet in the presence of anticipated wind gusts.

### 6.6.1 Typical Parachute Dynamics

Figure 62 indicates the geometry used in the analysis of wind-gust effects on a parachute system with the suspended capsule attached to the main-chute shroud lines by a single riser line. Figure 63 is presented to give the reader a physical picture of the parachute and suspended-capsule oscillations in the presence of wind-gusts. As is evident, the parachute has a long-term oscillation while the suspended capsule oscillates at a higher frequency about the riser-line suspension point. Minimization of parachute-capsule oscillations is clearly desirable.
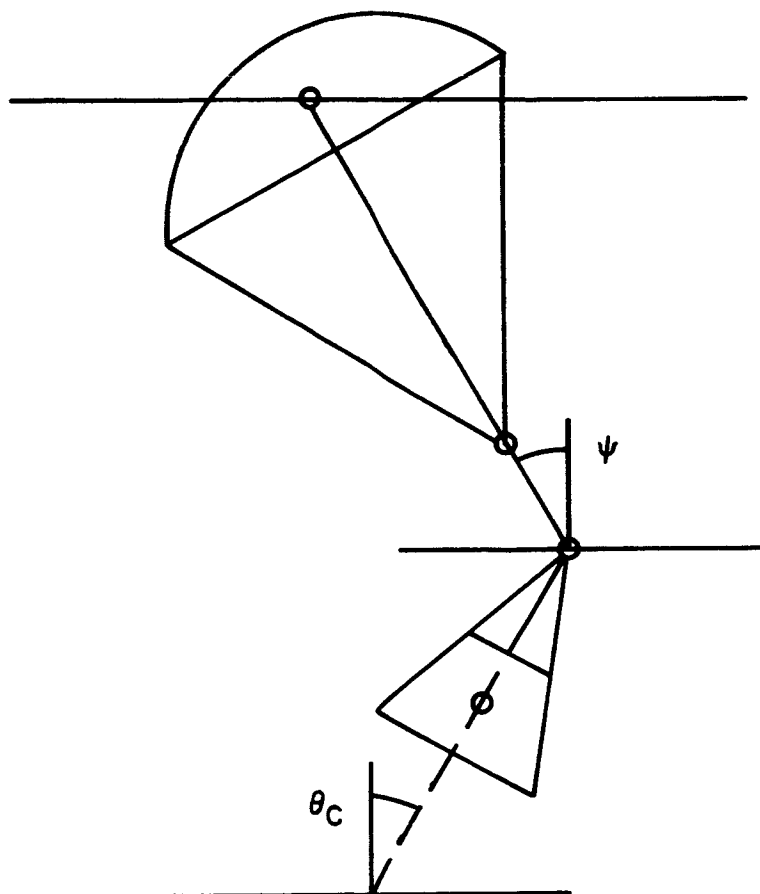
25-1084

Figure 62  PARACHUTE DYNAMICS
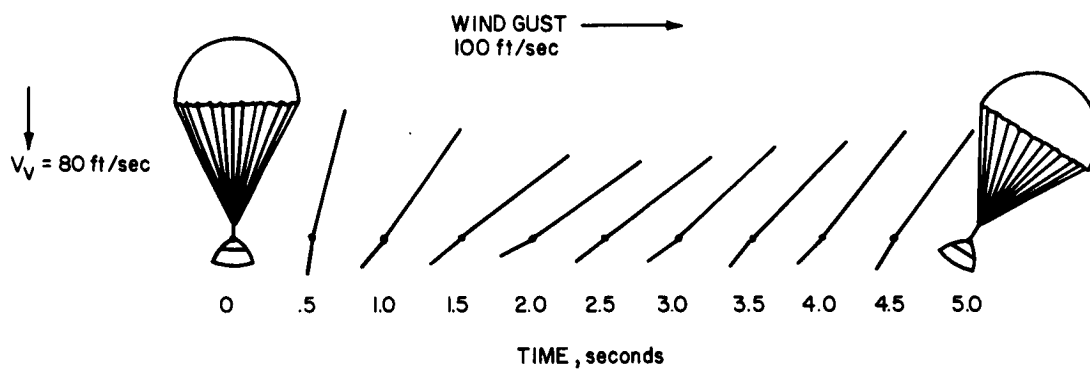
Figure 63  PARACHUTE DYNAMICS PICTORIAL

25-1229

Figure 64 indicates the effects of parachute size (area of main parachute/suspended capsule weight, A/W) on the flight capsule swing angle for planar motion. Note that the VM-4 atmosphere (highest dynamic pressure) is used in this and subsequent illustrations of parachute behavior. For large values of A/W, the suspended-capsule swing angle is very high (<90 degrees). As parachute size decreases down to values somewhat in excess of A/W = 3.5 $ft^2$/lb, the maximum value of swing angle decreases. Below A/W = 3.5 $ft^2$/lb, the swing angle excursions actually increase somewhat, but seem to damp more quickly because of the poorer overall stability of the smaller parachute and coupling of the suspended capsule oscillations into the parachute oscillations. The conceptual design utilizes an A/W = 5.0 $ft^2$/lb.

Figure 65 illustrates the capsule swing rate during the swing angle variations in the previous figure. This illustration also supports the conclusions that perhaps an optimum A/W exists above 3.5 $ft^2$/lb. Very high values of A/W produce look angles which are high and remain high for a long time. Very low values of A/W yield swing rates, $\dot{\theta}_c$ , which are high and damp slowly.

Figure 66 demonstrates the effects of gust-magnitudes on parachutes with A/W = 3.5 $ft^2$/lb. The same general behavior is evident for gust magnitudes between 100 and 200 ft/sec. The major difference is the increase in maximum suspended capsule swing angle from 60 to 85 degrees.

From the series of illustrations presented in this section, it is apparent that wind gusts will produce suspended capsule look angles and swing rates much higher than those allowed for non-smeared images at 1.0 ft/TV line resolution. Furthermore, the analysis is only indicative of parachute dynamics during planar motions. Cross gusts during the transients illustrated will, in general, give rise to complex coning motions for which both rates and angles can maintain excessive values for at least the 8 to 10 seconds characteristic of the planar motions.

## 6.6.2 Parachute/Harness Design Considerations

The previous parachute dynamic analyses showing the influence of a sudden wind gust, indicated excessive angular motions of both the complete parachute system and the suspended capsule with the actual angles and rates dependent upon wind-gust magnitude and parachute size. Furthermore, the very high angular rates of the suspended capsule which occured may be partly due to the attachment concept of a single riser line and swivel joint. The high angular rates of the suspended capsule can probably be reduced by a different suspension attachment, as indicated in the right-hand sketch in Figure 67 (i.e., dividing the shroud lines into four groups and attaching each group at a discrete point on the capsule). With this concept, the suspended capsule is not hinged at a single point. Further analyses are

Figure 64 PARACHUTE DYNAMICS -- CAPSULE SWING ANGLE
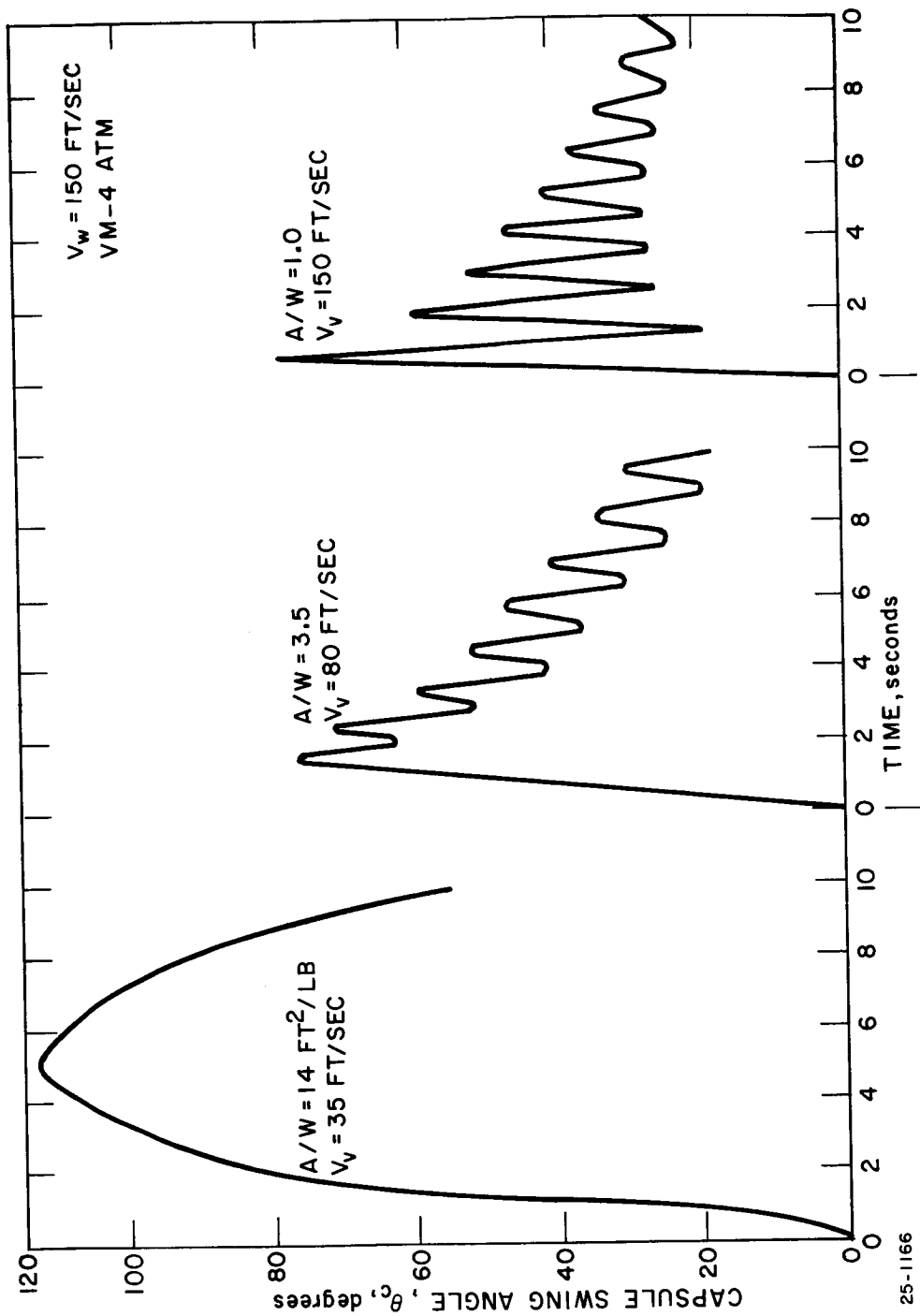
25-1166

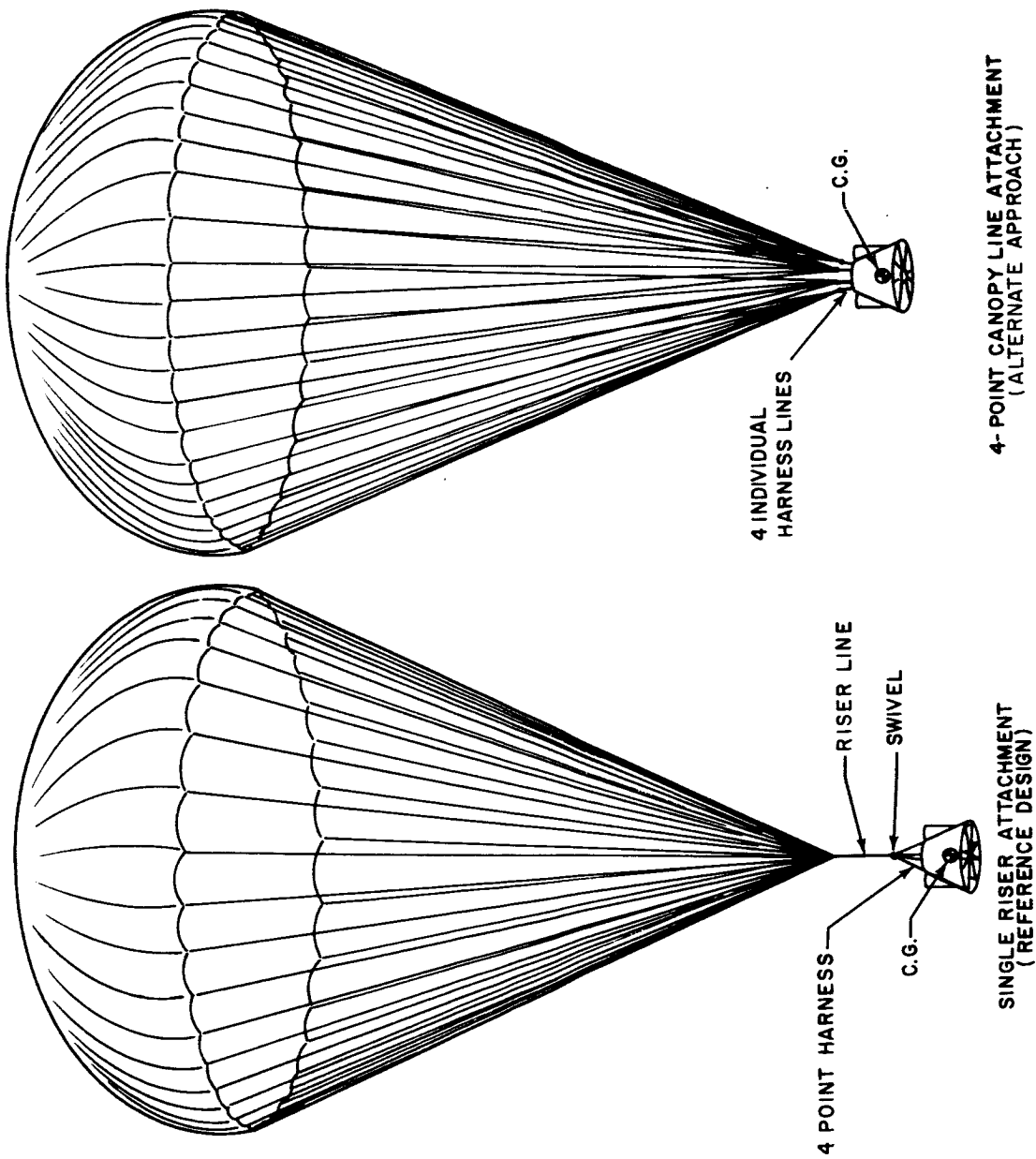-166-
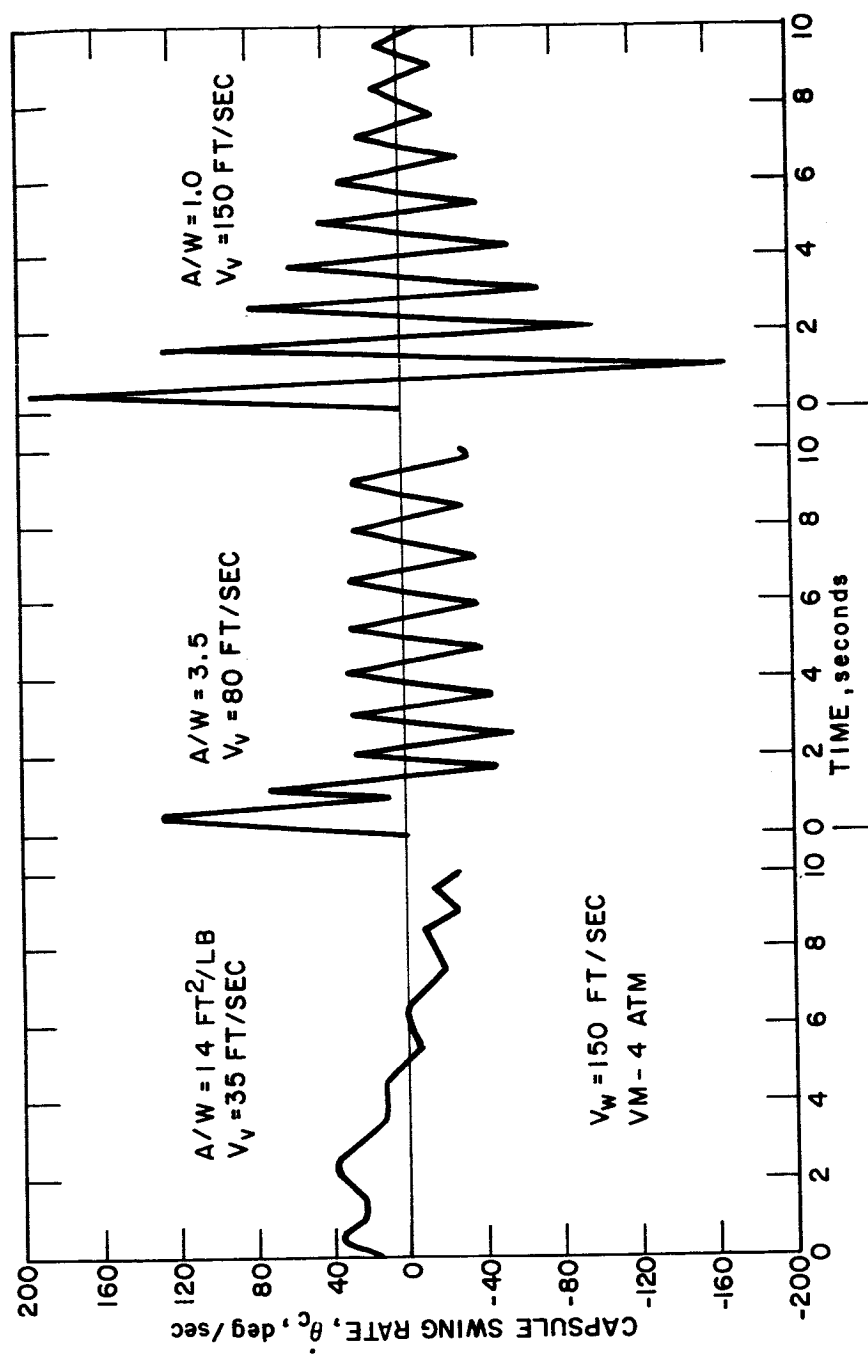
Figure 65 PARACHUTE DYNAMICS -- CAPSULE SWING RATE

25-1165

-167-
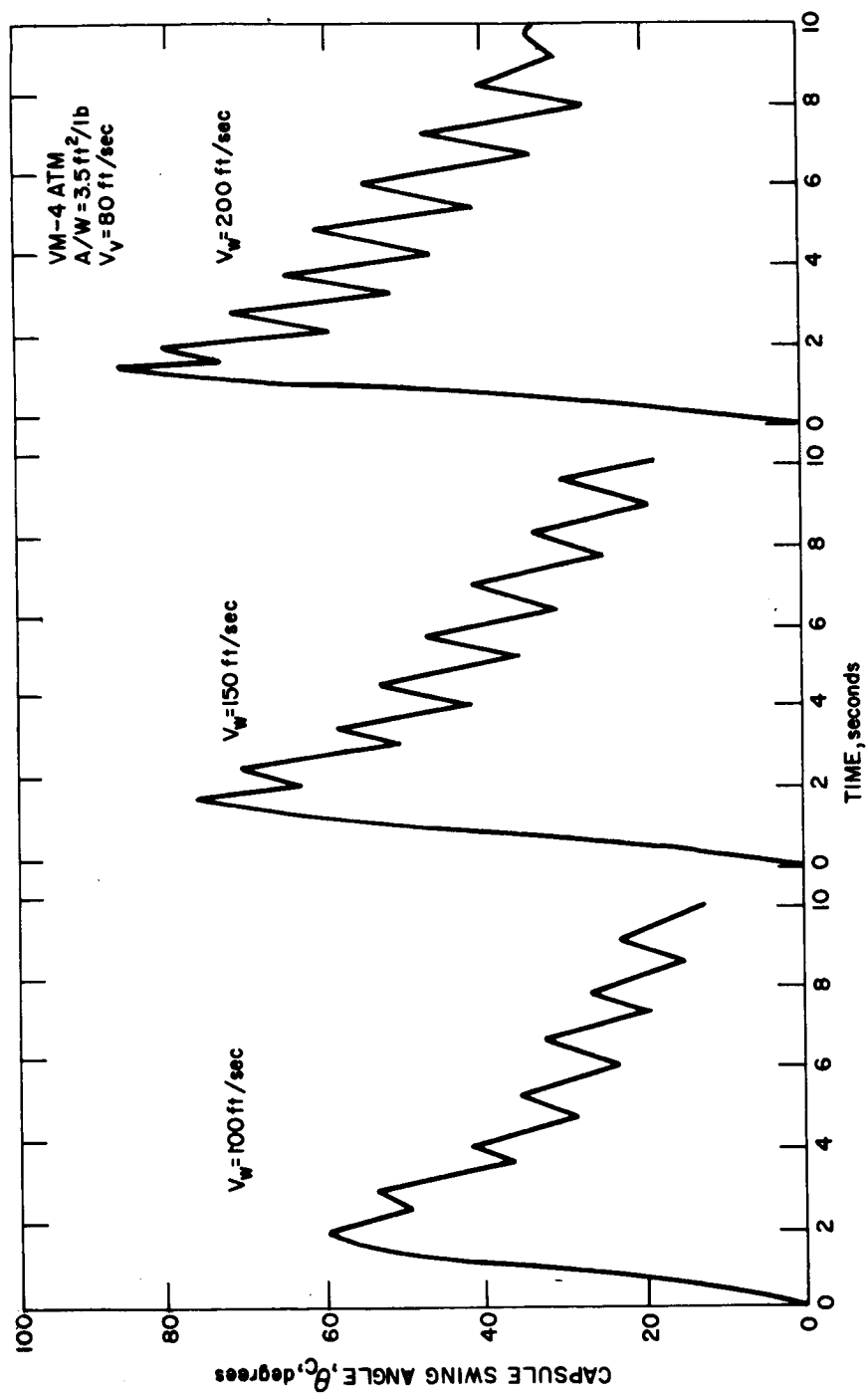
Figure 66 PARACHUTE DYNAMICS--CAPSULE SWING ANGLE

25-1161

-168-

C.G.

4 INDIVIDUAL
HARNESS LINES

4- POINT CANOPY LINE ATTACHMENT
(ALTERNATE APPROACH)

RISER LINE

SWIVEL

4 POINT HARNESS

C.G.

SINGLE RISER ATTACHMENT
(REFERENCE DESIGN)

25-1199

Figure 67   PARACHUTE ATTACHMENT CONCEPTS

required to verify these conclusions and to determine deployment procedures for the four-group attachment.

However, although several features of parachute design can reduce high look angles and high swing rates, it is unlikely that these variables can be maintained below the 30 and 4.5 deg/sec levels necessary to satisfy the high resolution television requirements.

### 6.6.3 Conclusions

The adverse camera dynamics on parachute coupled with the low sensitivity of standard vidicon tubes constitutes the major design problem of the television experiment. Two approaches to alleviating these dynamics effects have been considered in detail. The first involves waiting for favorable dynamics before exposing the cameras. For wind gusts up to 200 ft/sec., the capsule swing angle returns to less than 30 degrees within approximately 8 seconds of the onset of a gust. Furthermore, the planar-capsule oscillations produce swing rates which go through zero about twice each second (see Figure 65). Thus, it is likely that favorable dynamics will exist within 8 seconds of a wind gust. To implement this approach, capsule swing rate and swing angle are sensed and the camera shutters are inhibited while these motion parameters are outside of design limits. Of course, to remove the possibility that long periods of unfavorable dynamics will result in an excessive loss of communication time, a time-gated shutter logic override would be provided.

In using the wait for favorable dynamics approach, two potential problems still remain.

1. It is highly probable that unfavorable dynamics will exist for long periods due to parachute system coning induced by cross gusts.

2. The performance of the television experiment is highly sensitive to wind and wind gust models which cannot be verified prior to the mission.

As a result of these factors, a second approach involving camera stabilization was considered.

## 6.7 CAMERA STABILIZATION PLATFORM

### 6.7.1 Platform Requirements

The prime contribution to image smear are suspended capsule swing angle and swing rate. The television cameras can be stabilized against these motions by mounting them on a two-axis gimballed platform slaved to the four-axis inertial reference system platform.

-170-

Analysis of the required stabilization indicates that control of the camera pitch and yaw rates over suspended capsule swing angles up to 45 degrees from local vertical is sufficient to reduce smear to tolerable levels with a minimum of complexity. Stabilization of the camera in roll (or spin) is also desirable but the modest performance improvement which results from the inclusion of a third gimbal does not justify the additional complexity. This third gimbal would require a full 360 degrees of travel which generates requirements for slip rings or other moving electrical contacts.

The television-camera platform characteristics selected are given in Table XXX. * A pictorial representation of the three boresighted cameras mounted on the two-degree of freedom gimbal arrangement is shown in Figure 68. The three cameras are contained in a cylindrical environmental canister for thermal control. A thin optical quartz window at one end provides camera viewing. This canister is mounted on the inner gimbal inside the yoke of the outer gimbal. Electrical connection between the cameras and the television electronics, housed in the aft end of the outer cylindrical structure, is provided by circular loops around each of the gimbals. This arrangement minimizes cable bending and allows maximum movement of the camera. Each gimbal is actuated by electrical torque motors slaved to the inertial reference platform.

## TABLE XXX

### TV PLATFORM CHARACTERISTICS

2-Gimbal system (pitch and yaw)

Slaved to inertial reference system gimbals

Points camera within 1 degree of local vertical for
FC roll axis angles $\leq$ 45 degrees

TV shutters are inhibited to FC roll axis angles
> 45 degrees

Residual camera pitch and yaw rates < 0.001 deg/sec.

Total camera swing rate < 0.0014 deg/sec.

---

* Additional discussions of platform implementation appear in Volume V, Book 5 paragraph 8.5.

TV PLATFORM IS SLAVED TO
INERTIAL REFERENCE
SYSTEM PLATFORM

STRUCTURES

TV ELECTRONICS

2 - DEGREE OF FREEDOM GIMBAL

ENVIRONMENTAL
BOOT

3 - BORESIGHTED
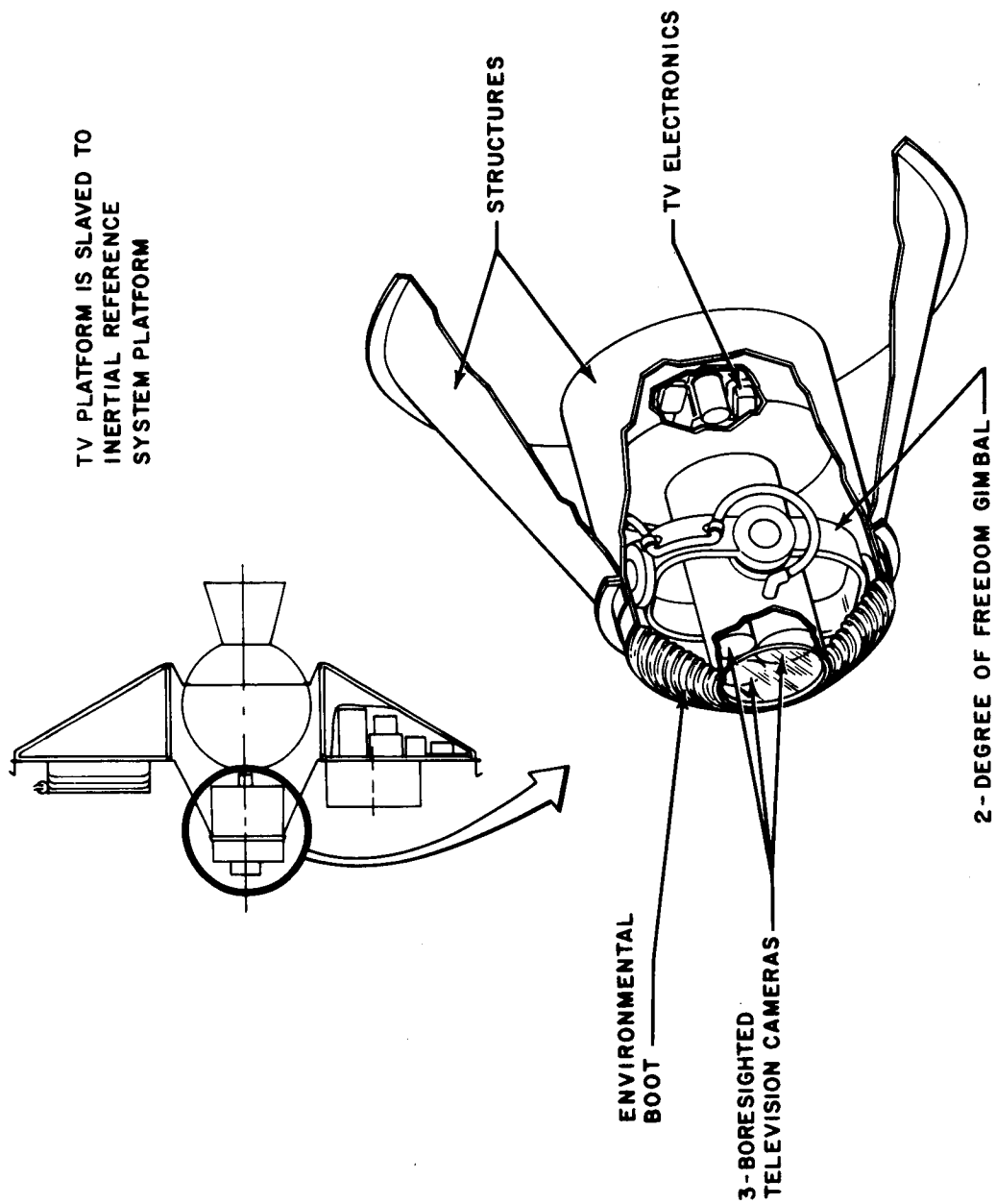TELEVISION CAMERAS

760200P-A

Figure 68 TELEVISION CAMERA PLATFORM

In selecting the platform characteristics given in Table XXX major consideration was given to the 1-degree pointing error (error in achieving a local vertical orientation of the camera axes). This error arises primarily from inertial reference-system platform misalignment at the time the flight capsule is separated from the flight spacecraft and gyro drift from separation to impact. From equation (1) in paragraph 6.5.1 it is apparent that this angle determines the extent to which vertical descent velocity and flight capsule roll pitch and yaw rates contribute to image smear. It is, therefore, desirable to reduce this error to as small a value as is practical. However, the highest resolution camera in the reference design has an angular field of view of 2.7 degrees; when this camera axis is precisely oriented along the local vertical, some image elements will be at off-axis angles up to 1.35 degrees. Figure 69 illustrates this condition. With a 1-degree pointing error, those elements, which experience minimum smear (along the vertical axis) merely appear at a different point in the image format. Some image elements will experience less smear than they would for correct point, while others will experience more smear. In general, pointing errors less than the camera-field half angle of 1.35 degrees are negligible. Pointing errors between 1.35 and 5 degrees are tolerable. A nominal 1 degree pointing error has been assumed in the analyses presented.

The residual pitch and yaw rates given in Table XXX are typical of such platforms. Actually, swing rate (for $\theta_c$ = 0 degree) does not become a significant smear contributor until it reaches about 0.1 deg/sec.
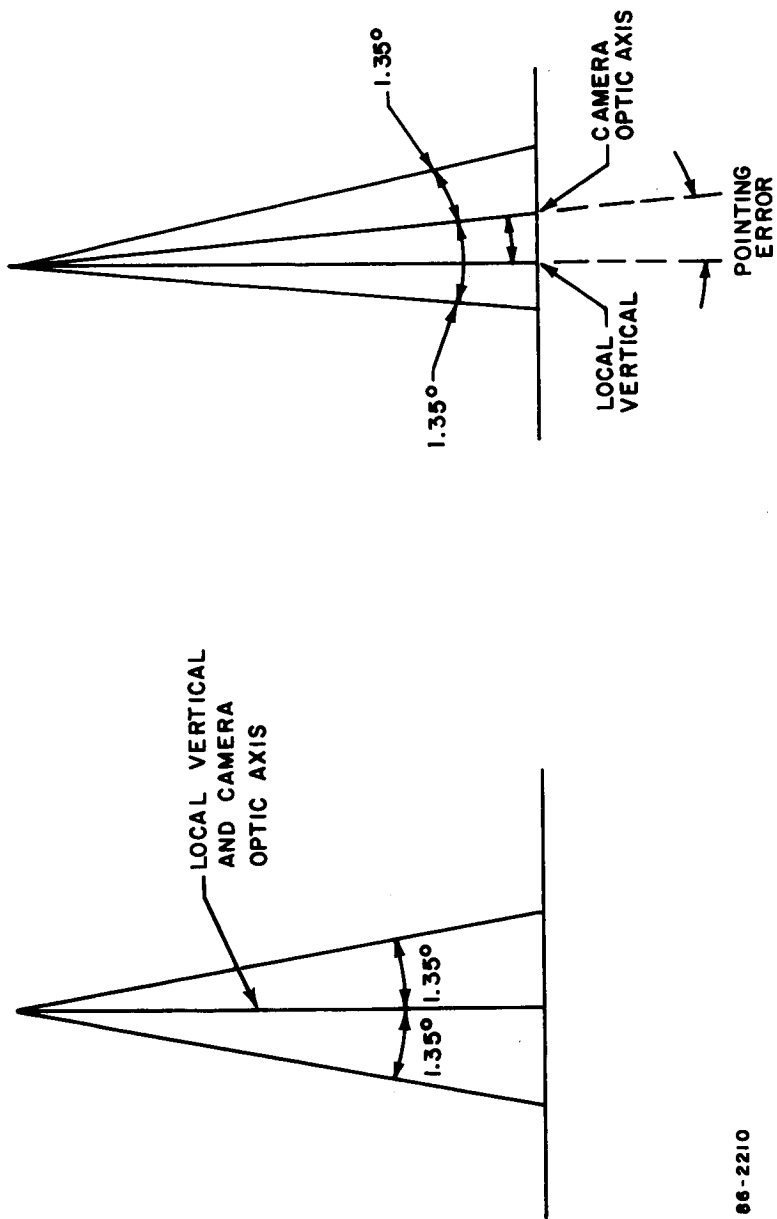
## 6.7.2 Television Resolution with Camera Platform

When the camera stabilization platform is used, resolution at low altitude is limited almost exclusively by horizontal drift velocity over the surface. At high altitudes, significant smear is generated by vehicle spin (or roll) for the pointing errors and camera angular aperatures in the reference design. Figure 70 illustrates the resolution limits imposed by the 1/2 television line smear criterion. It is apparent from the graph that the resolution objective of the television experiment can be achieved through the use of the stabilized platform.

In interpreting Figure 70,* several factors should be considered:

　　1. With the cameras oriented in the vertical direction, there are actually two distinct sources of horizontal drift velocity - the normal wind-induced steady translational component of the entire parachute and suspended capsule and main parachute and/or capsule coning motions which result in an effective translational velocity. This second component can be as great as 20 to 50 ft/sec even if the parachute system

---

* Note that the assumption on which the figure is based include $\theta_c$ = 1 degree; Figure 62 presents similar information for $\theta_c$ = 1 degree and thus, the two illustrations can be directly compared.

Figure 69 EFFECTS OF PLATFORM POINTING ACCURACY ON C-CAMERA SMEAR

86-2210

-174-
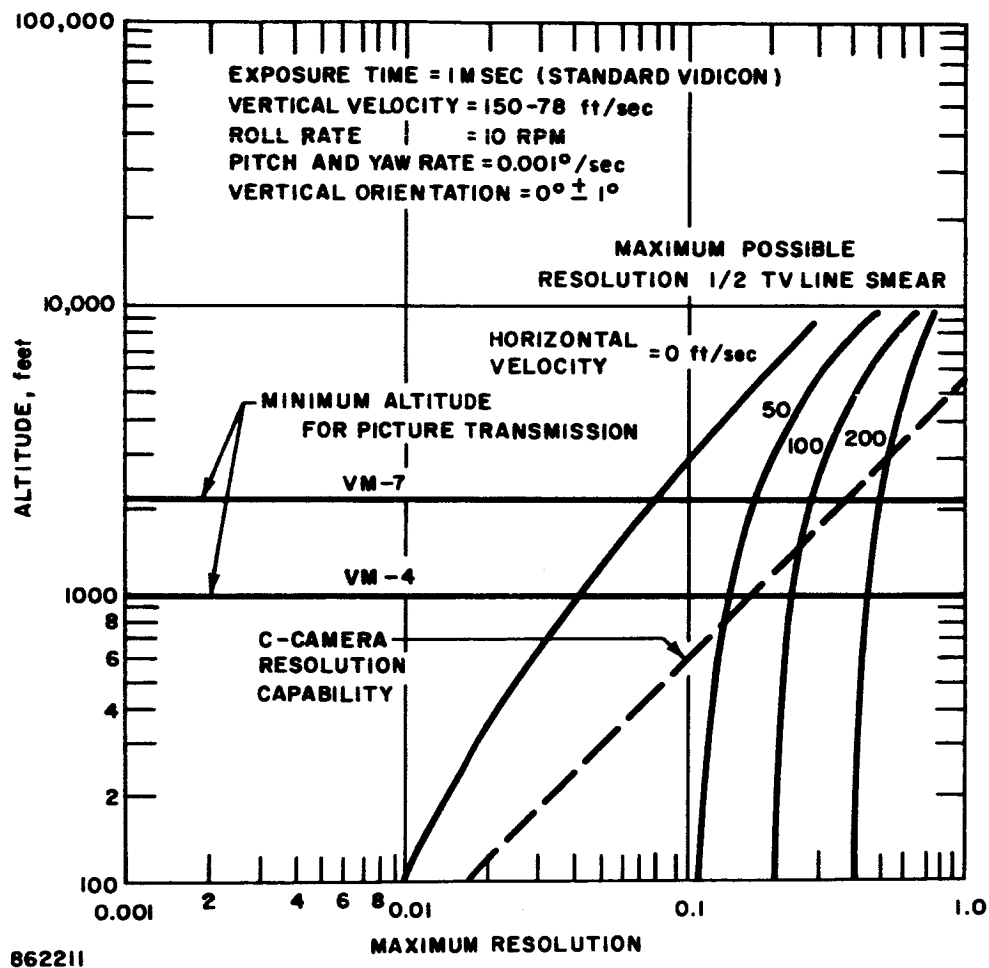
Figure 70  MAXIMUM TELEVISION RESOLUTION

862211

does not assume a long term translational component. Thus, the 0 ft/sec horizontal velocity performance may never be achieved.

2.   The actual C-camera (high resolution camera) resolution capability indicated implies that this camera will experience less than 1/2 television line smear at altitudes above about 2800 feet for all drift velocities considered. At lower altitudes, the smear may exceed 1/2 of a television line for high drift velocities.

3.   The camera system has a lower limit on operational altitude imposed by the requirement to transmit the last picture prior to impact. This low-altitude limit and its relation to both image-smear and C-camera resolution capability illustrates how close the reference design is to the ultimate experimental capability which can be achieved without major impact on many of the other flight capsule subsystems.

## 6.7.3   Failure Mode Considerations

Inclusion of the television camera platform in the reference design involves several additional failure-mode considerations. These include 1) failure of the gimbals to release from the locked position after parachute deployment, 2) failure of the gimbal system to perform properly after release, and 3) encountering long-duration intervals during which one or both of the gimbals remains against a stop ($\theta_c > 45$ degrees).

Prior to parachute deployment, the gimbals are mechanically locked, such that the camera axes are aligned with the flight-capsule roll axis. If the gimbals do not release after parachute deployment in accordance with the preset sequence, camera rates and angles will be equal to flight capsule rates and angles. In this operating mode, the shutter logic will be based on the wait for favorable dynamics approach, and the cameras will be inhibited for $|\theta_c| \geq 30$ degrees $|\theta_c| \geq 13$ deg/sec. With these dynamic constraints, the C-camera images will be excessively smeared, but there is a high probability that both the A- and B-cameras will operate properly.

There are many distinct ways in which the gimbals may not perform properly after release. The inertial reference system platform and design logic must be selected such that 1) camera rates and angles are no worse than capsule rates for the most likely failure modes, and 2) the shutter logic appropriate for the wait for favorable dynamics approach is used when such failures are sensed.

Even if the gimbal system operates properly, there is a low, but non-zero, probability that the gimbals will remain against a stop for periods longer than the 8.2-second duration of the shutter enable gate. Under these circumstances, the shutters will be opened while the platform is against a gimbal stop. However, the actual roll axis angle $\theta_c$ will be reduced by

45 degrees in this case and pitch and yaw rates may be partially compensated for especially for long-durations, slow-rate coning motions at high angle. In this operating mode the A- and B-cameras will operate properly and some smearing will occur on the C-camera pictures.

## 6.8 TELEVISION EXPERIMENT REFERENCE DESIGN SUMMARY

### 6.8.1 Cameras and Optics

Typical specifications for the three-camera TV system using standard state-of-the-art 1-inch vidicons are presented in Figure 71. In general, the A- and B-cameras are similar in many respects to Ranger cameras. The C-camera is closest to design limits. Double-blade mechanical shutters are contemplated to satisfy the short exposure time requirements. The requirement for a minimum detectable signal of 30-foot lamberts is based upon the assumed Martian surface photometric function and the desirability of maintaining high signal-to-noise ratio for adequate contrast. Two color filters are used on the A-camera only, since it is the only one with sufficient signal energy to accommodate filter losses.

### 6.8.2 Stabilization Platform

The characteristics of the stable, two-axis camera platform are summarized in Figure 72. With the platform, image resolution from 0.1 to 1.0 ft/TV line may be achieved depending on drift velocity at low altitudes. In addition, inclusion of the stable platform in the television subsystem reduces the dependence of television performance on wind and wind gust models as well as parachute and harness design constraints.

### 6.8.3 Anticipated Picture Yield

The television experiment yield is dependent upon the atmosphere encountered during parachute descent. Both the number of images transmitted and the altitudes at which images are taken (hence their resolution) are different in each Model atmosphere. In all cases, the highest resolution is adequate for the detection of object hazards and the lowest resolution is adequate for locating capsule pictures in flight capsule pictures. The shutter logic is designed such that active video data is transmitted during the entire descent interval (beginning immediately after the first image set is read-off the image tubes). Figure 73 indicates the anticipated image yield for each model atmosphere considered.

In all atmospheres at least one image at 1.0 ft/TV line resolution will be obtained. Additional higher resolution images to 0.25 ft/TV line will be transmitted in VM-3 and VM-4; these may be smeared if high horizontal velocities are encountered.

- Image Tubes — 3 Boresighted 1" Vidicons Mounted on 2-Axis Slaved Platform

- Optics

| | A Camera | B Camera | C Camera |
|---|---|---|---|
| Field | $24^0$ | $8.2^0$ | $2.7^0$ |
| Focal Length | 0.4" | 1.1" | 3.3" |
| Relative Aperture | f/2 | f/1.6 | f/1 |

- Sensitivity — Unity SNR at Surface Brightness of 30 Ft-Lamberts

- Weight — 60 Lbs. Including Platform, Power Supply, Camera Electronics

- Power — 27 Watts

- Pictures

  3 Sets of 3 Nested Images/Set Minimum

  200 x 200 Lines

  32 Grey Levels

  2-Color Filters on A-Camera

7601187P

Figure 71 TELEVISION CHARACTERISTICS, CAMERAS, AND OPTICS

2-Gimbal System (Pitch and Yaw)

Slaved to Inertial Reference System Gimbals

Vertical Pointing Error $<1^0$ For Capsule Elevation Angles $<45^0$. (TV Shutter Inhibited for Elevation Angles $>45^0$)

Residual TV Pitch and Yaw Rates $<0.001^0$/Sec.

Weight    -    10 Lbs.
Power     -    8 Watts

Figure 72  TELEVISION PLATFORM CHARACTERISTICS

760237P

-179-

|  | ATMOSPHERE | | | | |
|---|---|---|---|---|---|
|  | VM-3 | VM-4 | VM-7 | VM-8 |
| Number of Pictures | 16 | 22 | 11 | 12 |
| Altitude Range (1000 Ft.) | 24.3-2.8 | 24.5-1.4 | 23.9-5.3 | 18.3-5.4 |
| Resolution Range (FT/TV Line) | 36-0.5 | 36-0.25 | 36-0.9 | 28-0.9 |

SEQUENCE: First Picture Set Taken Less Than 10 Seconds After Chute Deployment;
Subsequent Sets at 43 Second Intervals.

760182P

Figure 73 TELEVISION CHARACTERISTICS, ANTICIPATED PICTURE YIELD

## 7.0 WIND VELOCITY EXPERIMENT DESIGN

### 7.1 EXPERIMENT OBJECTIVES

The primary reason for making wind-velocity measurements is to provide data necessary for the design of vehicles which will land and operate on the Martian surface. If a hard landing system which utilizes only a parachute or other aerodynamic terminal descent mechanism is to be used, then the wind velocity may well determine the maximum impact velocity. The parachute can be designed to reduce the vertical component of velocity dependent on the atmospheric model used, but relatively little can be done to prevent the whole assembly of parachute and lander from assuming the horizontal velocity of the wind. The present large uncertainty in the wind velocity will probably cause the design of the impact attenuation system for the lander to be fixed by the horizontal rather than the vertical velocity. In the design of soft landers, which utilize a propulsive terminal descent system, the wind velocity is less critical, since the thrust required to offset the low horizontal forces applied by even the highest wind-gust models will be small compared with the total thrust requirement. However, the wind velocity is also important after landing. If surface mission lifetimes of days or weeks are planned, the effects of wind-driven sand and dust must be considered. Such materials may bury the lander before its mission is completed. Even for lesser amounts of dust or sand, the erosive action of the particles on sensitive optical and mechanical parts might become a serious problem.

In addition to these engineering considerations, the nature of winds and wind-blown particles is of scientific interest. Apart from the obvious meteorological ramifications, winds and wind-blown particles may prove to be the major forces for geological change on a planet with negligible liquid water and perhaps a solid core and thus little tectonic or volcanic activity. The presence or absence of winds, particles, and dunes will also have a profound effect on the nature of possible Martian life forms. These factors may be among the dominant ones which shape evolutionary patterns.

Although the importance of making wind velocity measurements is readily demonstrated, a serious problem arises when the validity of a 2 to 4 minute sampling of wind velocity is considered. Such a time limitation is inherent in any wind-velocity measurement technique which has been proposed for nonsurvivable probes. A consideration of the use to which possible results may be put emphasizes this point. If zero or low wind velocities are measured even by several probes at a given opposition, lander designers will not design for these levels but will defer to the higher values previously determined from Earth-based observations and computations. They will argue that the few minutes of observation from the probes just didn't catch the high winds, and to base a multi-million dollar program on any other assumption would be absurd. If intermediate winds (25 to 75 ft/sec) are observed, similar arguments will be used to disregard the data.

-181-

Lander designs will be influenced only if high (200 to 500 ft/sec) winds are observed. The most probable effect then will be to increase the design ground rules to velocities two or three times those observed on the basis that it is unlikely that such a brief sampling would have observed maximum velocities. In spite of these factors, the determination of wind velocities is still a very important probe experiment, since it at least represents a start in the accumulation of wind statistics and could still have, in at least one case, an important impact on design.

## 7.2 CANDIDATE TECHNIQUES

To make wind velocity measurements from the suspended capsule, two general categories of experiments were considered: those which measure wind-induced motions of the capsule and those which observe wind velocity directly. The former technique has the disadvantage of making a sort of integrated wind-force measurement rather than an instantaneous velocity measurement. The motion of the massive Suspended Capsule will not respond rapidly to even major changes in wind magnitude or direction, because of the very low dynamic pressures associated with winds in low pressure atmospheres. Thus wind measurements deduced from capsule motions have in a sense been integrated over both time and distance, and near-surface wind velocities will not be obtainable. The direct measurements are certainly more desirable, but not readily accomplished.

## 7.3 COMPARISON OF TECHNIQUES

Several methods of making integrated measurements were considered. Initially it had been thought that dropping a reference marker on the surface and then measuring range or range rate to it was a promising technique which could be combined with the penetrometer experiment. Measurement of Doppler shift from a transmitter in the penetrometer was attractive and carried a low cost in weight. However, the frequency stability requirement was far beyond the state of the art, particularly when the impact shock loads were considered. Next, a transponder in the penetrometer was studied, this had two important disadvantages. Since only range and range rate along the line of sight to the reference point would be obtained, many possible motions due to changes in wind direction would be missed. More important, the weight of the penetrometer-transponder, when supplied with the necessary impact protection, would be in excess of 25 pounds. The problem of inadequately defining the motion could be resolved if two or more transponders were placed on the Martian surface, but only if the distance between them and the altitude difference were known. The difficulty of reliably implementing this requirement when combined with the additional weight penalty greatly reduced the desirability of this scheme.

Three additional integrated measurement techniques were then considered, all of which were confined to the suspended capsule. Two of these made use of radar techniques. One involved analysis of the return signal from the radar

altimeter to determine its Doppler shift. Although this would be a relatively light-weight experiment since the radar altimeter would already be on-board, transmission of samples of the radar return would require a large number of bits. Furthermore, no directionalty could be assigned to the movement. However, because of its dual utilization of equipment, this experiment was selected as a backup in spite of its limitations. The primary system is a three-leg Doppler radar. This provides three channels each of range, range rate, and Doppler information as well as cone angle. From these data, the track of the descending suspended capsule over the surface can be unfolded. This experiment, although heavy and requiring much power, has the additional advantage of being one which will certainly be needed for soft landing systems. Its actual flight qualification in the Martian environment before it is needed as a vital part of a soft landed mission would be a major advantage.

A second back-up experiment was also included because of its presence for other reasons. This was the use of the inertial reference system's outputs to define the motions of the capsule. Although the desired accuracy may not be achieved with such a system, the negligible cost makes it worthwhile.

The television experiment may also provide information on capsule horizontal motions if surface features can be identified in successive sets of images. This is not a high reliability technique for obtaining wind velocities, nor a major reason for carrying the television experiment (indeed, if it were, the picture-taking sequence would be modified), but it may provide additional backup.

In addition to these integrated wind velocity experiments, an instantaneous wind velocity experiment was very seriously considered and only deleted in the final payload evaluation. This was a set of smoke bombs to be released from the suspended capsule at an altitude of about 20,000 feet. Each bomb would release several puffs of smoke at timed intervals after impact. These puffs would travel with the surface winds, and thus the distance between puffs would give an estimate of surface-wind velocities. The actual inter-puff distance would be measured by the third and fourth sets of television pictures. It was demonstrated that the probability of seeing a pair of smoke puffs in the low resolution television pictures was 39 percent under worst case conditions with a simplified wind model. However, the problem of having significant portions of the high resolution television pictures obscured by the smoke could not be resolved. This risk of compromising one of the most valuable aspects of the mission resulted in the decision not to carry the smoke-bomb experiment.

## 7.4 SELECTED TECHNIQUES

As a result of the arguments presented in the preceding section, four experiments, which would provide wind velocity information, are included in the engineering payload. None of these will provide instantaneous velocity data, but all of the experiments have significant reasons, apart from their measurement of

wind velocity, for inclusion in the payload. The experiments are in order of decreasing value for wind velocity measurement: the Doppler radar or velocity-attitude sensor, the radar altimeter, the inertial reference system, and the television experiment.

## 7.5 ANTICIPATED PERFORMANCE OF EXPERIMENT

It is anticipated that the various wind-velocity experiments will provide with high reliability estimates of the wind velocity if the winds are in excess of about 100 ft/sec. If winds of lower velocity are encountered, the inherent accuracies of several of the methods will be decreased. Furthermore, it will be difficult to differentiate between the normal horizontal motions of the descending capsule, which would be present in still air, and the wind-induced motions. These random horizontal motions may be as much as 25 percent of descent velocity. However, as was noted earlier, the most important measurement is the detection of high-velocity winds. The important design decisions on future landers will be changed only if high winds are found. Thus, the most important objective of the experiment will be satisfied.

# 8.0 PENETROMETER EXPERIMENT DESIGN

## 8.1 EXPERIMENT OBJECTIVES

The primary objective of the penetrometer experiment is to provide the information on the nature of the Martian surface necessary to design landers which will impact the surface and survive in an operational mode for periods of weeks or months. Four types of information are required for such designs. First is the bearing strength of the surface. The concern over lunar dust layers is an excellent example of the problems that inadequate bearing strengths can cause. Designs which may sink deeply into surface layers are obviously to be avoided. However, it is usually expensive in weight and volume to design low unit area loading support systems when higher loadings can be tolerated. Similarly, design for impact on totally unyielding surfaces is also difficult. It is desirable to have information not only on mean bearing strength, but also to have some estimates of the ranges of bearing strengths which may be encountered. The second type of data required is the angle and distribution of slopes over areas large relative to the size of the lander. If landers are unable to remain erect and are subject to tumbling on slopes or even are unable to establish a required orientation relative to the local vertical, serious problems may arise with some experiments and with communications. The third requirement is for knowledge of the size and frequency distributions of surface features in the range of the size of the lander to about one tenth its size. These features can cause orientation problems as well as areas of high loading at impact. The fourth and probably least important requirement is for data on the vertical structure of the near-surface region. A foot of low bearing strength dust resting on bedrock presents vastly fewer problems than a layer 20 feet thick.

## 8.2 CANDIDATE TECHNIQUES

Several candidate techniques have been considered for meeting these objectives. None of the techniques seems to show promise for meeting all of them, and it appears that a combined approach will be essential. Information on bearing strength can be obtained from a non-survivable probe by measuring the deceleration-time history of a penetrometer impacting the surface. If the shape, mass, and velocity of the penetrometer are known, the nature of the surface can be determined either by calculation or by comparing with results on known surfaces. Use of several penetrometers over a wide area can provide the desired statistical weights for various types of surface which may be found. Experiments of this type also provide vertical profiles since some penetration will be achieved in most cases, and even a totally unyielding surface at least indicates an appreciable thickness. The penetrometer may be a small probe which separates from the descending capsule and precedes it to the surface, or it may be the capsule itself. This latter possibility has been rejected because of the added constraints it puts on the communications system and on the structure.

Penetrometers are not particularly well suited to providing the large and small scale surface features. This task has been relegated to the television, radar altimeter, and Doppler radar experiments. These experiments can also support penetrometer experiments by providing estimates of the frequency of occurrence of different types of surfaces, although it may be difficult to correlate specific surfaces which have been impacted with television-differentiable features.

A problem with all of these techniques as applied in a single probe mission is the extent to which the results obtained for a local area can be extrapolated to the entire planet. A suspended capsule television experiment well correlated with a flight spacecraft television experiment can greatly increase the reliability of such extrapolations, but in the final analysis, the validity of extrapolations can only be estimated after the results are in. If the capsule had the misfortune to land in an area of a type which could not be found in spacecraft pictures taken in other areas of the planet, then any extrapolation would be risky.

## 8.3 EXPERIMENT PROGRAMMING

In designing the penetrometer experiment a number of ground rules were initially established. The first was to utilize existing concepts wherever possible. The second was to measure deceleration history versus time, rather than just depth of penetration or peak loading, since these parameters could be derived from a deceleration history. The third was to make the penetrometers as simple as possible so that several could be carried. This meant centralizing all possible common operations on the suspended capsule rather than duplicating them in the individual penetrometer units.

Since study of a penetrometer experiment for lunar applications was already underway at the Aeronutronic Division of the Ford Motor Company for the Langley Research Center under contract number NAS1-4923, the basic design philosophy was to use that design as it evolved with as few changes as possible. Only two basic changes appeared necessary. The lunar device was designed to survive an impact on an unyielding surface at velocities of up to 200 ft/sec. After a brief analysis it became apparent that if release of the penetrometer were at such a low altitude that the impact velocity would stay below the lunar level, there would be inadequate time to relay the data from the suspended capsule to the flight spacecraft before the suspended capsule impacted the surface. To resolve this problem, the impact limiter was increased in size and weight to keep the internal shock loading below the 10,000 g-level of the lunar design. Starting with the time required to relay the data to the flight spacecraft, the release altitude in the least favorable atmosphere for the last penetrometer was calculated. The number of penetrometers and the interval between releases required to give the desired sampling of the surface was estimated at four penetrometers and two second intervals. From this, the release altitude of the first penetrometer was computed, adjusted for the maximum error in the radar altimeter which would trigger the release sequence, and the maximum impact velocity determined. The impact limiter was then optimized for that velocity, resulting in a 9 pound penetrometer.

A second problem, which was not as extensively treated, was the adjustment of the internal design of the penetrometer to make it compatible with the sterilization cycle. None of the components appear to have unresolvable sterilization requirements, but an extra contingency of more than thirty percent of the internal weight was allowed in case heavier components are required.

A data compression scheme is used for the suspended capsule to flight spacecraft link which involves digitizing and transmitting only the time intervals between the crossing of selected g level gates and the indixes of the gates, with allowance being made for at least two maxima in the signal.

## 8.4 INTERPRETATION OF RESULTS

Although in theory it is possible to calculate the results anticipated for various types of surfaces and to work back from deceleration histories to surface properties, in practice the results obtained to date by Aeronutronic indicate that there are significant discrepancies between theory and experiment. Thus, it will probably be desirable to attempt to match the results obtained on Mars after the fact with Earth-based experiments.

## 9.0 DE-ORBIT TECHNIQUE

This section examines the mission and system constraints upon the selection of a de-orbit technique. Several de-orbit techniques are considered, one is selected, and its performance capability is explored.

### 9.1 MISSION REQUIREMENTS AND CONSTRAINTS

The selection of a de-orbit technique must consider constraints upon the system from many sources. Once a planetary vehicle orbit and a flight capsule landing site have been nominally selected, several other parameters remain to be considered; the de-orbit true anomaly $(f_o)$, the magnitude of the de-orbit velocity increment, $(\Delta V)$, the thrust application direction $(\theta_{op})$, the entry angle, and the landing true anomaly. Some of these parameters are constrained by the flight capsule mission or system design. The landing true anomaly is fixed once the orbit and landing-site selections have been made. The entry angle is constrained by the planetary skipout for too shallow an entry angle, and the desired parachute deployment altitude and Mach number for too steep an entry angle. This constraint is more severe for high apoapsis orbits than for low apoapsis orbits since the skipout entry-angle limit is relaxed for lower entry velocities (lower apoapsis orbits). The requirement to maintain proper communication geometry during the entire flight capsule mission, constrains the selection of the remaining parameters. (The flight spacecraft and flight capsule must be within line of sight and, more important, each must lie within the antenna radiation pattern of the other.) For each value of entry angle there is now a unique combination of de-orbit true anomaly, magnitude of the de-orbit velocity increment, and thrust application direction which satisfy the communications maintenance requirement and places the flight capsule on a trajectory toward the desired landing site.

If the argument of periapsis of the planetary vehicle orbit remains a free parameter, to be determined by flight capsule requirements, one of the previous three parameters $(\Delta V, f_o, \theta_{op})$ can be fixed and the orientation of the orbit selected to accommodate landing site selection and communications maintenance requirements.

The selection of the de-orbit technique must further consider the dispersion in the achieved orbit and provide a sufficient degree of flexibility to avoid planetary vehicle orbit trim maneuvers except in the extreme.

### 9.1.1 Landing Site Selection

The landing site(s) selected for this mission, must satisfy several criteria:

1. The landing site must be sufficiently large to accommodate the expected dispersion in the impact point. This dispersion results from uncertainties in the orbital parameters, de-orbit parameters, and Mars atmospheric model.

2.  The landing site must be at a latitude consistent with the sub-Earth latitude during future landing opportunities. The lander vehicles of future missions will, in all probability, use a direct link communications system requiring the landing site to be near the sub-Earth latitude for that mission in order to provide proper communication geometry. The sub-Earth point on Mars varies between 25 degrees north and 25 degrees south latitude. Therefore, the landing site must lie relatively near the equator.

3.  The landing site should contain some characteristics or features of interest. The dark maria provide such areas of prime interest for early landing missions on which life detection is the basic objective. Other areas of some interest which may be selected for later landing missions are the desert regions, polar regions, or regions mapped by Mariner 4 or some later spacecraft.

Syrtis Major has been chosen as the primary landing site for this study since, of all possible choices, it best satisfies the requirements above. Other landing sites have been identified in Mare Sirenum, Mare Hadriacum, Mare Serpentis, Mare Erythraeum, Solis Lacus, Mare Cimmerium, and Mare Tyrrhenum. The selection of Syrtis Major is in no way restrictive but is primarily made to illustrate the system operation.

### 9.1.1.1 Landing Time of Day

The selection of a landing time of day is governed primarily by the lighting conditions necessary for good television photography. The degree of shadowing necessary to deduce something about the terrain features is an extremely important criteria. All of the television lighting criteria are best satisfied between 10 and 60-degree sun elevation angle with the optimum conditions occurring at between 20 and 30-degree sun elevation angle. These conditions occur at about 7:30 A.M. or 4:30 P.M. at the equator and slightly earlier or later in the region near the equator depending upon the local season on Mars. The choice between 7:30 A.M. and 4:30 P.M. is based upon the precession of the periapsis of the orbit due to the oblateness of Mars. The periapsis point precesses in a retrograde fashion for orbital inclinations between 40 and 60 degrees. Selection of a 7:30 A.M. landing would therefore imply that within a few days after flight capsule separation, the periapsis of the orbit would have precessed into the darkness beyond the morning terminator. The planetary mapping mission of the flight spacecraft would thus suffer. Selection of a 4:30 P.M. landing, however, leaves as long as is possible for further mapping by the flight spacecraft before the periapsis of the orbit precesses into the darkness. Therefore, a 4:30 P.M. landing at Syrtis Major has been selected as the reference landing conditions.
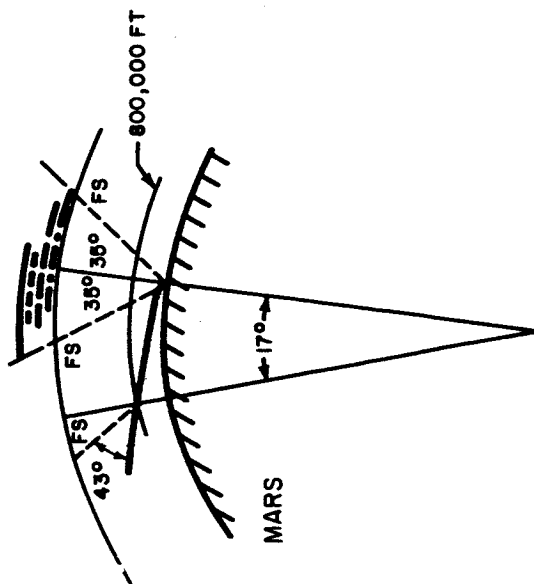
### 9.1.2 Communications Requirements

One of the primary requirements, in considering the de-orbit technique, is that proper communications geometry be provided throughout the entire flight capsule mission from separation until impact. This is especially important for the parachute descent portion of the flight capsule mission since the television and most of the important experiments are either performed or the data transmitted during this mission phase. It is desirable to angle center the flight spacecraft overhead during the parachute descent of the suspended capsule. This is shown pictorially in Figure 74.

A detailed analysis has been made to establish the duration of the period when the flight spacecraft must be overhead. The flight spacecraft must be overhead no matter which atmosphere is encountered. Furthermore, dispersion in the de-orbit conditions results in a dispersion in the entry conditions which must be accommodated. Analysis over the range of orbits being considered results in a requirement that a 6-minute period of the flight spacecraft trajectory be angle centered over the nominal parachute descent position. This analysis includes the variation in parachute descent time (170 to 322 seconds) resulting from the different atmospheric models, the variation in range angle from de-orbit to entry resulting from the dispersion in de-orbit conditions, the variation in time from de-orbit to entry resulting from dispersion in de-orbit conditions, the variation in range angle from entry to parachute deployment resulting from dispersion in entry conditions, and the variation in time from entry to parachute deployment resulting from dispersion in entry conditions. Combining these items, the variation in time from the earliest possible parachute deployment to the latest possible impact is about 6 minutes.

In order to angle center the flight spacecraft overhead for a 6 minute period during which parachute descent will occur, requires control over 2 of the 4 variables available at de-orbit, the entry angle, the de-orbit true anomaly, the magnitude and the direction of the de-orbit velocity increment. As previously discussed, the entry angle is fixed near -15 degrees by the entry angle skipout limit and by the selection of the $M/C_D A$ and the parachute deployment conditions in order to minimize the weight fraction which must be applied to the flight capsule entry shell (see paragraph 5.1). A unique combination of velocity increment magnitude, $\Delta V$, and direction, $\theta_{op}$, exists then for each value of de-orbit true anomaly, for each orbit considered. These values of $\Delta V$ as a function of de-orbit true anomaly are shown in Figure 75 for each of nine orbits considered. The thrust application direction, $\theta_{op}$, is the angle between the negative orbital velocity vector and the applied $\Delta V$ vector, with a positive angle being taken when the $\Delta V$ is applied downward. This angle is shown for each of the nine orbits in Figure 76 as a function of de-orbit true anomaly.
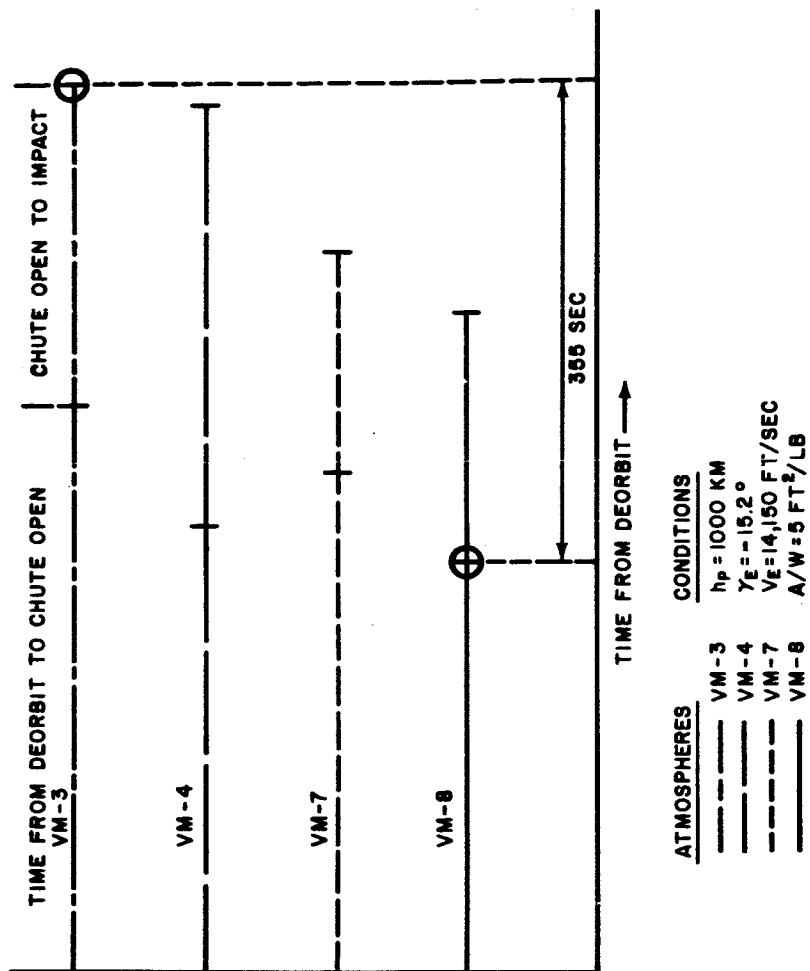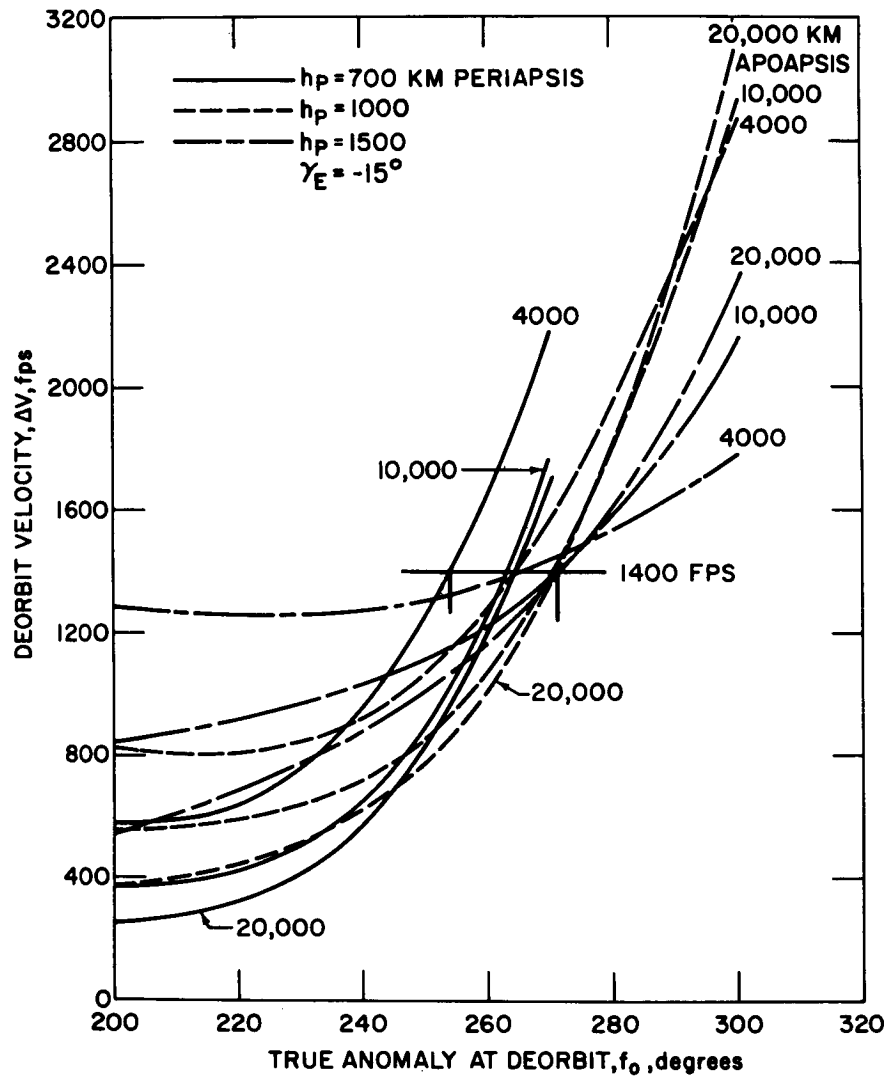
Figure 74  COMMUNICATION GEOMETRY DURING ENTRY

-191-

760146P

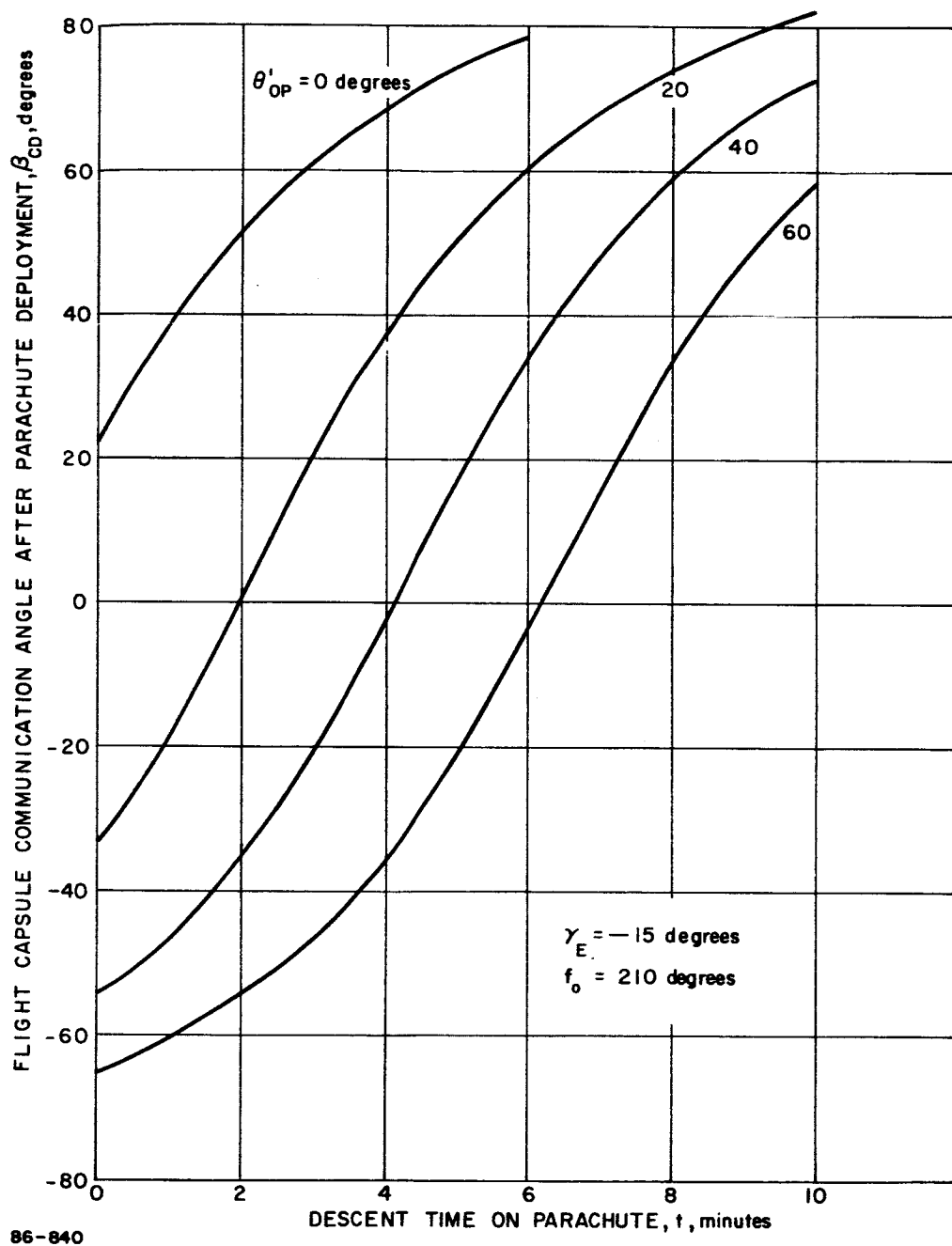Figure 75 DE-ORBIT VELOCITY REQUIREMENTS

760147P

-192-

**Figure 76  OPTIMUM THRUST APPLICATION ANGLES**

86-840

The communications geometry during the cruise portion of the flight can be accommodated by fixed antennas on both ends of the communications link. A typical example of this geometry is shown in Figure 77 for a 1000 x 10,000 kilometer orbit. The flight capsule is shown ejected from the flight spacecraft and de-orbited at a true anomaly of 270 degrees along the proper thrust application direction. The small arrows show the antenna pointing direction for antennas on the flight capsule and the flight spacecraft both of which are broad beam antennas. The look angles throughout the flight capsule cruise, as shown, are well within the beamwidth of each.

### 9.1.3 Operational Constraints

The selection of a de-orbit technique must consider the operational constraints necessary to accommodate the mission. The de-orbit technique must be sufficiently flexible to accommodate changes in the mission made necessary by failures of one or more subsystem. The de-orbit technique should easily handle off-nominal conditions created by dispersion about the nominal conditions of the mission.

#### 9.1.3.1 Sensitivity to Dispersion in the Orbital Parameters

The selection of a particular design orbit for the Voyager mission must necessarily be made well in advance of the actual operational flight. However, in the execution of the actual launch, interplanetary cruise, midcourse corrections, and orbit injection, various uncertainties, and execution errors will result in an orbit which is different from the desired orbit. The de-orbit technique must be selected to accommodate as large a variation as possible in the desired orbital parameters. It is assumed that as the orbital parameters depart from the design conditions, at some point, an orbit trim maneuver will be used to return the orbit to within tolerable limits. However, the risky nature of such a maneuver makes it highly desirable that the flight capsule as well as the flight spacecraft be capable of operating over as wide a range of orbital parameters as possible.

#### 9.1.3.2 Dispersion in Entry Parameters

For each true anomaly of each orbit there is a particular thrust application angle, ( $\theta_{op}$ ) which results in a minimum value of entry angle dispersion. The requirement for proper communication geometry during parachute descent, in general, requires a different thrust application angle. This results in a non-optimum value of entry angle dispersion. The same statement can be made for the other entry parameters: entry velocity, $V_e$ , entry time from de-orbit to entry, $t_e$ , and entry range from de-orbit, $R_e$ . The de-orbit technique selected must not allow the resulting dispersion in entry parameters to become excessively large by virtue of de-orbiting too far from the minimum dispersion points.
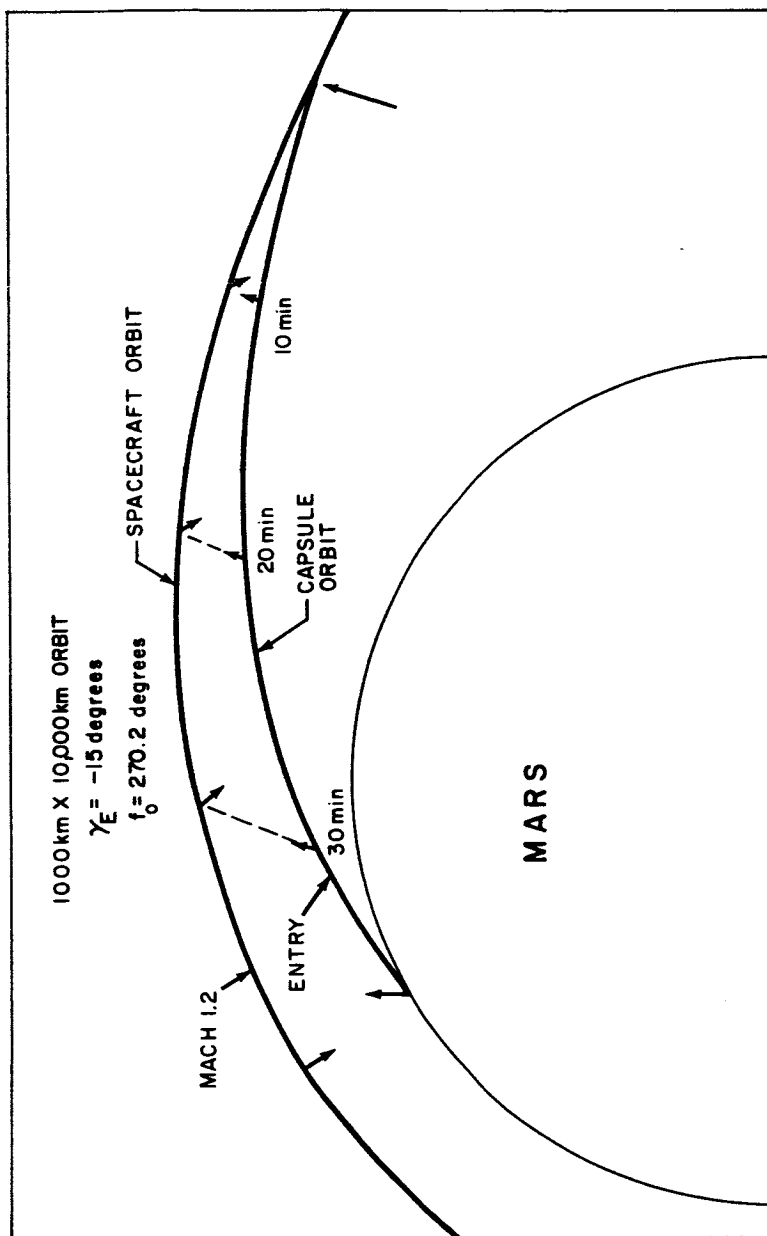
-194-

Figure 77 FLIGHT CAPSULE AND FLIGHT SPACECRAFT SEPARATION TO IMPACT TRAJECTORY

In general, these minimum dispersion conditions are not simultaneously satisfied. That is, the de-orbit conditions which produce minimum dispersion in entry angle do not minimize the dispersion in entry velocity.

9.1.3.3 Fixed $\Delta V$ versus Variable $\Delta V$

Four de-orbit methods have been considered as follows:

1. Fixed $\Delta V$ for use on all orbits

2. Fixed $\Delta V$ for each orbit, the $\Delta V$ selected for minimum entry angle dispersion

3. Fixed $\Delta V$ for each orbit, the $\Delta V$ selected for minimum magnitude

4. Variable $\Delta V$, fixed entry angle

Table XXXI compares the four de-orbit methods considered. The two techniques which employ a fixed $\Delta V$ which is selected for each orbit have the serious disadvantage of either requiring the development of a number of different engines if a range of orbits are to be maintained as options, or the early selection of one orbit if only one engine development is pursued. These approaches are also significantly more sensitive to dispersion in the achieved orbit.

The performance of the concept employing a fixed $\Delta V$ for use on all orbits and the variable $\Delta V$ concept are roughly comparable. The variable $\Delta V$ concept, however, requires that thrust-termination capability be designed into the engine. The engine must also be jettisoned prior to entry since, depending on the particular orbit, significant propellant may be left after thrust termination. If the engine were not jettisoned, the resultant penalty on entry weight and suspended capsule weight would be prohibitive. The additional event sequences and the engine jettison requirement lead to undesirable failure modes which significantly detract from this approach. The use of a fixed $\Delta V$ for all orbits is simple, flexible, meets all major requirements, and therefore has been selected as the reference design.

From Figure 75 it can be seen that a constant de-orbit velocity of 1400 ft/sec will ensure optimum communications for the entire range of orbits considered. The achievement of a constant de-orbit velocity requirement results in considerable engine simplification while retaining orbit selection flexibility.

At the selected de-orbit velocity of 1400 ft/sec, the de-orbit true anomaly is about 265 degrees, the range of true anomalies required to cover the

TABLE XXXI

DEORBIT METHOD SELECTION

| | Fixed ΔV All Orbits | Fixed ΔV Each Orbit | | Variable ΔV Fixed $\gamma_E$ |
| --- | --- | --- | --- | --- |
| | | Min $\Delta\gamma_E$ | Min ΔV | |
| • Engine design to provide orbit flexibility<br>   Single engine fixed total impulse<br>   Many engines fixed total impulse<br>   Single engine thrust cutoff | X | X | X | X |
| • Entry angle dispersion | Fair-Good | Good | Poor | Good* |
| • Entry angle of attack (requirement for maneuver) | Fair-Good | Fair | Poor | Good* |
| • Time to entry (battery weight) | Good | Fair | Poor | Good* |
| • Sensitivity to orbital dispersion (requirement for orbit trim) | Good | Fair | Poor | Good* |
| • Periapsis location adjustment (efficiency of orbit injection) | Good | Fair | Poor | Good* |
| • Engine size | Fair | Fair | Good | Poor |
| • Failure mode<br>   Engine ejection required (propellant remaining) | Good | Good | Good | Poor |
|    Thrust cutoff required (landing site miss) | Good | Good | Good | Poor |

*All "good" entries cannot be achieved simultaneously in this technique.

entire range of orbits being very small ($\sim$17 degrees). The resulting de-orbit, cruise, and entry conditions are very similar over the entire range of orbits. The sensitivity of these parameters to dispersion in the achieved orbit is, therefore, greatly reduced.

A weight optimization between the engine case weight and the required battery weight as a function of true anomaly has been performed for several orbits as shown in Figure 78. The engine propellant has not been considered in this tradeoff since it is entirely burned prior to entry and is not chargeable to entry weight. The battery system considered is a totally redundant nickel cadmium battery which operates the entire system for 30 minutes from separation to de-orbit and thereafter until impact. For true anomalies near apoapsis, the time of flight from de-orbit to entry is long, thereby increasing the battery weight requirement. For true anomalies near periapsis, the required $\Delta v$ increases, thereby increasing engine case weight. The sum of the battery and engine is minimum at a de-orbit true anomaly between apoapsis and periapsis. The resulting optimum true anomaly range for all orbits corresponds quite well with the de-orbit true anomalies (225 to 272 degrees) resulting from the selection of 1,400 ft/sec engine.

Figure 79 shows the flight capsule entry $V_e - \gamma_e$ contour on an entry velocity - entry angle map. The boundaries of the map labeled Nominal $V_e - \gamma_e$ Map, represent the three-sigma entry angle dispersion limits about a nominal entry angle.

A range extension $V_E - \gamma_E$ map is also shown. This boundary extends the range of entry angles to lower values constrained by the dynamic skipout contour at all velocities. With the fixed - $\Delta v$ de-orbit concept, it is possible to extend the impact point by using shallower entry angles.

The impact true anomaly can be extended by slightly reducing the entry angle and adjusting the de-orbit true anomaly and thrust application angle to maintain optimum communication geometry. This range extension capability is very significant, since it relaxes the orbit orientation requirements (argument of periapsis) and/or increases the number of de-orbit opportunities by tending to cancel the effect of apsidal line regression.

For the orbital range considered, the range extension capability is strongly dependent upon apoapsis altitude as shown in Figure 80 since increased apoapsis altitude results in increased entry velocity. Since the skipout entry-angle boundary increases with increasing entry velocity, smaller reductions in entry angle (less range extension) are permissible with increasing apoapsis altitude.
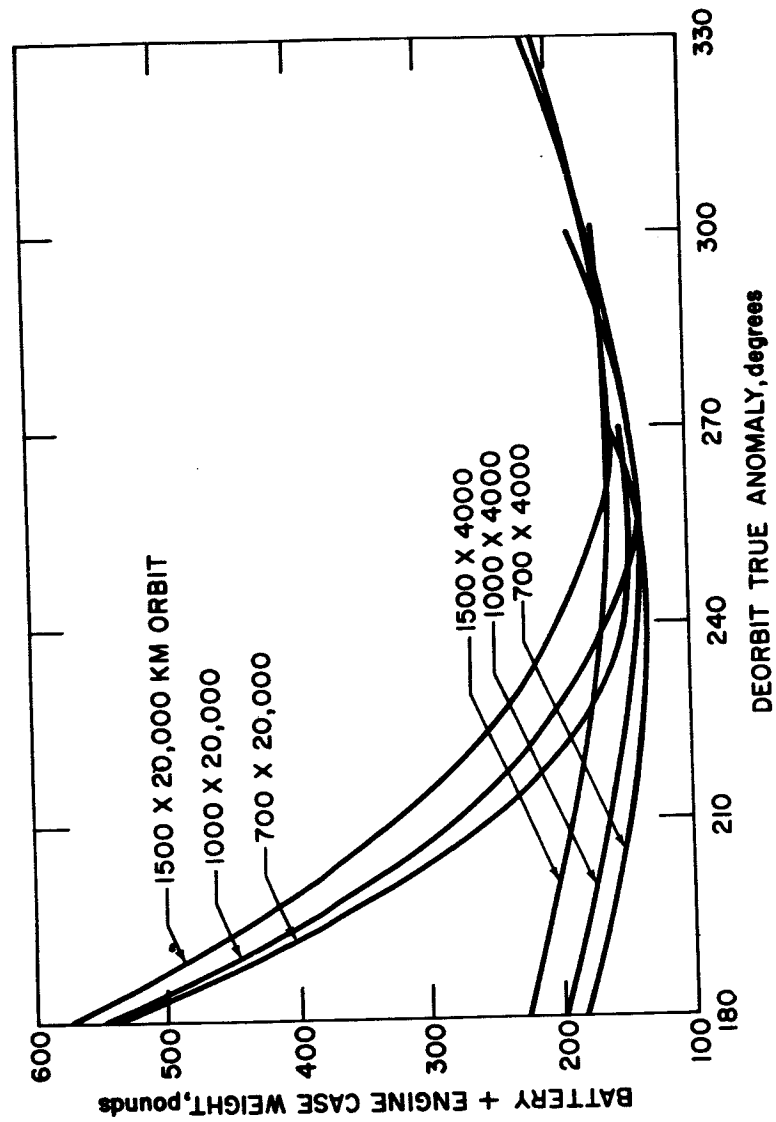
Figure 78 BATTERY PLUS ENGINE CASE WEIGHT VERSUS DE-ORBIT POINT
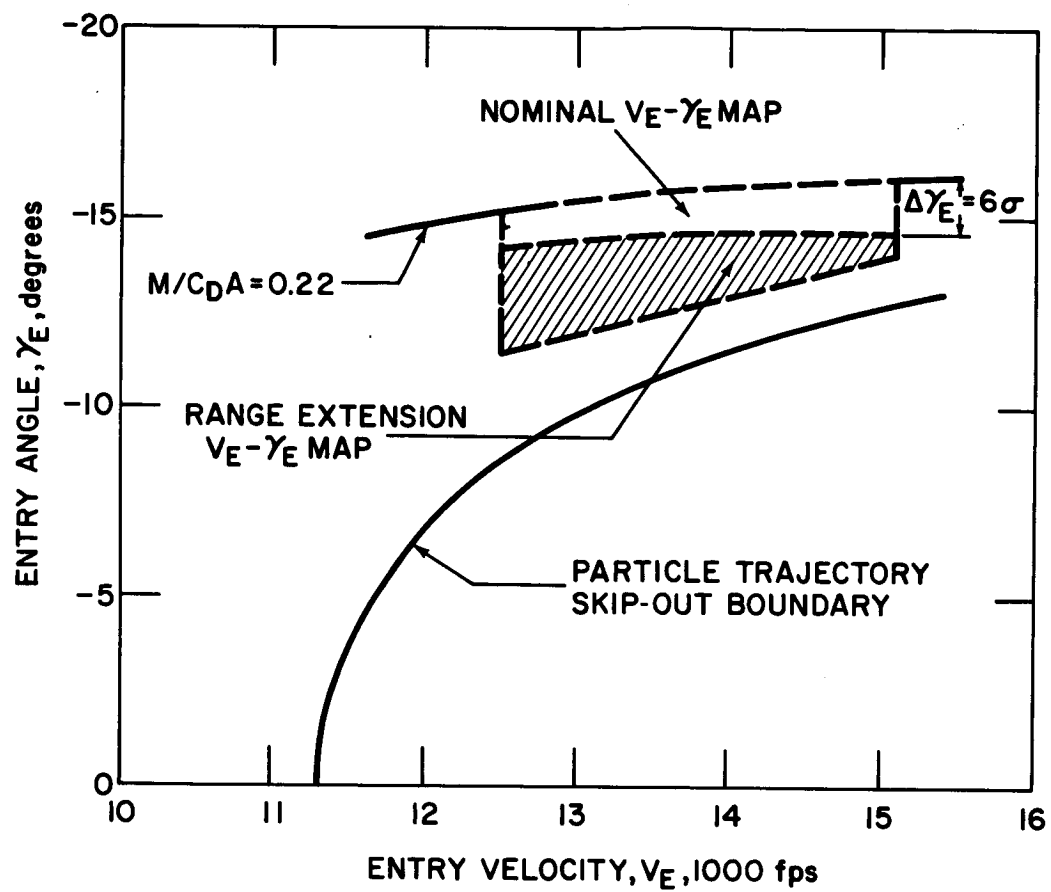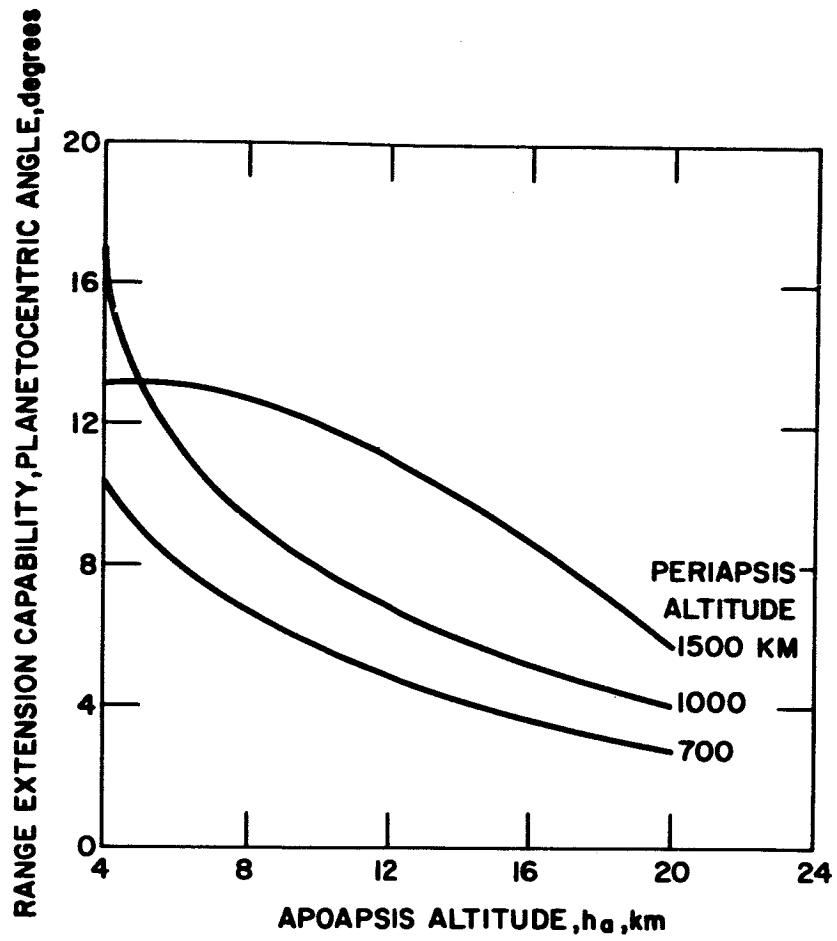
Figure 79  RANGE EXTENSION $V_e - \gamma_e$ MAP

760156P

Figure 80  RANGE EXTENSION CAPABILITY

For the fixed- $\Delta V$ de-orbit method, impact dispersion was determined for several orbits to show the effect of orbit on impact dispersion. Figure 81 shows that the maximum and minimum dispersions are obtained for orbits of 700 x 20, 000 kilometers and 1500 x 4000 kilometers, respectively. An intermediate value of dispersion is shown occurring for an orbit of 1000 x 10, 000 kilometers. The dispersion in entry angle and entry range was evaluated for $1\sigma$ uncertainties in the thrust application angle of 0.5 degree and de-orbit velocity of 0.25 percent $\Delta V$. The total impact dispersions shown combine the $\pm 3\sigma$ variation in entry angle with the extreme atmospheric models considered (VM-3 and VM-8). The impact dispersion is reduced as the periapsis altitude is increased and the apoapsis altitude is reduced.

Each of the impact dispersion contours is shown on a Syrtis Major contour to illustrate the relative size of a potential landing site.

Figure 82 shows the number of landing passes that can be obtained over Syrtis Major after orbit injection, for the fixed- $\Delta V$ method of de-orbit from a specific orbit. The natural periapsis is shown and the required periapsis location that must be achieved during orbit injection is also shown. All periapsis locations for subsequent passes over Syrtis Major consider the effect of nodal line precession and apsidal line regression. A fourth landing pass is possible, for this orbit, by use of the range extension capability. All passes shown have the proper landing time of day for proper television lighting.
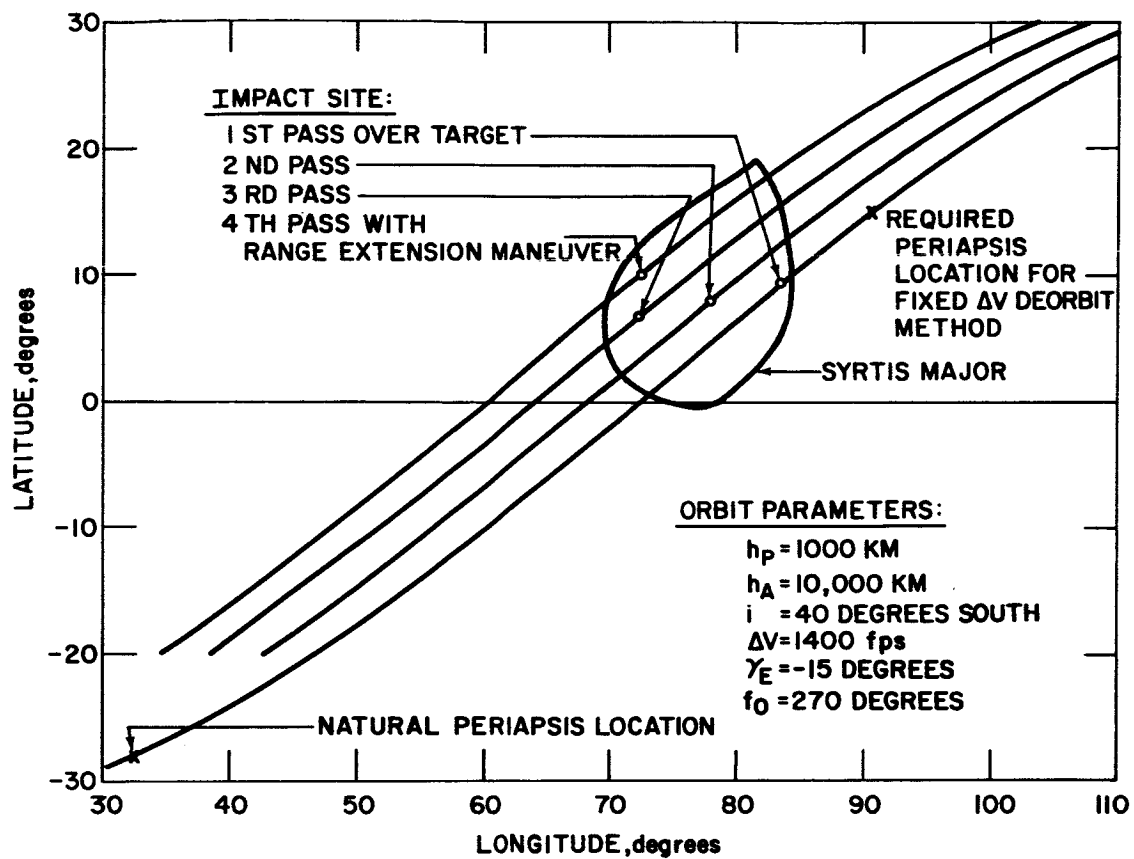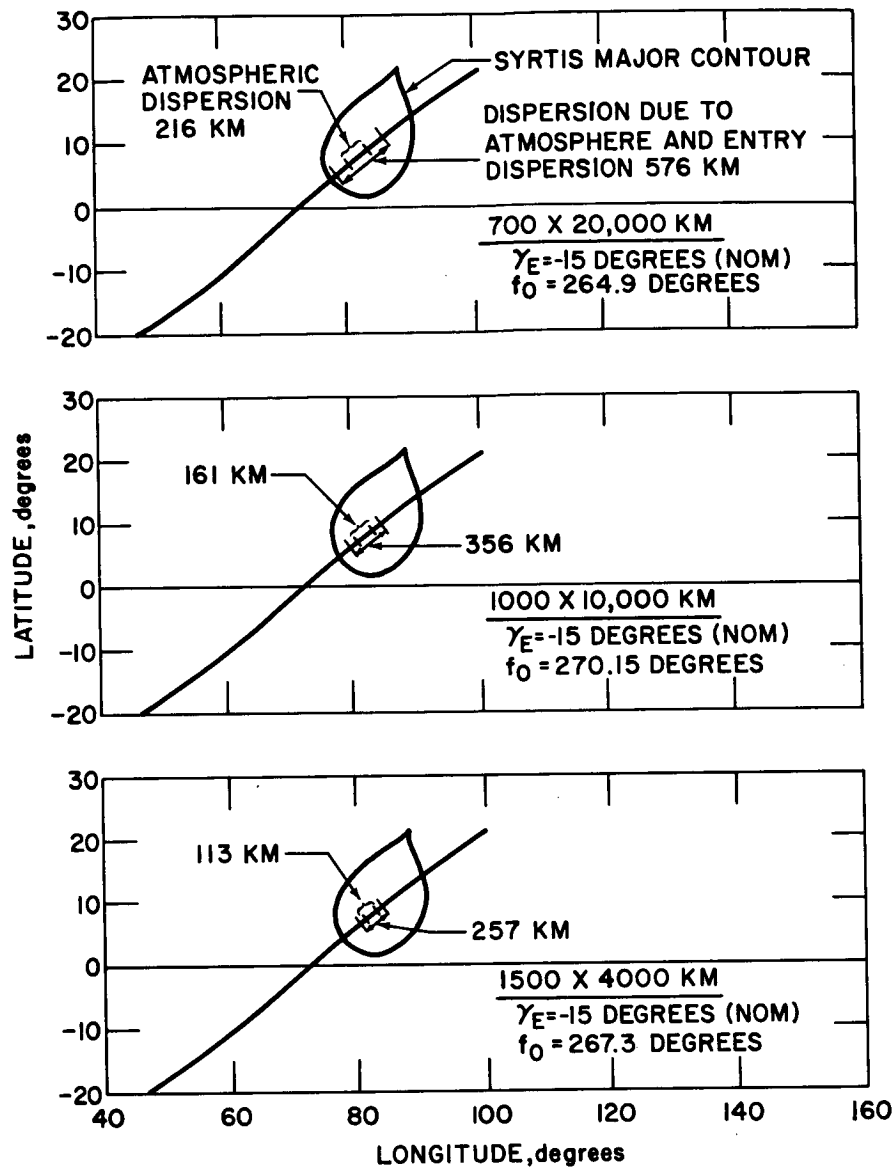
Figure 81 IMPACT SITE DISPERSION

Figure 82  PERIAPSIS LOCATION AND IMPACT SITE ACHIEVEMENT

# 10.0 ATTITUDE CONTROL SYSTEM TRADEOFFS

## 10.1 SYSTEM REQUIREMENTS/DESIGN GUIDELINES

The attitude control subsystem is required to orient the separated vehicle to the proper attitude for application of the velocity increment following separation from the flight spacecraft, to maintain it in this attitude while thrusting, and then to place the entry vehicle in the proper attitude to optimize communication and entry conditions and to maintain limit cycle conditions until entry. After entry, the inertial reference system will continue to act as a reference for the television camera.

## 10.2 CANDIDATE TECHNIQUES BY MISSION PHASE

The possible approaches for the design of the attitude control system can be conveniently discussed by examining the operation required during each phase of the mission and considering the candidate techniques which are suitable.

### 10.2.1 Orient Separated Vehicle to Thrust Attitude

The separated vehicle can be placed in the proper attitude for thrusting either by maneuvering the flight spacecraft prior to separation or by maneuvering the separated vehicle by means of an active control system.

### 10.2.2 Maintain Attitude During Thrust

The attitude of the separated vehicle can be maintained during thrusting by spin stabilization, by means of an active attitude control system (either hot or cold gas) or by gimballing the rocket engine.

### 10.2.3 Reorient for Proper Entry Attitude

The entry vehicle dynamic performance during entry will be improved if the angle of attack is nominally zero. If only spin stabilization is used, this cannot be achieved, unless the thrusting attitude and zero angle of attack attitude are the same, but at least the spin rate should be reduced so angle of attack convergence is not hindered. Convergences can further be improved if rate damping of the entry vehicle is effected. If an active attitude control system is used, it can perform the reorientation.

### 10.2.4 Maintain Attitude During Cruise

The attitude of the entry vehicle can be maintained during cruise by spin stabilization or by an active attitude control system.

## 10.3 COMPARISON OF CANDIDATE SYSTEMS

From the techniques cited, possible candidate systems can be synthesized, then compared and evaluated with respect to their performance, reliability and complexity, weight, flexibility, growth potential, and their effect on other subsystems.

### 10.3.1 Spin Only System

This system is oriented to the thrusting attitude by the flight spacecraft is spin stabilized after separation for thrusting and cruise; the spin rate is decreased prior to entry. This is the simplest and lightest system but requires a maneuver of the flight spacecraft which is the primary disadvantage. Performance is adequate for the entry from orbit mission.

### 10.3.2 Active Attitude Control System with Spin

This system used an active attitude control system for orientation. Spin stabilization is used to maintain attitude during thrusting and to entry. Adequate pointing accuracy can be achieved. It does not require a flight spacecraft maneuver and is more flexible; however, it is heavier than a spin only system.

### 10.3.3 Active Attitude Control System -- Cold Gas Reaction System

This system is the same as that previously described except that no spin stabilization is used. Control during thrusting and cruise is accomplished by a cold-gas reaction system. Due to the high thrust levels dictated by the disturbance torques occurring during thrusting, the total impulse requirements make system weight excessive.

### 10.3.4 Active Attitude Control System with Gimballing

This is the same as that previously described except that gimballing of the rocket engine provides pitch and yaw control during thrusting. The thrust levels of the reaction control nozzles can therefore be sized to be compatible with orientation and limit cycle requirements, bringing the weight down. Lower reliability and complexity, however, are major disadvantages, due to the engine gimbal and its associated mechanism.

### 10.3.5 Active Attitude Control System with Auxiliary Thrust-Vector Control

This system utilizes a separate hot-gas reaction control system for use during the thrusting phase. Thus, weight requirements are not excessive. In addition, the system is flexible, has growth potential, and reliability and complexity features are improved. Because of its efficiency, large c.g. offsets and thrust-vector misalignments can be tolerated, thus easing concern over variations in these parameters during the heat-sterilization process.

## 10.4 SELECTED APPROACH

The approach which has been selected is the active attitude control system with auxiliary thrust vector control, and is described in paragraph 4.6 of this book and in greater detail in Volume V, Book 5. An evaluation of the various candidate systems is presented in Table XXXII. It is seen then that on a relative basis the selected approach rates higher than the others. This system affords good performance. Weight was the major factor in the selection of this approach over the other active attitude control system combinations.

TABLE XXXII

ACS EVALUATION

| System / Criterion | 1 Spin Only | 2 Active ACS Plus Spin | 3 Active ACS (Cold Gas) | 4 Active ACS Plus Gimbal | 5 Active ACS (Cold Gas & Hot Gas) |
|---|---|---|---|---|---|
| Performance | Fair | Fair | Good | Good | Good |
| Complexity-reliability | Good | Good | Fair | Poor | Fair |
| Weight | Good | Good | Poor | Fair | Good |
| Maneuvering flexibility | Poor | Fair | Good | Good | Good |
| Effect on FS and other subsystems | Poor | Fair | Good | Fair | Good |
| Growth potential | Poor | Poor | Good | Good | Good |
| Failure modes | Good | Good | Fair | Poor | Fair |
| Communications maintenance | Poor | Poor | Good | Good | Good |

# 11.0 TELECOMMUNICATIONS

## 11.1 SUBSYSTEM REQUIREMENTS AND DESIGN GUIDELINES

The overall functional requirement for the flight-capsule telecommunication subsystem is to telemeter certain diagnostic and experimental data from the flight capsule to the flight spacecraft.

The following desing guidelines were established by Avco:

The design should allow the use of:

Body fixed flight spacecraft antenna

Low design-risk parachute

Solid state Flight Capsule transmitter

A wide range of orbits

The design should avoid necessity for:

Flight spacecraft maneuver

Flight spacecraft automatic tracking receiver

Flight capsule data mode change after separation

Flight capsule attitude control

Except for the entries concerning the solid-state flight capsule transmitter and flight capsule attitude control the reasons for the design guidelines are obvious. A solid state flight capsule transmitter is desired to avoid the high voltage arcing design problem that would be associated with the use of vacuum tube amplifiers. The flight capsule antenna beamwidth should be broad enough to avoid the necessity for flight capsule attitude control during entry or on the parachute.

## 11.2 ANTENNA REQUIREMENTS

### 11.2.1 Flight Spacecraft

The flight spacecraft to flight capsule look angle, which determines the flight spacecraft antenna beamwidth requirement and ultimately its gain, is defined as the angle between the main lobe axis of the antenna and the

line of sight to the flight capsule. Figure 83 shows the flight spacecraft
to flight capsule look angle for a body-fixed antenna orientation (cone angle
- 241 degrees, clock angle - 150 degrees) selected for the 1000 x 10,000
km orbit. The orientation selected is that which places the main lobe axis
of the flight spacecraft antenna along the line of sight from the flight space-
craft to a point along the descending parachute-suspended capsule flight
path. The point selected is one which occurs midway during the 6-minute
descent time interval allowed for atmosphere and entry angle dispersions.
For a body-fixed flight spacecraft antenna either a single orientation of the
antenna on the flight spacecraft can be selected for all orbits considered,
or the antenna can be reoriented for each orbit. The total flight spacecraft
look angle variation from separation to impact determines the flight space-
craft antenna beamwidth requirements. For orbits other than that illustrated
in the figure, larger look angle variations during parachute descent will
occur as periapsis is decreased and apoapsis is increased. Table XXXIII sum-
marizes the beamwidth requirements of three flight spacecraft antenna con-
cepts which could be employed. In the first concept, a single flight space-
craft body-fixed turnstile antenna is designed to accommodate the entire
range of orbits under consideration. A beamwidth of 130 degrees is re-
quired for this case. The second concept allows the antenna mount to be
adjusted prior to flight to provide the optimum pointing direction for the
particular orbit selected. In this case, the beamwidth of the flight space-
craft antenna could be reduced to 125 degrees. In the third case, the flight
spacecraft antenna requirements are examined as a gross function of orbit
range selected. For orbits with periapsis altitudes between 1000 and 1500
kilometers, a beamwidth of 100 degrees is required, while for orbits with
periapsis altitudes between 700 and 1000 kilometers, the 125-degree beam-
width determined previously is required. While the latter two concepts of-
fer potential antenna gain improvement due to the slightly narrower beam-
width required (once a nominal orbit is selected), they are more sensitive
to dispersions in the achieved flight spacecraft orbit, a potentially unde-
sirable operational penalty. Therefore, the first concept has been selected
as the reference design.

## 11.2.2 Flight Capsule

Figure 84 shows the variation in flight capsule to flight spacecraft look
angle from separation to impact for a typical orbit. The look angle is in-
creased significantly prior to entry when the flight capsule maneuvers to
a zero angle-of-attack attitude and, again, during parachute descent when
the suspended capsule may swing up to 90 degrees due to wind gusts. The
flight capsule antenna beamwidth requirements are determined by the total
look angle variation. The conditions during descent, then, indicate that
the beamwidth of the flight-capsule antenna must be very broad to accom-
modate the wide range of look angles that can be encountered. For the de-
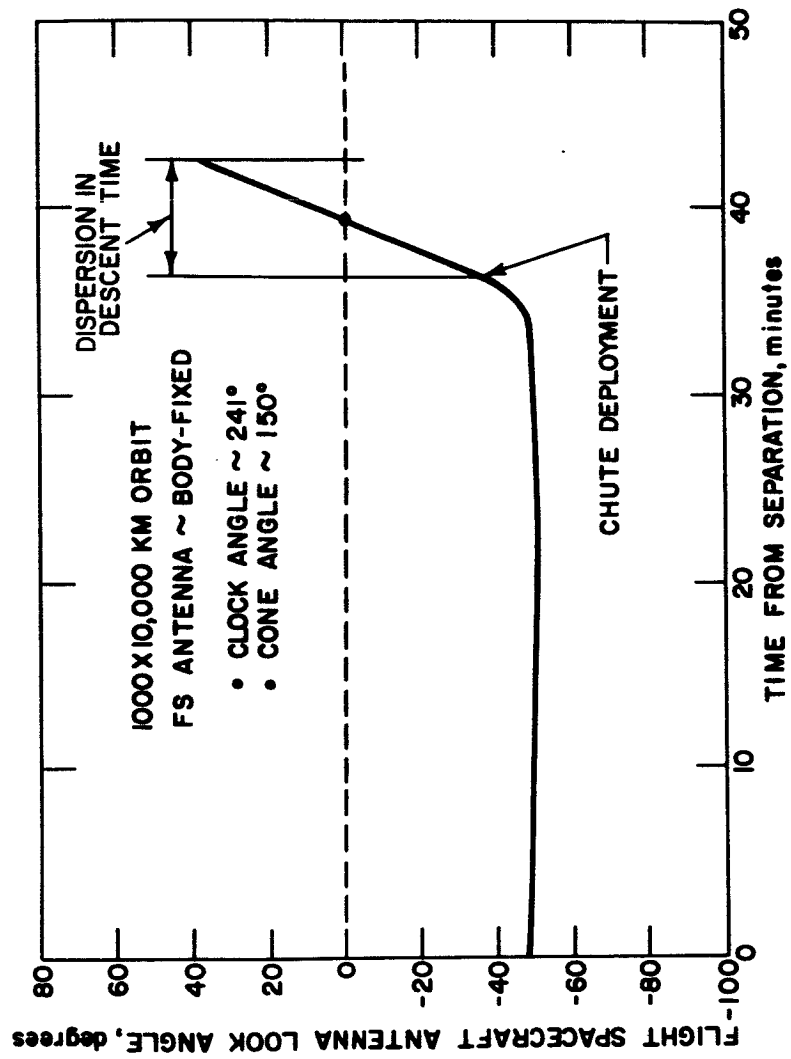sign, hemi-omni coverage is obtained until the entry shell is deployed,

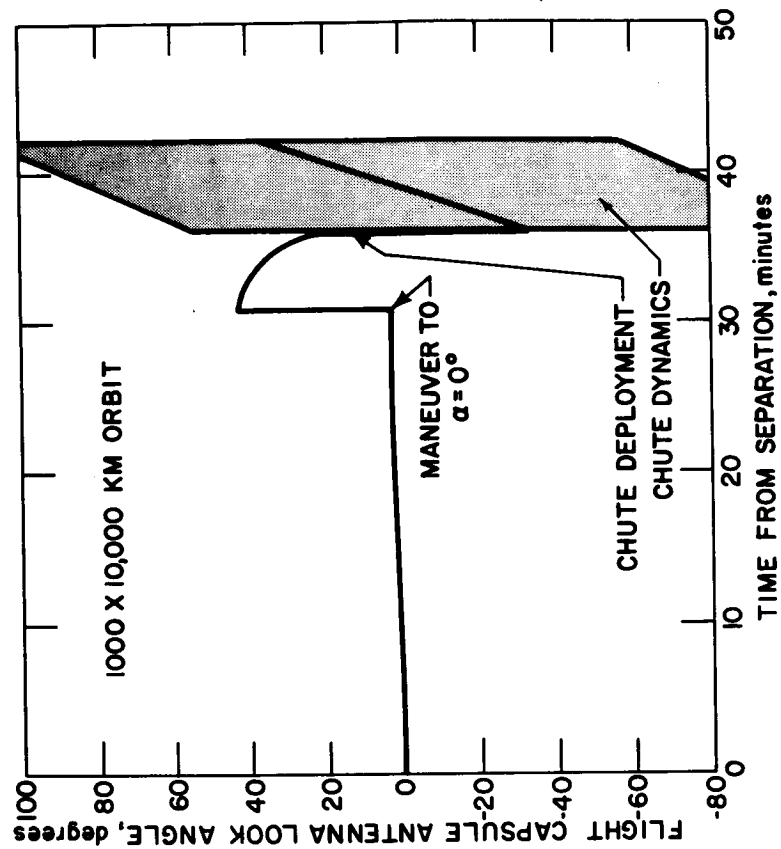Figure 83 FLIGHT SPACECRAFT ANTENNA LOOK ANGLE TO FLIGHT CAPSULE

-211-

760160P

Figure 84 FLIGHT CAPSULE ANTENNA LOOK ANGLE TO FLIGHT SPACECRAFT

-212-

TABLE XXXIII

FLIGHT SPACECRAFT ANTENNA SELECTION

| Concept | Single Antenna Type? | Adjust Antenna Position with Orbit? | Adjust Antenna Position Over Launch Window? | Beamwidth |
|---------|---------------------|-------------------------------------|---------------------------------------------|-----------|
| 1 | Yes - Turnstile | No | No | 130° |
| 2 | Yes - Turnstile | Yes | No | 125° |
| 3 | No<br>Turnstile - 700-1000 km periapsis | Yes | No | 125° |
|  | Helix - 1000 - 1500 km periapsis |  |  | 100° |

and slightly greater coverage thereafter. Antenna pattern measurements have been made by Avco, using appropriate flight capsule and suspended capsule models, so that antenna gains are accurately established.

## 11.3 FREQUENCY SELECTION

In the preceding section, it was shown that both the receiving and transmitting terminals of the relay link required broad beamwidth antennas. The performance of such broad beamwidth antennas will be essentially constant, over the frequency range of interest, regardless of the existing frequency. For such conditions, the received signal power at the flight spacecraft is inversely proportional to the square of the carrier frequency, hence, if no additional factors were to influence the decision, the selected relay frequency should be as low as possible. There are many additional factors which influence the frequency selection process (Volume V, Book 3 paragraph 5.4). The most significant were the following listed items:

- Cosmic Noise

- Receiver Noise Figure

- Transmitter Efficiency

- Antenna Size

- FCC Frequency Allocations

Figure 85 summarizes the results of the frequency selection analysis. First, the relative transmitter power required to overcome the propagation loss (the inverse square of frequency) is shown normalized to the power required by a 100 mc/sec transmitter and without regard for galactic noise. Second, the additional transmitter power required to overcome the effect of galactic noise is shown normalized to the power required by a 1000 mc/sec transmitter. Third, the additional transmitter power required to overcome the additional noise power introduced in the flight spacecraft receiver due to degraded amplifier noise figures at higher frequencies is shown normalized to a 100 mc/sec receiver. Fourth, the additional input power required to operate higher frequency transmitters due to decreasing solid state device efficiency is shown normalized to the input power required by a 100 mc/sec transmitter.

Finally, the total input power required as a function of frequency, which is the sum of the factors described above is shown and it can be seen that all relevant factors indicate that a broad optimum exists in the VHF band. Allocations in this band can be obtained at 137, 272 and 400 mc/sec. Of these, 137 mc/sec appears least attractive due to the relatively large flight capsule and flight spacecraft antennas that would be required. The selected design point is 272 mc/sec, which appears most attractive both from an efficiency viewpoint and
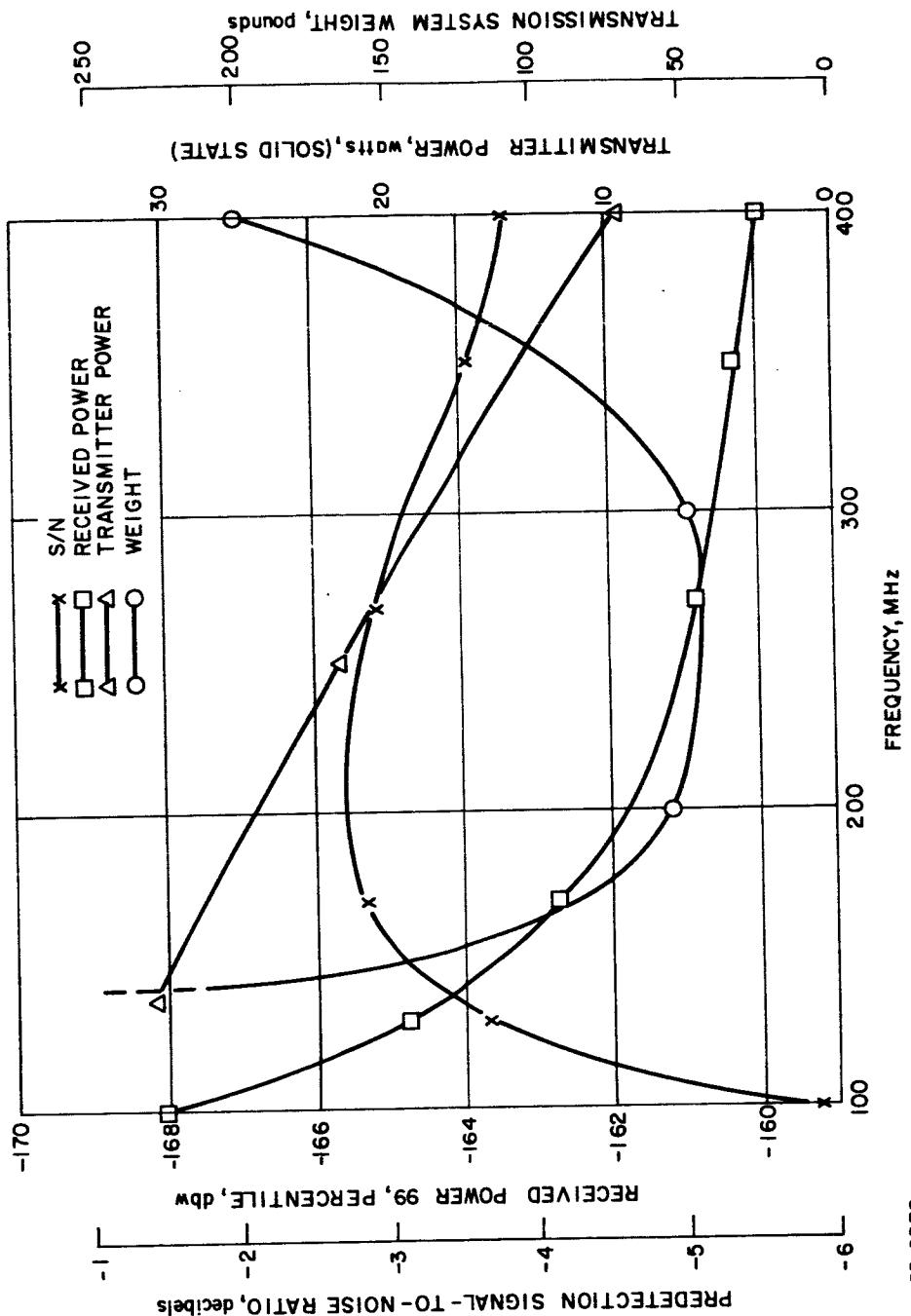
Figure 85  FREQUENCY SELECTION TRADEOFF

85-0570

-215-

availability of hardware in the existing (215 to 260 mc/sec) VHF band used on the test ranges. If vacuum tube rather than solid state devices were used, the effect of efficiency would not be as pronounced, however, the conclusions reached would not be altered.

## 11.4 FLIGHT CAPSULE TRANSMITTER POWER

The data rate required during descent, and correspondingly the transmitter power, is determined directly from the total bit content collected and the time available for transmission. A minimum descent mission, consisting primarily of television pictures, results in $2.5 \times 10^6$ bits collected. The transmission time during descent is related to the parachute diameter as shown in Figure 86. The data rate required to transmit the minimum bit mission is shown for various values of descent time and associated parachute diameters.

For a parachute 81 feet in diameter, about the size of the existing Apollo parachute, the required data rate is approximately 15,000 bps. Further reductions in required data rate by using larger diameter parachutes are considered an unnecessary design risk at this time.

A limiting value on data rate reduction is reached with descent times of 400 seconds and longer (not shown in Figure 86) due to low flight capsule - flight spacecraft elevation angles making multipath signal fading a severe problem.

Although 15,000 bps is required for the minimum descent mission, 18,000 bps was selected as the design data rate to allow a telecommunications subsystem design which does not require data-mode changes after separation.

At this data rate, approximately 240 watts of RF power would be required to maintain a simple relay link above threshold during conditions of large flight capsule sway during descent (see paragraph 11.8). At this height, a transmitter power is considered impractical in view of:

1) Potential antenna breakdown 2) Thermal control 3) State-of-the-art power device limitations 4) High voltage arcing.

Although, as shown in paragraph 11.8, various diversity techniques tend to mitigate this RF power level requirement, the factors listed above formed the basis for transmitter power selection; they are discussed briefly below.

### 11.4.1 Antenna Breakdown

The problem of antenna breakdown becomes serious at low atmospheric pressures and must be considered in selecting the power level. Although antennas can be designed to operate in any atmosphere at any power level, experience indicates that, for simple antenna configuration, and, in general,
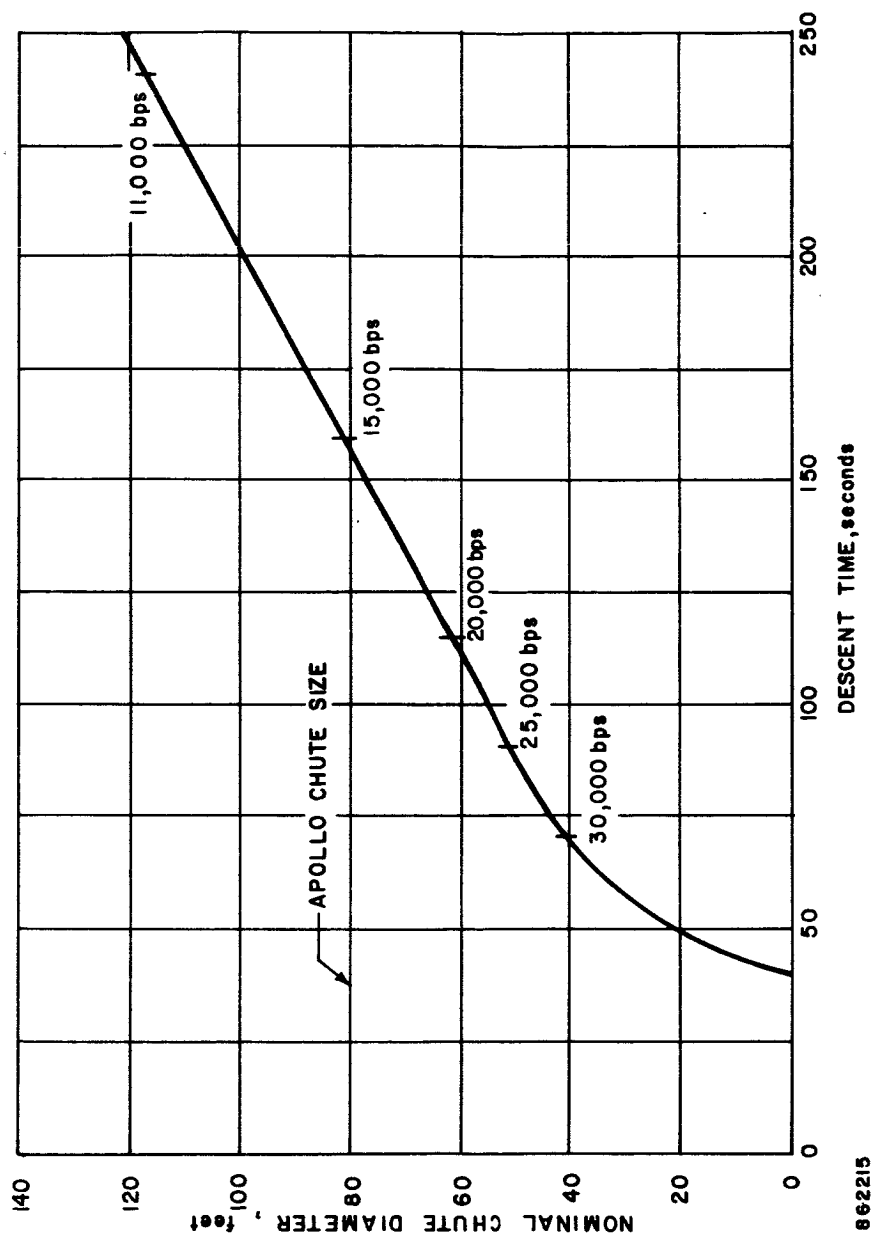
Figure 86 PARACHUTE SIZE VERSUS DESCENT TIME

862215

-217-

for antennas with a single radiating element, care must be taken in handling power in excess of 10 watts to ensure freedom from voltage breakdown in low pressure atmospheres. Since, during entry and descent, the flight capsule will be exposed to atmospheric pressures ranging from space vacuum up to possibly 10 millibars, it is considered a design risk at this time to consider transmitter power levels greater than 30 to 40 watts.

## 11.4.2 Thermal Control

As presently conceived, the flight capsule transmitter will be operating continuously for 5-1/2 hours; 4 hours before separation and up to 1-1/2 hours from separation to impact. With the transmitter efficiencies attainable with state-of-the-art devices, it is doubtful that adequate cooling can be provided with simple heat-sink configurations at power levels much above 50 watts if the transmitter is operated for this period of time. Above this level, active thermal control would probably be required. This is especially true when, in a nonoperating condition, the transmitter must be maintained above some minimum temperature and insulation is required.

This is the case with the flight capsule transmitter for, prior to separation, the transmitter requires insulation to maintain its nonoperating temperature above the specified lower limit of -55°C. During operation, the insulation prevents maximum heat sinking efficiency.

An alternative approach which would allow higher transmitter powers to be used is to operate the transmitter intermittantly during the preseparation phase. This has the undesirable feature of not allowing continuous monitoring of transmitter performance during the critical preseparation checkout and further, would make mission success dependent upon an additional discrete command from the flight spacecraft to turn the transmitter on shortly before separation.

## 11.4.3 State-of-the-Art Limitations on Device Power Handling Capabilities

Solid state devices (transistors) are currently available with power output capabilities in the 10 to 15 watt range for carrier frequencies in the 270 to 400 mc/sec band of interest. It is predicted, however, that by mid 1966 this capability will be increased to 15 to 30 watts in the same frequency band. Power levels above these values can be achieved using vacuum tube amplifiers.

## 11.4.4 Avoidance of High Voltages

It is desirable to avoid high voltage potentials when operating at the low atmospheric pressures expected during entry and descent because high voltage arcing is possible unless adequate precautions, such as pressurizing the high voltage components, are taken.

In summary, transmitter powers above 40 watts are unattractive because of potential antenna breakdown, powers above 50 watts are unattractive because of thermal control, devices requiring high voltages (vacuum tubes) are unattractive from the viewpoint of design risk in the event of pressurization failure, and solid state devices, which circumvent the high voltage problem, are not currently available and will not be available in the near future with output powers above 30 watts.

Since high voltage arcing will always constitute a design risk and passive thermal control is desirable. 30 watts was chosen as the transmitter power level with the recommendation that a solid state amplifier be developed for its provision.

## 11.5 MODULATION/DETECTION TECHNIQUES

In choosing a suitable modulation technique for the flight-capsule relay link, a number of criteria must be considered. The optimum choice necessitates a critical analysis of, and subsequent compromise among various conflicting selection criteria. Such an analysis was conducted during the study (see Volume V, Book 3 paragraph 5.4). A variety of communication systems were considered including systems for coherent and for noncoherent detection applications.

The major criteria upon which selection of the relay link modulation technique was based were:

- Relative communication efficiency

- Compatibility with mission requirements

- Compatibility with environment

- Equipment complexity

Evaluation of the results of the analysis led to the conclusions summarized below:

1. From the viewpoint of overall communication efficiency, the coherent pulse code modulation/phase shift keyed/phase modulation (PCM/PSK/PM) technique appears to be the best choice for a relay data link.

2. From the viewpoint of compatibility with mission requirements, either coherent PCM/PSK/PM or noncoherent frequency-shift-keyed (FSK) modulation will satisfy the mission requirements.

3. From the viewpoint of compatibility with environment, a noncoherent rather than a coherent modulation technique is more attractive since during entry, the radio link will experience blackout for a short period of time

-219-

and the coherent system will most likely experience loss of carrier phase lock and must reacquire lock after blackout. As the time duration allocated for reacquisition is decreased, the communication efficiency of the coherent system will degrade since larger amounts of carrier power must be allocated to the carrier phase lock loop. A similar argument applies for the descent phase when exposure to large wind gusts could cause conditions during which the relay link performance margin would drop below threshold and cause the coherent link to again lose carrier phase lock. This situation will not exist with a noncoherent modulation scheme.

4. From the viewpoint of equipment complexity, a noncoherent modulation technique is slightly favored over a coherent one since the requirement for carrier lock is eliminated in the noncoherent scheme.

The additional complexity of the coherent scheme is minor, however, since the phase lock loop does not contain complex circuitry, a noncoherent FSK modulation technique was selected.

## 11.6 PERFORMANCE MARGIN

The relay-link performance margin is shown in Figure 87 throughout the entire flight capsule mission for the case of de-orbit from a 1000 x 10,000 kilometer orbit. The margin is well above threshold (maximum adverse tolerance) over the entire trajectory except during two periods. During entry, the radio link signal is attenuated by the flight capsule plasma wake (blackout); the magnitude of attenuation depends upon the flight capsule entry velocity and the atmosphere encountered. For the case shown, it is assumed that the VM-3 atmosphere is encountered. If the VM-8 atmosphere is encountered, the degradation in margin due to plasma attenuation would be negligible. Provision is made in the design for continuous transmission during entry and, since blackout may occur, entry data are also stored and retransmitted after a delay of 100 seconds.

During parachute descent, exposure to wind gusts could cause the suspended capsule to sway up to 90 degrees. As the sway angle increases, the probability of data loss also increases due to both a reduction in flight capsule antenna gain and an associated increase in the probability of signal fading due to multipath reflections from the planet surface.

Figure 87 shows the effect on performance margin if time diversity is used in data transmission. Instead of transmitting the same signal simultaneously on the redundant transmitters, the data on one transmitter is slightly delayed to provide time diversity. The probability of signal fade, due to multipath effects, is high during the time when the capsule is at large swing angles.

However, time diversity more than compensates for this loss since, to lose information, the suspendend capsule must be at high swing angles during both separate periods of transmission when the same data is sent over each transmitter, a highly unlikely event. As can be seen from the figure, the probability of exceeding a bit error rate of $1 \times 10^{-3}$ is less than 1 percent for swing angles up to 90 degrees.
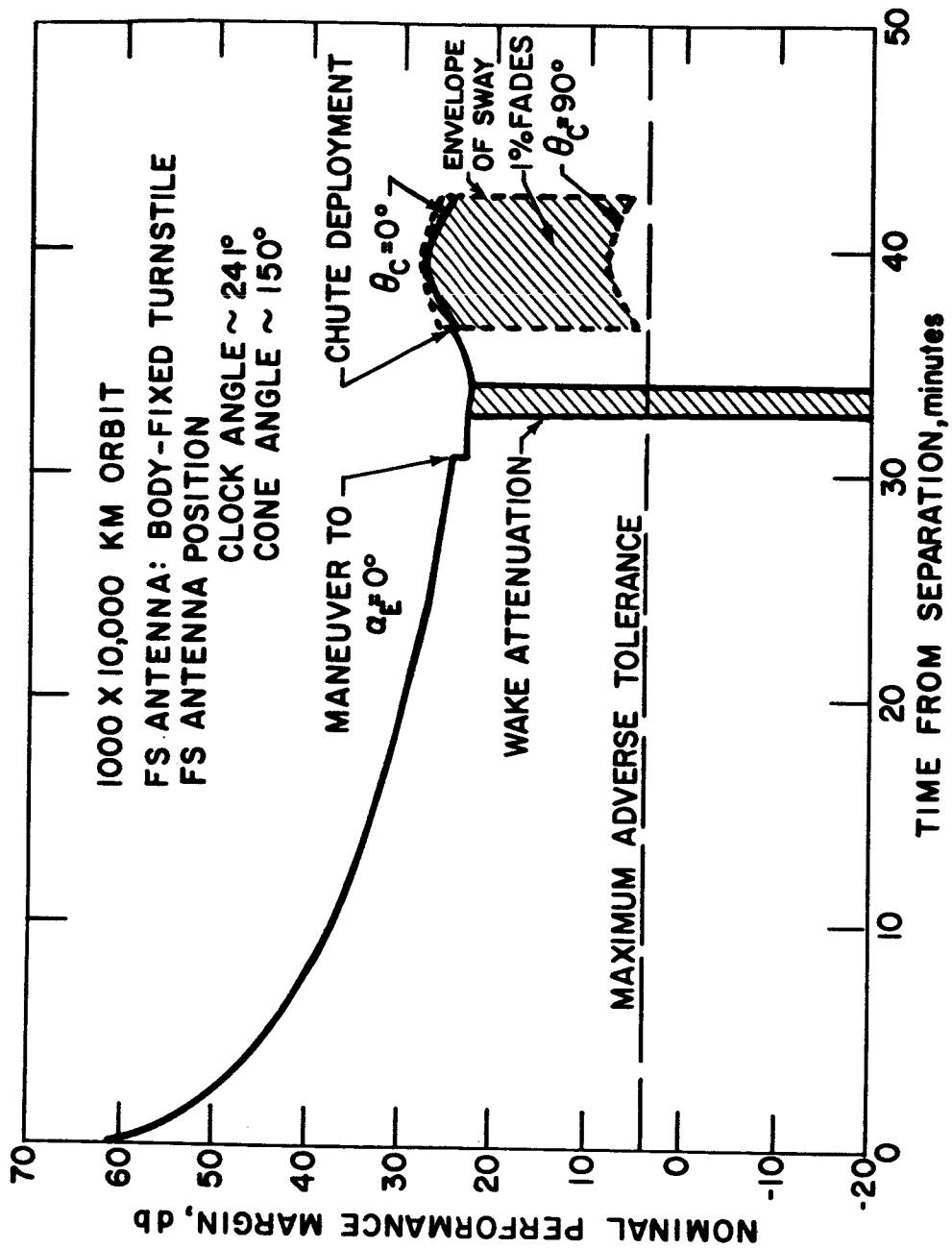
Figure 87 AVAILABLE PERFORMANCE MARGIN, WITH TIME DIVERSITY

## 11.7 FAILURE MODE CONSIDERATIONS

The design concept features totally redundant telecommunications systems.
This approach allows the use of time diversity to ensure data retrieval even
under the most adverse fading conditions experienced during the mission. As
shown in the simplified block diagram of the telecommunication subsystem in
Figure 88, all engineering and diagnostic data are fed to the corresponding data
handling equipment in both subsystems. Rather than modulate radio subsystem
1 entirely from data handling subsystem 1 and radio subsystem 2 entirely from
data handling subsystem 2, it is more advantageous to sequence the data alter-
nately to the RF subsystems from each data handling subsystem. This scheme
results in a recovery of all the data for any single failure and recovery of half
the data for any two nonredundant failures. If the one-to one relationship ra-
ther than the alternating scheme was employed, all data would be lost if two
nonredundant failures such as a failure in radio subsystem 1 and a failure in
data handling subsystem 2 occured.

## 11.8 ALLOWABLE CAPSULE SWING ANGLE ON PARACHUTE

In section 11.6, the relay-link performance margin during the descent portion
of the mission was shown to be well above threshold except during radio black-
out at entry and again during descent on the parachute when exposure to wind
gusts could cause the suspended capsule to sway up to 90 degrees (see Figure
89). Figure 90 shows the link performance margin as a function of capsule
sway angle ($\theta_c$) for a condition in which no form of diversity reception is used.
Diversity is defined as a general technique that utilizes two or more copies of
a signal to achieve, by a selection or a combination scheme, a consistently
higher degree of message-recovery performance than is achievable from any
one of the individual copies separately. As indicated in the figure, the link
performance will drop below threshold (maximum adverse tolerance line) for
capsule swing angles greater than 70 degrees. At 90 degrees, the design point,
the link performance is 9 db below threshold. To regain this lost margin by
simply increasing the flight capsule transmitter power would result in a 240
watt transmitter power requirement, an unacceptable condition. Various forms
of diversity reception were explored as more acceptable means for improving
the link margin at very large swing angles. They are summarized in Figure
91 where the probability of data loss at a capsule swing angle of 90 degrees is
shown as a function of periapsis altitude. As indicated earlier in paragraph
11.2, the nominal range of flight capsule look angles to the flight spacecraft
increases as periapsis altitude dereases, flight capsule increasing the probability
of data loss due to both a reduction in flight capsule antennas gain and an associ-
ated increase in the probability of signal fading due to multipath reflection from
the planet surface. With no diversity reception, the probability of data loss each
time the flight capsule swings 90 degrees from the local vertical is at least 20 per-
time is transmitted again, but delayed by fixed timed interval. If the wind gusts
are not time correlated, the probability of data loss with time diversity is the
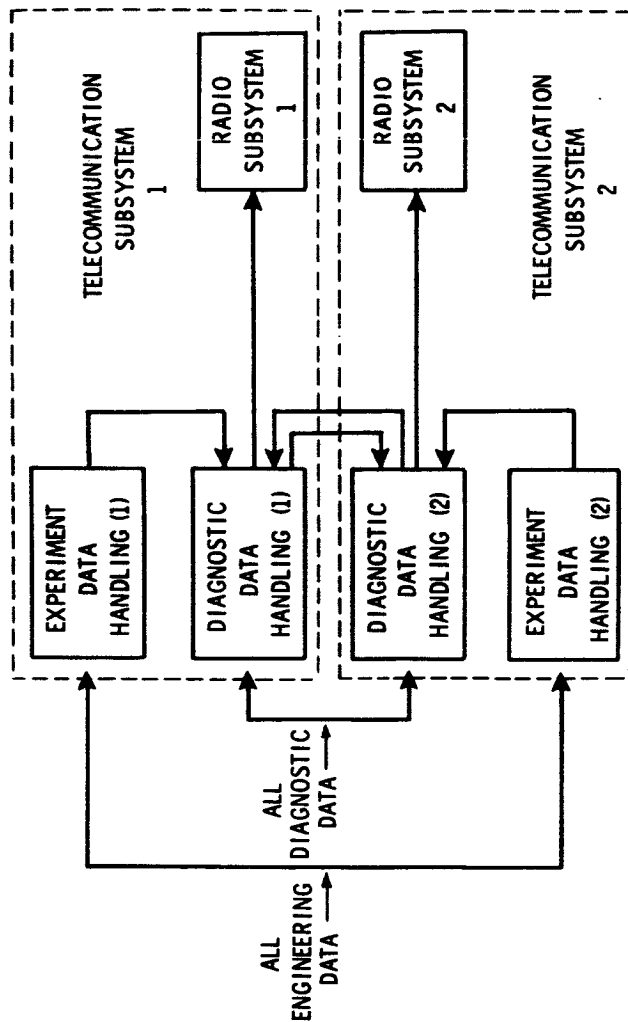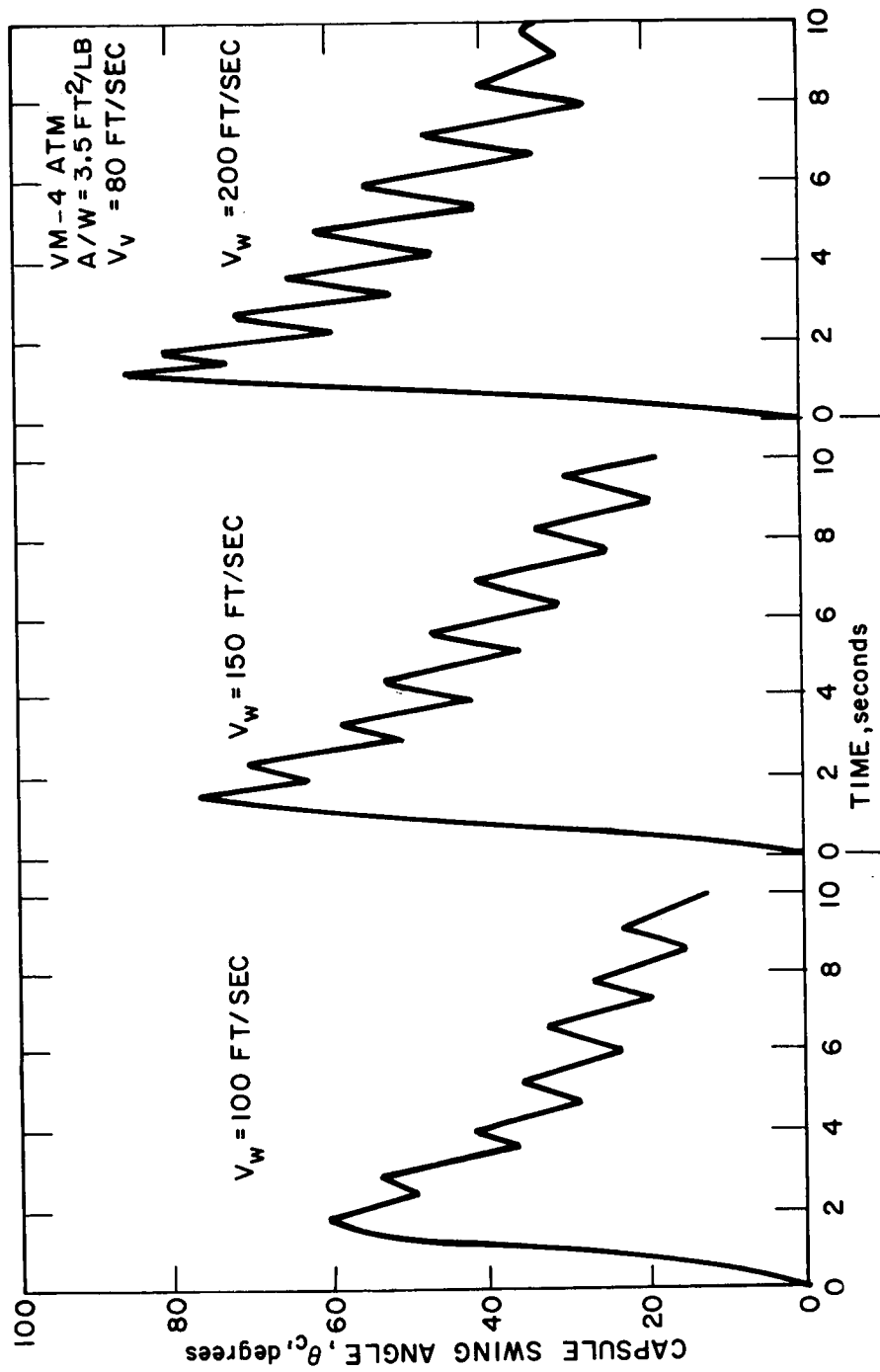
PROPOSED MECHANIZATION PROVIDES FOR:

- Total Data Retrieval For Any Single Failure
- Partial To Total Data Retrieval For Multiple Failures
- Time Diversity
- Delayed Transmission of Blackout Data

Figure 88  TELECOMMUNICATION SUBSYSTEM MECHANIZATION

760231P

-223-

Figure 89 PARACHUTE DYNAMICS - CAPSULE SWING ANGLE

25-1161

-224-
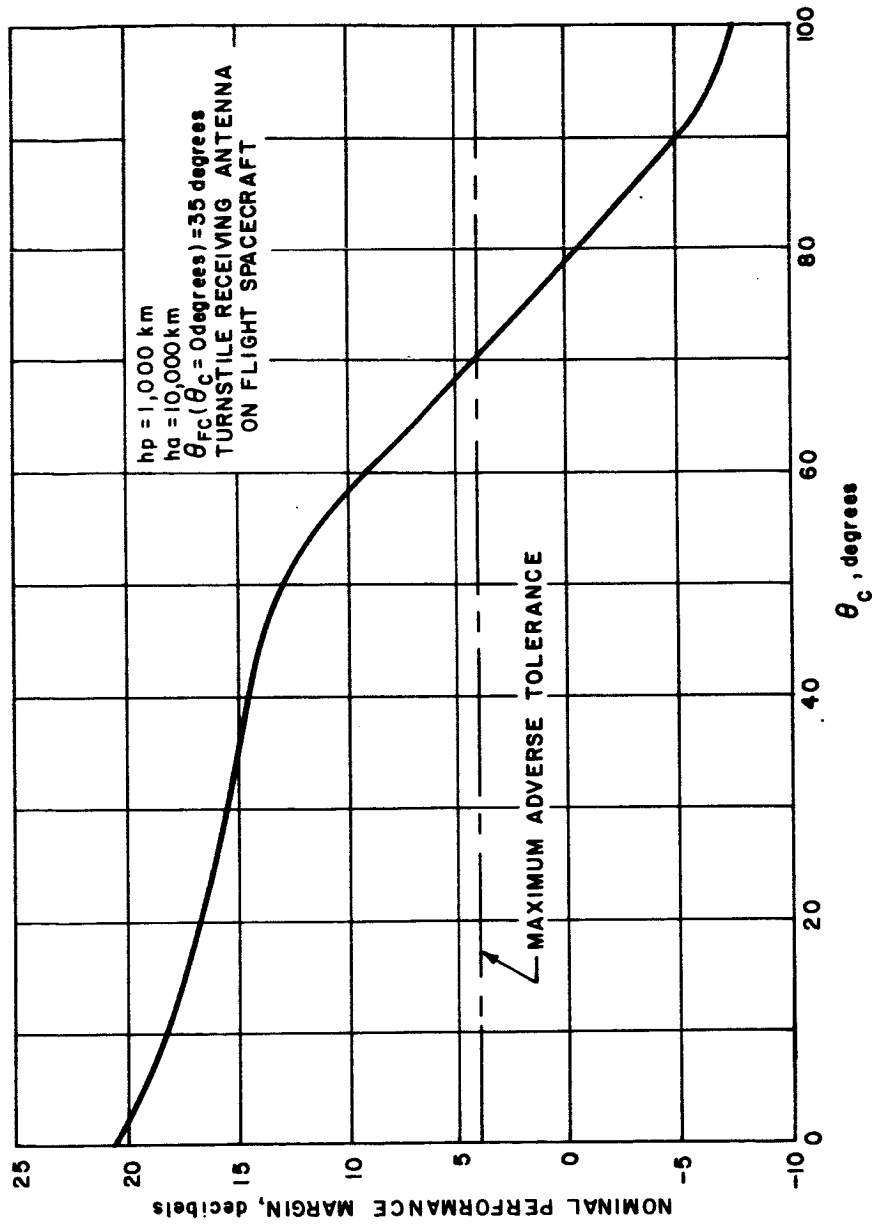
862216

Figure 90 PERFORMANCE MARGIN AT PARACHUTE DEPLOYMENT WITHOUT DIVERSITY RECEPTION
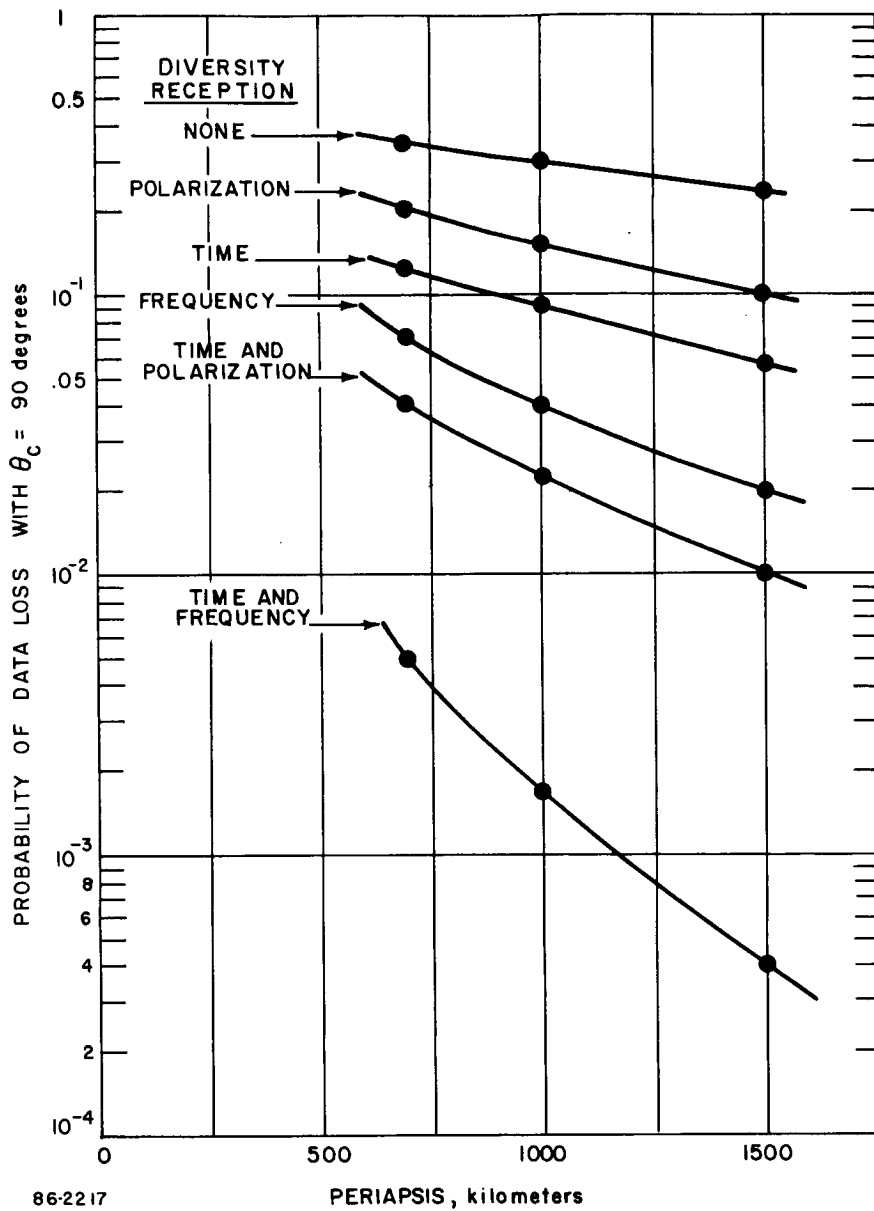
Figure 91 DATA LOSS AT CAPSULE SWAY ANGLE OF 90 DEGREES

86-22 17

square of the probability of data loss with no time diversity. Using a 1 percent probability of data loss as an acceptable performance criteria, it can be seen from Figure 91 that time, polarization (left circular and right circular) and frequency (two discrete carrier frequencies) diversities alone exhibit unacceptable performance. Additional improvement is obtained by combining time diversity with either polarization or frequency diversity. Time and frequency diversity combined satisfy the 1 percent criterion for all orbits considered while time and polarization diversity combined meet the criterion only with orbits having 1500 kilometer or higher periapsis altitudes. If no additional factors were to influence the decision, the selected diversity technique should be time and frequency combined. The improvement obtained, however, should be consistent with the price paid. The price in this case would be either a reduction in the data rate by a factor of 2 to maintain the 30 watt transmitter power level, or an increase in the power level by a factor of 2 to allow a doubling of the data rate to 36,000 bits/sec. These alternatives are required if both time and frequency diversity are used, since a condition necessary for frequency diversity is the simultaneous transmission of identical data over each of the two discrete frequency links. Inclusion of time diversity in addition to frequency diversity would of course require the same data to be repeated at a fixed time interval later and would therefore result in a doubling of the total data transmitted. Neither alternative is attractive since a reduction in data rate will compromise the mission performance and an increase in the power level would constitute a design risk from the viewpoint of high voltage arcing that is associated with vacuum tube amplifiers required at power levels above 30 watts. Of the two alternatives, the latter would be the recommended approach if both frequency and time diversity were selected.

Examining time and polarization diversity combined, it is shown that the highest probability of data loss is 4 percent occuring at a periapsis altitude of 700 kilometers. Although this technique does not meet the 1 percent criterion, it has the attractive feature of not requiring a change in the design data rate. Since two independent radio links are included in the telecommunication subsystem design for redundancy, each discrete radio link will require polarization diversity reception at the flight spacecraft. The objective of using polarization diversity here is not to transmit one sense of polarization, say right hand via antenna 1 and the alternate polarization sense via antenna 2. Both antennas would transmit the same polarization sense, but both left and right polarization would be sensed by the flight spacecraft antenna subsystem (see Volume V, Book 3 paragraph 5.4 for a complete treatment). With this condition, identical data are not required to be transmitted simultaneously as was the case with frequency diversity. Time diversity can be added here by simply delaying the data transmitted on the alternate radio link.

In selecting the form of diversity reception to be employed, it is important to consider that both the 1 percent acceptance criterion and the uncorrelated wind gust model assumed here are both subjective constraints, however, it is clear

that time diversity and either polarization or frequency diversity are required for acceptable performance. Of these two alternatives, it can be argued that with proper selection of the time diversity interval, say a few seconds, the capsule sway angle will be reduced to 70 degrees or less (see Figure 89) and the link performance margin would be above threshold without polarization or frequency diversity as long as another wind gust does not occur before the flight capsule oscillation transient has decreased sufficiently. With this consideration in mind, time and polarization diversity combined was selected as the diversity technique to be synthesized in the conceptual design since it has the least impact on other system parameters.

## 11.9 DATA FORMATTING -- TIME DIVERSITY

The selected data format scheme interlaces 34 frames on television data with 9 frames of non-television data every 2.5 seconds as shown in Figure 92. The radar, engineering, diagnostic, and penetrometer frames shown in the first 2.5 second interval of radio subsystem (1) via data handling subsystem (1) are repeated 2.5 seconds later; but this time over radio subsystem (2) via data handling subsystem (2). The data frames transmitted over radio subsystem (1) during the first 5 second interval are entirely from data handling subsystem (1) and those transmitted over radio subsystem (2) are entirely from data handling subsystem (2). During the next 5 second interval, each of the two data handling subsystems feeds data to the alternate radio subsystem. In this way, no data are lost in the event of a single failure of any subsystem.

The television transmission sequence is similarly shown in Figure 92. Each television camera has two redundant memories except the A-camera, which has four memories. After a set of three television pictures is taken, each picture is read into both memories for that camera. The picture transmission sequence is C, B, A. Camera A has four memories to allow the next set of pictures to be taken before all the stored data of the first Camera-A picture has been transmitted. The second set of Camera-A memories is used to store the second Camera-A picture while the first Camera-A picture is still being transmitted. As shown in Figure 93 radio subsystem (1) transmits even numbered lines of the Camera-C picture from the prime Camera-C memory via data handling subsystem (1). This data is repeated 2.5 seconds later from the redundant Camera-C memory via data handling subsystem (2) providing the 2.5 seconds of time diversity. Odd numbered lines of the camera-C picture are transmitted first over radio subsystem (2) from the prime Camera-C memory via data handling subsystem (1) and then 2.5 seconds later over radio subsystem (1) from the redundant Camera-C memory via data handling subsystem (2). The second block of 34 lines of Camera-C data are interleaved in the second block of 34 television lines transmitted to be repeated redundantly in the third block of 34 television lines and so on. Each block of 34 television lines is thus transmitted twich with complete redundance, and with 2.5 seconds time diversity except the first 34 lines of Camera-B which are transmitted first interleaved with the Camera-C data in the first block of 34 television lines and redundantly 14 seconds later. This was done to eliminate transmitter dead air time otherwise occuring every other frame in the first 2.5 second interval.

-228-

Figure 92  DATA TRANSMISSION SEQUENCE

-229-

Figure 93 TELEVISION TRANSMISSION SEQUENCE

RADIO SUBSYSTEM NO.1

RADIO SUBSYSTEM NO.2

KEY

A — TV CAMERA A
B — TV CAMERA B
C — TV CAMERA C

DHS NO.1

DHS NO.2

2.5 SECONDS

862185

-230-

Every other frame in the first 2.5 second interval, the first 34 frames of B camera data are also transmitted. These 34 frames of B data will still enjoy time diversity, but delayed by approximately 14 seconds rather than the 2.5 seconds used for all other frames.

## 11.10 DATA STORAGE

Storage of bulk data is required during entry when the radio link may experience blackout for a short period of time, and later during television data collection when the data recorded on the image tubes of the three television cameras must be erased simultaneously in 6 seconds. Both the rate that the image tubes must be erased and the fact that they must be erased simultaneously preclude the use of the image tubes themselves as a data storage medium.
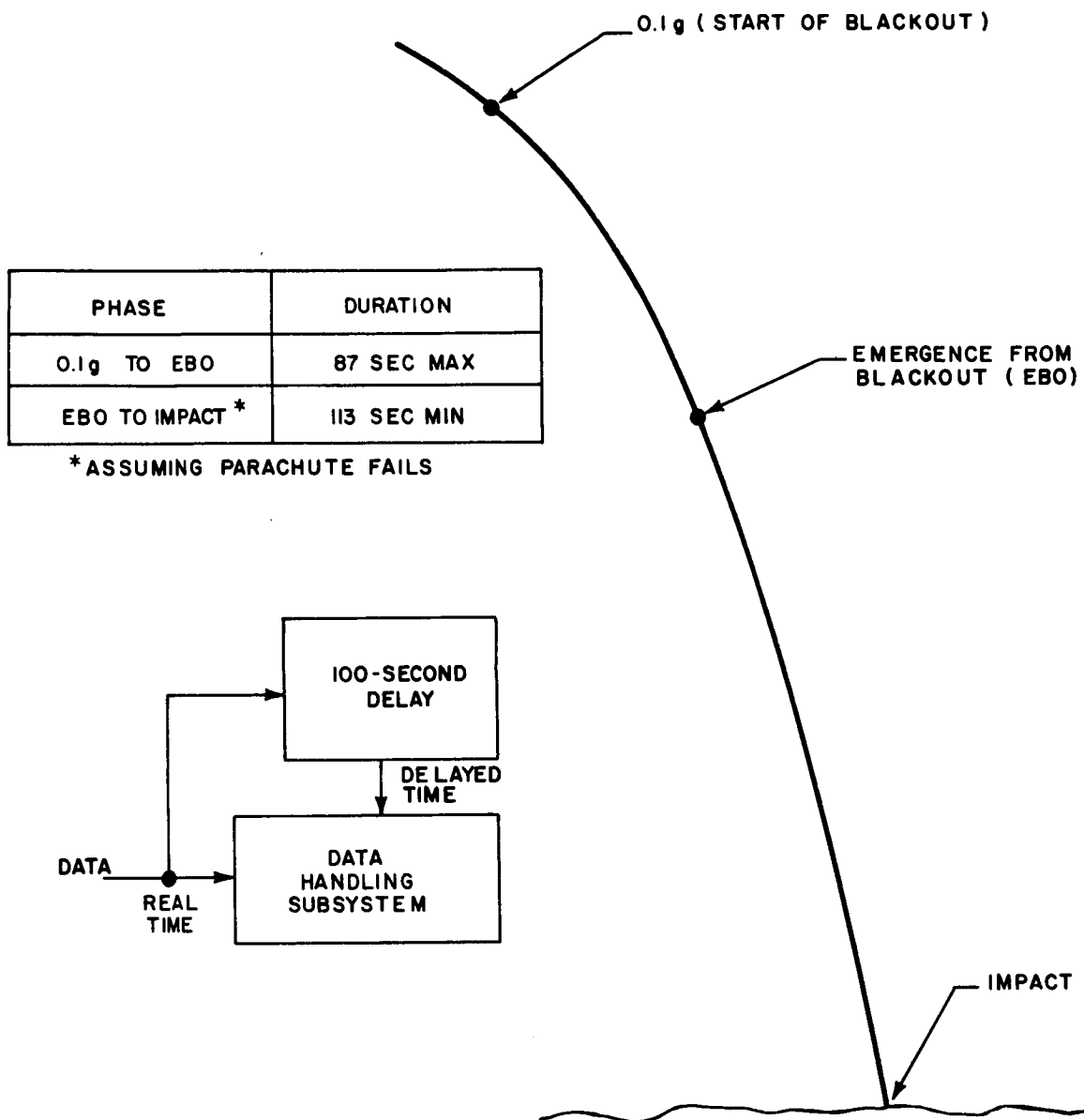
### 11.10.1 Blackout Storage Requirements

During entry radio-link blackout will probably begin near the first sensible deceleration level, shown in Figure 94 as 0.1g, and end when the flight capsule velocity is reduced to approximately 11,000 fps. To prevent loss of the data collected during this critical phase of the mission, the data transmitted in real time will also be stored in a first in-first out buffer memory creating a 100-second delay in data transmission. The maximum time from start-to-end of blackout is 87 seconds for all trajectories considered. There would always be ample time to retransmit this data if the parachute worked correctly. In the event the parachute is not deployed, the minimum time from blackout emergence to impact is 113 seconds for all trajectories considered. Therefore, by selecting the mean time between these extremes; namely 100 seconds, as the delay time, there is additional allowance for blackout periods slightly longer than expected and also additional retransmission time in the event the impact point is higher than the mean surface level.

### 11.10.2 On-Parachute Storage Requirements

While on-chute, three-picture sets of television data are acquired, the image tubes are erased simultaneously during the 6-second interval immediately following exposure. Three schemes for sequencing the storage and transmission of television data are shown in Figure 95. Each scheme provides a 10-second Take Picture period during which a set of three pictures is taken as soon as the television platform is vertically oriented (i.e., whenever the suspended capsule swing angle is less than 45 degrees). Immediately following exposure; the pictures are transferred to storage during a 6-second interval.

In paragraph 11.9, it was shown that 68 lines of television data are read out of storage every 5 seconds. Transmission of a set of three 200 line

0.1g ( START OF BLACKOUT )

| PHASE | DURATION |
|---|---|
| 0.1g  TO EBO | 87 SEC MAX |
| EBO TO IMPACT * | 113 SEC MIN |

*ASSUMING PARACHUTE FAILS

EMERGENCE FROM
BLACKOUT ( EBO)

```
            ┌──────────────┐
            │ 100-SECOND   │
            │   DELAY      │
            └──────────────┘
                   │ DELAYED
                   │  TIME
                   ▼
            ┌──────────────┐
  DATA      │    DATA      │
 ──────●───▶│  HANDLING    │
   REAL     │  SUBSYSTEM   │
   TIME     └──────────────┘
```

IMPACT

86-2218

Figure 94  BLACKOUT DATA RECOVERY CONCEPT

-232-

SCHEME 1 ONE MEMORY PER CAMERA
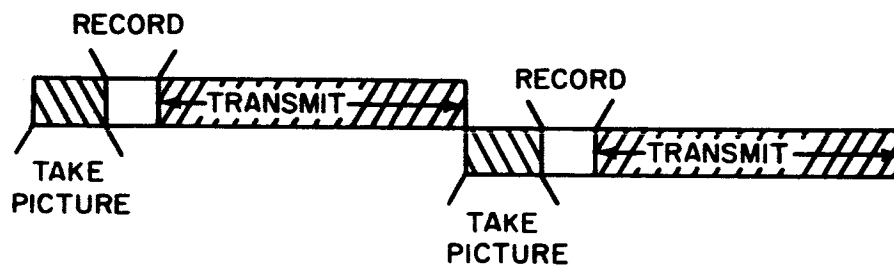


SCHEME 2 ADDITIONAL STORAGE FOR ONE PICTURE



SCHEME 3 SIMULTANEOUS READ IN-READ OUT



862219

Figure 95 TELEVISION DATA STORAGE

pictures will therefore require approximately 44 seconds. Scheme 1 is a completely serial sequence in which transmission of television data is delayed until the data are completely read into storage. This could result in a loss of up to 16 seconds per picture set (the equivalent of more than one more television picture per set).

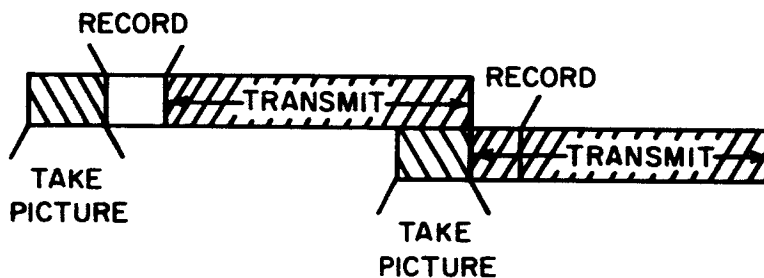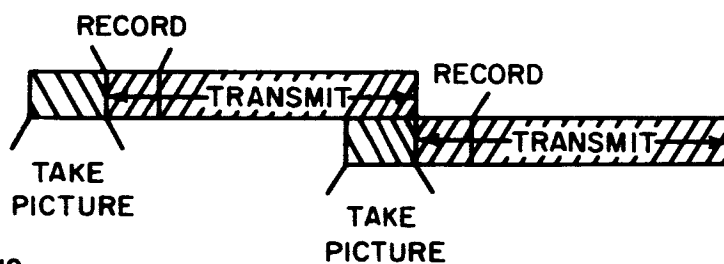In scheme 2, transmission of television data is delayed only during the read-in of the first set of three pictures. Subsequent sets are read into storage while the previously stored data are being read out. This can be accomplished by adding storage capacity for one additional picture for the A camera. As pointed out in paragraph 11.9, camera data are played out in the series camera C, B, and then A, hence, in two thirds of the time required to transmit a complete set of three pictures storage for pictures C and B will be empty and capable of receiving new data. By including storage capacity for one additional A camera picture, a new set of pictures can be taken during the interval that the A camera memory is being played out. The new picture from Camera A will be stored in the additional storage. The time required to empty A camera memory is approximately 15 seconds or not quite long enough to satisfy the 10 second Take Picture interval and subsequent 6 second record interval. However, it is close enough to be acceptable. This scheme (2) results in obtaining one additional picture (this picture will be the high resolution picture from camera C, making its inclusion desirable). However, the scheme could result in the loss of approximately one half picture in the sequence C, B, A due to the first 6 second dead time that data is being read into storage and none is being read out. In scheme 3, a simultaneous read-in read-out memory is provided to eliminate the first 6 second delay while the pictures are transferred from the vidicon to storage. Although somewhat complicated in mechanization, this scheme is feasible and would result in the possibility of obtaining half of an additional one half picture. The scheme selected for mechanization is scheme 2 to avoid the simultaneous read-in read-out complexity.

## 12.0 <u>FAILURE MODE ANALYSIS</u>

During the design synthesis, a concerted effort has been made to select only those concepts which can accommodate signel failures without catastrophic interruption of the planned mission sequence. This approach is possible because the weight constraints, which limited design flexibility and the use of redundancy, have been relaxed. As a result, the design has a high degree of inherent reliability. Moreover, those few residual failure modes have been restricted to the class of items, such as parachute and rocket motor, which do not easily lend themselves to the application of redundancy.

The analysis of each failure mode was based on:

1.  Definition of the failure mode.

2.  Identification of a diagnostic method to determine whether a failure had in fact occurred.

3.  Identification of the back-up command necessary either to reactivate the appropriate mode or to select an alternative mode of operation.

4.  Identification of an alternative or redundant mode of operation capable of compensating for the original failure.

5.  Analysis of the effect on the over-all mission if:

    a.  back-up command activated the original mode of operation.

    b.  The alternative or redundant mode of operation was successful.

    c.  No alternative or redundant mode of operation was available or successful.

## 12.1 FAILURE MODE SUMMARY

The preliminary design presented in Sections 3.0 and 4.0 includes sufficient redundancy and design margin to accommodate most single failures. Table XXXIV presents an abbreviated flight sequence with failure mode provisions indicated for each major event.

Events with unprotected failure modes are:

a)  Sterilization canister jettison

b)  Flight capsule - flight spacecraft separation, and

c)  Solid engine thrust.

-235-

TABLE XXXIV

FAILURE MODE SUMMARY

| Event | Time | Failure Mode Provision | Effect on Mission |
|---|---|---|---|
| Jettison sterilization canister | Approach trajectory | Jettison flight capsule | Flight Capsule mission failure |
| Planetary vehicle orbit inject | At approximately periapsis | None | Planetary Vehicle mission failure |
| Initiate relay communications | Preseparation | Redundant power, communication, antennas | No effect |
| Separate flight capsule | In-orbit | Backup separation joint | Flight Capsule mission failure |
| Orient flight capsule | Postseparation | Redundant reaction control system | No effect |
| Thrust vector control | Postorientation | Redundant TVC system | No effect |
| Thrust-solid engine | Postorientation | None | Flight Capsule mission failure |
| High altitude radar information | 250,000 ft to 25,000 ft | G-switch for parachute deployment | None → minor |
| Deploy parachute jettison shell | 27,500 feet or altitude where Mach = 1.2, whichever altitude is lower | Jettison nose cap to accommodate TV | Fewer TV pictures no wind measurements no penetrometers |
| Doppler information | Entry shell jettison | Low altitude radar | Possible wind measurement degradation |
| Initiate picture-taking | Entry shell jettison +5 sec | Three-camera design | Minor → no TV |
| Drop penetrometers | 3500 feet | Multiple penetrometers | Minor no hardness measurement |

-236-

## 12.2 FAILURES BEFORE SEPARATION

Prior to separation, a programmed checkout sequence will be completed. The sequence will include circuit warm-up where necessary and will determine the status of power, communications, attitude control system, thrust vector control, CC&S, instrumentation, and pyrotechnics through continuity loops, monitors, and performance measurements. Upon detection of failure or discrepancy, the checkout program will correct the problem by calibration, switching to a back-up mode or requesting disposition from the mission operation system. At the completion of checkout the batteries will be recharged.

Removal of the sterilization canister is also required (on the approach trajectory) prior to flight capsule separation. The pyrotechnic circuit used for the canister removal is redundantly activated; any one of four signals can remove the canister. The thermal coatings on the flight capsule have been designed to allow early removal of the canister.

## 12.3 SEPARATION FAILURES

The physical attachment of the flight capsule to the flight spacecraft will be accomplished by a V-clamp with four explosive clamp release mechanisms. Each release mechanism has dual squibs. The signal to initiate separation is provided by the flight spacecraft to each squib of each clamp release mechanism, providing an extremely reliable separation device since any one of the eight separation impulses will accomplish separation. In the event that separation does not occur, the base of the sterilization canister, together with the flight capsule, will be jettisoned and the flight capsule mission lost. This backup separation will occur at the field joint between the flight capsule and the flight spacecraft. The command required for the jettison is supplied by deep space network via the flight spacecraft.

## 12.4 ATTITUDE CONTROL SYSTEM FAILURE

Particular attention has been given to the design of the attitude control system to ensure backup modes in the event of system failure. The cold-gas reaction control system consists of two completely redundant systems, either one of which is capable of performing all required functions. In addition, sufficient extra gas is provided so that in case of a single failure in one system, the other system will continue to maintain control and will have enough gas remaining to overpower the failure and complete the mission. The hot-gas system is also completely redundant, so that any single failure will not affect its performance.

A sentry system, consisting of body-mounted rate gyros, is used to detect high angular rates which could occur if the inertial reference system fails in certain ways and the reaction control system continues to operate. If angular rates exceed 6 deg/sec, the reaction control system is deactivated by the sentry to prevent the uncontrollable high-rate tumbling during entry.

## 12.5 PROPULSION SYSTEM FAILURE

The propulsion system aboard the flight capsule is required to provide sufficient $\Delta V$ capability to de-orbit the flight capsule from orbits having periapsis altitude from 700 to 1500 km and apoapsis altitude from 4000 to 20,000 km. The de-orbit philosophy requires a fixed value of $\Delta V$ eliminating the requirement for thrust cut-off capability. The characteristics of a solid engine are such that once the system has been ignited, it will burn to depletion and provide the required total impulse. To assure ignition, redundant bridge wire is used.

## 12.6 ENTRY SHELL FAILURE

The failure of the entry shell during entry would naturally have catastrophic results on the flight capsule mission. Therefore, the early results of the failure effects analysis were incorporated into the entry-shell design. The entry shell was designed to survive entry for the worst entry conditions that could be realized entering from any of the postulated orbits into the worst model atmosphere. The structure was designed for $\gamma_E$ = -16 degrees at $V_E$ = 15,200 ft/sec. As previously mentioned, a failure of the attitude control system would result in a spin rate of 6 deg/sec limited by the rate sentry incorporated into the attitude control system. To account for this failure mode, a weight penalty of 18 pounds in the primary structure and a heat shield weight penalty of 114 pounds has been included in the design.

In addition to the weight penalty associated with the primary heat-shield and structure weights, the possibility of rearward entry requires additional heat-shield material on the back side of the shell weighing 55 pounds. The design also incorporates an afterbody to provide a righting moment to the vehicle in the event of rearward entry at an additional weight of 186 pounds. The secondary heat shield and afterbody also protect the subsystems from wake heating during normal entry, however, much lighter elements are required.

## 12.7 PARACHUTE FAILURE

Early in the study it became obvious that failure of the parachute system would result in a severe restriction of the time available for data transmission from the flight capsule to the orbiting flight spacecraft, and reduced time for television and penetrometer experiments. The parachute canopy utilized a design factor of safety of 2.7, while the shroud and riser lines were designed using a safety factor of 1.7. In addition to the increased strength given to the material to assure successful operation, backup deployment devices were employed to provide redundancy in the parachute deployment system. In the normal mode, parachute is initiated at an altitude of 27,500 feet or the altitude where Mach = 1.2, whichever altitude is lower, by a combination of accelerometer and radar altimeter readings. In the event either the accelerometer or radar altimeter fails, the remaining device is capable of deployment initiation at Mach = 0.85 or an altitude of 20,000 feet. This failure mode would result, for the worst

atmosphere, in a degradation in descent time of approximately 20 percent. A complete failure of the parachute system would result in a descent time from the required parachute deployment point to impact of 40 seconds or approximately 130 seconds less than required.

The actual parachute deployment is performed by a pilot parachute ejected by a mortar. A failure of the primary ejection system would automatically initiate the backup system, a gas generator used to simultaneously deploy and inflate the main parachute. Additionally, all pyrotechnic charges in the deployment mechanism contain dual igniters as backup.

## 12.8 COMMUNICATIONS FAILURE

Totally redundant telecommunications subsystems have been selected for the design since weight is not critical. Total rather than partial redundancy was selected to maximize allowance for failure. Since the flight capsule contains two independent communication subsystems, it is more advantageous to sequence the data alternately to the RF subsystems from each data handling subsystem, rather than to sequence each radio subsystem with its own data handling subsystem. The data sequence from both data handling subsystems is not synchronous; therefore different data are transmitted from each RF subsystem simultaneously. The scheme provides time diversity in the data sequence and provides for recovery of all the data twice. If any signal fading occurs, the data can be recovered later when it is repeated. This scheme also results in a recovery of all the data for any single failure and recovery of half the data for two non-redundant failures.

## 12.9 POWER FAILURE

The power system consists of two completely redundant lines of battery, battery charger and discharge regulators. Each system is capable of powering the entire mission. Both systems are coupled to the entire load through a network of protective diodes and switches. The battery chargers are installed in the flight spacecraft and are disconnected from the flight capsule at separation. The control section consists of silicon control rectifiers arranged to perform switching of power on receipt of signals from the flight spacecraft CC&S.

## 12.10 PROGRAMMING FAILURE

The CC&S has several internal failure mode back-ups. Commands stored in memory are redundant within the core matrix such that if part (less than half) of the memory is lost (electrically isolated) it is still possible to extract the command. The CC&S has seven stored sequences, such as checkout, calibration, separation, and deployment. Each sequence has at least two alternate functionally redundant means of initiation so that any single failures can be

accommodated. Since the master clock function is critical, a slave clock is synchronized to it. Should the master clock fail, the slave would be used to complete the mission.

## 12.11 INSTRUMENTATION FAILURES

If entry and descent are executed successfully, the experimental phase of the mission should present no major problems. However, if the parachute fails or nose cap is not removed, not all experimental objectives can be realized.

Within the experimental design, all experiments have some form of back-up. Altitude measured by the radar altimeter will be verifiable with the doppler radar. Atmospheric composition can be determined by both the mass spectrometer and gas chromatograph; however, only the mass spectrometer is used for high altitude measurement. Measurement of water with the water detector can be verified if an abundance of hydrogen and oxygen are observed in the gas-chromatograph experiment. Redundant devices exist for accelerometer and gyro packages and for temperature and pressure devices. Finally, atmospheric density measurement can be verified using pressure, acceleration and composition data from other experiments. (See Paragraph 4.2)

## 12.12 FAILURE MODE AND RELIABILITY DESIGN PHILOSOPHY

The nature of the Mars atmospheric mission is such that the capsule design is a compromise among many factors in order to realize the mission goals. Since reliability is one such factor, it has been important to establish the extent to which failures could be tolerated and the conditions under which reliability compromise could be considered.

To develop optimal or even satisfactory performance, a design often employs complex schemes based upon presumably untested or at least unproven hardware. These practices severely reduce reliability. Yet, to the extent that reduced performance is equivalent to reduced reliability, no compromise was possible. To sterilize and subsequently to maintain sterility until transit phase extends the thermal environment, forces remote checkout and maintenance, and complicates separation of the flight capsule from the flight spacecraft. No compromise in sterilization or sterility was permitted. Although pyrotechnic devices are highly reliable and have desirable functional characteristics (as stored energy sources for initiating or terminating discrete events), these same devices will present safety hazards during assembly, test, and launch operations. For adequate protection, pyrotechnic devices have been given elaborate safing, arming, and initiating schemes. With every safing feature added, reliability was proportionately reduced. Yet safety has been primary.

Therefore, in recognition that the best design for performance, sterility, and safety would not necessarily result in satisfactory reliability, the following design approach has been used to enhance reliability and provide for failures:

1.  Use of simple designs with a minimum number of events. The fewer things which must happen, the fewer things that could go wrong.

2.  Use of concepts and hardware which have been used successfully before. When the capabilities are well known, there is less chance that serious problems will develop.

3.  Provisions for potential failures. This has been done 1) by including either block or functional redundancy, or 2) by permitting the system to adapt to an alternate functional mode with a possible reduction of mission objectives.

4.  Use of broad rather than selective design limits to achieve satisfactory performance capability over the full range of design conditions. This permits 1) local design changes without major redesign ramifications, 2) acceptable performance despite production variability, and 3) minimum performance degradation for poorly defined environmental limits.

5.  Use of standard designs each time a function (say, safing) must be performed. More effort can then be expended on developing and qualifying relatively few items to be used in relatively large quantities.

6.  In designing for safety, use of at least two independent events in prescribed prior sequence in order to accept an initiation signal.

## 13.0 MISSION TRADEOFFS

### 13.1 ORBIT COMPARISON

The flight capsule has been designed to operate over the entire range of orbits considered, 700 to 1500 kilometer periapsis altitude and 4000 to 20,000 kilometer apoapsis altitude. Flight capsule requirements, therefore, do not restrict the selection of orbital altitude or the operational flexibility of the mission. The design orbit can be determined entirely by the flight spacecraft requirements. However, if there are no strong flight spacecraft requirements for selection of a particular orbit, there is a moderate preference for a high periapsis altitude - low apoapsis altitude orbit on the part of the flight spacecraft. Table XXXV presents the preferred altitudes for several primary and secondary design considerations. The selection of orbital altitudes can be made to favor any of these considerations. The table is also helpful in flight spacecraft - flight capsule tradeoffs involving selection of orbital altitude.

### TABLE XXXV

### ORBIT COMPARISON

| Primary Considerations | Favors | |
| --- | --- | --- |
| | Periapsis | Apoapsis |
| • Allowable suspended capsule swing angle on chute | 1500 km | 4000 km |
| • Required periapsis adjustment | 1500 km | --- |
| Secondary Considerations | | |
| • Entry angle of attack (Requirement for Maneuver) | 700 km | ----- |
| • Entry angle dispersion | 1500 km | 4000 km |
| • Range extension capability | --- | 4000 km |
| • Sensitivity to de-orbit timing | 1500 km | 20,000 km |

The range of orbital inclination used in the design studies is 40 to 60 degrees. This range of inclinations allows good flexibility in planetary mapping from the flight spacecraft as well as access to any of the desired landing sites for the 1971 mission (see Section 9.0).

The fixed $\Delta V$ de-orbit method places one constraint on the orbit selection and also fixes the de-orbit and impact true anomalies. Some flexibility in impact true anomaly can be realized by allowing small variation in the entry angle (see Section 9.0), however, at best, a range extension capability of about 1000 kilometers can be achieved. Therefore, the orbit must be initially oriented to allow landing at the desired latitude at the time of day which provides proper lighting and shadowing for maximum return from the television experiment (4:30 PM). This necessitates initial orbital orientation with the subperiapsis point on or beyond (on the dark side) the evening terminator. Periapsis regression due to planetary oblateness places the subperiapsis point at the appropriate latitude for flight capsule mission after 3 or 4 days in orbit. Several passes over a landing site of the size of Syrtis Major can thus be achieved for some orbits; a minimum of two passes over the landing site can be realized from any of the orbits considered (see Section 9.0).

## 13.2 FLIGHT SPACECRAFT - FLIGHT CAPSULE TRADEOFFS

### 13.2.1 Flight Spacecraft Relay Receiving Subsystem

Several tradeoffs exist between the flight spacecraft relay receiving subsystem complexity, the relay link performance, and the flight capsule complexity.

#### 13.2.1.1 Flight Spacecraft Relay Antenna

It is desirable to employ a single body-fixed relay antenna at the flight spacecraft relay link terminal. For a body-fixed flight spacecraft antenna, either a single orientation of the antenna can be selected for all orbits considered, or the antenna can be reoriented for each new orbit. In Paragraph 11.2, the flight spacecraft antenna beamwidth requirements resulting from three alternative concepts are shown. The summary table of beamwidths presented in Paragraph 11.2 is repeated as Table XXXVI, with the addition of the relay link performance margin attainable relative to concept (1) in which a single body-fixed turnstile antenna is designed to accommodate the entire range of orbits considered. A beamwidth of 130 degrees is required for this case. The second concept allows the antenna mount to be adjusted prior to flight to provide the optimum pointing direction for the particular orbit selected. In this case, the beamwidth of the flight spacecraft antenna could be reduced to 125 degrees giving a 1 to 1.4 db improvement in the available performance margin over the previous case. In the third case, the flight spacecraft antenna

TABLE XXXVI

FLIGHT SPACECRAFT ANTENNA SELECTION

| Concept | Single Antenna Type | Adjust Antenna Position with Orbit | Adjust Antenna Position Over Launch Window | Beamwidth | Δ Margin |
|---------|---------------------|-----------------------------------|--------------------------------------------|-----------|----------|
| 1 | Yes - Turnstile | No | No | 130° | Reference |
| 2 | Yes - Turnstile | Yes | No | 125° | +1 to 1.4 db |
| 3 | No | Yes | No | 125° | +1 to 1.4 db |
| | Turnstile - 700 - 1000 km periapsis | | | | |
| | Helix - 1000 - 1500 km periapsis | | | 100° | +2 to 3.9 db |

type is changed as a gross function of orbit range selected. For orbits with periapsis altitudes between 1000 and 1500 kilometers, a helix antenna of a 100-degree beamwidth is used, which gives a 2 to 3.9 db improvement in available performance margin over that of the first case.

While the latter two concepts offer more performance margin once a nominal orbit is selected, they are more sensitive to dispersions in the achieved flight-spacecraft orbit, a potentially undesirable operational penalty. Therefore, concept (1) has been selected as the reference design.

### 13.2.1.2  Flight Spacecraft Relay Receiver

In Paragraph 11.8, it is shown that unless some form of diversity reception is employed at the flight spacecraft relay terminal, there is a high probability that at very large flight capsule sway angles certain flight capsule data may be lost in the process of data transmission to the flight spacecraft. A combination of time and polarization diversity reception was selected for the conceptual design. This results in a somewhat complicated flight spacecraft relay receiver (see Paragraph 3.4). Since the criterion for acceptable relay link performance (probability of data loss less than one percent) and the wind model postulated (uncorrelated wind gusts) are both subjective constraints, it is entirely possible that the performance attainable with time diversity alone, which is obtainable with no additional flight capsule complexity, would be an acceptable performance criterion thus eliminating the need for polarization diversity combining flight spacecraft receivers. The reduction in flight spacecraft complexity would be the elimination of one turnstile antenna, two receivers and both polarization diversity combiners shown in Figure 4.

Although the reduction in flight spacecraft receiver complexity stated above is very desirable, polarization diversity is included in the conceptual design to maintain the consistently conservative approach to the overall telecommunication subsystem.

### 13.2.1.3  Flight Spacecraft Relay Data Storage

In Paragraph 3.2.1.4, the flight spacecraft data handling subsystem is described as consisting primarily of two data storage subsystems, one consisting of a buffer memory for operation during the cruise portion of the flight capsule mission after separation, and the other consisting of a tape recorder for storing all data transmitted during flight capsule entry and descent. This approach was selected so that there would be no requirement for a flight capsule data-mode change after separation. This does require a mode change in the flight

spacecraft relay subsystem, however, by requiring the flight space-
craft to turn the recorder on shortly before flight capsule entry.
Alternatively, to allow a single flight spacecraft relay mode also, a
single data storage medium could be employed in the flight spacecraft,
but operated for the entire post separation flight capsule mission.  At
a data rate of 18, 000 bits/sec from each of the redundant relay links,
the data storage required in 1 hour (total time from flight capsule
separation to impact) is approximately 130 million bits.

The amount of data storage required with the alternative approach
described above is roughly an order of magnitude more than would
be required with the concept described in paragraph 3. 2. 1. 4.  Since
the reference concept requires data storage nearly the same as has
been required on previous deep space programs, it was selected for
the conceptual design.

13. 2. 2  Flight Capsule Thermal Control

The importance of proper definition of the flight spacecraft flight capsule
thermal interface and its effect on the flight capsule thermal control de-
sign and performance was emphasized previously in paragraph 4. 9.
Physically, this influence of the interface is reflected in the heat-flow
patterns to and from the base of the sterilization canister, and in the
base temperatures.

A tradeoff study indicating the effect on average flight capsule temperature
of various assumptions concerning the thermodynamic state of the interface
boundary as represented by the sterilization canister base reference design
approach, (adiabatic, insulated, isothermal, etc.) is summarized in Fig-
ure 96 for various flight capsule heater power levels.  The selected approach
is shown to be conservative for realistic conditions and power levels re-
quired (200w).  The interaction of the interface assumptions with the power
levels indicated should also be noted, as well as the advantage of a solar
panel configuration permitting direct impingement of solar radiation on
the sterilization canister base.  The effect of various isothermal inter-
face assumptions on heat-shield temperatures is shown in Figure 97 again
for various heater-power levels.  Component temperatures would follow
a similar trend. Such isothermal conditions could result from a variety of
interface configurations and spacecraft solar panel selections.
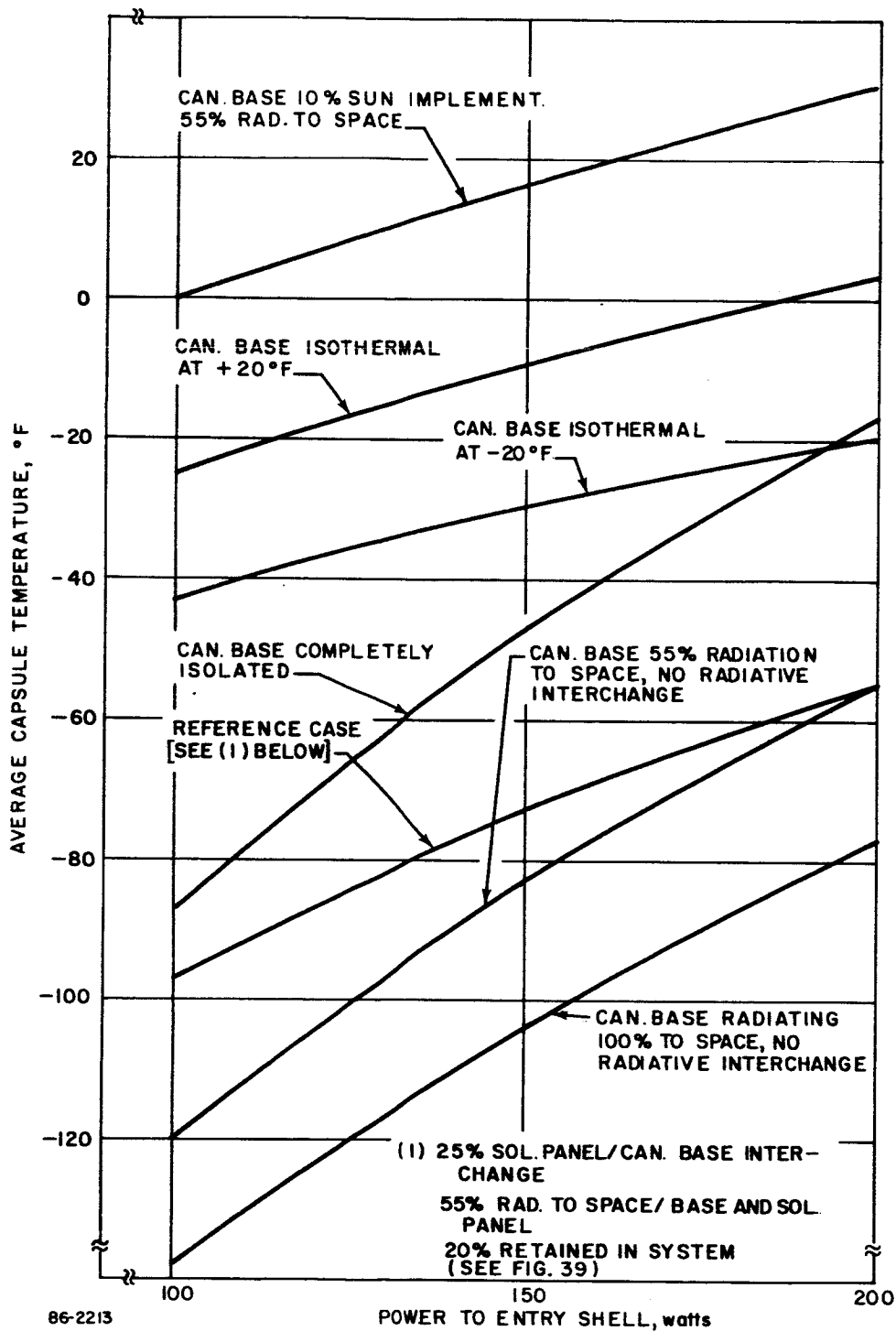
Figure 96 COMPARISON OF THE EFFECT OF INTERFACE ASSUMPTIONS ON FLIGHT
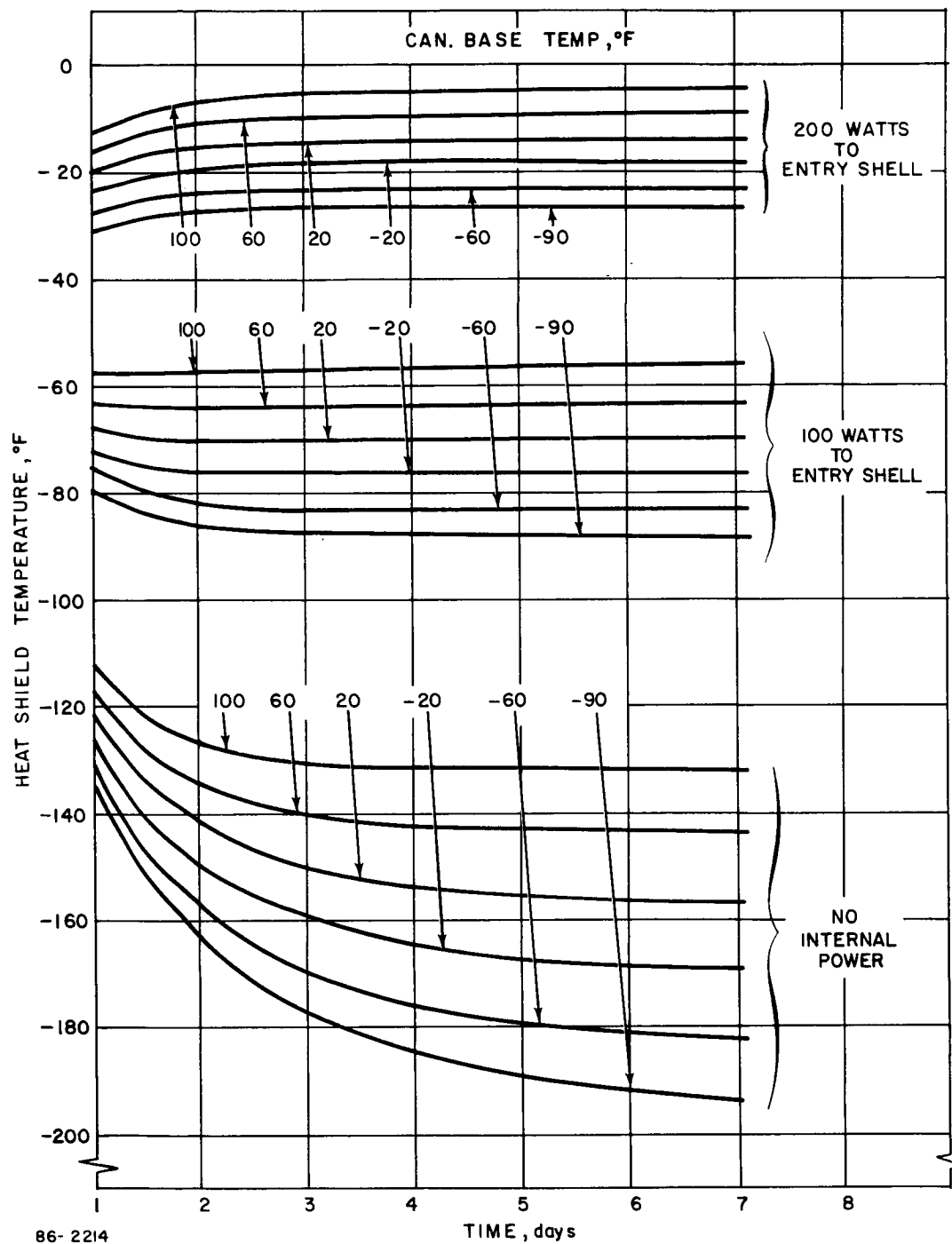CAPSULE AVERAGE TEMPERATURE NEAR MARS

Figure 97  EFFECT OF CANISTER BASE TEMPERATURE VARIATION ON HEAT SHIELD
TEMPERATURE

86-2214

-248-